The Electrophysiological Detection of Subclinical Abnormalities in Asymptomatic Members of Lebers Hereditary Optic Neuropathy Pedigrees

By:

Lisa Kleiner Hoffman

A dissertation submitted to the Graduate Faculty in Psychology in partial fulfillment of the requirements for the degree of Doctor of Philosophy, The City University of New York.

2006

UMI Number: 3205024

Copyright 2006 by
Kleiner Hoffman, Lisa

All rights reserved.

UMI Microform 3205024
Copyright 2006 by ProQuest Information and Learning Company.
All rights reserved. This microform edition is protected against
unauthorized copying under Title 17, United States Code.

ProQuest Information and Learning Company
300 North Zeeb Road
P.O. Box 1346
Ann Arbor, MI 48106-1346

©2006

Lisa Kleiner Hoffman

All Rights Reserved

This manuscript has been read and accepted for the Graduate Faculty in Psychology in satisfaction of the dissertation requirements for the degree of Doctor of Philosophy

1/18/06	Louise Hainline, PhD.
Date	Chair of Examining Committee
1/18/06	Joseph Glick, PhD.
Date	Executive Officer

Vance Zemon, PhD.

James Gordon, PhD.

Jerome Sherman, O.D.

Daniel Kurylo, PhD.

Supervisory Committee

THE CITY UNIVERSITY OF NEW YORK

Abstract

The Electrophysiological Detection of Subclinical Abnormalities in Asymptomatic Members of Lebers Hereditary Optic Neuropathy Pedigrees

By:

Lisa Kleiner-Hoffman

Adviser: Louise Hainline, PhD.

Background: Lebers Hereditary Optic Neuropathy (LHON) is a mitochondrial DNA (mtDNA) disorder where primarily male descendents are at greater risk for near or complete vision loss.

Purpose: Subclinical VEP abnormalities are hypothesized in normal asymptomatic LHON maternal relatives positive for the 11778 mtDNA mutation. Specifically, magnocellular and ON cells are hypothesized to express neurotoxic damage earlier in LHON. Firstly, larger cells, which are more metabolically active, may be more susceptible to compromises in oxidative phosphorylation and the derivative cycling effects of neurotoxicity. Secondly, the magnocellular pathway has been implicated in other disease states such as glaucoma, retinitis pigmentosa, Duchenne muscular dystrophy, and early-onset Alzheimers. The ON pathway has been implicated in other disease states as well, including nocturnal vision deficits, such as melanoma-associated retinopathy and congenital stationary night blindness.

Methods: Classic VEP stimuli and VEP stimuli aimed at probing ON/OFF and M/P specificity were employed. The first stimulus was a steady state spatial frequency (SF) sweep with horizontal square-wave grating patterns with contrast reversals at 7.5 Hz and a square-wave temporal signal. The second involved a conventional 32x32 contrast

reversing checkerboard pattern (15 min checks), and contrast reversals at 1 Hz with a square wave temporal signal to evaluate transient VEP records. The third comprised checkerboard patterns where check size was swept and contrast reversals were modulated by a 1 Hz square wave temporal signal. The fourth employed a sweep through an array of isolated checks of increasing check size, where luminance was modulated sinusoidally in time, either above (positive contrast) or below (negative contrast) the luminance of the static background, producing appearing-disappearing bright or dark checks. The fifth employed a depth of modulation (DOM) sweep varying between 0% to 32% contrast across a 16x16 array of isolated checks in a similar appearance disappearance paradigm.

Results: Results indicated greater amplitude responses, vector mean amplitudes and signal-to-noise ratios in the asymptomatic LHON population as opposed to controls in both dominant and nondominant eyes, in both steady state and transient stimuli and in both the spatial and contrast domains. Significant responses, evaluated by means of a statistical application of magnitude-squared coherence (MSC) revealed greater coherence in the LHON population in the high frequency band correlated with P0, input to the cortex, which is consistent with an increased afferent signal in LHON. Intact and possibly enhanced magnocellular and parvocellular function was evidenced in the majority of LHON individuals. Analysis of an affected LHON individual and an anomalous asymptomatic participant with corroborative evidence of subsequent initial visual abnormalities indicated apparent magnocellular deficits.

Conclusion: Subclinical abnormalities are evidenced in asymptomatic LHON maternal relatives, consistent with a chronic progressive disorder of oxidative stress endemic to mtDNA mutations.

Acknowledgements

With gratitude to G-d for all of His gifts and help in actualizing this goal.

I would like to extend my heartfelt thanks and appreciation to all those who helped and supported me throughout this extensive process:

To Dr. Louise Hainline, who was truly more than a dissertation adviser - thank you for your sage advice, perpetual encouragement, and unfaltering patience. Thank you for having the uncanny ability to know when I needed a prod and when I needed praise. Thank you for being a model of intelligence, efficiency, and capability – always with a smile and positive outlook.

To Dr. Vance Zemon whose patience knew no bounds – thank you for the countless hours spent on data analysis and reanalysis, for sharing your encyclopedic knowledge and for your keen insights into the orphan disease of my dissertation. Most of all, thank you for caring as much about my deadlines as you did for your own.

To Jane Zemon who always welcomed me into her home with a smile – even when I interfered with dinner time and every other time.

To Dr. Jerry Sherman, who not only piqued my interest into the subject area but also imparted a contagious enthusiasm with every breakthrough in the field – thanks for your insight and your uncanny omniscience in the field – where somehow you knew about all current research even before publication.

To Dr. Shlomo Shinnar, whose kindness and friendship are matched only by his brilliance and invaluable insight. Thank you for being a lot more than just my Saturday night adviser.

To Dr. James Gordon and Dr. Daniel Kurylo, my other committee members – thank you not only for your timely reading of the manuscript, and multiple revisions, but more importantly for your critical insights.

To Dr. Elisabeth Brauner who has always been there to ensure that all technical difficulties were smoothed out with as little pain as possible with such grace.

To my brother-in-law, Dr. Simcha Pollack, for all his statistical assistance and more. Thank you for the long hours of programming and analysis and reanalysis and late night-early morning chats about the data. Thank you Debbie, for giving up your husband so graciously.

To my brother, Mendy Kramer, for always being there to assist with the myriad of computer-related and other assorted logistical issues.

To Bruce Benet who would drop everything at a minute's notice to fix endless computer bugs, viruses and crashes - thank you for your time and saintly patience. Bruce, I truly could not have done it without you. Thank you to Danny Wunder who pitched in when Daddy Benet was not around.

To Dr. Robert Tolz who saved me from Trojans and worms that managed to corrupt my files at the 11th hour. To Hopie Burgess for always extending her secretarial proficiency to the wife and family.

To Ron, Debbie, and Rivki Levitan who spent hours decoding corrupted software and personify friendship.

Most importantly, to my family - thank you for your unimaginable patience and encouragement. Thank you for allowing me to be negligent in my other roles in life as mother, daughter, daughter-in-law, sister, sister-in-law, aunt and wife. Thank you for picking up the endless slack in food preparation, running errands, child care, paying the bills etc.

To my beloved children (particularly Miri, Shiri, Tova who suffered the longest) – I love you and am sorry for not always being there when you needed me. For missing out on Mommy- daughter togetherness, for not always being around to pick you up at the train station, for not always having enough time to edit your papers. Thank you for cooking, cleaning and taking care of the babies. Thank you for helping with the spreadsheets. I especially thank you, Tova, for the "togetherness" we shared manipulating graphs and fixing spreadsheets until the sun rose. Thank you Shelly for all the time you spent taking care of the children so that I could get to the computer. Thank you Shimmy for your insight into my EXCEL bugs and how to circumvent them. Thank you all for your empathy and negating your needs in light of mine.

To my parents – thank you for your support for so many years – both financial and emotional. Thank you for not only being my parents but parents to my children as well. You were and continue to be a central force in the girls' lives. Thank you for picking up the endless slack to give me the time and lack of worry to devote to my work. Thank you for the gourmet meals, running errands, taking the girls driving, the shuttle service and the myriad of the tiny details to afford me the time and ability to pursue this dream. Thank you for your open home, but more importantly, for your open hearts.

To Ima and Abba Kleiner – thank you for always being there for us and for the children. Thank you for your love and encouragement and for allowing me to be remiss of some of my familial obligations.

Thank you Mom and Dad Hoffman – thank you for being so close despite the distance. Thank you for your constant love and support. Thank you Daddy David Hoffman for helping to revise the abstract to fit the word requirement and for your helpful edits.

To my dear, beloved husband, Mat – thank you for being both father and mother. Thank you for your belief in me and for your encouragement. Thank you for your support both financial and emotional. Thank you for perpetually helping to make it happen despite my frustration. Thank you for actualizing this dream. "What is mine is truly his."

And finally, to my first husband Chesky (alav hashalom) who initially inspired me to embark on this path. We all love and miss you.

Once again, to my family – thank you all for sustaining me with your love. I love you.

Table of Contents

CHAPTER 1: OVERVIEW **1**

HISTORY AND CLINICAL PRESENTATION 1
MITOCHONDRIAL MUTATIONS 2
HYPOTHESES: SUBCLINICAL VEP ABNORMALITIES 3
Selective Pathway Involvement: Clinical Evidence *3*
Selective Pathway Involvement: Anatomical and Biochemical Evidence *3*
PURPOSE 5

CHAPTER 2: LHON **6**

HISTORY 6
CLINICAL PRESENTATION 9
OPHTHALMOSCOPIC FINDINGS 10
COLOR VISION 11
ELECTROPHYSIOLOGICAL INDICES 12
Electroretinogram Recordings *12*
Pattern Electroretinogram Recordings *13*
Visual Evoked Potential Recordings *14*
Anatomical Imaging *15*
Functional Imaging *17*
EPIDEMIOLOGY 17
ETIOLOGIC DETERMINANTS 18
DIAGNOSIS 21
PRECLINICAL DIAGNOSIS 21
MISDIAGNOSIS 23
ASSOCIATED NEUROLOGICAL FINDINGS 24
Association of LHON and MS *25*
PROGNOSIS 27
HISTOPATHOLOGICAL FINDINGS 28

CHAPTER 3: LHON MITOCHONDRIAL MUTATIONS **31**

MITOCHONDRIA AND OXIDATIVE PHOSPHORYLATION 31
MITOCHONDRIAL MUTATIONS IN LHON 33
BIOCHEMICAL RAMIFICATIONS OF MITOCHONDRIAL MUTATIONS 38
HOMOPLASMY VS HETEROPLASMY 40
EPIGENETIC FACTORS 41
Smoking: Abnormal cyanide metabolism *41*
Multiple Sclerosis *44*
Metabolic Pathogenesis *45*
Cuban Optic Atrophy: Nutritional Pathogenesis *45*
Tobacco/alcohol amblyopias *47*

CHAPTER 4: PHYSIOLOGY OF THE HUMAN VISUAL SYSTEM: RETINOGENICULATE PATHWAY **49**

THE RETINA: 49
GANGLION CELLS 51
LATERAL GENICULATE NUCLEUS 52
VISUAL CORTEX 53
PARALLEL PATHWAYS - ON AND OFF PATHWAYS 53
Retinal Bipolar cells *53*
Ganglion Cells *55*
MAMMALIAN X AND Y PATHWAYS 56
HUMAN MAGNOCELLULAR AND PARVOCELLULAR PATHWAYS 58

The Lateral Geniculate Nucleus ... *62*
Visual Cortex ... *63*

CHAPTER 5: RELATED BIOCHEMISTRY OF THE VISUAL SYSTEM ... 64

FREE RADICALS AND OXIDATIVE DAMAGE ... 64
SELECTIVE NEUROTOXICITY: EXCITATORY AMINO ACIDS ... 68
GLUTAMATE TRANSPORTERS ... 70

CHAPTER 6: VEP ... 74

THEORETICAL OVERVIEW ... 74
HISTORY ... 75
COMPARISON OF ELECTROPHYSIOLOGICAL METHODOLOGIES ... 77
RECORDING THE VEP ... 80
ELECTRODE PLACEMENT ... 80
STIMULI ... 81
Transient VEP ... *81*
Steady-State VEP ... *82*
Swept -Parameter VEP ... *82*

CHAPTER 7: HYPOTHESIS ... 84

METHODOLOGY ... 86

PARTICIPANTS ... 86
PROCEDURES ... 87
EQUIPMENT ... 88
RATIONALE ... 89
STIMULI ... 90
Steady State Spatial-Grating Sweep ... *90*
Transient Contrast reversing checkerboard ... *91*
Transient Checkerboard Sweep ... *92*
Steady State Check size sweep ... *92*
Steady-State VEPs to Isolated-Check Luminance-Contrast Sweeps ... *94*
ELECTRODE PLACEMENT ... 94
VEP RECORDING ... 95
ANALYSIS OF THE VEP ... 95
ESTIMATION OF NOISE IN STEADY-STATE VEPS - T^2_{CIRC} ANALYSIS ... 96
ESTIMATION OF NOISE – MAGNITUDE SQUARED COHERENCE (MSC OR γ^2) ANALYSIS ... 97
ANALYSIS OF THE TRANSIENT VEP ... 99
ANALYSIS OF THE TRANSIENT SWEEP VEP ... 99
ANALYSIS OF THE STEADY-STATE VEP ... 100
ANALYSIS OF THE STEADY-STATE SWEEP VEPS ... 100
STATISTICAL ANALYSIS: ... 101

CHAPTER 8: RESULTS ... 104

NONPARAMETRIC VARIABLES ... 104
WITHIN-SUBJECT-VARIABILITY ... 104
ANALYSIS OF THE STEADY-STATE VEPS TO A GRATING-SPATIAL FREQUENCY SWEEP ... 105
Analysis of Individual Functions and Grating Acuity ... *105*
Analysis of Mean Amplitude Functions ... *107*
Mean Grating Acuity ... *107*
ANALYSIS OF THE TRANSIENT 32X32 CHECKERBOARD ... 108
Analysis of Individual Amplitude and Phase functions: ... *108*
Analysis of Individual MSC ... *110*
Analysis of Group Mean Amplitude ... *111*
Analysis of Group Mean Latency ... *111*

Analysis of Group Mean MSC ... *112*
ANALYSIS OF TRANSIENT VEPS TO A CHECKERBOARD SWEEP ... 113
Analysis of Individual MSC ... *115*
Analysis of Individual Checkerboard Acuity Estimates ... *117*
Analysis of Group Mean Amplitude ... *117*
Analysis of Group Mean Latencies ... *119*
Analysis of Group Mean MSC Values ... *122*
Analysis of Group Mean Checkerboard Acuity Estimates ... *124*
ANALYSIS OF STEADY-STATE VEPS: APPEARANCE-DISAPPEARANCE OF ISOLATED CHECKS ... 125
Analysis of Amplitude: Individual Functions ... *125*
Analysis of Amplitude: Group Mean Functions ... *129*
Analysis of Noise: Individual Functions ... *133*
Analysis of Noise: Group Functions ... *134*
Analysis of SNR: Individual Functions ... *134*
Analysis of SNR: Group Functions ... *137*
Analysis of Phase: Individual Functions ... *139*
Analysis of Phase: Group Functions ... *141*
ANALYSIS OF STEADY-STATE-CONTRAST VEPS: APPEARANCE-DISAPPEARANCE OF ISOLATED CHECKS ... 143
Analysis of Amplitude: Individual Functions ... *143*
Analysis of Amplitude: Group Functions ... *145*
Analysis of Vector Mean Amplitudes: Group Functions ... *147*
Analysis of Noise and SNR: Individual Functions ... *149*
Analysis of Noise and SNR: Group Functions ... *151*
Analysis of Phase: Individual Functions ... *154*
Analysis of Phase: Group Functions ... *157*

CHAPTER 9: DISCUSSION ... 160

SUMMARY OF OVERALL FINDINGS ... 160
Replication of Findings From Prior Experimentation ... *160*
Increased Cortical Signals ... *160*
Selective Pathway Involvement ... *161*
Enhanced OFF Pathway ... 161
Enhanced ON pathway ... 162
Enhanced P Pathway ... *162*
Magnocellular Deficits ... *163*
M Pathway Deficits ... *163*
WITHIN-GROUP VARIABILITY ... 164
TRANSIENT 32X32 CONTRAST REVERSING CHECK ... 165
SPATIAL SWEEP ... 165
LUMINANCE CONTRAST SWEEPS ... 166
ENHANCED MAGNOCELLULAR RESPONSE ... 169
SUPRANORAMAL ERG RESPONSES IN OPTIC NERVE ATROPHY ... 170
HYPOTHESIZED ETIOLOGICAL DETERMINANTS OF THE CURRENT FINDINGS ... 171
ARGUMENTS SUPPORTING THE COMPENSATORY MODEL ... 173
Histopathological Evidence ... *173*
Ophthalmoscopic Evidence ... *175*
Retinal Nerve Fiber Layer ... *175*
ARGUMENTS AGAINST THE COMPENSATORY MODEL ... 178
HYPERTOXICITY AND SELECTIVE PATHWAY INVOLVEMENT ... 179
SUMMARY OF HYPOTHESIZED ETIOLOGICAL PROGRESSION ... 182
LIMITATIONS OF THE CURRENT STUDY: ... 183
FUTURE RESEARCH ... 185
VEP Analyses of Other LHON Mutations ... *185*
Association of LHON and MS ... *185*

Association with DOA and Other Optic Atrophies *186*
Longitudinal Analysis *187*
Inclusion of Parvocellular Specific Stimuli *188*
Prophylactic Intervention Protocols *189*

APPENDIX 1: ASSOCIATION BETWEEN LHON AND MS 191

APPENDIX 2: SECONDARY LHON MTDNA MUTATIONS 193

APPENDIX 3: CLINICAL CASE HISTORIES OF LHON SECONDARY MTDNA MUTATIONS 196

APPENDIX 4: HOMOPLASMY VS. HETEROPLASMY 198

APPENDIX 5: EXCITATORY AMINO ACIDS 203

GLUTAMATE RECEPTORS 204
Iionotropic Glutamate Receptors *204*
Metabotropic Receptors *205*

APPENDIX 6: METABOLIC INHIBITION AND MEMBRANE POTENTIAL 207

APPENDIX 7: CONSENT FORMS 209

APPENDIX 8: FUTURE RESEARCH 215

METABOLIC BYPASS THERAPIES 215
MINOXIDIL 218
NEUROPROTECTIVE AGENTS 218
GENE THERAPY 222

REFERENCES 225

List of Illustrations and Charts

Figure 1: Fundus photos indicating telangiectatic microangiopathy and vascular tortuosity in an asymptomatic LHON individual positive for the 11778 mtDNA mutation prior to disease onset. 11

Figure 2a: Simple organization of the retina Figure 2b: 3-D Block of a segment of human retina. Reprinted with permission from: Kolb, H., Fernandez, E., and Nelson, R. (2005) http:// webvision.med.utah.edu. 51

Figure 3: Golgi staining of human ganglion cells in central retina. Reprinted with permission from: Kolb, H., Fernandez, E., and Nelson, R. (2005) http:// webvision.med.utah.edu. 62

Figure 4: The projections of the small P, and large M ganglion cells from the two eyes to parvocellular and magnocellular layers of the LGN respectively. Reprinted with permission from: Kolb, H., Fernandez, E., and Nelson, R. (2005) http:// webvision.med.utah.edu. 62

Figure 5a: Classic grating stimulus Figure 5b: Classic checkerboard pattern 92

Figure 6: Appearance (left) and Disappearance (right) checkerboard stimulus patterns..... 93

Figure 7: T^2_{circ} analysis: The T^2_{circ} statistic, applied to this vector model, calculates a circular 95% confidence region around the mean amplitude and phase. The T^2_{circ} value is the calculated distance (radius) from the tip of the vector to any point on the circular confidence region. The length of the vector divided by the radius yields the SNR for the 95% confidence region. A SNR of one, obtained when the length of the radius is equal to the vector, indicates that the circular confidence region touches the origin. A SNR above one indicates a response out of noise, whereas a SNR below one indicates a response embedded in noise where the circular confidence region encompasses the origin. Criterion was therefore, the interpolation of SNR equal to one. 97

Figure 8: Second harmonic amplitude and phase values for a control. An acuity estimate was obtained through linear interpolation between two successive steps to a signal-to-noise ratio of one..... 106

Figure 9: Second harmonic amplitude and phase values for LHON individuals. Acuity estimates were obtained through linear interpolation between two successive steps to a signal-to-noise ratio of one. 106

Figure 10: Mean amplitude measurements for both LHON individuals and controls given stimulation of both dominant (left) and nondominant (right) eyes. Error bars indicate ± 1 SEM. 107

Figure 11: Mean grating acuities measured in cycles/degree given stimulation of the dominant (left) and nondominant (right) eyes in asymptomatic LHON individuals and controls. Error bars indicate ± 1 SEM. 108

Figure 12: VEP trace from a control reflecting the normal amplitude and latency measurements elicited from the transient 32x32 contrast reversing checkerboard..... 108

Figure 13: VEP trace from an asymtomatic LHON individual reflecting amplitude and latency measurements elicited from the transient 32x32 contrast reversing checkerboard. Note the significantly higher amplitude and the normal latencies. 109

Figure 14: VEP trace from an asymtomatic LHON individual reflecting amplitude and latency measurements elicited from the transient 32x32 contrast reversing checkerboard. Note the low P100 associated with magnocellular input to the cortex and the significantly higher amplitude of the subsequent positive wave associated with parvocellular input to the cortex. 109

Figure 15: Decreased amplitude and increased latency measurements were obtained from the anomolous asymtomatic LHON individual from the transient 32x32 contrast reversing checkerboard. 109

Figure 16a: MSC values plotted for even frequency components between 2 and 50 Hz. in a normal control. The critical value for individual harmonics is 0.28. Figure 16b: Pooled MSC values plotted for low, middle and high frequency components. Low frequencies include 4-12 Hz., middle frequencies include 14-26 Hz. and high frequencies include 28-42 Hz. The critical value 0.174 for low frequencies, 0.162 for middle frequencies and 0.158 for high frequencies. 110

Figure 17a: MSC values plotted for even frequency components between 2 and 50 Hz. in an asymptomatic LHON individual. The critical value for individual harmonics was 0.28. Figure 17b: Pooled MSC values plotted for low, middle and high frequency components. Low frequencies included 4-12 Hz., middle frequencies included 14-26 Hz. and high frequencies included 28-42 Hz. The critical value was 0.174 for low frequencies, 0.162 for middle frequencies and 0.158 for high frequencies. 110

Figure 18: Mean amplitudes from the transient 32x32 contrast reversing checkerboard in the dominant (left) and nondominant (right) eyes in both asymptomatic LHON individuals and controls. Error bars indicate ± 1 SEM. 111

Figure 19: Mean latencies elicited from the transient 32x32 contrast reversing checkerboard in the dominant (left) and nondominant (right) eyes in asymptomatic LHON individuals and controls. Error bars indicate ± 1 SEM. 112

Figure 20: Mean magnitude squared coherence values for low, medium and high frequency bands elicited from the transient 32x32 contrast reversing checkerboard stimulus given stimulation of the dominant (left) and nondominant eyes (right) in asymptomatic LHON individuals and controls. Error bars indicate ± 1SEM. 113

Figure 21: Individual amplitude and latency functions for each checkerboard size in the transient sweep for a control (left) and a LHON individual (right). Note the higher amplitudes in the LHON individual even at high spatial frequencies..... 114

Figure 22: Magnitude squared coherence for a control (dominant eye) for each checkerboard size within the sweep. The left set of graphs plots MSC for each even harmonic until 50 Hz. The critical value for individual harmonics was 0.28. The right set of graphs pooled the low (4-12), middle (14-26) and high (28-42) frequency harmonics. The critical value was 0.174 for low frequencies, 0.162 for middle frequencies and 0.158 for high frequencies. 115

Figure 23: Magnitude squared coherence for a LHON individual (dominant eye) for each checkerboard size within the sweep. The left set of graphs plots MSC for each even harmonic until 50 Hz. The critical value for individual harmonics was 0.28. The right set of graphs pooled the low (4-12), middle (14-26) and high (28-42) frequency harmonics. The critical value was 0.174 for low frequencies, 0.162 for middle frequencies and 0.158 for high frequencies... 116

Figure 24: MSC values for a control (dominant eye) as a function of spatial frequency for low, middle and high frequencies. Checkerboard acuity estimates were calculated via extrapolation of the MSC function to the critical value. Bias (solid line) was 0.1 and the critical value (dashed line) was 0.174 for low frequencies, 0.162 for middle frequencies and 0.158 for high frequencies. 117

Figure 25: MSC values for a LHON individual (dominant eye) as a function of spatial frequency for low, middle and high frequencies. Checkerboard acuity estimates were calculated via extrapolation of the MSC function to the critical value. Bias (solid line) was 0.1 and the critical value (dashed line) was 0.174 for low frequencies, 0.162 for middle frequencies and 0.158 for high frequencies..... 117

Figure 26: Amplitude measures from the transient checkerboard sweep through incremental check sizes given stimulation of the dominant (left) and nondominant eyes (right) in asymptomatic LHON individuals and controls. Error bars indicte ± 1 SEM. 119

Figure 27: Mean latency values from the transient checkerboard sweep through incremental check size given stimulation of the dominant (left) and nondominant (right) eyes in asymptomatic: LHON individuals and controls. Error bars indicate ± 1SEM. 121

Figure 28: Mean magnitude squared coherence values of the low, middle and high frequency components from the transient checkerboard sweep through incremental check size given stimulation of both the dominant (left) and nondominant (right) eyes in asymptomatic LHON individuals and controls. Error bars indicate ± 1 SEM. 123

Figure 29: Checkerboard acuities measured in cycles/degree for low, medium and high frequency components, obtained from the transient checkerboard sweep in the dominant (left) and nondominant (right) eyes in asymptomatic LHON individuals and controls. Error bars indicate ± 1 SEM. 125

Figure 30: Individual amplitude plotted as a function of incremental check number from a spatial sweep of isolated bright and dark checks in the dominant (top 2 sets) and nondominant (bottom 2 sets) eyes of asymptomatic LHON individuals (left), controls (right), and one LHON affected individual with recovery of visual function (left). The amplitude function for the affected LHON individual is depicted in all graphs with a dashed line. Error bars indicate ± 1 SEM. 129

Figure 31: Mean amplitude as a function of incremental check number from a spatial sweep of isolated bright (left) and dark (right) checks in the dominant (top) and nondominant (bottom) eyes of asymptomatic LHON individuals and controls. Error bars indicate ± 1 SEM. 131

Figure 32: Individual signal-to-noise-ratios plotted as a function of incremental check number from a spatial sweep of isolated bright and dark checks in the dominant (top 2 sets) and nondominant (bottom 2 sets) eyes of asymptomatic LHON individuals (left), controls (right), and one LHON affected individual with recovery of visual function (left). The SNR function for the affected LHON individual is depicted in all graphs with a dashed line. SNR values below criterion indicate ratios indistinguishable from noise. Error bars indicate ± 1 SEM .. 136

Figure 33: Mean signal-to-noise ratios as a function of incremental check number from a sweep employing isolated bright (left) and dark (right) checks given stimulation of both the dominant (top) and nondominant (bottom) eyes of asymptomatic LHON individuals and controls. SNR values below criterion indicate ratios indistinguishable from noise. Error bars indicate ± 1 SEM. 138

Figure 34: Individual phase plotted as a function of incremental check number from a spatial sweep of isolated bright and dark checks in the dominant (top 2 sets) and nondominant (bottom 2 sets) eyes of asymptomatic LHON individuals (left), controls (right), and one LHON affected individual with recovery of visual function (left). The phase function for the affected LHON individual is depicted in all graphs with a dashed line. 141

Figure 35: Mean phase as a function of incremental check number from a sweep employing isolated bright (left) and dark (right) checks in the dominant (top) and nondominant (bottom) eyes of asymptomatic LHON individuals and controls. Error bars indicate ± 1 SEM. 142

Figure 36: Individual amplitude plotted as a function of incremental depth of modulation (% contrast) from a contrast sweep of isolated bright and dark checks in the dominant (top 2 sets) and nondominant (bottom 2 sets) eyes of asymptomatic LHON individuals (left), controls (right), and one LHON affected individual with recovery of visual function (left). The amplitude function for the affected LHON individual is depicted in all graphs with a dashed line. 144

Figure 37: Mean amplitude as a function of incremental depth of modulation (% contrast) from a contrast sweep employing isolated bright (left) and dark (right) checks in the dominant (top) and nondominant (bottom) eyes of asymptomatic LHON individuals and controls. Error bars indicate ± 1 SEM. 146

Figure 38: Vector mean amplitude as a function of incremental depth of modulation (% contrast) from a contrast sweep employing isolated bright (left) and dark (right) checks in the dominant (top) and nondominant (bottom) eyes of asymptomatic LHON individuals and controls. Error bars indicate ± 1 SEM. 148

Figure 39: Individual signal-to-noise-ratios plotted as a function of incremental depth of modulation (% contrast) from a contrast sweep of isolated bright and dark checks in the dominant (top 2 sets) and nondominant (bottom 2 sets) eyes of asymptomatic LHON individuals (left), controls (right), and one LHON affected individual with recovery of visual function (left). The SNR function for the affected LHON individual is depicted in all graphs with a dashed line. SNR values below criterion indicate ratios indistinguishable from noise. 151

Figure 40: Mean signal-to-noise ratios as a function of incremental depth of modulation (% contrast) from a sweep employing isolated bright (left) and dark (right) checks in the dominant (top) and nondominant (bottom) eyes of asymptomatic LHON individuals and controls. SNR values below criterion indicate ratios indistinguishable from noise. Error bars indicate ± 1 SEM. .. 153

Figure 41: Individual phase plotted as a function of incremental depth of modulation (% contrast) from a contrast sweep of isolated bright and dark checks in the dominant (top 2 sets) and nondominant (bottom 2 sets) eyes of asymptomatic LHON individuals (left), controls (right), and one LHON affected individual with recovery of visual function (left). The phase function for the affected LHON individual is depicted in all graphs with a dashed line. 156

Figure 42: Mean phase as a function of incremental depth of modulation (% contrast) from a sweep employing isolated bright (left) and dark (right) checks in the dominant (top) and nondominant (bottom) eyes of asymptomatic LHON individuals and controls. Error bars indicate ± 1 SEM. 157

Figure 43: Vector mean phase as a function of incremental depth of modulation (% contrast) from a sweep employing isolated bright (left) and dark (right) checks in the dominant (top) and nondominant (bottom) eyes of asymptomatic LHON individuals and controls. Error bars indicate ± 1 SEM. 158

Chapter 1: Overview

History and Clinical Presentation

Historically, Leber's Hereditary Optic Neuropathy has been described as an acute or subacute disease resulting in a characteristic sudden, painless bilateral loss of central vision, and ultimately in the formation of central scotomata (Lundsgard, 1944; Newman et al. 1991; Nikoskelainen et al. 1987, 1985). Risk of disease expression is predominant in males (Nikoskelainen et al., 1987; Seedorff 1970; van Senus 1963; Lundsgard 1944), with onset of visual dysfunction typically occurring between the ages of 18 and 30 (Carroll & Mastaglia, 1979; Imachi, 1967; Taylor & Holmes, 1913). Visual deterioration is extreme, with visual acuities often plummeting to worse than 20/200 in each eye (Newman et al., 1991; Nikoskelainen et al., 1983, 1977; Carroll & Mastaglia, 1979; Smith et al., 1973).

Classic, early ophthalmoscopic findings in LHON include a glistening opacity of the peripapillary nerve fiber layer due to dilation of the ganglion cell axons, blurred disc margins, telangiectatic microangiopathy, disk pseudoedema, and vascular tortuosity. Fundus findings indicate a gradual progression toward ultimate disc pallor, reflective of the associated optic nerve atrophy. The atrophy in the papillomacular fibers result in the temporal pallor observed a few months after the initial expression of the clinical symptomology. Progression of the clinical course results in the attenuation of retinal vessels and a resultant atrophy that may include the whole nerve fiber.

Mitochondrial Mutations

Recent advances in the field of molecular genetics have yielded insights into the etiological determinants underlying the clinical expression of LHON. Whereas the nuclear genome has been implicated in most inherited diseases, LHON has been associated with mutations in the mitochondrial genome.

To date, twelve mutations have been identified, the most common of which is the primary 11778 mutation. Mutations at nts 3460, 4160, 11778, and 15257 and 14484, designated as class I mutations, are considered high risk for they can occur singly in an LHON pedigree, and probands harboring these mutations have a higher probability for blindness than probands harboring any of the other mutations. Mutations at nts 4216, 4917, 5244, 13708, and 15812, designated as class II mutations, are considered low risk for they generally present in combination with another mutation, and the probability for experiencing blindness is comparatively low for individuals harboring a single class II mutation.

The current supposition from the literature is that the mtDNA mutations establish a risk for developing the optic neuropathy at a specific frequency, i.e. the penetrance of the disease. Specifically, a synergistic interaction of primary mtDNA mutations with other primary or secondary mutations establishes a degree of oxidative stress (Johns et al, 1991, 1992). The risk of disease expression is mediated by both genetic and epigenetic factors, including potential nuclear encoded factors (Vilkki et al, 1991; Brown et al., 1992b), which may either increase the risk of penetrance and/or exacerbate the underlying dysfunction, or decrease the risk of penetrance and/or ameliorate the disease process (Howell et al, 1991a). This is also consonant with the strong male bias, the strict

tissue specificity, reduced penetrance, the later age of onset for females, and the delayed expression of the disease suggesting that LHON cannot be explicated with a single mitochondrial gene defect.

Hypotheses: Subclinical VEP Abnormalities

Endemic to mtDNA mutations is the axiom of oxidative phosphorylation (OXPHOS) compromise which renders the biological system more vulnerable to excitatory amino acid (EAA) toxicity. Although the exact mechanism of neurotoxicity is not established, subclinical VEP abnormalities are hypothesized in LHON, as with other mitochondrial diseases which express selective impairments.

Selective Pathway Involvement: Clinical Evidence

The juxtaposition of visual impairment in LHON with evidence of both normal pupillary responses (Sherman & Kleiner, 1994) and normal Critical Fusion of Photic Driving (CFPD) values (Kothe et al, 1990) in at least some LHON patients, has led to the hypothesis of selective pathway involvement in LHON. Specifically, selective damage to the pathway synapsing at the LGN is postulated, whereas the pupillary pathways to the midbrain remain primarily intact in LHON. Similarly, the CFPD may correspond with a pathway that synapses at the brainstem primary visual nuclei, as opposed to the LGN, and then projects to the occipital cortex (Rodieck, 1979).

Selective Pathway Involvement: Anatomical and Biochemical Evidence

Analysis of the variability in the regulation of excitatory amino acid (EAA)

reuptake both by endogenous and exogenous variables has led to a derivative postulate of selective vulnerability and ultimate apoptotic outcome in different neuronal populations (Fletcher & Johnston, 1991). The cells most sensitive to glutamate hypertoxicity, namely amacrine and bipolar cells (Brandstatter, 1994), may be more easily predisposed to neurotoxic damage. Hence, subclinical abnormalities in the M/P and ON/OFF responses in LHON probands may be able to be detected in their VEP signals due to the oxidative compromise in the presynaptic amacrine and bipolar cells.

M/P and ON/OFF pathway involvement cannot be hypothesized as a result of differential hypertoxic outcomes. Specifically the relative amplitudes of M/P responses to NMDA and non-NMDA agonists are similar across all cell types. Similarly, research has not implicated a selective predisposition in the ON/OFF pathway for neurotoxic damage. On the one hand, research has shown that the ON bipolar cell appears uniquely vulnerable. For example, the mGluR6 receptor can be selectively removed via selective pharmacological blocking agents (i.e., APB) or site directed mutagenesis techniques designed to eliminate the mGluR6 receptors, without major effect on other neural pathways. On the other hand, the extracellular recordings from ON/OFF and X/Y ganglion cell types were most transient in OFF cells with the application of PTX, native BCC, or BCC MeBr (Frumkes et al., 1995).

Selective pathway involvement is thus hypothesized as a derivative outcome of a faulty oxidative phosphorylation (OXPHOS) system affecting larger cell types, like magnocellular and ON cells, believed to be more metabolically active. Furthermore, the magnocellular pathway has been implicated in other disease states such as glaucoma (Greenstein et al., 1998), retinitis pigmentosa (Alexander et al., 2005), schizophrenia

(Butler et al., 2001; 2005), Duchenne muscular dystrophy, and early-onset Alzheimers. Nocturnal vision deficits, such as melanoma-associated retinopathy (Alexander et al., 1992; Berson and Lessell, 1988) and congenital stationary night blindness (Alexander et al., 1992) appear dependent on the physiological integrity of ON bipolar cells.

Purpose

Evidence supporting abnormalities in the VEP recording prior to presentation of symptomology in LHON (Mondelli et al, 1991; Walsh 1985; Sherman, 1984; Carroll & Mastaglia, 1979) renders the VEP a possible preclinical indicator of this chronic progression before disease onset. Therefore, the current VEP protocol investigated asymptomatic individuals genetically positive for the 11778 LHON mutation for subclinical abnormalities in the VEP both in terms of the magnitude of the responses and selective ON/OFF and M/P pathway involvement.

The ensuing chapters develop this background research in greater depth followed by the detailed methodology and results of the VEP protocol that was undertaken with the LHON sample. It is my hope that this methodology will enable the clinician to identify individuals who might progress into an active state of disease. Prophylactic intervention protocols could then be employed to arrest disease progression to a state of near or complete vision loss.

Chapter 2: LHON

This chapter describes the history, clinical presentation, mtDNA diagnostic criteria, histopathology, past research and potential future research in LHON. Historically, LHON was believed to present clinically in an acute stereotypical presentation with devastating visual ramifications. However, its variable and oftentimes bizarre clinical symptomology, variable associated neurological complications and a maternal inheritance pattern with an atypical male predilection has yielded a myriad of etiological hypotheses. Modern genetic technology has established LHON as a mtDNA disorder with variable penetrance as of 1988. This has opened the field to molecular biological and pathophysiological research that attempts to analyze the complex etiological determinants of this disease.

History

In 1871, Theodor Leber accurately described the clinical features of a nosologically distinct form of optic atrophy with its unique pattern of inheritance. This eponymous disease has been recognized as a familial optic neuropathy since its categorical inception. Moreover, it is precisely this strict maternal inheritance that had helped to differentiate LHON from other forms of optic atrophies prior to the more recent molecular diagnostic techniques. Furthermore, LHON has been notorious for the inherent variability in its clinical course and permutations thereof, both between and within familial pedigrees. Albeit, multiple large pedigrees throughout the world have been analyzed, the clinical reports of this disorder overall, remain consonant with the original, classic description.

LHON has been the source of much controversy in the creation of eclectic hypotheses whose aim was to discover its elusive etiology. The enigmatic pattern of inheritance yielded the very early hypothesis of cytoplasmic transmission of an X- linked recessive trait (Imai & Moriwaki, 1936; Went, 1963, 1964). However, the inheritance patterns were inconsistent with a classic X-linked inheritance pattern. Specifically, the incidence of affected males did not proportionally decrease in subsequent generations and the occurrence in females was higher than is expected for a true X-linked inherited disorder (Miller, 1982).

Initially, postulates of a slow virus-like transfer via maternal ooplasm or transplacentally (Asseman et al., 1989; Rogers, 1977) were investigated (Harper, 1977; Erikson, 1976; Francois, 1968; Colenbrander, 1962; Ronne, 1944; Imai & Moriwaki, 1936), based on reports of the similarity of LHON to some slow virus diseases (Wallace, 1970). This postulate relied on the supposition of cytoplasmic transmission of the virus-like agent in the non-nuclear substance of the ovum (Carroll & Mastaglia, 1979). Hence, the failure of paternal transmission might have resulted from the small percentage of cytoplasm in the zygote (about 1%) derived from the spermatozoon (Fine, 1977). However, serological investigations have yielded negative results and have been unable to identify any viruses that play a precipitating role in the pathogenesis of LHON (van Gemert & Versteeg, 1989).

Hypotheses of environmental etiologies such as tobacco smoking (Wilson, 1965), nutritional deficiencies (Denny-Brown, 1947), and excessive alcohol use (Cullom et al., 1993) have also been postulated.

Mitochondrial inheritance was later hypothesized on the basis of the maternal transmission of mtDNA to the fetus (Nikoskelainen et al., 1987, 1984b, c; Novotny et al., 1986; Egger & Wilson, 1983; Fine, 1978). Extensive data confirm that not only is LHON never transmitted via the paternal lineage (Carroll & Mastaglia, 1979; Krill, 1977), but also that every sibling of an affected carrier inherits the trait (Nikoskelainen et al., 1987; van Senus, 1963). Mitochondrial transmission supports the purely maternal inheritance pattern characteristic in LHON due to the fact that mtDNA is transmitted exclusively from the cytoplasm of the ovum (Phillips & Gosden, 1991). The observation of enlarged subsarcolemmal mitochondria in LHON probands further supported this postulate of mitochondrial inheritance (Nikoskelainen et al., 1984b, c).

Whereas the nuclear genome has been implicated in most inherited diseases, genetic analysis has established that LHON is determined by mutations in the mitochondrial genome. This, however, was not established until a century after Leber's original report.

Unfortunately, the sophistication obtained through modern genetic diagnostic techniques and the research investigating the myriad of potential etiologies has not yet afforded a comprehensive understanding of the intricacies involved in the expression of LHON. More importantly, it is perhaps this lack of knowledge that is impeding on our most important criteria and ultimate goal - an effective therapeutic intervention and cure.

Clinical Presentation

LHON has historically been described as an acute or subacute disease resulting in a characteristic sudden, painless bilateral loss of central vision, and ultimately in the formation of centrocecal scotomata (Lundsgard, 1944; Newman et al. 1991; Nikoskelainen et al. 1987, 1985). Generally, vision loss is sequential, with involvement of the second eye occurring weeks to months after the first (Nikoskelainen et al., 1986; Wallace, 1970). This asymmetric involvement of the second eye has been observed even after prolonged intervals, reportedly up to eight years after initial vision loss (Taylor & Holmes, 1913). Accounts of both simultaneous involvement (Newman et al., 1991; Johns, 1990; Berninger et al., 1989; van Senus, 1963) and monocular involvement (Nikoskelainen et al., 1983; Carroll & Mastaglia, 1979; Wallace, 1970) have also been reported.

The onset of clinical visual dysfunction usually occurs between the ages of 18 and 30 (Carroll & Mastaglia, 1979; Imachi, 1967; Taylor & Holmes, 1913), yet it has been observed in a male as late as 70 years (Seedorf, 1985). Unpublished data extend this range from age 3 to age 80 (personal communication, Johns, 1993). The duration of vision loss is variable with reported stabilization after days, weeks, or months (Newman et al., 1991; Nikoskelainen et al., 1983, 1977; Carroll & Mastaglia, 1979; Bird & McEachern, 1949).

Visual deterioration is extreme, with visual acuities often plummeting to worse than 20/200 in each eye, with light perception not an uncommon remnant of a once versatile visual system (Newman et al., 1991; Nikoskelainen et al., 1983, 1977; Carroll & Mastaglia, 1979; Smith et al., 1973). Most clinical cases have described its rapid course

of visual deterioration, with the exception of Nikoskelainen et al. (1977) who have reported cases of slow and insidious visual loss.

Uhthoff's phenomenon, a transient form of visual deterioration due to exercise or metabolic warming most common in demyelinating disease, has also been observed occasionally in LHON (Newman et al., 1991; Miller, 1982; Nikoskelainen et al., 1977).

Ophthalmoscopic Findings

Classic, early ophthalmoscopic findings in LHON include a glistening opacity of the peripapillary nerve fiber layer due to dilation of the ganglion cell axons, blurred disc margins, telangiectatic microangiopathy, disk pseudoedema, and vascular tortuosity. In the acute phase, fluorescein angiography indicates an absence of leakage from the vessels around the disc margin reflective of the disc psuedoedema characteristic in LHON (Nikoskelainen et al., 1984a; Rogers, 1977; Smith et al., 1973), in contrast to true disc leakage resulting from other sources such as papillitis and papilloedema. There have been reports however, of flame-shaped hemorrhages on the disc and the surrounding retina (Miller et al., 1982; Krill, 1977). Peripapillary arteriovenous shunting, most commonly demonstrated infero-temporal to the disc in the acute phase, has not been demonstrated in the early phase, suggesting that AV shunting may be a useful index for preclinical diagnosis (Nikoskelainen et al., 1984c). Disc atrophy, which may affect the entire disc (Berninger et al., 1989), beginning between 2 and 4 weeks after the initial onset of visual deterioration, tends to be temporal. Maximum disability has been reported to occur within days (Miller et al., 1982; Smith et al., 1973), and tends not to deteriorate further beyond 6 months (Perkin et al., 1979; Duke-Elder et al., 1971). Visual

fields commonly reveal a relative or absolute centrocecal scotoma (Newman, 1991; Nikoskelainen et al., 1984, 1977; Berninger et al., 1989).

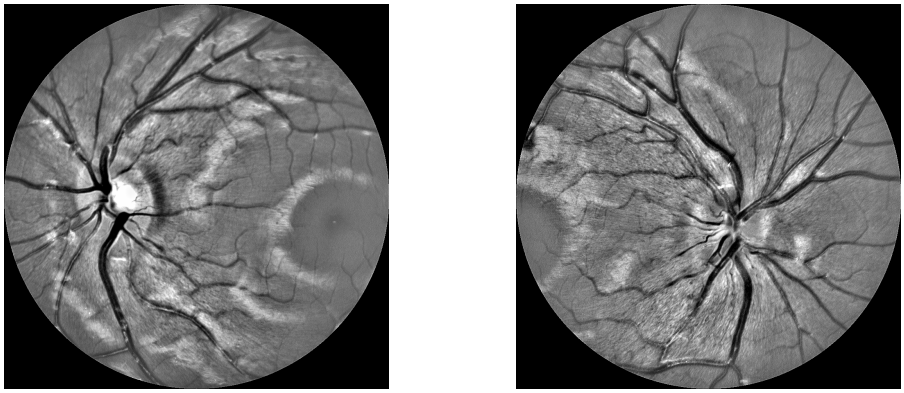

Figure 1: Fundus photos indicating telangiectatic microangiopathy and vascular tortuosity in an asymptomatic LHON individual positive for the 11778 mtDNA mutation prior to disease onset.

Fundus findings indicate a gradual progression toward ultimate disc pallor, reflective of the associated optic nerve atrophy. The atrophy in the papillomacular fibers result in the temporal pallor observed a few months after the initial expression of the clinical symptomology. Progression of the clinical course results in the attenuation of retinal vessels and a resultant atrophy that may include the whole nerve fiber. The microangiopathy disappears completely (Berninger et al., 1989) and the optic atrophy, occasionally with evidence of cupping (Trobe et al., 1980) or arteriolar attenuation (Nikoskelainen et al., 1983), is often the only funduscopic signs that remain.

Color Vision

Color vision alterations, most commonly assessed by means of the Farnsworth-Munsell 100 (FM-100) hue test, reveal dyschromatopsia in all three axes (Livingstone et al., 1980; Gittinger et al., 1979; Nikoskelainen et al., 1977) in affected LHON probands.

Color vision abnormalities tend to be synchronous with visual acuity deterioration (Krill, 1977), yet more interestingly, have also been reported to precede acuity deterioration in asymptomatic individuals (Miller, 1982; Livingstone et al., 1980; Nikoskelainen et al., 1977). The most common dyschromatopsia is in the principal axis of deuteranopia or is intermediate between deuteranopia and protanopia (Francois, 1968). Color vision abnormalities have also been reported in female carriers, predominantly indicating a tritan defect (Mueller-Jensen et al., 1978).

FM-100 hue color vision tests performed on 91 members of a giant Brazilian LHON pedigree spanning seven generations, revealed color vision defects in 27 of 55 carriers (49.1%) in one or both eyes (Quiros et al., 2003). 13 of the 27 (48%) indicated tritan defects, the remaining 14 (52%) indicated deutan defects, and 9 of the 27 (33%) were identified with bilateral defects. These findings of abnormalities in asymptomatic carriers is consistent with the current view that LHON is not a disease characterized by a sudden devastating vision loss, but rather a chronic progressive disease with subtle abnormalities which given the appropriate genetic and epigenetic milieu may cascade into the devastating vision loss.

Electrophysiological Indices

Electroretinogram Recordings

Electroretinogram (ERG) recordings, reflecting activity of the photoreceptors and the bipolar cell layer, and electrooculogram (EOG) recordings, reflecting activity of the retinal pigment epithelium, tend to remain intact (Berninger et al., 1989; Lessell et al., 1983; Syme et al., 1983; Smith et al., 1977). A recent ERG investigation with four

members from a newly discovered extensive Brazilian family with the 11778A mutation revealed normal rod and cone ERG responses in two affected members. However, one unaffected female and one affected male showed reduced amplitude for both single-flash cone response and 30 Hz flicker with normal *b*-wave latencies, suggesting that LHON can also affect retinal elements, even preceding fundus changes (Salomao et al., 2002).

Pattern Electroretinogram Recordings

Unlike the flash ERG which clearly has its origin in the photoreceptor layer (the *a* wave) and the bipolar cell layer (the *b* wave), the origin of the pattern electroretinogram (PERG) remains controversial. Research has demonstrated in cats that the pattern ERG was generated by the ganglion cell layer since the pattern ERG was lost after sectioning of the optic nerve (Maffei & Fiorentini, 1981). However, research with clinical correlates revealed that the PERG could still be recorded after total nerve atrophy (Sherman, 1986, 1982). Recently it has been postulated that the P-50 component of the PERG arises from preganglionic elements while the N-95 component arises from the ganglion cells and their axons which comprise the optic nerve.

PERG data from LHON patients reveal a normal positive (P-50) component, indicating the preservation of the retinal mechanism responsible for contrast sensitivity (Berninger & Schuurmans, 1985b). However, there is evidence for the complete extinction of the negative (N-95) component, a finding compatible with other optic nerve diseases (Ryan & Arden, 1988; Berninger & Schuurmans, 1985b).

Visual Evoked Potential Recordings

VEP recordings, which measure the integrity of electrical conduction from the retina to the occipital cortex, are desynchronized with a reduction in peak amplitude and prolonged latencies to spatial stimuli in the early stages of the disease (Mashima et al., 1997; Walsh, 1985; Halliday, 1982; Livingstone et al., 1980). With the progression of the disease, the VEP deteriorates to the point of extinction (Walsh, 1985). However, although mean amplitudes from flash VEP (FVEP) stimuli were reduced in patients with LHON, the mean latency was not delayed in patients with LHON as compared with normal subjects or patients with optic neuritis (ON) (Mashima et al., 1997). Therefore, spatial-vision-related fibers may be preferentially affected over luminance-related fibers in early LHON.

VEP abnormalities have been reported in both the asymptomatic eyes of some patients diagnosed with LHON (Mondelli et al., 1991; Walsh 1985; Sherman, 1984; Carroll & Mastaglia, 1979), as well as in asymptomatic patients at risk for developing the disease (Salomao et al., 2003; Livingstone et al., 1980; Carroll & Mastaglia, 1979). Transient pattern-reversal VEPs were monocularly recorded from the asymptomatic members of a large Brazilian 11778 pedigree with 20/20 corrected visual acuity (Salomao et al., 2003). Statistically prolonged latencies were found in carriers with stimulus size 15’ for the P100 and N135 components, and with stimulus size 60’ for the N135 component as well. Furthermore, prolonged latencies were also seen with stimulus size 60’ for the N75 component in the descendents of affected males as compared to the descendents of non-affected males.

Steady-state pattern reversal VEP recordings reveal waveforms with irregular morphology and the absence of correlative periodicity. Morphological distortions for transient pattern reversal VEP recordings, typically a double positive peak, correlate with the delays in VEP recordings characteristic of LHON (Kothe et al., 1990; Halliday et al., 1979; Dorfman et al., 1977; Halliday, 1976). The presence of a central scotoma has been associated with this positive-negative-positive (PNP) component. However, this has been refuted by the claim that similar PNP components were seen in patients with autosomal dominant optic atrophy, a condition with no measurable scotoma (Flanagan & Harding, 1986; Harding & Crews, 1982; Miller et al., 1982).

Anatomical Imaging

Magnetic resonance imaging (MRI) data of patients at different stages of LHON progression have yielded contradictory findings. Whereas some reports indicate no significant abnormalities of the optic nerve signal characteristic of LHON (Dotti et al., 1992), investigators who employed short time inversion recovery (STIR) sequences to image the optic nerve, report increased signals in the mid and posterior intraorbital sections. These increases have been attributed to possible gliosis in the chronic phase and, perhaps, edema in the acute phase (de Gottrau et al., 1992; Wilson, 1992; Kermode et al., 1989).

High-resolution microMRI was employed to examine the three dimensional images of the optic nerve in a 75 year old asymptomatic LHON individual positive for the 3460 mtDNA mutation. Axonal bundles were atrophic and the pial-collagen septae markedly thickened. The entire nerve had shrunk, creating space under the arachnoid,

down and around the central ophthalmic artery and vein (Sadun et al., 2002). These types of atrophic lesions, normally visible only by histopathologic examination, were visualized in the Lebers optic nerve, rendering microMRI a potentially useful clinical tool in the visualization of lesions in or about the optic nerve in vivo.

Magnetization transfer imaging (MTI) and diffusion tensor (DT) MRI was employed to investigate the integrity of the optic radiations and calcarine cortex in LHON patients (Inglese et al., 2001). No abnormalities were detected in the MT ratio (MTR), average diffusivity (D), and fractional anisotropy (FA) values for the white matter of the optic radiations and MTR and D values for the calcarine cortex both on a macroscopic and microscopic level.

The severity of optic nerve damage and the presence and extent of macroscopic and microscopic pathology in the brain and cervical cord was assessed in LHON and LHON-MS patients using MRI and MTI and MRI, MTR and mean diffusivity (D) histogram analysis respectively (Inglese et. al, 2001). Results indicated that the mean values of optic nerve volumes, MTR values and normal appearing brain tissue (NABT) – MTR histogram peak height were significantly lower in LHON patients than in healthy controls, and lower still in patients with LHON-MS than in those with only LHON.

Retinal nerve fiber layer (RNFL) measurements were obtained from a large Brazilian LHON pedigree, haplogroup J, with the 11778 mtDNA mutation (Sherman, et al., 2003). About half of the 200 members evaluated were LHON-carriers, 20 were LHON-affected, and the remainder was off-pedigree. With one exception, all LHON-affected participants had profound and quite symmetric RNFL loss with more profound atrophy correlated with longer durations of vision loss. All LHON-carriers had normal or

nominally reduced RNFL measurements that often corresponded to minor field defects and Tritan-axis dyschromatopsia, perhaps an indication of the chronic progressive nature of the disease. All off-pedigree participants had normal RNFL measurements. In LHON, functional vision loss precedes structural RNFL loss as measured with the GDx, with apparent gradual loss for the first year with a slow, progressive deterioration for at least a decade with eventual, profound and symmetric RNFL reduction.

Functional Imaging

Phosphorus-31 magnetic resonance spectroscopy (31P-MRS) has indicated impaired mitochondrial metabolism in muscle limbs and in the occipital lobes (decreased PCr/Pi ratios) of LHON probands (Cortelli et al., 1991). Although indices of brain energy metabolism on 31P-MRS were abnormal in four members of a family positive for the nt 3460 mutation, the muscle OXPHOS rate was normal suggesting that extramitochondrial factors, such as nuclear genes, may influence expression of this mutation in vivo (Lodi et al., 2002).

Epidemiology

The risk of disease expression is predominant in males, with clinical case histories indicating an overall male/female ratio of 5:1 (Nikoskelainen et al., 1987; Seedorff 1970; van Senus 1963; Lundsgard 1944). The frequency of affected males ranges from 80% to 90% in some Caucasian pedigrees (Newman et al., 1991; Nikoskelainen et al., 1987; Miller, 1982; Carroll & Mastaglia, 1979), to approximately 60% in Japanese pedigrees (Yamanaka, 1971; Imachi, 1967). Female incidence ranges from 8% to 32%

(Nikoskelainen et al., 1987; Seedorf 1985, 1968). The age of disease onset is on average, 2-15 years earlier in males than in females (Black et al., 1995). This male predilection, inconsistent with the incidence data in other mtDNA disorders, has yielded the hypothesis of an X-linked cofactor in disease expression. At present, the etiology of the male incidence predilection is unknown and remains the subject for future research.

Etiologic Determinants

Advances in molecular diagnostic techniques have established LHON as a mtDNA disease with the identification of multiple mitochondrial mutations. Extensive data confirm that not only is LHON never transmitted via the paternal lineage (Carroll & Mastaglia, 1979; Krill, 1977), but also that every sibling of an affected carrier inherits the trait (Nikoskelainen et al., 1987; van Senus, 1963). Mitochondrial transmission supports the purely maternal inheritance pattern characteristic in LHON due to the exclusive transmission of mtDNA from the cytoplasm of the ovum (Phillips & Gosden, 1991).

However, the enigmatic pattern of inheritance of LHON subverts both the classic principles of both Mendelian and mitochondrial genetics. The higher incidence of affected males, the variation in the clinical expression of the disease and even more significantly, the proportion of asymptomatic individuals among members of the same familial pedigree, have yet to be explained.

The hypothesis of a simple X-linked inheritance pattern (Went, 1963, 1964) was discredited when research revealed that the incidence of affected males did not proportionally decrease in subsequent generations, as predicted by classic inheritance patterns. Furthermore, the occurrence in females is higher than is expected for a true X-

linked inherited disorder (Miller, 1982). In essence, the concept of a simple X- linked inheritance had been undermined due to the absolute failure of male transmission of the disease (Chen et al., 1989).

The postulate of an X-linked nuclear encoded modification of mtDNA was reinvestigated based on extension of segregation analysis methods which have shown LHON pedigrees to be consistent with a two-locus disorder, implicating one mitochondrial gene and one nuclear, X-linked gene (Bu & Rotter, 1992, 1991). Furthermore, extension of the two-locus analytic method has suggested that a proportion of affected females are likely heterozygous at the X chromosome-linked locus, thus explaining the later age of onset in females due to inactivation of the X chromosome.

Although there have been unsuccessful attempts at linking LHON with markers on the X chromosome (Chen et al., 1989; Newman et al., 1991; Carvalho et al., 1992; Sweeney et al., 1992; Juvonen et al., 1993), there have been reports of successful linkage data in LHON pedigrees, both with and without the ND4/11778A mutation to the locus DXS7 on the proximal Xp of X-chromosomal gene (Vilkki et al., 1991). This specific locale has been linked to three other hereditary eye diseases; Norrie's disease (Ngo et al., 1989), X-chromosomal congenital stationary night blindness (Gal et al., 1989), and X-linked retinitis pigmentosa (Chen et al., 1989). Furthermore, as is the case in retintis pigmentosa where distinct loci have been shown to cause similar diseases (Ott et al., 1990), perhaps a similar mechanism is involved where more than one nuclear X-linked factor is involved.

Clinical data has been presented that is consistent with the aforementioned postulates of an X-linked recessive factor interacting with mitochondrial factors (Black et

al., 1995). A study of over 30 LHON families positive for the nt 3460A mtDNA mutation, consistent with other published data on the sex distribution with the nt 3460A mutation, indicates a male female ratio of 3:1. However, 12 of the families contained only one affected member, and of those, only one was female. This suggests a marked bias in the ascertainment of males over females.

Furthermore, the compatibility of disease segregation with the existence of a nuclear modifier gene was evaluated in a large Brazilian family of Italian ancestry, haplogroup J, carrying the homoplasmic 11778 mtDNA mutation (Carelli et al., 2003). Data indicated that penetrance was 47.7% in offspring of affected females (66.7% in males, 30% in females) as opposed to 16.6% in offspring of unaffected females (19.04% in males, 0% in females). The strong male bias and the threefold higher penetrance in offspring of affected females as compared with unaffected females is consistent with the existence of a nuclear modifying gene , most probably X-linked or autosomal recessive.

Moreover, the recent identification of mutations in the nuclear gene OPA1 as the causative factor in dominant optic atrophy (DOA, Kjer's type) has confirmed a nuclear encoding of a mitochondrial protein, perhaps suggesting that DOA and LHON may be linked by similar pathogenesis (Cardaioli, 2005). Polymorphisms in this very same gene may be associated with normal tension glaucoma (NTG), which may be considered a genetically determined optic neuropathy that also shows similarities with both LHON and DOA (Woo et al., 2004).

Diagnosis

Despite this controversy concerning the etiologic determinants of the disease, mitochondrial genetics have afforded the reliable identification of specific point mutations in the mitochondrial genome via restriction fragment length polymorphisms (RFLP) of polymerase chain reaction (PCR) amplified mtDNA (Ara et al., 1991; Howell et al., 1991; Huoponen et al., 1991, 1990; Johns et al., 1991; Johns, 1990; Wallace et al., 1988, 1985), thus positively confirming a diagnosis of LHON. Furthermore, analysis of both muscle and blood samples of LHON probands have demonstrated deficiencies in respiratory chain complex I function (Larsson et al., 1991; Howell et al., 1991; Parker et al., 1989). Muscle biopsy, on the other hand, rarely indicates ultrastructural changes in the mitochondria (Larsson et al., 1991).

Preclinical Diagnosis

It remains unclear what genetic and epigenetic variables influence whether individuals positive for LHON mtDNA mutations will remain asymptomatic (and if female be labeled a carrier), or whether such individuals are simply in a preclinical state until they eventually become symptomatic. Due to the fact that the penetrance rate is not fully established, there is to date no reliable way to distinguish or predict who will and who will not express symptomology. Research has discovered some interesting and varied preclinical indices which require further analysis.

The early ophthalmoscopic findings, indicative of peripapillary microangiopathy, comprising the characteristic tortuosity, disc hyperemia, and optic nerve head margin blurring have been observed not only in the presymptomatic phase of LHON, but also in

a significant number of unaffected individuals in the maternal pedigree (Nikoskelainen et al., 1986). In contrast, increased microangiopathy and disc hyperemia, demonstrated by sequential fundus photography, become more severe during the acute phase of visual loss, whereupon nonedematous opacification occurs in the peripapillary retinal nerve fiber layer, particularly in the dense arcuate bundles above and below the disc. These differential fundal findings are considered to be valid and reliable indicators of the stage and extent of disease expression, and hence increased telangiectatic microangiopathy is recommended as a preclinical indicator.

The reliability of these fundal findings in symptomatic, and some presymptomatic and asymptomatic cases (Nikoskelainen et al., 1986), had supported an exclusionary diagnosis of LHON in patients exhibiting acute vision loss with the absence of these findings. However, there has been evidence of LHON probands who never exhibited the characteristic fundus findings (Borruat et al., 1992; Newman et al., 1991; Smith et al., 1990; Lopez & Smith, 1986), suggesting that the typical funduscopic appearance in an LHON proband, or in an asymptomatic relative should be employed as a corroborative measure, or as a preclinical predictor. Furthermore, research indicates that there is little correlation between funduscopic appearance and severity of visual deterioration (Nikoskelainen et al., 1982).

The dissociation of the VEP with classic acuity measures (Walsh, 1985; Sherman, 1984; Carroll & Mastaglia, 1979) has been offered as a possible preclinical indicator for onset of disease expression in LHON. VEP recordings of the unaffected eye in one LHON patient, employing a typical checkerboard stimulus pattern with a standard reversal rate of 7.5 reversals/sec. resulted in VEP records that were indistinguishable

from background noise in both the 7 and 14 min. checks, despite clinical evidence of perfect visual acuity. VEP amplitude reductions, and to a lesser degree increased latencies, which have been seen to occur as early as two months prior to the eventual synchrony of a flat VEP and deceased visual acuity (Sherman, 1984), have been implicated as precursors to clinical visual deterioration. Conversely, other research has not found the VEP to be a reliable preclinical indicator (Dorfman et al., 1977). However, the checkerboard element size employed was 1 deg. 50 min., perhaps too coarse a stimulus parameter to detect early foveal pathway dysfunction.

Misdiagnosis

Currently, misdiagnoses are rare due to genetic testing of the mitochondrial genome (Jacobson & Stone, 1991). Specifically, false negatives are more of a concern clinically, because not every variable presentation of visual abnormalities would necessitate genetic analysis. The clinical diagnosis of LHON is often difficult due to the transient nature and variable phenotypic expression of the classic symptomology. LHON patients display optic atrophy, variable centrocecal field loss, and a flat VEP recording, findings that are virtually indistinguishable from other etiologies of optic atrophy. Hence, historically, the incidence of LHON has more than likely been underrepresented.

An exemplary case described a 63 year old male who presented with a monocular, progressive central vision loss and optic nerve atrophy, followed 11 months later by involvement of the second eye. A diagnosis of chronic ischaemic optic neuropathy was subsequently disconfirmed despite a negative family history, lack of electrocardiographic

abnormalities, and minimal fundus changes characteristic of LHON, when testing positively identified the mtDNA LHON mutation at nt 11778A (Borruat et al., 1992).

Associated Neurological Findings

It is well established that mtDNA disorders affect other multiple organ systems, specifically those that are associated with a greater oxidative need. Although neurological and systemic examinations are generally considered normal in LHON, there is evidence of a variety of central nervous system disorders and the incidence of abnormalities in all aspects of cognitive and motor function. These abnormalities include an increased incidence of cardiovascular abnormalities, specifically preexcitation syndromes (Bower et al., 1992; Banerjee et al., 1990; Nikoskelainen et al., 1985, 1984; Rose et al., 1970), Wolff-Parkinson-White and Lown-Ganong-Levine (Nikoskelainen et al., 1985), including cerebellar and pyramidal tract disorders (Glaser, 1988; Rogers, 1977), palpitations and syncope (Nikoskelainen et al., 1987, 1985), neurological MS-like symptoms (Franks & Sanders, 1990; Palan et al., 1989; Adams et al., 1966), hereditary spastic dystonia (Bruyn et al., 1991), skeletal abnormalities (Miller, 1982; Wallace, 1970; Wilson, 1963; Ferguson & Critchley, 1928), hearing loss (Hagemoser et al., 1989), and auditory nerve damage (Mondelli et al., 1990). Leber himself, reported that even the unaffected members of an LHON family, typically suffer from associated abnormalities including migraine, nausea, palpitations, lethargy, and nervousness (Leber, 1871). These neurophysiological abnormalities seem to implicate a multisystem, yet often subclinical, involvement of the underlying disease.

Onset of neurological impairments has been reported both prior to (Bruyn & Went, 1964) and after visual involvement (Wilson, 1965). The variability within and between families is profound. Whereas, some individuals only experience optic atrophy (Carroll & Mastaglia, 1979), there have been reported fatalities perhaps due to hypothalamic involvement with polydipsia in one case, and polydipsia and bulimia in another (Wallace, 1970). An Australian pedigree has been described as exhibiting not only variable permutations of optic atrophy, but also movement disorders, spasticity, psychiatric disturbances, and acute encephalopathic episodes (Wallace, 1970). Furthermore, evidence of dystonia and basal ganglial lesions has been associated with a California pedigree (Novotny et al., 1986; Wallace et al., 1985), and Charcot-Marie-Tooth disease has also been associated with at least two familial pedigrees (McCluskey et al., 1986; McLeod et al., 1978).

Mitochondrial genetic analysis has implicated a higher incidence of neurological complications in probands harboring the LHON mutation at nt 15257 (Johns et al., 1993). However, the predisposing mechanisms inherent in this association remain unresolved.

Association of LHON and MS

Evidence of excess female transmission of multiple sclerosis and the incidence of MS-like illness in patients with LHON has led researchers to postulate that mtDNA mutations contributes to the genetic susceptibility to MS. The incidence of MS-like symptomology is commonly associated with LHON mtDNA mutations at bps 11778A and 3460A (Riordan et al., 1995; Kellar-Wood et al., 1994), whereas it has not been shown to be associated with the bp 14484C mutation (Kellar-Wood et al., 1994;

Chalmers et al., 1996). Research has suggested an increased incidence of mutations at bps 4216 and 4917 in MS patients than in normal controls (Hanefeld et al., 1994; Kalman et al., 1995), whereas bp 13708 mutations have been shown not to have an increased frequency in MS (Kellar-Wood et al., 1994). A more in-depth analysis of the correlation between LHON primary and secondary mutations and MS can be found in Appendix 1.

Delays in VEP recordings, common in demyelinating disorders such as multiple sclerosis, are often indistinguishable from the delays seen in LHON (Walsh, 1985). Research has indicated, however, that the differentiation between the optic neuritis common in multiple sclerosis and LHON may not lie in the typical morphological abnormalities evidenced in steady-state or transient pattern reversal VEP recordings, but rather in the critical frequency of photic driving (CFPD) for each eye. The CFPD is considered the electrophysiological counterpart of the psychophysically measured critical fusion frequency (CFF), indicating the highest frequency of photic driving in response to repetitive flash stimulation (Cohen et al., 1980; Celesia & Daly, 1977). Normal CFPD values indicate photic driving beyond 40 Hz, whereas patients with demyelinating disorders typically exhibit diminished CFPD values (Cohen et al., 1980). A case report of a Lebers patient with monocular involvement indicated normal CFPD values of greater than 50 Hz in both eyes, despite clear evidence of an optic nerve disorder, both clinically and electrophysiologically, with evidence of aberrant VEP recordings to both steady state and transient stimuli (Kothe et al., 1990).

The postulate that autoimmune mechanisms may play a contributory role in LHON (Harding et al., 1992) has not been overruled. The subacute onset of vision loss and the similarity in fundal appearance to an inflammatory microangiopathy have helped

sustain the hypothesis. Furthermore, increased immunoglobulins in the CSF of some patients with only optic nerve involvement (Riordan et al., 1995) and antibodies to tubulin, an optic nerve protein (Smith et al., 1995), have both been demonstrated in LHON. Evidence that mtDNA encoded peptides can act as transplantation antigens in rodent models further substantiates this premise (Loveland et al., 1990).

Prognosis

Whereas recovery of function after an acute episode is typical in other mtDNA disorders, visual loss in LHON is generally permanent. However both unilateral and bilateral recoveries of visual function have been reported, including citations of excellent central vision recovery (Holt et al., 1989; Lessell et al., 1983; Brunett & Bernier, 1969; Bird & McEachern, 1949). Recovery of function has been inversely correlated with age of onset, such that a better prognosis is more likely with an earlier disease expression (Johns et al., 1993; Holt et al., 1989).

Gradual improvement in acuity has been reported in approximately 10% of LHON patients, usually occurring within 2 years of initial onset of the disease (Beck and Smith, 1988). There are, however, reports of spontaneous improvement in LHON probands after years of visual dysfunction (Lessell et al., 1983; van Senus, 1963; Constantine, 1955; Bird & McEachern, 1949; Lundsgaard, 1944). Reports of the incidence of spontaneous improvement have been variable, ranging from 29% (Holloway, 1933) to 45% (van Senus, 1963), and even a reported improvement in 11 of 13 probands in a Canadian pedigree (Bird & McEachern, 1949). Leber himself described

visual improvement within one LHON family, without an accompanying change in the disc pallor associated with the optic disc atrophy (Leber, 1871).

Advances in the field of mitochondrial genetics have correlated the degree of visual improvement to both type and number of specific mitochondrial point mutations present in a particular gene sequence (Brown et al., 1992; Johns et al., 1992). The poorest prognosis occurs in probands harboring the primary LHON mutation at nt 11778A, with only a 4% recovery encompassing a range of visual capability from NLP (no light perception) to 20/50. Twenty-two percent recovery was reported for LHON patients with the nt 3460A mutation with a reported range of visual recovery from LP (light perception) to 20/100, and 28% with the nt 15257 mutation, with a recovery range of HM (hand motion) to 20/100. The best prognosis was evidenced in probands who were nt 14484C positive with a 37% recovery of visual function ranging from CF (counting fingers) to 20/200 (Johns et al., 1993; Stone et al., 1992).

Histopathological Findings

Early histopathology studies reported marked atrophy of the nerve fiber and ganglion cell layers and diffuse and shrunken optic nerve, chiasm, and tracts (Rehsteimer, 1930; Kwitken & Barest, 1958). No evidence of meningeal thickening, adhesion, or inflammatory lesions was obtained. The pituitary gland and fossa were normal (Adams et al., 1966; Kwittken & Barest, 1958; Rehsteiner, 1930). Distension of the dura mater and arachnoid of the optic nerve has been reported (de Gottrau et al., 1992), corroborating CT and MRI studies describing occasional optic nerve sheath distention in LHON (Smith et al., 1990). One report described thickening of the pia and septa with

hyaline degeneration in both the orbit and the canal of the optic nerve and indications of severe demyelination, gliosis and atrophy of the axis cylinder (Imachi, 1973).

More recent histopathological findings include the molecular genetic data. Morphometric analysis of a female positive for the 11778A mutation has revealed striking axonal loss primarily in the temporo-ventral region of the optic nerve. A count of the remaining axons totaled approximately 48,000 as compared to age matched normals with counts of 1 million per optic nerve. These remaining fibers were found to be clustered in the ventro-lateral optic tract after decussation of the chiasm with evidence of a glial zone separating these intact fibers from the hypothalamus. Nominal degenerative debris was found in both optic nerve and tract, suggesting the absence of an inflammatory process (Sadun et al., 1994). Decreased cellularity was observed in the retinal ganglion cell layer with remaining nuclei significantly smaller than normal and a nearly absent nerve fiber layer. The optic nerve, atrophic and shrunken, was 1.5 mm in diameter even in the posterior orbit. Gliosis and a moderate increase in astrocytes and oligodendrocytes, with few phagocytic microglia were observed (Sadun et al, 1994).

A considerable amount of tightly bunched neurofilaments, small organelles, multivesicular bodies, and intra-axonal myelin loops were observed in most axons in the optic nerve and peripheral optic nerves. Abnormal cristae were evidenced in the mitochondria in the extra-ocular muscles clustered in the periphery. Furthermore, a relative scarcity of microtubules as well as a small axon-to-fiber ratio was observed, suggesting axoplasmic stasis and axonal involution. There was an increase in mitochondria, approximately two-thirds of the cell mass, as opposed to a normal one-third, in the vicinity of the microtubules, and yet the microtubules themselves were

depleted, perhaps the result of a deficiency in net ATP. Histopathological research has also supranormal densities of mitochondria in the optic nerve itself (Carelli & Sadun, 2004). The most remarkable aspect of this seeming proliferation is the stacking of mitochondria posteriorally in the optic nerve, in the myelinated portion, where there is generally a sparsity of mitochondria. Similarly, the excess debris observed in the optic nerve may further represent a faulty axonal transport system that is incapable of maintaining internal integrity. Evidence of similar debris has been noted in other systems following axonal transport inhibitions (Brady, 1991). Insufficient neurofilament phosphorylation resulting from compromised ATP production has been hypothesized (Carelli & Sadun, 2004; Sadun et al., 1994).

In conclusion, this chapter described the multivariate permutations affecting the clinical expression of this mitochondrial disease. The chapter attempted to intertwine this myriad of minutia into a cogent model of the implications of mitochondrial vulnerability which will be analyzed further in the next chapter.

Chapter 3: LHON Mitochondrial Mutations

This chapter describes the features of exclusive maternal transmission of mtDNA mutations, concepts of oxidative phosphorylation and the biochemical impairments in the respiratory chain as a result of the particular LHON mutations. Endemic to the concept of mtDNA mutations are the derivative constructs of oxidative compromise and neurotoxic stress. The probability of disease expression is further comediated by other genetic and epigenetic variables.

Mitochondria and Oxidative Phosphorylation

Human mitochondria, transmitted exclusively by the female, are unique among cellular organelles in that they contain their own genetic material, consisting of approximately 2-10 copies of a double-stranded, closed, circular DNA molecule (mtDNA). This genome is distinctive in its lack of introns and noncoding sequences, and in overlap of contiguous genes in certain regions of the genome. Both the manner of replication and the transcription of mtDNA differ from that of nuclear DNA, and even their genetic codes are disparate. As a result, translation of mtDNA is constrained to the mitochondrion, and that of nuclear DNA to the cytoplasmic ribosomes (Shoffner & Wallace, 1990; Harding, 1989; Zeviani et al., 1989).

Although mitochondria exhibit different sizes, shapes and densities in different tissue (Wallace 1992; Wallace 1986: Hatefi 1985), all consist of two phospholipid bilayers. The inner membrane contains the protein complexes that catalyze oxidative phophorylation (OXPHOS), and the matrix, the area enclosed by the inner membrane, is the site of the tricarboxylic acid cycle.

The 16,569 base pairs (bp) of human mtDNA have been entirely sequenced and have been found to encode 2 rRNA, 22 tRNA, and 13 polypeptides of the mitochondrial respiratory chain and OXPHOS system (Chomyn et al., 1985; Anderson et al., 1981). The 13 mitochondrially encoded polypeptides are critical components of four of the five mitochondrial inner-membrane respiratory enzyme complexes involved in electron transport (complexes I-IV) and ATP synthesis (complex V). Complex I (NADH:ubiquinone oxidoreductase) contains seven polypeptides encoded by mtDNA; ND1, ND2, ND3, ND4, ND4L, ND5, and ND6. Complex III (ubiquinone:cytochrome *c* oxidoreductase) contains one; cytochrome *b*. Complex IV (cytochrome *c* oxidase) contains three; COI, COII, and COIII. Complex V (ATP synthase) contains two; ATPase 6 and 8 (Anderson et al., 1981).

Mitochondrial DNA is dependent upon structural and enzymatic proteins encoded by the nuclear genome for its replication and transcription; in turn, the cell itself is dependent upon the mitochondrion for a normal level of ATP production. This symbiotic interplay may be further enhanced by a nuclear regulatory process of mitochondrial activities (Shoffner & Wallace, 1990; Zeviani et al., 1989).

Inherent in the theory of mitochondrial diseases is the axiom that tissue with the highest requirements for ATP will be most affected by the respiratory deficiencies that result from deleterious mutations. The central nervous system, including the optic nerve and retina, are the most vulnerable, and potentially the most irreversibly compromised.

Mitochondrial mutations in LHON

The hypothesis of mutations within the mitochondrial genome was confirmed with the positive identification of a mitochondrial mutation in 9 of 11 LHON families (Wallace et al., 1988). A single nucleotide change at position 11778A (nt 11778A) in the mtDNA resulted in the substitution of an arginine with histidine in the highly conserved codon 340 of the ND4 subunit of NADH-ubiquinone oxidoreductase. This point mutation (ND4/R340H) removes a *Sfa*NI restriction site, thereby providing a simple detection of the mutation through restriction site analysis of mtDNA amplified by polymerase chain reaction (PCR). Mapping with other restriction endonucleases can rule out deletion or rearrangement of mtDNA (Yoneda et al., 1989; Wallace et al., 1988). Nucleotide sequence analysis of amplified mtDNA can be used to confirm the G-to-A transition at this nucleotide, commonly dubbed the "Wallace Mutation". Subsequent research has supported these original findings in culturally diverse matrilineal pedigrees (Brown et al., 1992; Sudoyo et al., 1992; Ara et al., 1991; Carducci et al., 1991; Hiida et al., 1991; Kormann et al., 1991; Bolhuis et al., 1990).

Maternally related members of a Leber's pedigree carry the mtDNA mutation, regardless of phenotypic presentation. Subsequent research has confirmed that approximately 50% of LHON pedigrees have been positively identified with the nt 11778A mutation (Newman et al., 1991; Poulton et al., 1991; Holt et al., 1989; Vilkki et al., 1989; Wallace et al., 1988).

A large Queensland family has been described exhibiting a severe form of LHON, as evidenced not only in the large proportion of affected members, but also in the incidence of extreme neurological complications, such as dysarthria, ataxia, tremors,

posterior column signs, skeletal deformities, and a severe infantile encephalopathy, fatal in at least three cases (Wallace, 1970). Biochemical defects in the mitochondrial respiratory chain, specifically a marked decrease in the specific activity of complex I, were first documented in platelet mitochondria in four members of this family (Parker et al., 1989). Subsequently, two ND1 mtDNA mutations were identified (Howell et al., 1991; Howell & McCullough, 1991).

Alternative LHON mutations were sought by sequencing the mitochondrial genes for NADH-ubiquinone oxidoreductase subunits (ND genes). When no further mutations were found in the ND4 gene (Huoponen et al., 1990), other ND genes were investigated, leading to the discovery of another single base mutation at nucleotide position 3460A (nt 3460A) in the ND1 gene, indicating the second instance of a biochemical defect in mitochondrial complex I specific activity. The G-to-A mutation converts an alanine to a threonine at position 52 of the ND1 protein (ND1/A52T). The mutation also obliterates an *Aha*II restriction site, thus affording simple detection by means of RFLP analysis.

The 3460A mutation has been identified in 7 English and Australian LHON pedigrees (Howell et al., 1991) and in three Finnish LHON pedigrees (Huoponen et al., 1991). Estimates of the incidence of the nt 3460A as the primary etiologic event in LHON are 15%-25% (Howell et al., 1992, 1991b; Huoponen et al., 1991).

A third mtDNA mutation was identified at position 171 in the apocytochrome b gene (Complex III); including a G-to-A transition at nucleotide position 15257 which changes a highly conserved aspartate to asparagine (Johns et al., 1991; Anderson et al., 1981). The demonstration of mtDNA mutations in Complex III established that LHON is not mutually exclusive to Complex I dysfunction. However, the presence of the three

primary LHON mutations affecting two respiratory complexes, has led to the suggestion that LHON results from a nonspecific reduction in mitochondrial energy production (Brown et al., 1992a).

Research has thus identified these three primary mtDNA mutations to be proximate causative mutations including the nt 11778A of the ND4 gene (Wallace et al., 1988), the nt 3460A of the ND1 gene (Howell et al., 1991; Huoponan et al., 1991), and the nt 15257 of the apocytochrome b gene (Johns et al., 1991; Anderson et al., 1981).

Although both the nt 11778A and the nt 3460A primary mutations have not been detected in normal controls, the nt 15257 mutation has been detected not only in 4 of 23 non-11778A LHON patients, but also in 1 of 362 normal controls (Brown et al., 1992a). Furthermore, the research described the first instance of a phylogenetic clustering of the four LHON families harboring the nt 15257 mutation. Although there has been no recorded evidence of the nt 15257 mutation occurring in LHON probands harboring another primary mutation (Brown et al., 1992a; Johns & Neufeld, 1991), two LHON families have been identified who carry both the nt 11778A and the nt 15257 mutations (Howell et al., 1993).

Several other mutations have been identified that appear to be of secondary importance with regard to not only the probability and severity of LHON symptomology, but also to later prognosis and recovery of function. These include mutations at nucleotide positions 4216 of the ND1 gene (Johns et al., 1992), 4917 of the ND2 gene (Johns et al., 1992), 5244 of the ND2 gene (Anderson et al., 1981), 13708 of the ND5 gene (Johns et al., 1991; Anderson et al., 1981), 14484C of the ND6 gene (Johns et al.,

1992), and 15812 of the apocytochrome b gene (Johns et al., 1991; Anderson et al., 1981).

The current hypothesis suggests either the synergistic action of these mutations with the primary mutations, or their inherent linkage with another primary pathogenic mutation (Johns et al., 1991, 1992). For example, research indicates the presence of the 15257 apocytochrome b mutation in LHON probands who were negative for the nt 11778A, but were positive for the nt 13708. This finding is suggestive of the possibility that mutations such as nt 13708 occurring in low percentages in normals, and with increased frequency in LHON, are not the primary pathogenic mutations, yet serve as synergistic mutations for the expression of LHON symptomology in certain genotypic pedigrees (Brown et al., 1992a; Johns & Neufeld, 1991). Preliminary results comparing the frequency of affected males in three Australian families suggest that increased penetrance may occur in probands harboring both the 4216 and 13708 mutations, but is not affected by the presence of the cytochrome b mutation (Howell et al., 1993). For a more detailed discussion on the identification of other secondary mtDNA mutations, see Appendix 1.

Although LHON probands exhibit similar symptomology, further analysis of their clinical presentation reveals vast differences. For example, probands harboring the nt 3460A have a better prognosis for visual recovery, and are more highly correlated with tobacco and alcohol abuse and a positive family history than probands harboring the nt 11778AA (Johns et al., 1992). There have been reports, however, of spontaneous visual recovery up to six years after initial onset in probands harboring the nt 11778AA

mutation (Stone et al., 1992). However, this mutation is still considered the most incompatible with visual improvement (Holt et al., 1989).

Molecular genetic analysis has been reported to be between 70% - 90% sensitive, and between 95% - 100% specific for mtDNA mutations in LHON (Johns et al., 1992; Johns & Berman, 1991; Norby et al., 1991). The incidence of complex I mutations in LHON pedigrees has been reported at 56% for nt 11778A, 28% for nt 13708, 17% for nt 4917, and 38% for nt 4216 (Johns & Berman, 1991). Current research is currently investigating the incidence of other mtDNA mutations in LHON pedigrees. Unfortunately, there is a paucity of data on the epidemiological incidence of these mutations, implicating the need for cross-sectional study. Two interesting case studies of LHON probands positive for the 4216 and 4917 secondary mutations are described in Appendix 2.

The molecular mechanisms of the pathogenesis of this disease still remain elusive. The etiology underlying enigmatic axioms are left unanswered. For example, probands are typically healthy except for visual deterioration. Relatives of the proband may carry mutant DNA in their blood and hair follicle cells, and yet, not exhibit vision loss. Furthermore, the proband himself does not typically experience visual deterioration until the second or third decade in life.

In summary, twelve mutations have been identified. Mutations at nts 3460A, 4160, 11778AA, and 15257 and 14464, designated as class I mutations, are considered high risk for they can occur singly in an LHON pedigree, and probands harboring this mutation have a higher probability for blindness than probands harboring any of the other mutations. Mutations at nts 4216, 4917, 5244, 13708, and 15812, designated as class II

mutations, are considered low risk for they generally present in combination with another mutation, and the probability for experiencing blindness is comparatively low for individuals harboring a single class II mutation.

Class I mutations generally involve evolutionarily conserved amino acid substitutions within functionally significant polypeptide sequences, whereas class II mutations create both conservative and nonconservative amino acid substitutions. Class I mutations are rarely identified in control populations of unaffected individuals, whereas class II mutations are both rarely identified (nts 5244 and 15812), and frequently identified (nts 4216 and 13708) in the unaffected controls. However, there appears to be a significant positive correlation between low incidence and linkage to another specific class I mutation; e.g. the incidence of nts 5244 and 15812 are positively correlated with the class I nt 15257 mutation (Brown et al., 1992; Johns & Neufeld, 1991).

Mutations at nts 7444 and 3394 are designated as class I/II, for they appear to be intermediaries between class I and class II. Significant substitutions in respiratory polypeptides are resultant from both these mutations, yet their incidence is relatively uncommon not only in LHON pedigrees, but in unaffected controls (about 1%) as well. Linkage is nonspecific to both class I and class II mutations (Brown et, al., 1992).

Biochemical Ramifications of Mitochondrial Mutations

Respiration studies from lymphoblasts and transmitochondrial cybrids harboring the three most common LHON mutations at nts 11778AA, 3460AA and 14484CC revealed that the 11778A mutation reduced the maximal respiration rate 30-36%, the 3460AA mutation 20-28%, and the 14484C mutation 10-15% (Brown et al., 2000).

Furthermore, the 3460AA mutation reduced specific activity in Complex I enzymatic assays by 79%, the 11778AA mutation resulted in a 20% reduction, whereas the 14484CC did not affect Complex I activity. The more severe biochemical defects in 11778AA and 3460AA, and the milder biochemical defects in 14484CC corroborate well with the reported LHON pathogenesis. Similarly, microphotometric analysis obtained from skin fibroblasts from patients with the 11778 mtDNA mutation revealed a 30% lower fibroblast NADH-tetrazolium reductase activity even at the single-cell level (Malik et. al, 2001).

Osteosarcoma-derived cybrid cells carrying the most common and severe mutations at nts11778 and 3460 were shown to be sensitized to Fas-induced apoptotic death as opposed to control cells that bore the same mitochondrial genetic background (the J haplogroup) without the pathogenic 11778 mutation and other controls (Danielson, et al., 2002). Furthermore, research employing osteosarcoma-derived cybrid cell lines harboring one of the three most common LHON mutations at nts 11778/ND4, 3460/ND1 and 11484/ND6 reveals that when galactose replaces glucose in order to produce a metabolic stress forcing the cells to rely on mitochondrial respiratory chain to produce ATP, the cells undergo apoptosis as evidenced by chromatin condensation and nuclear DNA laddering (Ghelli, et al., 2002). The increased release of cytochrome c into the cytosol in LHON cybrid cells implicates the mitochondrial involvement in the activation of the apoptotic cascade. Interestingly, cybrids bearing the 3460/ND1 and 14484/Nd/6 mutations seemed more readily prone to undergo apoptosis than the 11778/ND4 mutation.

Reduced concentrations of plasma alpha-tocopherol/cholesterol+triglyceride ratios were seen in both patients carrying the 11778 mtDNA mutation and asymptomatic carriers (Klivenyi et al., 2001) perhaps reflecting the consumption of the antioxidant by the affected tissues. Furthermore, alpha-tocopherol may be the primary scavenger molecule against the free radicals induced by Complex I deficiencies, since no differences were evidenced neither in other non-enzymatic antioxidants such as beta-carotene, lycopene, glutathione, and free sulphydryl groups nor in other lipid peroxides in the blood.

Homoplasmy vs Heteroplasmy

Mitochondrial diseases have highly variable expression, even within kindreds (Shoffner and Wallace, 1992), and the specific mechanisms linking genotype and phenotype remain unknown. The relative proportion of wild-type and mutant mtDNA appears to be a critical variable in disease expression in many diseases arising from primary mutations in the mitochondrial genome (Boulet et al., 1992; Chomyn et al., 1992). The proportions of mutant and wild-type mtDNA vary between different individuals and can vary between tissues within individuals as well (Ciafaloni et al., 1991; Matthews et al., 1994).

In vitro studies typically reveal that a respiratory deficient phenotype is expressed when the proportion of mutant mtDNA exceeds a disease-specific threshold level in clonal cells in culture, thereby impairing mitochondrial protein synthesis (Chomyn et. al, 1994; Kobayashi et al., 1992). However, in vivo LHON studies have failed to show a consistent relationship between the degree of heteroplasmy and biochemical expression

of the specific visual defect. This may be due to variable heteroplasmy in individual cells that does not adequately reflect the mean heteroplasmy of a given tissue as evidenced in fibroblast clones derived from two LHON probands positive for the nt 11778A mutation (Matthews et al., 1995).

The heteroplasmy or tissue variability identified in both the ND4/11778A (Bolhuis et al., 1990; Lott et al., 1990; Vilkki et al., 1990; Holt et al., 1989), and the ND1/3460A (Howell et al., 1991) mutations, was initially believed to be partially responsible for the variability in phenotypic presentation of LHON symptomology. The underlying premise asserts that the presence of wild type mtDNA molecules would mitigate the extent of the respiratory Complex I deficiency, such that probands whose optic nerve cells contained heteroplasmic mtDNA would be less prone to experience visual deterioration. Although a correlation between the proportion of mutant DNA and the severity of the optic nerve disease has been documented (Isashiki & Nakagawa, 1991), the existence of homoplasmy found to occur in all mitochondrial mutations with no apparent correlation to phenotypic severity, engenders skepticism for the underlying hypothesis. For a more detailed analysis of this controversy including issues of segregation and transmission analysis, see Appendix 3.

Epigenetic Factors

Smoking: Abnormal Cyanide Metabolism

Given the condition of a necessary, but not sufficient mitochondrial mutation for overt symptoms, additional precipitating exogenous and epigenetic factors were investigated that might be causally related to the onset and variable expression of the

disease. Animal data such as the chronic exposure of primates and rodents to low levels of respiratory inhibitors resulting in optic neuropathy and basal gangliar lesions (Berridge & Irvine, 1984), coupled with the fact that the mutation itself alters respiratory chain complex I, has broadened the investigation into other possible determinants of LHON. Environmental stressors, such as smoking, which mitigates OXPHOS efficacy by means of carbon monoxide inhibition of Complex 1 in optic nerves characterized by high oxidative activity (Shoffner & Wallace 1990), may be responsible for augmenting the expression of symptomology. The severity of LHON was correlated to tobacco smoking (Wilson, 1965), and cyanide was implicated as a possible precipitant of vision loss in LHON. Furthermore, the onset of optic neuritis as a direct consequence of cyanide intoxication from the ingestion of bitter cassava in man (Osuntokun, 1973; Montgomery, 1965), and in animals (Lessel, 1971), has prompted research into abnormal cyanide metabolism in LHON.

Increased urinary thiocyanate excretion was observed in healthy smokers as compared to non-smokers, but this difference was not observed in a population afflicted with LHON (Rogers, 1977; Wilson, 1965). The relatively low levels of thiocyanate may be indicative of an inability of LHON individuals to respond to an increased intake of cyanide with increased detoxification.

Research investigating rhodanese, the primary enzyme involved in cyanide detoxification has yielded conflicting data. Whereas significantly reduced rhodanese activity was observed in the liver parenchymal cells (Cagnianut et al., 1984), in the rectal mucosa (Poole & Kind, 1986), and in whole blood samples taken from LHON patients (Berninger et al., 1989; Goadsby & Fine, 1988), normal rhodanese levels were reported

in the liver (Whitehouse et al., 1989; Wilson, 1965), in the red cells (Syme et al., 1983), and in the mitochondria of muscle samples taken from LHON patients (Nikoskelainen et al., 1984).

Cyanide normally conjugates with sulfur from the liver to form non toxic thiocyanate. Due to the postulated compromise in cyanide detoxification in LHON, treatments involving agents that were believed to accelerate detoxification were implemented. Hydroxycobalamin, sulphur containing amino acids, namely cystine (Syme et al., 1983; Foulds & Pettigrew, 1977), and sodium thiosulfate (Berninger et al., 1989) were treatments of choice for all three have no known side effects.

Reduction in blood cyanide levels was achieved with the administration of cyanide antagonists to patients with acute LHON, without the anticipated visual recovery. Furthermore, data indicated that whereas elevated blood cyanide levels were obtained at the acute stage of disease, normal levels of both rhodanese activity and blood cyanide levels were obtained at the chronic stage of the disease. This data may serve to clarify existing inconsistencies regarding the status of rhodanese activity with respect to the differential stages of the disease. These results implicate a temporary imbalance of cyanide metabolism only at the acute stage of LHON (Berninger et al., 1989).

The mitochondrial data may further substantiate the hypothesis of an imbalance in cyanide metabolism in LHON. The 11778A mutation may result in only a partial reduction in the mitochondrial production of energy. Potassium cyanide, a chemical inhibitor of complex I activity, produces an energy deficit similar to the one produced by the nt 11778A mutation (Jay, 1992). The postulate that the mitochondrial energy deficit may be exacerbated by elevated levels of blood cyanide requires further investigation.

Furthermore, an atypical case of LHON described a 15 year old Chinese boy with no evidence of a family history and involvement of the second eye occurring after an interval of more than five years (Chew, 1990). An intramuscular hydroxycobalamine therapy was administered achieving a bilateral improvement of Snellen acuity of 6/9 within six months. Interestingly, the eye with a longer history of poor vision responded first to the therapy. Hence, a controlled study implementing a regimen with hydroxycobalamine must be further evaluated.

Multiple Sclerosis

The incidence of neurological complications indistinguishable from multiple sclerosis, predominantly in affected female probands, has led researchers to postulate an immunologically mediated process in which mitochondrial genes may be primarily responsible for increased susceptibility to MS (Harding et al., 1992). Many LHON probands have increased immunoglobulins in their CSF (Pallini et al., 1988). One study reported that a significant number of LHON patients have circulating antibodies to tubulin protein in their blood; supporting the theory that autoimmunity may somehow play a role in the pathogenesis of LHON (Smith et al., 1995). The absence of anti-HON antibodies in non-genetic optic neuropathies, specifically ischaemic and compressive optic neuropathies refutes the premise that these antibodies are simply the result of a non-specific immune response to damaged optic nerve proteins.

As such, protocols involving effective drug therapies in MS should be investigated for their clinical efficacy in LHON. Immunosuppressors, such as

cyclosporine or beta interferon (Arnason, 1993), may serve as initial drugs of choice for future investigations.

Metabolic Pathogenesis

Interestingly, the mitochondrial data require the renewed investigation of the otherwise unsubstantiated postulate of a metabolic pathogenesis. A case history was cited describing a 9 year old female, diagnosed with juvenile onset diabetes mellitus, who also presented with symptoms suggestive of bilateral optic neuropathy. Mitochondrial DNA was positive for LHON, suspected on the basis of family pedigree. Once the diabetes was controlled, visual recovery followed, suggesting that a metabolic compromise, occurring in such disorders as diabetes, may precipitate other inherent, but otherwise latent dysfunctions, such as LHON (DuBois & Feldon, 1992).

A case history of a male with normal vision with onset of blindness after a failed suicide attempt with an aspirin overdose further implicates the possibility of a metabolic trigger (Sherman, personal communication). The patient subsequently tested positive for one of the primary LHON mutations, consistent with the notion that aspirin, toxic to mitochondria, was the precipitating factor of disease expression.

Cuban Optic Atrophy: Nutritional Pathogenesis

An epidemic of blindness due to an optic neuropathy with occasional mild neurological complications affected more than 48,000 Cubans (Cotton, 1993; Lincoff et al., 1993). The Cuban Ministry first reported that the disease mostly affected young males, between the ages of 15 and 65, who smoked tobacco and/or drank alcohol.

However, later reports included women, nonsmokers and nondrinkers. Researchers in both Cuba and the United States investigated possible pathogenic factors, including viruses, nutritional deficiencies and toxins.

Data ruled out a viral cause since no viral cultures were grown from the Cuban samples. Furthermore, the disease was not spread by contact with no reported outbreaks in institutions like schools or army barracks. Hypotheses included Strachnan's disease, an optic neuritis with numbness, cramps and a burning sensation in the hands and feet believed to be due to a vitamin B deficiency (Denny-Brown, 1947; Spillane, 1947). Beriberi, a thiamine deficiency was also hypothesized due to the similarity of the clinical features of the Cuban population to other prisoners of war diagnosed with known nutritional deficiency syndromes (Denny-Brown, 1947). Dry beriberi causes peripheral neuropathy and wet beriberi causes peripheral edema when the cardiovascular system is involved. The Wernicke-Korsakoff thiamine deficiency syndrome causes ocular motility disturbances and mental status changes (Victor et al., 1989). Although optic neuropathy is not typical of beriberi or Wernicke-Korsakoff syndrome, it is nonetheless the dominant finding in nutritional amblyopias (Carroll, 1966).

Interestingly, the aforementioned nutritional deficiencies and toxic and/or nutritional amblyopias correlate well with current standards of living in Cuba. Firstly, the Cuban government implemented stricter food rationing, specifically of milk, eggs and meat, due to the loss of trade and direct help from the Soviet Union (Lincoff et al., 1993). This lack of animal protein results in not only a lack of B group vitamins which may allow for damage from high, but otherwise tolerable levels of cyanide in tobacco and foods like cassava and black beans, staples in the Cuban diet, but also from a lack of

methionine, a sulfur-containing amino acid that normally counteracts cyanide poisoning. Children younger than 7 years, adults older than 65 years, and pregnant women who receive larger rations have rarely been affected by this outbreak. Secondly, chronic methanol toxicity from bootleg rum, analyzed at 1% methanol, may be responsible for subacute poisoning which may serve as a contributing factor for disease expression. A wedge defect affecting a select bundle of nerve fibers between the retina and optic nerve was identified which correlates with a previously identified wedge defect in tobacco/alcohol amblyopias and LHON.

Tobacco/Alcohol Amblyopias

Patients diagnosed with classic tobacco/alcohol amblyopias were genetically evaluated in an attempt to decipher any genetic parallels with the LHON mtDNA mutations. Genetic testing identified two (17%) of twelve patients who tested positive for LHON mutations (Cullom et al., 1993), and 6 of 11 affected Cubans with the same classic LHON mutations at nts 11778A and 3460A (Sadun, et al., 1993).

Research has shown that smoking tobacco, a rich source of cyanide, increased the risk of the neuropathy eightfold. Early treatment with parenterally administered B-group vitamins has been reported to result in decreased symptomology (Cotton, 1993).

On the other hand, conflicting research has found no significant deleterious correlation between tobacco or alcohol consumption and vision loss among sibships harboring LHON mutations at nts 11778A, 14484C and 3460A based upon self-reported exposure prior to vision loss (Kerrison et al., 2000).

Nonetheless, most researchers still believe that the genetic mutations create an inherent predisposition that can be triggered via epigenetic factors. Environmental stressors such as nutritional deficiencies, smoking and drinking may exacerbate disease expression. Low levels of dietary folic acid compromise mitochondrial efficiency of net ATP. Cyanide may also block ATP production and methanol depletes folic acid in the body with the conversion of folic acid to formic acid. These epigenetic factors, namely toxins related to cyanide and methanol, are hypothesized as causing a toxic-nutritional insult to compromised mitochondria resulting in differential disease expression.

Chapter 4: Physiology of the Human Visual System: Retinogeniculate Pathway

This chapter describes the basic physiology of the human visual system. The specific pathways and differential cell types with their respective response characteristics are delineated. The physiology and morphology of these specific pathways are critical in evaluating the hypothesized selective pathway involvement in LHON both in terms of the precise biochemical vulnerability of the differential cell types (chapter 5) and the particular types of VEP stimuli (chapters 6 and 8) that were designed to differentially assess those explicit pathways.

The Retina

The visual pathway consists of the eyes which capture and respond to light energy, the lateral geniculate nucleus (LGN) the neural circuitry which transmit signals from the eye to the brain and the visual cortex which interprets these signals into meaningful images. The key components of the eye include the image focusing structures including the cornea, lens, iris and pupil and the image recording component, namely the retina. Visual sensations result when patterns of light that enter the eye are focused on the light-sensitive retina.

The retina is composed of three major layers of cell bodies separated by two layers of synaptic connections. The outer nuclear layer, the layer nearest the pigment epithelium, contains the cell bodies of the photoreceptors which absorb the light and transduce it into nervous energy. Specifically, the rods and cones hyperpolarize in response to light absorbed by their individual outer segments. These receptors terminate in the outer plexiform layer, where these discrete receptors are potentially presynaptic and/or postsynaptic to different cell types. There is even evidence that receptors

themselves are influenced by neighboring receptors (Scholes, 1975; Gold & Dowling, 1979). Horizontal cells are both presynaptic and postsynaptic for although they contain vesicles, they are in a position that indicates receptors are presynaptic to them. Bipolar cells are postsynaptic to both receptors and horizontal cells.

The next layer of cell bodies is the inner nuclear layer consisting at the outer margin with horizontal cells, lateral cells that interconnect with distant areas, provide the first stage of visual processing. Horizontal cells have large receptive fields, even larger than the lateral spread of the cell presumably due to its interconnection with neighboring horizontal cells (Kaneko, 1971).

The bulk of the inner nuclear layer consists of the bipolar cells which interconnect between the outer and inner plexiform layers. The receptive fields of bipolar cells are spatially antagonistic, with bipolars responding to relative amounts of light, namely contrast based upon their center/surround receptive field. Most invaginating bipolars are center-depolarizing, while most flat bipolars are center-hyperpolarizing (Famiglietti & Kolb, 1976; Stell et al., 1977). Although this division by anatomical type is imperfect, the division into mirror-image systems persists throughout the retina (Saito et al., 1983; Sterling, 1983).

At the inner margin are the amacrine cells, whose cell bodies are in the inner plexiform layer while their dendrites project into the synaptic layer, are the lateral interconnections required for the second stage of visual processing. At the inner plexiform layer, bipolar cells are presynaptic to amacrine and ganglion cells; and amacrine cells are presynaptic to other amacrine, bipolar and ganglion cells. This organization affords vertical information flow from photoreceptors to bipolars to

ganglion cells and lateral flow mediated by horizontal and amacrine cells. Amacrine cells process temporal contrast and depolarize both to Onset and Offset.

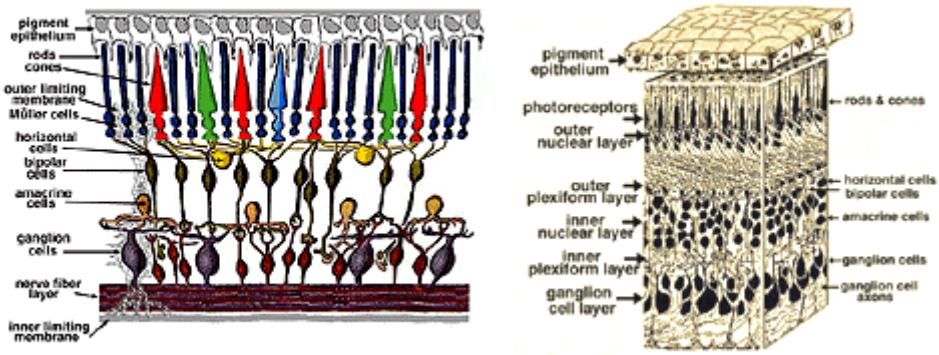

Figure 2a: Simple organization of the retina Figure 2b: 3-D Block of a segment of human retina. Reprinted with permission from: Kolb, H., Fernandez, E., and Nelson, R. (2005) http:// webvision.med.utah.edu.

Ganglion Cells

The final level consists of the ganglion cells with dendrites in the inner plexiform layer, cell bodies in the ganglion cell layer and axons across the surface of the retina that terminate in the optic nerve. Information flows vertically from photoreceptors to bipolars to ganglion cells and there is a lateral information flow mediated by horizontal and amacrine cells. The pooled signals form several photoreceptors determines the electrical responses evoked in ganglion cells. The response of the ganglion cell critically depends on the precise pattern of light that stimulates the retina and how this pattern changes over time (Hubel, 1988, Kaplan, 1989).

Individual ganglion cells differ not only in their location in reference to the portion of the retina sampled, but also in the size of their receptive field, namely their spatial selectivity. Hence, although several ganglion cells may respond to a given

stimulus, the neuron that optimally responds is contingent upon the particular size of the pattern elements. This lateral antagonism or lateral inhibition, allows a single ganglion cell to be selectively sensitive to contrast within its receptive field, rather than responding to the total amount of light directed onto the field. This organization which mediates spatial frequency selectivity is even more strongly expressed in the cortex.

Selectively sensitive ganglion cells have been described in frog retina including sustained contrast detectors, net convexity detectors, moving edge detectors and net dimming detectors (Lettvin et al., 1959). Direction-selective ganglion cells (Barlow et al., 1964) and orientation selective ganglion cells (Levick, 1967) have been described in rabbit retina.

Axons leaving the temporal half of the retina traverse the optic nerve to the optic chiasm where they join the optic tract and project to ipsilateral structures, while axons leaving the nasal half of the retina cross the midline at the chiasm and terminate in contralateral structures. This structural arrangement affords that all axons in one optic tract carry information about the contralateral visual field, a pattern of hemispheric reversal consonant with the motor and somatosensory systems with respect to the external world. Axons of the optic tract terminate in the right lateral geniculate nucleus and axons from the left optic tract terminate in the left lateral geniculate nucleus.

Lateral Geniculate Nucleus

Axons of the optic tract terminate in the LGN, a bilateral structure which is the principal subcortical structure that processes visual information. The LGN has six layers.

The contralateral fibers of the optic nerve terminate in layers one, four and six. The ipsilateral fibers terminate in layers two, three and five.

Visual cortex

Visual information passing through the LGN projects to area V1 of the cortex, also known as striate cortex due to its striped appearance. A separate parallel pathway through the pulvinar projects to all other cortical visual areas. Much of the information form V1 goes to the secondary visual cortex (V2) which also receives input from the thalamus. Information from V2 branches to area V3, V4, and V5 while some information travels back to V1 (Mignard & Malpeli, 1991). Each of these areas further subdivides and sends the visual information to additional brain areas. Neuroscientists have identified more than twenty brain areas receiving visual input which occupy more than half of the primate cerebral cortex (Kaas & Krubitzer, 1991; Knierim & Van Essen, 1992).

Parallel Pathways - ON and OFF Pathways

Retinal Bipolar cells

Bipolar cells in the primate retina have been classified into distinct subtypes based upon both anatomical and physiological characteristics. Processes from bipolar and horizontal cells fit into invaginations and form a triad where the dendrite of a bipolar cell is flanked on either side by processes from horizontal cells (Dowling & Boycott, 1966). Midget bipolar cells synapse with only one cone pedicle and their axons project onto many levels of the inner plexiform layer (IPL), as opposed to diffuse bipolar cells which

receive input from several cones (Polyak, 1941). Two types of midget bipolars have been described through electron microscopy (Kolb et al., 1969; Kolb, 1970). Flat midget bipolars make only basal contacts with cone pedicles, while invaginating midgets synapse opposite the cone ribbons as the central elements in cone triads. The axons of flat midgets terminate in the outer part, the OFF sublamina of the IPL, whereas the axons of the invaginating bipolars terminate in the inner half, the ON sublamina of the IPL. Midget bipolars form the first distinct step in the P pathway of the primate visual system and are the major determinant of the receptive field properties of color selective midget ganglion cells. Midget bipolars contact a single photoreceptor, acquire the photoreceptor's spectral sensitivity, and communicate this to the inner retina (Rodieck, 1988; Boycott & Hopkins, 1991; Waslle & Boycott, 1991).

Diffuse bipolar cells also maintain the distinction of flat (OFF) and invaginating (ON) cells (Mariani, 1981; Boycott & Hopkins, 1993). However, at least six different morphological types have been described in Golgi-stained retinae (Boycott & Wassle, 1991). Diffuse bipolars contact all cone pedicles, generally between five and ten, within their dendritic field. However, it is unlikely that they are carrying a specific chromatic signal into the inner retina because the irregular sizes of the clusters, or cells contacting cone pedicles of adjacent clusters, or summation by ganglion cell dendrites would all cause a degradation of the chromatic signal (Wassle et al., 1994). As such it has been proposed that diffuse bipolars, like H_1 and H_2 horizontal cells (Boycott et al., 1987; Wassle et al., 1989), carry a luminosity signal (Boycott & Wassle, 1991).

The spatial density of midget bipolars, cones and ganglion cells were compared in an immunocytochemical study of monkey retina stained with antibodies against

cholecystokinin (CCK) and recoverin (Wassle et al., 1994). Results indicated that although CCK-immunoreactive midget bipolars were found throughout the retina, recoverin-labeled sections revealed a different population of midget bipolars. The researchers concluded that ON-midget bipolars were immunoreactive for CCK and Off-midget bipolars were immunoreactive for recoverin based on convergent data from Golgi-stained retinae (Milam et al., 1993). The spatial density of recoverin labeled midget bipolars matches the cone density to an eccentricity of about 10mm, whereas the ratio drops to about 60% of cone density with eccentricity. This suggests convergence of several cones to individual midget bipolars in peripheral retina, and as such, the peripheral as well as the central retina, could provide chromatically specific input to the P pathway.

Ganglion Cells

Ganglion cells have spatially antagonistic receptive fields (Kuffler, 1953; Rodieck & Stone, 1965; Enroth-Cugell & Robson 1966) and may either be transient in their response characteristics like amacrine cells or sustained like bipolar cells. Like the hyperpolarizing and depolarizing bipolars that form mirror-image pairs, there are ganglion cells with ON-center and OFF-center receptive fields. As such, a response may either be an increase or a decrease from the mean firing rate, or maintained discharge of the cell; specifically the neural response is a modulation around some steady level of neural spikes per unit time. However, when both center and surround are illuminated, a subtraction process limits or even cancels the net response, or departure from mean firing rate (Kuffler, 1953). A third type of ganglion cell evidenced in frog retina, the ON-OFF

cell, has both an excitatory onset and offset, and thus its function is to signal a change in light level regardless of an increase or decrease in luminance (Hartline, 1938).

The two systems continue in parallel throughout the retina, where ON-center ganglion cells project to the IPL directly above the ganglion cell layer, where mostly ON-center invaginating cone bipolar cells synapse. The OFF-center ganglion cells project to the outer portion of the IPL where mostly flat hyperpolarizing bipolar cells terminate (Famiglietti & Kolb, 1976; Nelson & Kolb, 1983).

On-center ganglion cells receive direct excitatory from depolarizing bipolars, and OFF-center ganglion cells from hyperpolarizing bipolars (Miller & Dacheux, 1976; Naka, 1977). On the other hand, ON-center ganglion cells receive inhibitory signals from depolarizing bipolars (Sterling, 1983).

Mammalian X and Y Pathways

Most ganglion cells that have been recorded from the retinae of higher mammals, mainly cat and monkey, have concentric center-surround receptive fields. Three morphological classes of ganglion cell in cat retina, namely the alpha, beta, and gamma cells, were correlated with three main classes of physiological response types namely X, Y, and W (Boycott and Wassle, 1974; Enroth-Cugell and Robson, 1966; Cleland and Levick, 1974). 21 different morphological types of ganglion cell were of the non-alpha/non beta cells classes (Kolb et al., 1981).

Two types of ganglion cells were identified based upon their responses to grating stimuli (Enroth-Cugell & Robson, 1966). The X and Y pathways initiate in the retina, project in parallel to the LGN, and continue in parallel pathways to the visual cortex. Y-

cells correspond to a relatively rare, large cell called the *alpha* cell with fast axon conduction velocities, while X-cells correspond to a smaller cell called the *beta* cell with moderate axon conduction velocities. Y-cells, perhaps due to their large receptive field organization, are important for orienting to novel stimuli and for detection of motion (Marr, 1982), whereas X-cells, due to their small receptive field organization, provide the detail of the novel stimulus once there is foveal fixation. Both Y-cells and X-cells have center-surround receptive field organizations, with a nonlinear spatial summation for the Y-cell and a linear spatial summation for the X-cell. Y-cells contribute 4% of the total retinal ganglion cell population with a relatively even distribution throughout the retina, whereas the X-cells contribute 55% of the total retinal ganglion cell population with its highest density in the central retina decreasing proportionally with eccentricity. X-cells project almost exclusively to the LGN, whereas Y-cell projections divide synapsing both in the LGN and in the brainstem.

A third retinal system, the W-cell, corresponds anatomically to the *gamma* cell, which is a heterogeneous group of cells with large, yet sparse dendritic fields and small cell bodies with thin axons (Boycott & Wassle, 1974; McGuire et al., 1986), corresponding with slow axon conduction velocities (Cleland & Levick, 1974). The receptive fields of W-cells vary and include motion selective and other specialized cell types as well as the more common center-surround cells (Rodieck, 1979). W-cells may be either spatially linear like X-cells, or nonlinear like Y-cells (Sur & Sherman, 1982). The W-cell is almost as numerous as the X-cell, contributing 41% to the total retinal ganglion cell population (Stone & Hoffman, 1972). W-cells terminate on groups of cells near, or inside the LGN, or go to the brainstem.

Human Magnocellular and Parvocellular Pathways

The initial discovery of X and Y ganglion cells in the cat retina led to the ensuing discovery mostly from psychophysical investigations, of dichotomous subsystems in human vision (Breitmeyer & Ganz, 1976; Kulikowski and Tolhurst, 1973). The sustained system is mostly sensitive to high spatial frequencies and low temporal frequencies, while the transient system is mostly sensitive to low spatial frequencies and high temporal frequencies. The transmission time in the sustained system is generally slow with responses occurring throughout stimulus presentation, while transmission time is generally fast in the transient system with response to stimuli mainly at onset and offset. The sustained system predominates in central vision while the transient system predominates in peripheral vision and each may inhibit the other system (Lovegrove, 1991).

According to the prevailing view, two major human ganglion cell classes have been identified, namely the midget and parasol cells which project in parallel to the LGN and convey all the requisite information to the cortex for processing. These two major pathways are named magnocellular (M) and parvocellular (P) for the layers in the lateral geniculate nucleus with which they are associated (Shapley & Perry, 1986; Merigan & Maunsell, 1993). Both cell types can be further subdivided into a and b subtypes according to the level of their dendritic stratification in the inner plexiform layer (IPL). A fifth cell type, small bistratified cells, has also been identified (Dacey, 1994) with some blue-on ganglion cells associated with the koniocellular pathway (K) (Hendry and Reid, 2000; Xu et al., 2001).

Parasol cells, providing most of the input to the magnocellular layers of the LGN, are believed to correspond with the physiologically defined ON- or OFF-center phasic response and a non-opponent receptive field organization (M-type). M cells have larger perikarya and dendritic trees than P cells, and they are much less numerous, comprising at most, 10% of the retinal ganglion cells (Silveira & Perry, 1991). Although there are a and b subtypes of the parasol cells, they are not broadly stratified like the midget ganglion cells, but instead, their dendrites are confined to two narrow strata close to the center of the IPL (Dacey & Peterson, 1992; Watanabe & Rodieck, 1989). $GABA_A$ receptors are found exclusively on inner and outer foveal parasol cells. Immunostaining for this receptor led to the conclusion that about 6% of foveal ganglion cells are parasol cells with a three to four cell dendritic tree overlap (Grunert et al., 1993), whereas in the periphery, density varied between 3% and 27%, increasing proportionally with eccentricity, with a dendritic tree overlap of 3.4 (Silveira &Perry, 1991).

M cells are more sensitive to stimulus contrast, but they are not selective for stimulus wavelength (Kaplan et al., 1990). M cells exhibit a more transient response at all adaptation levels, and are also sensitive to moving or other rapidly changing stimuli (Purpura et al., 1990).

Midget cells (P-type) have small perikarya and project to parvocellular layers of the LGN, forming two cellular mosaics with dendritic stratification that branch either to the distal half (sublamina a), or the proximal half (sublamina b) of the IPL, and consequently are named type a and b (Dacey & Peterson, 1992; Watanabe & Rodieck, 1989). Midget cells indicate increased dendritic field size with eccentricity and a constant dendritic coverage factor of one indicates that there is no overlap of dendritic

trees of neighboring cells. Unlike parasol and small bistratified cells whose spacing is equivalent to the radius of the dendritic field, midget cells have spacing equivalent to the diameter of the dendritic field (Dacey, 1994). Hence, midget cells increase in relative numbers foveally to about 80% to 90% of the ganglion cells in the macaque retina, whereas this decreases proportionally to about 45% to 50% peripherally (Leventhal et al., 1981; Perry et al., 1984; Rodieck & Watanabe, 1993). This increase in the ratio of magnocellular to parvocellular geniculate cells with eccentricity (Connolly & Van Essen, 1984; Malpeli et al., 1993) is commensurate with a hypothesized increase in the ratio of parasol to midget retinal ganglion cells and that the density gradient of the midget ganglion cells projecting to the parvocellular layers is sufficient to account for the V1 cortical magnification factor (Schein & De Monasterio, 1987).

In the central retina, each midget ganglion cell receives input from a single cone (Watanabe & Rodieck, 1989), via a single midget bipolar cell (Kolb & DeKorver, 1992), with glutamate considered the neurotransmitter mediating synaptic transmission. Amacrine cells also synapse with midget ganglion cells, most of which use either GABA or glycine (Crooks & Kolb, 1991; Davenger et al., 1991; Hendrickson et al., 1988; Grunert & Wassle, 1990).

P cells have relatively sustained responses to light, which can either be hyperpolarizing or depolarizing, such that the amplitude and phase of the response varies with stimulus wavelength (Kaplan et al., 1990). Although midget ganglion cells provide the major projection to the parvocellular layers of the LGN, other non-midget ganglion cell types also project to the parvocellular layers (Rodieck & Watanabe, 1988), rendering the etiology of the color opponent signal ambiguous. However, the large numbers and

small receptive fields of the red-green opponent cells with center-surround organization have been shown, through intracellular recordings from peripheral macaque retina, to belong to the midget ganglion cell (Dacey, 1994). It is still unclear whether the receptive field structure of midget cells corresponds exclusively to the common center-surround pattern (Type I) or whether in some cases it has coextensive ON and OFF regions (Type II) (Reid & Shapley, 1992).

The small bistratified cell projects to the intercalated (interlaminer) layers of the LGN (Kaplan, 2003), and its dendritic morphology and coverage of about three is similar to that of the parasol cells. The dendritic tree of the small bistratified cell is divided into two strata that occupy positions close to the inner and outer portions of the IPL, with the inner tier creating a larger diameter field, denser branching and dendrites that contain complex spinelike appendages relative to the outer tier (Dacey, 1993a). These cells contact other small bistratified cells and a population of amacrine cells that also have small, bistratified dendritic fields. Small bistratified cells in both human and macaque contribute about 1% of the foveal ganglion cell population, increasing to about 6% to 10% in the far retinal periphery.

In vitro extracellular recordings from the small bistratified cell has been shown to correspond exclusively to the blue ON yellow OFF type of color opponent cell in the both the macaque retina and LGN (Dacey & Lee, 1994). Thus, the red-green and blue-yellow color opponent signals originate from other morphologically distinct ganglion cell mosaics that project in parallel to the LGN.

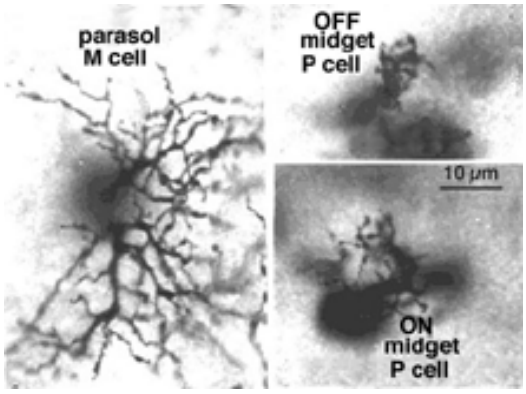

Figure 3: Golgi staining of human ganglion cells in central retina. Reprinted with permission from: Kolb, H., Fernandez, E., and Nelson, R. (2005) http:// webvision.med.utah.edu.

The Lateral Geniculate Nucleus

The ventral medial layers (one and two) contain large cells called the magnocellular layers and layers three to six contain small cells called the parvocellular layers. Neuronal receptive fields in the LGN retain the ON-center and OFF-center dichotomy as well (Hubel & Wiesel, 1959, 1962).

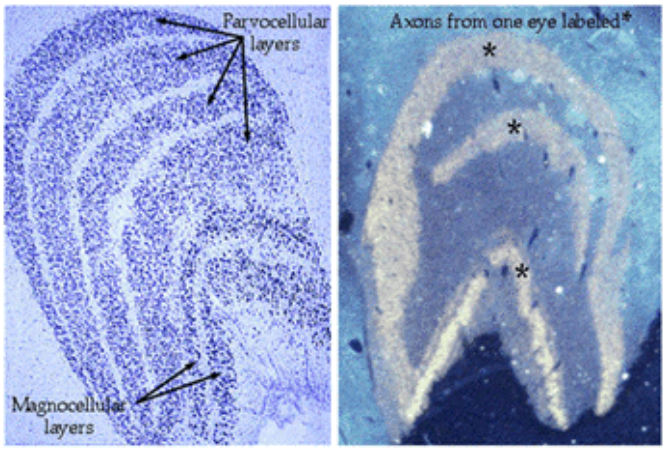

Figure 4: The projections of the small P, and large M ganglion cells from the two eyes to parvocellular and magnocellular layers of the LGN respectively. Reprinted with permission from: Kolb, H., Fernandez, E., and Nelson, R. (2005) http:// webvision.med.utah.edu.

Visual Cortex

The parvocellular pathway synapses to layer IVc*B*, while the magnocellular pathway synapses more superficially to layer IVc*a* (Hubel & Wiesel, 1972; Hendrickson et al., 1978). Within the cerebral cortex, the M and P pathways split from two pathways into three. M neurons from lamina IVc*a* travel to IV*B* of V1 send information to the thick stripes of V2, which then sends information to both V3 processing detailed spatial perception and V5 processing movement perception. P neurons from the interblobs of V1 send information to the pale stripes of V2 which send information to the inferior temporal cortex for complex shape analysis. Mixed M and P neurons in the blobs of V1 send information to the thin stripes of V2, which send information to V4 where the M cells process black and white brightness and the P cells process color (Tso & Gilbert, 1988).

Chapter 5: Related Biochemistry of the Visual System

This chapter describes the specific biochemical findings that led up to the hypothesis of selective pathway involvement. Furthermore, the chapter describes the links between the mitochondrial mutations, the subsequent oxidative compromise and the ultimate derivative apoptotic outcome in a hypertoxic milieu. Different prophylactic protocols are evaluated as they relate to the specific neurotoxic abnormalities.

Free Radicals and Oxidative Damage

Free radicals exist independently and contain one or more unpaired electrons (Halliwell, 1987; Borg, 1993). Through oxidation and reduction reactions, free radicals may damage a variety of macromolecules including DNA strand breaks (Devasagayam et al., 1991), DNA adduct formation (Dizdaroglu, 1991; Shigenaga & Ames, 1991), lipid peroxidation (Schaffer & Thorling, 1990), and the generation of protein carbonyl groups (Levine et al., 1990; Smith et al., 1991). Oxidative damage to macromolecules may alter their function leading to impaired cellular functioning and/or cellular death.

There are significant interactions between oxidative damage and energy metabolism. Oxidative phosphorylation generates most of the free radicals in the cell (Boveris & Chance, 1973), primarily ubiquinone and cytochrome $_{b566}$ of complex III (Nohl et al., 1978). Increases in free radical generation are typically concomitant with inhibitions of the electron transport chain (Turrens & Boveris, 1980).

A cycling process may occur between oxidative damage and OXPHOS since the OXPHOS system is not only responsible for generating free radicals, it is also vulnerable to damage by free radicals. Mitochondrial DNA is particularly susceptible to oxidative

damage probably due to its lack of protective histones, limited repair capabilities, and proximity to the electron transport chain (Linnane et al., 1989; Miquel, 1991; Wallace, 1992).

Another cycling mechanism may occur through cytochrome $_{b566}$ which may increase free radical generation due to reduced levels of ATP, which may in turn further increase oxidative damage to the OXPHOS system thereby further curtailing ATP levels (Nohl & Jordan, 1986). Furthermore, calcium cycling may further play a role in exacerbating the oxidative damage since oxidative stress may impair mitochondrial function due to excessive release and reuptake of mitochondrial calcium (Schlegel et al., 1992; Reichman et al., 1994).

The implications of these cycling processing are consistent with the mitochondrial dysfunction evidenced in LHON. Firstly, minor defects that mildly impair OXPHOS may become amplified over time. This is consonant with the majority of LHON probands with acute onset of the disease in the second or third decade of life after a longstanding period of free radical elevation and subsequent exacerbation of the oxidative stress. Similarly, mitochondrial dysfunction and oxidative stress have been implicated in other progressive, age-related neurodegenerative diseases, including Parkinson's disease, Alzheimer's disease, Huntington's disease and amyotrophic lateral sclerosis (Bowling & Beal, 1994). Furthermore, different combinations of genetic and epigenetic variables may differentially alter mitochondrial function and oxidative damage. These differential rates of amplification may explain the variable amounts of oxidative damage observed between and within LHON familial pedigrees.

Additional cycling mechanisms responsible for cell death may be due to interactions between oxidative damage and excitotoxicity. Impaired energy metabolism may enhance excitotoxic damage by several mechanisms including decreases in ATP levels, reduced sodium-potassium ATPase activity, partial cell-membrane depolarization, and relief of the voltage-dependent Mg^{2+} block of N-methyl-D-aspartate (NMDA) associated receptors (Beal, 1992).

NMDA receptor activation generates superoxide (Lafon-Cazal et al., 1993a, 1993b) and stimulates production of nitric oxide synthase which consequently generates nitric oxide (N0) (Moncada & Higgs, 1993), superoxide (Pou et al., 1991) and hydrogen peroxide (Heinzel et al., 1992). These reactive oxygen species may further impair the functioning of many macromolecules (Bowling & Beal, 1994). NO may react with superoxide to produce peroxynitrite, a powerful oxidant (Beckman & Crow, 1993). Furthermore, NMDA receptors contain redox modulatory sites where oxidized nitric oxide congeners may react with thiol groups to downregulate channel activity (Lipton et al., 1993). Ionotropic GABA, an inhibitory transmitter, has also been shown to inhibit NO production, which in turn inhibits NO-stimulated transporter-mediated GABA release, indicating a mutual feedback mechanism regulating the NO/cGMP signal transduction pathway and GABA in the retina (Yu & Eldred, 2003).

Antioxidants have been shown not only to decrease kainate-induced neurotoxicity (Dykens et al., 1987; Puttfarcken et al., 1993), but also have been associated with the generation of free radicals (Sun et al., 1992b) and increased lipid peroxidation (Puttfarcken et al., 1993; Sun et al., 1992). Free radicals have been shown to be

associated with both the increased release (Pellegrini-Giampetro et al., 1988; Gilman et al., 1994) and decreased uptake of excitatory amino acids (Volterra et al., 1993).

Interestingly, a recent study evaluating serum and plasma samples from 43 male and female affected and unaffected members of a large Brazilian 11778 pedigree, haplogroup J, revealed no significant differences in circulating levels of total antioxidants, lipid peroxidation products, interleukin-3 (IL-3), and tumor necrosis factor-α, (TNF-α). However, neuron-specific enolase (NSE) levels were significantly elevated in male carriers as compared to male normal controls. These carriers also manifested other subtle subclinical abnormalities such as Tritan color defects and prolonged latencies in pattern reversal VEP (Lam, et al., 2003).

Ultimately, what may be critical to a successful therapeutic intervention is the understanding that these cycling processes that produce cellular death may involve similar pathways responsible for both defects that initially increase oxidative damage and for defects that initially impair mitochondrial function. As such, antioxidants and other compounds that improve mitochondrial function may be critical in retarding and even arresting the cellular death evidenced in LHON and other neurodegenerative diseases.

On the other hand, it is still unclear why the optic nerve, which is not as sensitive to a hypoxic insult as other cortical structures like the hippocampus, cerebellum and/or basal ganglia, is so selectively vulnerable in LHON. For example, in Leigh's Disease, calcifications in the basal ganglia are indicative of acute oxidative failure, which can be elicited via carbon monoxide poisoning. The underlying mechanism subserving the selectivity of optic nerve in LHON remains unresolved.

Selective Neurotoxicity: Excitatory Amino Acids

Excitatory amino acids (EAAs), critical in neurotransmission in the retina, brain and spinal cord, bind onto postsynaptic receptors and typically stimulate, or depolarize the postsynaptic neuron (Watkins & Evans, 1981; Miller & Slaughter, 1986; Mayer & Westbrook, 1987). Glutamate, considered to be the major excitatory neurotransmitter in the retina, is used in the synthesis of proteins, other amino acids and even other neurotransmitters (Stryer, 1988).

In a study investigating the role of excitatory amino acids (EAA) receptors in primate retinal ganglion cell function, APB (30-100 *u*M) was found to reduce or block the light-evoked responses and resting firing rates of the extracellular recordings from all ON-center ganglion cells, while higher doses (100 *u*M) were necessary to block the light-evoked responses of ON-transient cells (Cohen & Miller, 1994). Conversely, an increase in resting firing rates was observed when L-APB was applied to some OFF-center ganglion cells. Furthermore, the EAA agonist kainate (10-20 *u*M) and NMDA (200-350 *u*M) increased the firing rate in virtually all ganglion cells.

Similarly research with $GABA_A$ (γ-amino butyric acid) agonists and antagonists is consistent with the aforementioned research. GABA is considered to be the most common neurotransmitter in all vertebrate classes (Marc, 1992) and is released, sometimes with other cotransmitters, by a variety of amacrine cell types (Massey & Redburn, 1987, Daw et al., 1989; Freed, 1992). The intracellular recordings from perfused cat retina indicated that the $GABA_A$ agonists dAVA (δ-amino valeric acid), THIP, or muscimol reduced the photic-response amplitude, slowed response onset and offset and depolarized the dark membrane potentials in cat retinal horizontal cells

(Frumkes & Nelson, 1995). Similarly GABA agonists influenced amacrine and ganglion cells in that their responses were also slower and less phasic. In all cell types, response kinetics was most affected with flicker stimuli, indicating susceptibility to a transient response, as opposed to a sustained one.

However, the ON bipolar cell appears uniquely vulnerable. For example, the mGluR6 receptor can be selectively removed via selective pharmacological blocking agents (i.e., APB) or site directed mutagenisis techniques designed to eliminate the mGluR6 receptors, without major effect on other neural pathways. Furthermore, mutations and disease processes unrelated to mGluR6 selectively target ON bipolar cells. Nocturnal vision deficits, such as melanoma-associated retinopathy (Alexander et al., 1992; Berson and Lessell, 1988) and congenital stationary night blindness (Alexander et al., 1992), appear dependent on the physiological integrity of ON bipolar cells.

On the other hand, GABAergic mechanisms were studied (Frumkes et al., 1995) in the cat retina by exogenous application of the $GABA_A$ antagonists picrotoxin (PTX), native bicuculline (BCC), and bicuculline methyl bromide (BCC MeBr). Both PTX and BCC MeBr had relatively little influence upon the response characteristics of horizontal cells, while BCC tended to decrease the amplitude of, to slow the photic response to light onset, and to both quicken and increase the amplitude of the photic response to light offset. Furthermore, the extracellular recordings from ON/OFF and X/Y ganglion cell types became considerably more transient with the application of PTX, native BCC, or BCC MeBr. This tendency was greatest in OFF ganglion cells. A more detailed analysis of EAA's, specifically glutamate receptors can be found in Appendix 4.

Glutamate Transporters

Glutamate transporters have been identified on photoreceptors and Muller cells (Marc & Lam, 1981; Tachibana & Kaneko, 1988). The average concentration of glutamate, from glutamate labeling studies, in photoreceptors, bipolar cells, and ganglion cells is 5mM (Marc et al., 1990). Physiological studies using isolated cells indicate that only *u*M levels of glutamate are necessary for glutamate receptor activation (Aizenman et al., 1988; Zhou et al., 1993). Thus, the amount of glutamate released into the synaptic cleft is several orders of magnitude higher than the concentration required for receptor activation. High affinity glutamate transporters rapidly remove excess glutamate from the synaptic cleft to prevent neurotoxicity (Kanai et al., 1994).

Two classes of glutamate transporters have been identified. One reflects the transporters located on synaptic vesicles within presynaptic terminals. These vesicular transporters selectively concentrate glutamate into synaptic vesicles in a Na+-independent, ATP-dependent manner that requires chloride (Tabb & Ueda, 1991; Fykse & Fonnum, 1996). The second type of transporter, located in the plasma membrane of neuronal and glial cells, transports glutamate in a Na+-and voltage-dependent manner independent of chloride (Brew & Attwell, 1987, Kanai et al., 1994)

Glutamate receptors with transporter-like pharmacology have also been identified in photoreceptors (Picaud et. al, 1995a,b) and ON-bipolar cells (Grant & Dowling 1995,1996). These receptors are similar to glutamate transporters in that the glutamate-elicited current is dependent upon external NA+, is reduced by transporter blockers and is insensitive to glutamate agonists and antagonists (Connaughton, 1997). At the

photoreceptor terminals, this glutamate-elicited chloride current may regulate membrane potential and subsequent voltage-gated channel activity (Picaud et al., 1995a).

The unique status of the NMDA receptor as both a ligand and a voltage-dependent ion channel has led many researchers to hypothesize that neuronal membrane potential is a critical variable in modulating excitotoxicity (Zeevalk & Nicklas, 1992; Beal et al., 1993c). Specifically, membrane depolarization has been proposed as one mechanism linking metabolic compromise and excitotoxicity. When a system is metabolically compromised, there is insufficient neuronal ATP to sufficiently activate the membrane ion pumps, particularly the Na+, K+ -ATPase (Erecinska and Dagani, 1990; Haddad & Jiang, 1993). The resultant neuronal depolarization may relieve the voltage-dependent magnesium blockade of the NMDA receptor ion channel, leading to toxic receptor activation by ambient glutamate (Zeevalk & Nicklas, 1991, 1992; Albin & Greenamyre, 1992; Beal et al., 1993c).

Various in vitro and in vivo paradigms have shown that metabolic inhibition can lead to NMDA receptor-mediated ecitotoxic neuronal death (Novelli et al., 1988; Zeevalk & Nicklas, 1990; Turski et al., 1991; Beal et al., 1992, 1993a). Graded titration of membrane potential by increasing extracellular K+ levels has been shown to mimic the excitotoxicity produced by graded metabolic inhibition (Zeevalk & Nicklas, 1991). Furthermore, it has been shown in chick retina that following mild metabolic inhibition, cells undergo an NMDA receptor-mediated excitotoxic death without elevations in levels of extracellular EAAs (Zeevalk & Nicklas, 1992). Perhaps more importantly, in the same paradigm, the neuronal death was prevented by increasing the extracellular magnesium concentration, suggesting that the excitotoxic NMDA receptor activation and subsequent

relief of the magnesium blockade, was a result of the magnesium blockade of the ion channel (Zeevalk & Nicklas, 1992). This hypothesis is further supported by the finding that potassium channel activators abolished the excitotoxicity produced by magnesium-free, glycine-supplemented solutions in cultured hippocampal neurons (Abele & Miller, 1990).

Stereotaxic, intrastriatal injection of the competitive, reversible, succinate dehydrogenase (SDH) inhibitor malonate has been shown to cause dose-dependent neurotoxicity by inhibition of SDH and depletion of striatal ATP (Beal et al., 1993b, Greene et al., 1993; Greene & Greenamyre, 1995b). The overt toxicity of malonate is mediated almost exclusively by the NMDA receptor (Henshaw et al., 1994; Greene & Greenamyre, 1995a) and has been shown to exacerbate the toxicity of direct-acting glutamate agonists in vivo (Greene & Greenamyre, 1995b). In subsequent research, it was shown that the coinjection of the K+ channel activator minoxidil to reduce depolarization attenuated the toxicity without affecting malonate-induced ATP depletion (Greene & Greenamyre, 1996). Specifically, injection of minoxidil had no effect on ATP levels in both control striatum or on ATP levels following malonate injection, thereby precluding a simple interference of minoxidil with malonate inhibition of metabolism. These results suggest that membrane depolarization exacerbates malonate neurotoxicity, whereas conversely, membrane hyperpolarization protects against malonate-induced neuronal damage. It is as yet unclear whether minoxidil injection in vivo directly induces membrane hyperpolarization, or simply attenuates the malonate induced membrane depolarization, but in vitro studies more strongly supports the latter (Ben-Ari et al.,

1990). A more detailed discussion concerning metabolic inhibition and membrane potential is included in Appendix 5.

Chapter 6: VEP

This chapter reviews the history and progress in the evoked potential literature and discusses the rationale for selecting VEP as a means to investigate the current hypothesis of subclinical involvement of the visual system. The ability to differentially assess specific pathway involvement rendered the VEP a critical tool in evaluating these subclinical abnormalities.

Theoretical Overview

The human cerebral cortex, although only 2 mm thick, has a surface area of 2000 cm^2 with an estimated 10^{10} neurons, due to its many folds and invaginations (Hubel and Wiesel, 1977). Despite impressive advances in the understanding of the physiological and pharmacological codes of the central nervous system, the inherent complexity and intricacy of the neural networks of the human cerebral cortex still results in an enormous gulf between the realm of cellular neurobiology and that of human perception and cognition.

Historically, studies investigating the relationship between responsivity and the underlying cortical activity did so via direct, albeit gross, intracortical (microelectrode) monitoring of sets of neurons as they responded to differing stimuli. These methods, however, do not yield precise information on the time course of the neural activity that underlies perceptual and cognitive brain functions.

Electrical activity recorded from the scalp is reflective of the neural pathways engaged in sensory, motor, or cognitive processing. The electrical activity of the brain is generated by electrical potential changes from the membranes of cortical neurons in response to a variety of neuronal inputs from neighboring cells as well as from the

generator of rhythmic activity in the thalamus. The resting potential of all neurons represents a difference in electrical potential between the interior of the cell and the extracellular space. Each neuron contacts an estimated 3000-5000 other neurons potentiating a multitude of inputs, some excitatory and some inhibitory, that are summed within the cell body. Changes in the potential reflect the spatial and temporal summation of neuronal post-synaptic activity. An excitatory postsynaptic potential (EPSP) reflects the depolarization caused by transmitter released from a presynaptic cell, and an inhibitory postsynaptic potential (IPSP) reflects the hyperpolarization caused by transmitter released from a presynaptic cell. Thus, either an action potential will be generated that will travel to the axon terminal, or an action potential will be prevented due to the sign (positive or negative) and magnitude of ionic flow.

The nerve action potentials (NAPs) of presynaptic neurons cause the release of neurotransmitter from the nerve terminal which then diffuses across the presynaptic space to the postsynaptic neuron. An interaction with the receptor occurs producing a change in the permeability of the membrane to some specific ions, resulting in the change of the postsynaptic membrane potential. These potential differences that can be recorded between surface electrodes of amplitudes between 5 and 100 *u*V, constitute the ongoing electrical brain activity and the elicited electrical activity from specific stimuli that are being measured in EEG and VEP techniques.

History

About a century ago, both spontaneous brain rhythms and evoked potentials were reported (Caton, 1875). Spontaneous or intrinsic brain rhythms reflect the random

fluctuations of electrical activity that can be recorded from the scalp with surface electrodes. Evoked potentials, on the other hand, are not spontaneous and reflect the electrical activity elicited by specific sensory stimulation.

Electroencephalography (EEG) was ideal for human research for it established the first *noninvasive* monitor of widescale cortical activity (spontaneous brain rhythms). The EEG measures areas of neuronal activity as records of voltage fluctuations across a wide range of frequencies and is best used to record neocortical alterations in activity across a time continuum of a few seconds. The most well-known rhythm, the alpha wave has a frequency of about 10 hertz (Hz), or cycles per second. Other waves are slower (i.e. delta at 0.5-3.5 Hz and theta at 4-7 Hz), while others are faster (i.e. beta at 13-30 Hz).

Evidence of cortical responsivity to visual stimuli had been documented since the inception of EEG research, with the demonstration of a 10cps *a*-rhythm only present in the EEG when a participant's eyes were closed (Berger, 1932). The viability of recording from the occipital cortex was first demonstrated in studies employing regularly repeated flashes of light (Adrian and Mathews, 1934). These original studies were of scientific interest only, since the evoked response was only demonstrated in a small percentage of normal participants (Harding, 1974). Essentially, it has been the growth in computer technology that has potentiated our current ability to record the evoked electrical responses of human participants reliably. The inherent problem with the signal to noise ratio is that the evoked response is marginal as compared to the background EEG. These computer averaging techniques rely on the axiom that the evoked response is time-locked to the stimulus whereas the underlying EEG is random in its relationship to the stimulus. As a result, common features in the signal will sum to produce a clear signal while

random, biological EEG noise will approximate to zero. In essence, this technique of time-locking affords the capability of seeing the stimulus evoked waveform, which prior to computer averaging techniques, used to be embedded in the EEG noise. The signal is further enhance via However, if stimulus induced changes exist in the background EEG, they may contaminate the evoked potential signal by reducing a true response to noise.

The visual evoked potential (VEP) is the sum of a large number of excitatory and inhibitory postsynaptic potentials occurring on apical dendrites of pyramidal cells in the occipital cortex in response to visual stimulation (Creutzfeldt & Kuhnt, 1973; Zemon et al., 1986). These electrical potential differences are designated both in terms of their polarity and peak latency. Scalp electrodes monitor and transmit this cortical response originating primarily from the central retinal cones. The participant is treated as a "black box" to which the presentation of a stimulus will elicit a specific and measurable response.

Comparison of Electrophysiological Methodologies

In essence, the VEP differs from the EEG in three basic ways. First, an identifiable latency period can be measured from stimulus onset to evoked potential recordings from the scalp (Regan, 1979). This latency is contingent upon several neurological factors including the conduction velocity of the neural impulses and the conduction distance between the point of stimulation and the point of scalp recording (Chang, 1959). Latency measurements are considered a clinically useful parameter since these measurements remain relatively fixed and consistent within individual experimental

trials. Latency has been shown to decrease with increasing stimulus pattern size, increasing luminance and increasing contrast (Sokol, 1990).

The second difference relates to the anatomical correlate of the electrical activity. Specifically, VEP traces reflect activity from the occipital cortex.

The third difference is that the VEP produces characteristic waveforms reproducible under similar experimental conditions (Chang, 1959) as opposed to the ongoing electrical activity of the EEG which does not conform to any specific response characteristic. The VEP components that are typically measured in clinical research include P0 (P naught), occurring approximately 60 msec after stimulus onset, N1 occurring approximately 80 msec after stimulus onset, P1, occurring approximately 100 msec after stimulus onset and N2 occurring approximately 130 – 200 msec after stimulus onset .

The initial positive wavelet, P0, is thought to reflect afferent activity arriving at the cortex from the LGN and an initial depolarization deep in the cortex as a result of afferent activity from the lateral geniculate nucleus (LGN). The subsequent negativity, N1, is thought to reflect the spread of the initial depolarization and/or excitatory postsynaptic potentials mediated via intracortical pathways generated on superficial segments of apical dendrites. The later positive wave has been associated with GABA-mediated intracortical inhibition and superficial hyperpolarization (Zemon, Kaplan & Ratliff, 1980; 1986). Interestingly, many of the GABAergic synapses are located on apical dendritic shafts and spines of pyramidal cells (Somogyi et al., 1989), the site of VEP electrogenesis.

It is critical for one investigating cerebral recordings to appreciate that although evoked potential recording is the only method to date that yields precise information on the time course of the neural activity underlying higher brain functions, it is as yet a relatively undifferentiated response. This is because it reflects a net electrical response from parallel processing within the various subsystems of the visual system at large. Thus, the VEP waveform, the timing of each peak and trough, and the duration of the potential, have been a largely controversial issue regarding absolute criteria for extricating the evoked response embedded in the EEG noise.

The etiology of background EEG noise is complex and multivariate. Noise may be due to afferent flux from interoceptors and proprioceptors independent of any specific sensory stimulus (Linasley & Wicke, 1974), muscle activity, electrode motion artifacts and thermal noise in the EEG amplifier (Norcia, 1992). 60Hz currents, introduced into the system by inductive, resistive coupling from power lines have been reported to account for over 90% of instrumental difficulties (Stacy, 1960). VEP researchers are therefore careful to properly shield electrical connections, thus controlling for one source of this bias. The difficulty in measuring a true response is exacerbated by the fact that EEG signals typically reach amplitudes between 50 and 100 μV, whereas VEP signals can be as small as 0.5 and 1 μV (Regan, 1989).

Due to the inherent inability of precise neuronal input localization with EP recordings, many researchers complement EP studies with other brain imaging techniques such as nuclear magnetic resonance (NMR) imaging, positron emission tomography (PET scan), and regional cerebral blood flow. Whereas EP recordings offer excellent temporal, but poor spatial resolution, these powerful imaging techniques offer

precise spatial, but poor temporal resolution. An emerging technique, neuromagnetic recording, promises the spatial precision of the imaging techniques with the temporal resolution of the electrophysiological techniques in the hope of establishing the neural correlates of both sensory perception and cognitive decision making.

Recording the VEP

Scalp electrodes from an observer viewing a pattern on a video monitor record the underlying electrical activity elicited by modulation of a specific pattern. The electrical brain potentials transmitted into a differential amplifier serves to augment the EEG signal. This analog EEG signal, measured in volts, is then transmitted to an analog-to-digital-converter (ADC), which digitizes the individual voltages represented by a sequence of numbers rather than as a continuous function of time. This is achieved by the consistent sampling of the analog signal at regular intervals which is then numerically expressed as a sequence of voltage levels. The EEG voltage expressed in numerical form can then be stored and later retrieved as binary data (Regan, 1989).

Electrode Placement

Attempts to standardize electrode placement in order to reduce waveform variability resulting from differential electrode sites have yielded the ten-twenty electrode system with electrode placement over specified areas of the brain independent of skull size. The anterior-posterior (A-1) measurements are based on distance between the nasion[1] and the inion[2] as measured along the midline of the head over the vertex. Five

[1] The bridge of the nose, level with the eyes.

points are marked along this line, designated frontal pole (Fp), frontal (F), central (C), parietal (P), and occipital (O). Point Fp is 10% of the nasion-inion distance above the nasion point; F is 20% of the distance from point Fp and so on in 20% steps for points C, P, and O. Lateral measurements are based on the distance between the left and right preauricular points measured through point C at the vertex. 10% of the distance from the preauricular points[3] gives the right and left temporal point (T), and 20% above the temporal points lay the central points (C).

Stimuli

Transient VEP

Transient visual evoked potentials represent cortical responses to visual stimuli elicited typically by contrast reversing spatial patterns such as gratings and checkerboards (Regan, 1989). The neural mechanisms associated with the transient evoked potential return to their resting potential before each successive stimulus, yielding in theory, independent waveforms.

In theory, this type of analysis would require data collected from independent epochs, which is both inconsistent with conventional VEP recording techniques and impractical with any population with limited attention. Furthermore, this method of repeated stimulus presentations has been shown to cause adaptation and thereby distort the recorded response (Mackey, 1977; Jeffreys, 1977; Barber & Galloway, 1977).

Analysis of the derivative transient waveform from the signal averaged EEG has also been criticized for its inherent subjectivity in selecting positive and negative

---

[2] The bony lump at the base of the skull on the midline, at the back of the head.

[3] The points where the external ear flaps merge with the scalp on the face side.

deflections from the raw EEG waveform. Hence, true amplitude and latency values from the transient waveform have always been suspect. A relatively new technique (discussed below) has been introduced (Zemon et al., 1999), based on statistical estimates of magnitude-squared coherence (MSC), which yields an objective criterion for determination of a significant transient VEP.

Steady-State VEP

Steady-state evoked potentials represent cortical responses to visual stimuli at relatively high frequencies. The repetitive nature of the steady-state evoked potential yields a waveform whose constituent discrete frequency components remain constant in amplitude and phase for the duration of the stimulus presentation. The temporal rate that distinguishes these two methods of VEP recordings occurs somewhere around 4Hz; temporal rates above 4Hz would be classified as steady-state, and temporal rates below 4Hz would be classified as transient.

The fast, repetitive nature of the stimulus presentation is not associated with any distinctive characteristics in the recorded waveform but rather, the response is precisely defined within the frequency domain where the power resides at the harmonic multiples of the fundamental frequency. Extraction of the steady-state VEP is thus possible via Fourier analysis of the waveform and rejecting all those frequencies that are not harmonic multiples of the fundamental frequency.

Swept -Parameter VEP

Sweep VEPs reflect an efficient method of VEP recording where only one

parameter is varied rapidly in time, such as contrast, spatial frequency, or check size (Regan, 1973; Tyler et al., 1979; Nelson et al., 1984; Seiple et al., 1984; Norcia & Tyler, 1985; Norcia et al., 1989; Zemon et al., 1997). Sweep VEPs allow for the measurement of a variety of visual functions in a short period of time (10 seconds as opposed to a minute or more), rendering this type of stimulus presentation valuable in probing visual processes in observers with a limited attention span. The brief presentations reduce the possibility of extraneous variables such as loss of fixation, biological noise or neural changes over time distorting the evoked signal. Furthermore, the sweep method affords the recording of independent multiple samples, which by definition improves the signal-to-noise-ratio by the square root of the number of stimulus presentations.

By means of synchronous data collection and signal averaging of independent samples along with Fourier analysis, swept-transient VEPs are able to be analyzed in the frequency domain (Zemon & Ratliff, 1982; Zemon et al., 1995). Synchronous data collection guarantees the sampling of the EEG at precisely the same points in time in sequential stimulus presentations. As such, the response can be broken down into a series of bins of data whereby one bin lasts about one second and each bin contains the data from one complete cycle of a contrast-reversing stimulus.

Data collected from each run from a sweep is Fourier analyzed and then averaged. MSC estimates quantify signal-to noise-ratios and provide an objective measure of visual acuity.

Chapter 7: Hypotheses

Endemic to mtDNA mutations is the axiom of oxidative phosphorylation (OXPHOS) compromise which renders the biological system more vulnerable to excitatory amino acid (EAA) toxicity. Although the exact mechanism of neurotoxicity is not established, subclinical VEP abnormalities are hypothesized in LHON, as with other mitochondrial diseases which express selective impairments.

Magnocellular and ON pathways are hypothesized to express neurotoxic damage earlier in LHON. This hypothesized specificity is contingent upon research implicating these larger cell types as more metabolically active, thus rendering them more susceptible to compromises in net ATP from a faulty OXPHOS system. Furthermore, the magnocellular pathway has been implicated in other disease states such as glaucoma (Greenstein et al., 1998), retinitis pigmentosa (Alexander et al., 2005), schizophrenia (Butler et al., 2001; 2005), Duchenne muscular dystrophy, and early-onset Alzheimers. Nocturnal vision deficits, such as melanoma-associated retinopathy (Alexander et al., 1992; Berson and Lessell, 1988) and congenital stationary night blindness (Alexander et al., 1992) appear dependent on the physiological integrity of ON bipolar cells.

VEP technology has afforded the ability to differentially assess the contributions of these subsystems and the dissociation of one pathway from the other has potentiated the assessment of the contribution of each in various disease states. VEP stimuli aimed at probing ON/OFF and M/P specificity were used to evaluate this hypothesized selective pathway involvement. Low standing contrast, broadband spectral stimuli accentuates the VEP recordings from the M pathway, while high standing contrast, or isoluminant stimuli accentuates the P pathway VEP recordings. The M and P pathways, further subdivided

into ON and OFF pathways reflect the differential response to stimulus onset and offset, which can be assessed via positive and negative contrast stimuli, respectively.

Based on these hypotheses, the aims of the current protocol included:

1. The utilization of classic VEP stimuli to detect subclinical abnormalities in asymptomatic LHON individuals positive for the 11778 mtDNA mutation.
2. The utilization of specialized VEP stimuli aimed at probing ON/OFF and M/P specificity to detect selective pathway involvement.

Methods

Participants

Eligibility criteria for the LHON group included positive confirmation of the 11778 mtDNA mutation and normal or corrected to normal visual acuity. Exclusion criteria included positive confirmation of other primary or secondary mtDNA mutations. Six LHON participants, positive for the 11778 LHON mutation exclusively, were recruited from the International Foundation for Optic Nerve Disease (IFOND) registry. All LHON families on the registry were contacted. However, due to the rarity of the disorder, recruitment was, disappointingly low.

A baseline group of eight controls similar in age, race and sex was also evaluated. Initially, a matched design was intended. However, after testing two additional controls in anticipation of recruited LHON participants who never took part in the study, an unmatched design with unequal N had to be employed.

All participants were tested with a Snellen eye chart. The mean visual acuity, either normal or corrected-to-normal, was 0.8 (20/25) for the unaffected LHON participants in both eyes and better than normal VA averages were obtained for the controls of 1.2 (20/16) in both eyes.

A 72-year old affected male LHON participant, with a previous history of heavy alcohol consumption, positive for the 14484 mtDNA mutation was tested as well. His best corrected visual acuity on initial evaluation was 20/400 in each eye. Folow- up exams over the next four years indicated that the patient's visual acuity gradually returned to 20/20 in each eye along with bilateral improvement in visual fields, VEPs and color vision. Surprisingly, the discs developed pallor and the nerve fiber layer (NFL)

thinned as the vision improved. Mitochondrial DNA testing revealed a 14484 mutation, associated with a 50% spontaneous remission rate.

The patient's present Snellen acuity was 0.5 (20/40) in both eyes (20 years after initial improvement in visual function). While recognizing that this patient harbored another mutation, and that in general, patients exhibiting recovery of function still express abnormalities in the VEP, (e.g. multiple sclerosis patients with nearly complete visual recovery after onset of optic neuritis), the VEP records from the affected LHON individual were used to evaluate the correlation between clinical visual symptomology within the context of potential subclinical differences or deficits within the unaffected LHON sample.

Tenets of the Declaration of Helsinki were followed, and approval for human testing was obtained from the institutional review board (IRB) of the Nathan Kline Institute for Psychiatric Research in Orangeburg, N.Y. Informed consent, outlining both the purpose and the procedure of the study, was obtained from all participants before participation in the protocol (see Appendix 4).

Procedures

1. Snellen Acuity testing was performed on each participant to ensure that he/she met visual eligibility criteria.
2. Participants were also tested with two techniques for eye dominance to ensure convergent validity. In the first technique, participants were asked to look through a tube monocularly and to decide which eye provided a more optimal view. The preferred eye was the dominant eye. In the second technique, each

participant was asked to cover one eye, and to look at a corner of the room with the other eye with his/her thumb directly in that corner in the center of his/her field of vision. The participant was then asked to cover the other eye and to determine through which eye it appeared that there was more movement of his/her thumb. The eye through which there was less apparent motion was the dominant eye.

3. Participants in the asymptomatic LHON group all carried the same 11778 mtDNA mutation.
4. Participants were tested in one day at the Nathan Kline Institute. VEP testing was monocular. Sessions were approximately an hour and a half in duration.

Equipment

A VENUS system (Neuroscientific Corp., Farmingdale, NY) was used to generate the stimuli, record the electrophysiological signals and initially analyze the data. The VENUS system includes optically-isolated differential amplifiers, an analog-to-digital-converter, hardware and software capabilities for stimulus generation, and linearization software that incorporates look-up-tables to correct for distortions in the visual display. A photometer was also used for calibration and luminance measurements, and a photo-diode calibrator was used to linearize the monitor. Stimuli were displayed on a Princeton Ultrasynch RGB monitor with a frame rate of 119.03 Hz (noninterlaced). The EEG sampling rate was four times per frame.

Rationale

The paradigm included stimulus conditions such as conventional checkerboard and grating stimuli to assess visual function in general and other stimulus conditions aimed at probing magnocellular vs. parvocellular and ON vs. OFF pathways. These preferential testing paradigms have been used previously in retinitis pigmentosa (Alexander et al., 2005), glaucoma (Greenstein et al., 2001), and schizophrenia (Butler et al., 2001).

The magnocellular pathway is more sensitive to low luminance contrast than the parvocellular pathway, and therefore saturates more quickly with increasing luminance contrast (Kaplan, 1991). In fact, the contrast sensitivity of M cells is nearly ten times greater than that of P cells (Kaplan & Shapley, 1982; 1986). Research has further shown that parvocellular cells do not even respond below 8% contrast (Tootell et al., 1988). Therefore, low luminance stimuli are biased for a magnocellular response whereas high standing luminance contrast levels are biased for a parvocellular response. Furthermore, the magnocellular pathway is also preferentially sensitive to larger element size (low spatial frequency), whereas the parvocellular pathway is preferentially sensitive to smaller element size (high spatial frequency) (Merigan & Maunsell, 1993). The stimuli employed were designed to accentuate these differences.

The luminance contrast sweep has been shown to elicit differences in amplitude compression and phase advance ascribed to differential contrast gain control mechanisms. Contrast-response functions elicited from the M and P pathways indicate differential contrast sensitivities (Kaplan & Shapley, 1986). The M pathway exhibits high contrast sensitivity whereas the P pathway exhibits low contrast sensitivity.

Neurons from the M pathway produce contrast-response functions that rise steeply in the low contrast range (~0-10%) and tend to saturate or asymptote at low contrast. The slope of the initial segment of the function defines the contrast gain control. On the other hand, contrast response functions elicited from the P pathway rise gradually and uniformly with increasing contrast.

The isolated, positive-contrast (bright check) and negative-contrast (dark check) stimuli have been shown to elicit responses suggestive of asymmetries in contrast gain and spatial tuning between the ON and OFF subsystems. Specifically, the OFF subsystem has been shown to exhibit greater contrast gain and process finer spatial detail than the ON subsystem (Zemon et al., 1988), which is consistent with the morphological evidence of smaller dendritic fields in human OFF ganglion cells (Dacey & Petersen, 1991).

Stimuli

Viewing distance was at 114 cm, such that the square display subtended a visual angle of 8 deg. The display always had a static background luminance of 100 cd/$m^{2.}$ Presentation of stimuli was counterbalanced for both eye and order of stimuli, to mitigate confounds of order effects and eye dominance effects

Steady-State VEPs to a Grating-Spatial Frequency Sweep

The first stimulus condition used was a grating spatial frequency sweep with horizontal square-wave grating patterns of 4, 8, 16, 32, 64 and 128, contrast reversing at ~8 Hz with a square-wave temporal signal. A square-wave pattern was employed because

the sharper edge provided a better accommodative stimulus for visual acuity assessments and it also diminished the effects of residual nonlinearities in the display. Contrast was fixed at 80%. Gratings were swept in six discrete octave steps of increasing spatial frequency which helped reduce the effects of adaptation within spatial frequency channels. The stimuli spanned the broad spatial frequency spectrum of human vision in a brief interval of time, which not only facilitated correct accommodation but also increased the likelihood of collecting uninterrupted useable data (Zemon et al., 1997). Each octave step was one second in duration, which resulted in a six second sweep. The square-wave gratings were measured in cycles per degree of visual angle (c/d), ranging from 0.5 c/d to 16 c/d. Figure 5(a) represents a classic grating pattern.

Transient VEPs to a Contrast-Reversing Checkerboard

The second stimulus condition in the series involved a conventional contrast-reversing 32x32 checkerboard pattern (15 min checks), with a contrast-reversal frequency of ~1Hz and a square wave temporal signal to evaluate transient VEP records. Stimulus duration was 60 s. Contrast was fixed at 30%. Contrast may be defined by the *Michelson* equation:

$$C_M = (L_{max} - L_{min})/(L_{max} + L_{min})$$

where C_M is the contrast and L_{max} and L_{min} represent the maximum and minimum luminance values of the stimulus. Figure 5(b) shows a classic checkerboard pattern.

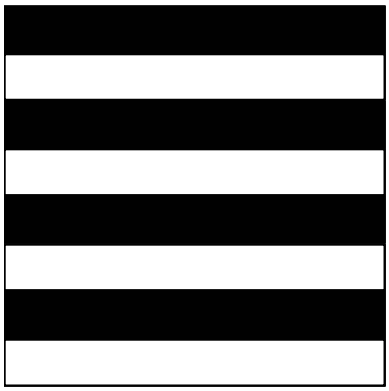

Figure 5a: Classic grating stimulus

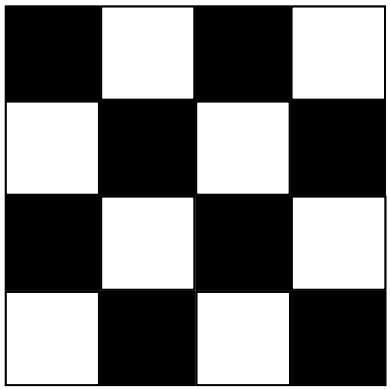

Figure 5b: Classic checkerboard pattern

Transient VEPs to a Checkerboard Sweep

The third stimulus condition in the series comprised checkerboard patterns of 8x8, 16x16, 32x32, 64x64 and 128x128, where size of check was swept in decreasing size (increasing check number) and contrast reversals were modulated by a ~1 Hz square-wave temporal signal. Contrast was set at 100%. Each of the five check sizes, presented for two seconds, comprised two cycles of contrast modulation. The first second served as an adaptation stimulus, and was not included in the analysis.

Steady-State VEPs to an Isolated-Check Size Sweep

The fourth stimulus condition employed a sweep through an array of isolated check patterns of 2x2, 4x4, 8x8, 16x16, 32x32, 64x64, and 128x128, with fewer checks corresponding to larger check sizes. Luminance of the isolated checks was modulated sinusoidally in time, either above (positive contrast) or below (negative contrast) the luminance of the static background, producing appearing-disappearing bright or dark checks. In the positive contrast condition, the peak (positive) contrast occurred when the

luminance of the checks was at a maximum whereas in the negative contrast condition peak (negative) contrast occurred when the luminance of the checks was at a minimum. Similarly, zero contrast (uniform field) occurred when the luminance of the checks was at a minimum (equal to the background luminance) in the positive contrast condition, while zero contrast occurred when luminance of the checks was at a maximum (equal to the background luminance) for the negative contrast condition. Hence, the luminance modulation signals employed to produce these stimuli were 180 deg out-of-phase with one another. Contrast of these stimuli can be expressed by the *Weber* equation:

$$C_w = (L_c - L_b)/L_b$$

where L_c is the maximum or minimum of the bright or dark checks, and L_b is the luminance of the background.

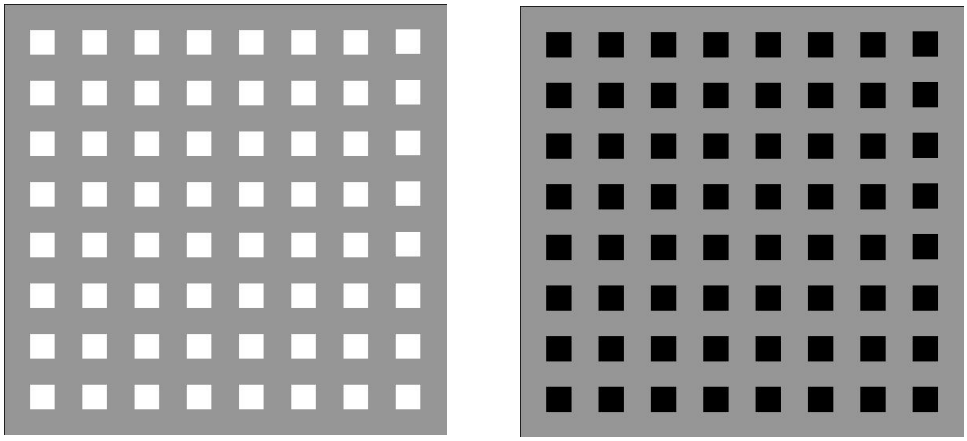

Figure 6: Appearance (left) and Disappearance (right) checkerboard stimulus patterns.

Temporal frequency for both bright and dark conditions was set at ~6 Hz. Mean contrast was set at 8% with depth of modulation (DOM) fixed at 8%. 8% contrast was chosen to accentuate a magnocellular response for it represents a contrast midrange that elicits magnocellular pathway involvement. Every sweep began with a uniform field of

background luminance to initiate a transient response at the onset of each run. Single sweeps lasted eight seconds with the initial second of background luminance not included in the analysis. Each sweep was run 10 times.

Steady-State VEPs to Isolated-Check Luminance-Contrast Sweeps

The fifth stimulus condition employed a 16x16 array of isolated checks in a similar appearance disappearance paradigm. DOM was sinusoidally swept from 0- 32%, with mean contrast equal to DOM. Thus if the DOM was, for example 8%, modulated around a mean contrast of 8%, peak luminance contrast would be 16% and minimum luminance contrast would be 0%. Temporal frequency for bright and dark conditions stimuli was set at ~6 Hz. Every sweep began with a uniform field of background luminance to initiate a transient response at the onset of each run. Single sweeps lasted eight seconds with the initial second of background luminance (0% contrast) not included in the analysis. Each sweep was run 10 times.

Electrode Placement

Placement of scalp electrodes is based on the International 10-20 System (Jasper, 1958). Standard gold cup electrodes will be placed along the following midline sites: An electrode at O_z will be referenced with another at C_z, with a floating ground electrode at P_z. All inputs to the amplifiers (Neuroscientific 600) are optoelectrically isolated. The low and high band pass filter of the differential amplifier was set at 0.01 and 100 Hz respectively. Amplification gain was set at 20,000.

VEP recording

The EEG was sampled synchronously with the signal used to modulate the stimulus at a frequency that was twice the frame rate of the display (238.1 Hz). Data collection was thus time-locked to the stimulus cycle and the EEG was measured only at discrete points that corresponded to fixed phase values of the modulation signal. A Fourier transform performed on a rectangular window function applied to the data, (such that data within the epoch was weighted with a coefficient of 1, whereas data outside the epoch was weighted with a coefficient of 0), yielded a corresponding amplitude characteristic in the frequency domain of the form {sinx/x}, where $x = \pi fT$, such that f is frequency and T is the period of the data epoch in seconds. The advantage of synchronous data collection is that any frequency components present in the EEG that are harmonics of the fundamental frequency do not leak through this filter function and distort the relevant response components.

Analysis of the VEP

Signal averaging of the output signal over the stimulus period enables its extraction from the underlying EEG output. Signal averaging is contingent upon the assumption that the individual potentials are equal in magnitude and that the response elicited is time-locked to the stimulus onset. Although any single record is embedded in noise, the VEP emerges as the computed average response with successive stimulus presentations. The signal-to-noise-ratio is improved by a factor of ten with one hundred times the number of stimulus presentations (Regan, 1979; 1989; Norcia, 1992).

Jean Baptiste Fourier in 1822 demonstrated that periodic wave forms can be analyzed into the sum of harmonically related sine waves of specific frequencies, phases and amplitudes. In essence, Fourier analysis affords a mathematical transformation from a time domain to a frequency domain.

Estimation of Noise in Steady-State VEPs - T^2_{circ} Analysis

Estimates of noise were obtained to assess the reliability of the VEP signal. Other noise estimates are based on undriven components at frequencies similar to the driven components. This rationale is flawed because EEG noise at neighboring frequency components tends to be considerably smaller than the noise at the driven frequency (Mast & Victor, 1991).

The application of a multivariate statistic T^2_{circ} (Victor & Mast, 1991), a modification of the Hotelling T^2 statistic, was employed in analyzing the data from this research to estimate the variability in the response. Noise was estimated by calculating the variances of the sine and cosine coefficients at the driven frequency, based on the assumption that these statistics are independent and not normally distributed with equal variance. In addition, T^2_{circ} increases its statistical power by gaining one degree of freedom based upon this independence assumption.

T^2_{circ} analyzes both amplitude and phase and calculates their respective 95% confidence intervals. T^2_{circ} can be represented in the complex plane as a circular confidence region around the mean of the vector response (see Figure 7).

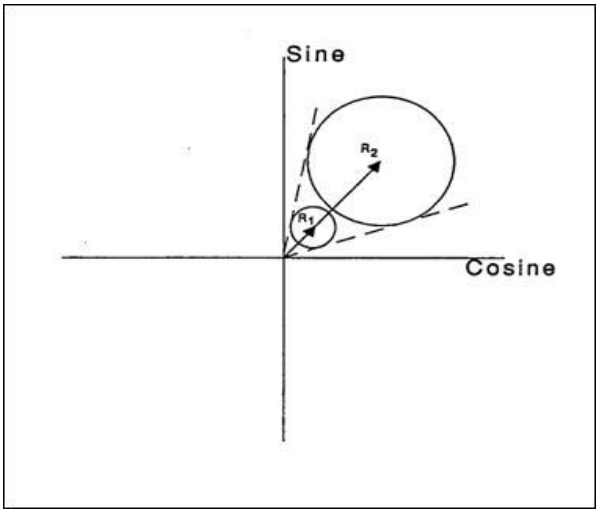

Figure 7: T^2_{circ} analysis: The T^2_{circ} statistic, applied to this vector model, calculates a circular 95% confidence region around the mean amplitude and phase. The T^2_{circ} value is the calculated distance (radius) from the tip of the vector to any point on the circular confidence region. The length of the vector divided by the radius yields the SNR for the 95% confidence region. A SNR of one, obtained when the length of the radius is equal to the vector, indicates that the circular confidence region touches the origin. A SNR above one indicates a response out of noise, whereas a SNR below one indicates a response embedded in noise where the circular confidence region encompasses the origin. Criterion was therefore, the interpolation of SNR equal to one.

Mean amplitude is represented by the length of the vector while mean phase is represented by the direction of the vector. The signal-to-noise ratio (S/N) is determined by the ratio of the response amplitude to the radius of the confidence circle. In this example, the mean amplitude of the hypothetical vector responses R_2 is significantly greater than R_1, whereas the mean phases and the S/N ratios of the two responses are identical. Confidence limits about the mean phase values are depicted as the angles subtended by radial lines from the origin that form tangents to the circles. When the confidence region encompasses the origin, the S/N is less than one and the response is considered too fraught with noise to be reliable.

Estimation of Noise in Transient VEPs – Magnitude-Squared Coherence (MSC)

MSC, initially a statistic used in the engineering literature (Bendat & Piersol,

1986), has been applied to auditory electrophysiology (Dobie & Wilson, 1989), electrocardiology (Fendelander et al., 1997), and visual electrophysiology (Zemon et al., 1999) as well. MSC is used to measure the proportion of a response that is attributable to a specific input signal in terms of power in frequency components. Specifically, it is the ratio of signal power to signal plus noise power for a given frequency component. In vision research, MSC is used to detect the presence of a true signal in a transient VEP record, and to quantify the magnitude of the response over a range of harmonic frequency components.

In theory, a pure (noise-free) signal is obtained when the response from each trial is equivalent to the mean response, rendering an MSC value of one. If the response is increasingly driven by noise, the MSC value decreases from one, and theoretically, a record determined by noise alone, would be represented by a value of zero. With a finite number of epochs, however, estimates of MSC ($\hat{\gamma}^2$) are biased by an amount that depends on sample size: bias[$\hat{\gamma}^2$]=1/q, where q is sample size. Thus, given no signal, $\hat{\gamma}^2$ would be equal to 1/q. Here, q=10 and the bias level is 0.1. Noise is reduced by a factor of q. The estimate of MSC is given as follows:

$$\hat{\gamma}^2 = \frac{(\frac{1}{q}\sum_{i=1}^{q} A_i \cos\theta_i)^2 + (\frac{1}{q}\sum_{i=1}^{q} A_i \sin\theta_i)^2}{\frac{1}{q}\sum_{i=1}^{q} A_i^2}$$

In this study, critical values for individual (m) and averaged MSC estimates were computed. For individual frequencies, MSC estimates had a critical value (1-tail, α= 0.05) =0.28. Specifically, the critical value for the low frequency band, consisting of frequencies between 4 and 12 Hz, is 0.174, for middle frequencies between 14 and 16 Hz,

the critical value is 0.162, and for high frequencies between 28 and 42 Hz, the critical value is 0.158. The sampling distribution approximated that of a normal distribution for averaged MSC estimates. The critical value was computed by:

$$CV_{\alpha} = \frac{\sqrt{m} + z}{q\sqrt{m}} = \frac{1}{q} + \frac{z}{q\sqrt{m}}$$

where m is the number of frequencies averages, q is the number of epochs, and z is the one-tail z value for α.

Analysis of the Transient VEP

A discrete Fourier transform (DFT) on the signal-averaged transient waveform was performed in order to obtain its frequency spectrum. A digital filtering technique was employed to remove all odd harmonics, since a symmetrical contrast-reversing stimulus should only produce even harmonic frequency components. As such, all odd harmonics can be considered noise and can only degrade the VEP waveform if not rejected. A low-pass filter with a high frequency cut-off of 50 Hz was used as it ensures negligible distortion of the VEP waveform (Zemon et al., 1994).

Analysis of the Transient Sweep VEP

Ten values for corresponding epochs collected from ten sweeps were vector-averaged for each harmonic component. A filtered transient waveform was constructed by means of an inverse Fourier transform. Measures of latency and peak-to-peak amplitude were obtained including times from stimulus onset to peaks of the first and second positive and negative wavelets, specifically P0, N1, P1 and N2, and N1-P1 and

P1-N2 amplitudes. Significant responses were evaluated by means of a statistical application of magnitude-squared coherence (MSC or γ^2) (Dobie &Wilson, 1993; Zemon et al., 1999)

Analysis of the Steady-State VEP

Fourier analysis of the output signals was used to measure amplitudes in microvolts and phases in degrees relative to the cosine of the relevant frequency components. Ten values for the fundamental frequency and second harmonic obtained from the ten sweeps were vector-averaged for corresponding epochs to yield mean amplitude and phase responses for each participant. 95% confidence limits were also obtained for each response component in terms of the sine and cosine coefficients based on the T^2_{circ} statistic. The statistic was used to derive signal-to-noise ratio (S/N) which can be represented both as a complex number and plotted in polar coordinate form.

Analysis of the Steady-State Sweep VEPs

A DFT was performed on each VENUS raw data file producing amplitude and phase values per each ~1-s epoch of EEG (corresponding to each step in the sweep). The mean and 95% confidence limits for both phase and amplitude values of the fundamental and second harmonic frequency components were also calculated for the set of 10 epochs associated with each stimulus condition. For the grating sweep, an acuity estimate was obtained through linear interpolation between two successive steps to a signal-to-noise ratio of one.

Statistical Analyses:

The statistical package SAS 9.1 (SAS Institute, Inc., Cary, N.C.) was used to analyze the data. A repeated measures mixed model ANOVA was employed because of its philosophical and quantitative advantages over traditional ANOVA models. Firstly, the mixed model is sound even with unbalanced and missing data, as long as the missing data are random. Secondly, the underlying assumption of independent errors made by most traditional models is rarely true. Finally, the mixed model approach affords a more flexible modeling of the covariance structure and can be expanded to analyze multivariate dependent measures.

Akaike's Information Criterion was used to assess which of the various covariance structures were optimal to analyze the data. Among the structures tested were compound symmetry (correlations are the same between any two time points), autoregressive order one (the correlations decrease with distance between time points), random regression model (the variables analyzed are repeated twice) and an unstructured covariance matrix (no structure is imposed on the assumed correlations). The unstructured covariance matrix was employed for all variables except for the pooling of dominant and non dominant eyes for each of the variables where the random regression model was implemented using Proc Mixed in SAS.

The random regression model was employed because it not only compares the group means across the repeated measure components (i.e. check size, DOM etc.), it also models the covariance structure of the data (Diggle et al., 1994). The assumption is that each repeated measures component is not necessarily independent and discrete from one another and as such modeling the appropriate covariance structure that is inherent in

these variables is essential so that inferences about means are valid (Littell et al., 1996). These methods also enable analyses with missing data points.

After initial analysis with the mixed model ANOVA, all significant repeated measures were analyzed for any interactions between group and condition with P>.10. If there was no significant interaction (i.e. p>.10) between group (mutation vs. normal) and the within-subject factor (e.g. check size, depth of modulation etc.) the significance of group was examined. If the two groups differed significantly (p<.05) the gradations specific to the within subject factor (i.e. individual check sizes) were then compared by computing a least squares estimate for the difference between the two groups at that point. A t-value (difference of the estimates/standard error of the difference) was examined for significance. A 95% confidence interval for this difference was also computed to allow for a measure of the precision of this estimate.

Model parameter estimates and their standard errors were generated by use of maximum likelihood functions. Lack of normality in particular data was addressed by transformations (e.g. log) and the use of nonparametric methods.

Comparisons of categorical variables among the groups (e. g. sex) were analyzed using Fischer's Exact test and continuous variables (e.g. age) were analyzed using independent t tests.

Nominal two-tailed significance was set at α <.05, and trend significance was set at α. < .10. One may argue that a correction for multiple analyses and multiple comparisons, such as the Bonferroni correction, should be employed to protect against the possibility of committing a Type I (false positive) error. However, such a correction

confounded by the small sample size, would increase the likelihood of a Type II (false negative) error.

Chapter 8: Results

Nonparametric Variables

Mean age for controls was 34.13 (SD = 15.21) and mean age for the LHON group was 38.83 (SD = 14.05). No significant differences between experimental group and controls were found in terms of mean age with t (1, 12) =.59, p = 0.5651. Fischer's Exact test was used to establish that there were no significant differences in sex distribution between the two groups as well χ^2 (1, 11) = 1.1667, p = 0.2801. Snellen acuities indicated a nonsignificant greater mean acuity for controls as opposed to the LHON group with t (1, 12) = -2.13, p = 0.0625. Mean acuity for controls was 1.23 c/deg (SD = 0.39) and 1.2 c/deg (SD = 0.39) in the dominant and nondominant eyes respectively, whereas mean acuity for the LHON participants was 0.87 c/deg (SD = 0.15) and 0.81 c/deg (SD = 0.13) in the dominant and nondominant eyes respectively. It is interesting to note that consistent with the general population, seven out of the eight controls were right-eye dominant, whereas four out of the six LHON participants were left-eye dominant.

Within-Subject-Variability

The LHON data overall evidenced greater within-subject variability. Due to the small N, individual functions for every stimulus condition are first analyzed and group means are evaluated within the fit of the individual functions. Analysis of the individual plots is also informative with respect to consistent subclinical dysfunction across stimulus conditions.

The VEP records from one LHON participant, L1, were mostly embedded in noise and were therefore considered anomalous. Subsequent communication with this participant indicated initial clinical visual abnormalities, although a clinical diagnosis of LHON has not been given. Group data was therefore analyzed both including and excluding his VEP records. A separate analysis of his VEP records was included for it evidenced the hypothesized abnormalities.

Notwithstanding the greater within subject variability and the small N, both of which would decrease the likelihood of obtaining significance, significantly enhanced amplitudes were evidenced in the LHON group under all stimulus conditions. Furthermore, significant specific enhanced magnocellular and ON pathway responses were noted from the group means. Positive findings under these conditions emphasize the magnitude of these differences. On the other hand, interestingly, the individual LHON traces indicated opposite findings of a deficit in these pathways. It is specifically for this reason, that the individual plots are being so intensely evaluated. Although these individual findings are not significant, they are consistent within the specific LHON individuals tested and perhaps reflect another dimension of the pathology. These provocative findings will be addressed in the discussion section.

Analysis of the Steady-State VEPs to a Grating-Spatial Frequency Sweep

Analysis of Individual Functions and Grating Acuity

Characteristic second harmonic amplitude and phase functions are presented for both controls and LHON individuals. Note the consistent morphology in the functions from the LHON individuals in the dip at 6 c/d, subsequent rise at 12 c/d, and fall again at 32 c/d. This morphology was seen in eight of twelve eyes in the LHON population.

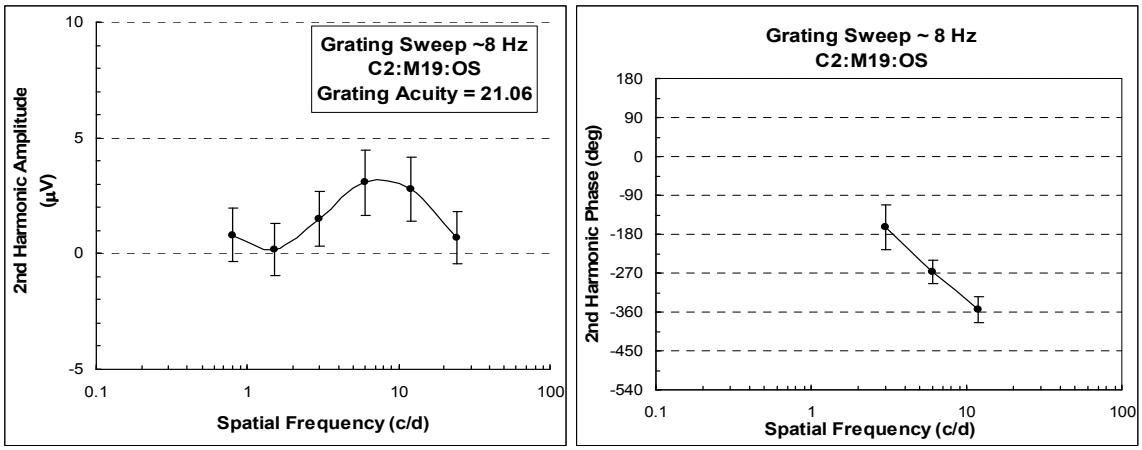

Figure 8: Second harmonic amplitude and phase values for a control. An acuity estimate was obtained through linear interpolation between two successive steps to a signal-to-noise ratio of one.

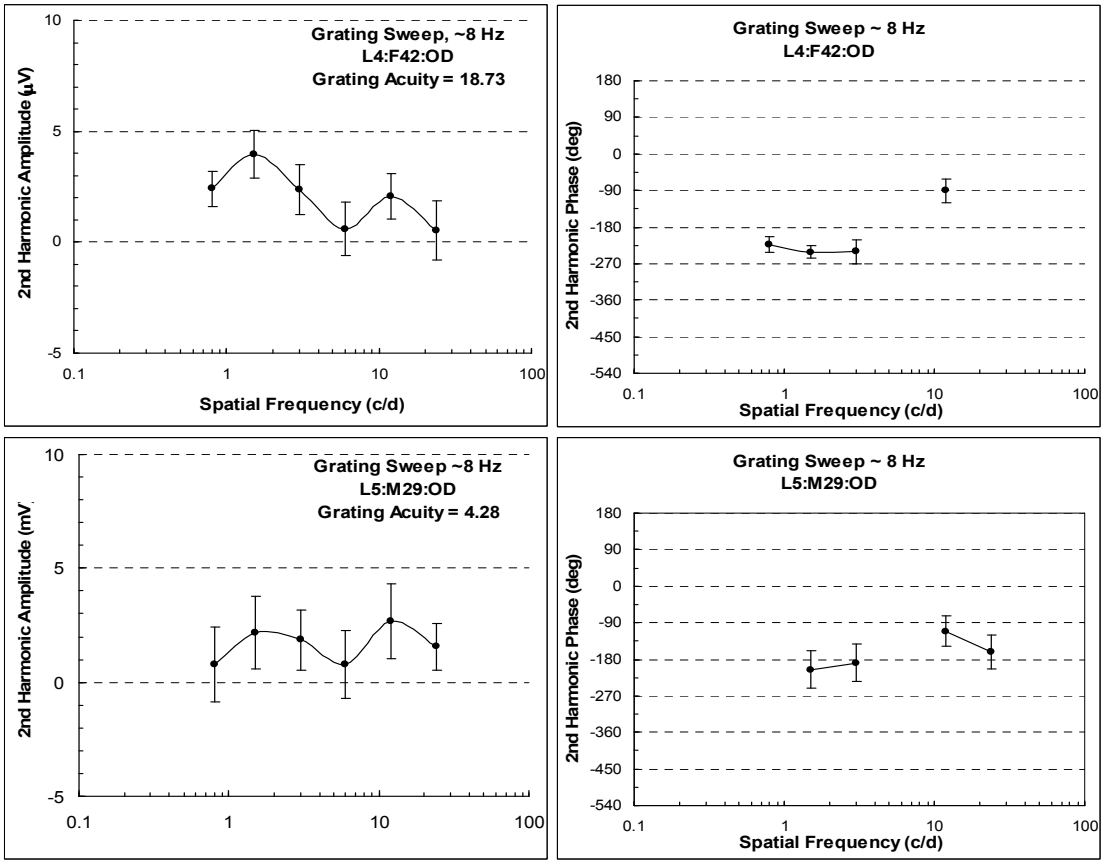

Figure 9: Second harmonic amplitude and phase values for LHON individuals. Acuity estimates were obtained through linear interpolation between two successive steps to a signal-to-noise ratio of one.

Analysis of Mean Amplitude Functions

Although differences in mean amplitudes were not statistically significant between the two groups, the morphology of the group functions still maintained the aforementioned "notch" in the middle spatial frequencies in the LHON group.

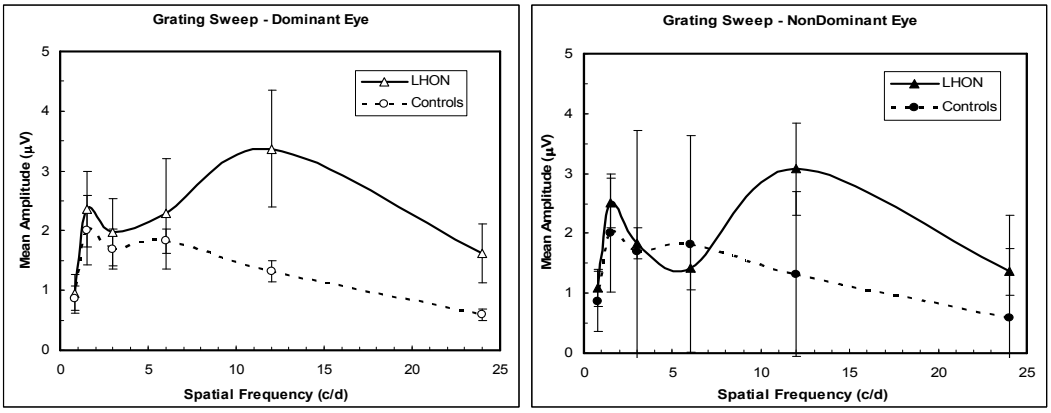

Figure 10: Mean amplitude measurements for both LHON individuals and controls given stimulation of both dominant (left) and nondominant (right) eyes. Error bars indicate ± 1 SEM.

Mean Grating Acuity

Mean grating acuities, unlike mean Snellen acuities, were greater for the LHON group as compared to controls with a mean grating acuity of 26.71 c/d (SD = 9.7) for the LHON group and 13.71 c/d (SD = 5.37) for controls given stimulation of the dominant eye, and 17.11 c/d (SD = 12.73) in the LHON group and 11.53 c/deg (SD = 6.7) for controls given stimulation of the nondominant eye. In a number of LHON individuals, the SNR did not dip below a value of one, even at the highest spatial frequencies. In these cases, a linear extrapolation to a SNR of one was necessary in order to obtain acuity estimates.

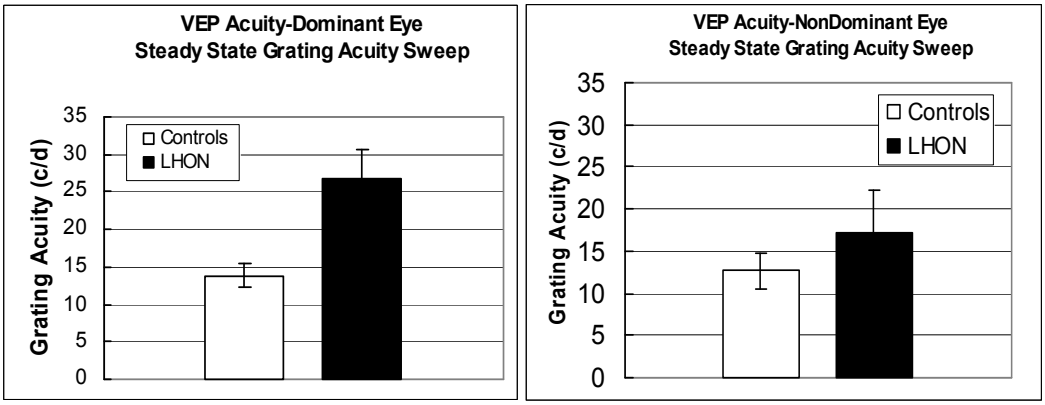

Figure 11: Mean grating acuities measured in cycles/degree given stimulation of the dominant (left) and nondominant (right) eyes in asymptomatic LHON individuals and controls. Error bars indicate ± 1 SEM.

Analysis of the Transient VEPs to a 32x32 Contrast-Reversing Checkerboard

Analysis of Individual Amplitude and Phase functions:

Individual VEP traces were representative of the groups at large. Significantly greater amplitudes were seen in the LHON group as compared to controls. On the other hand, no significant differences in latencies were detected between the two groups. A few classic VEP records are depicted below illustrating the noted differences.

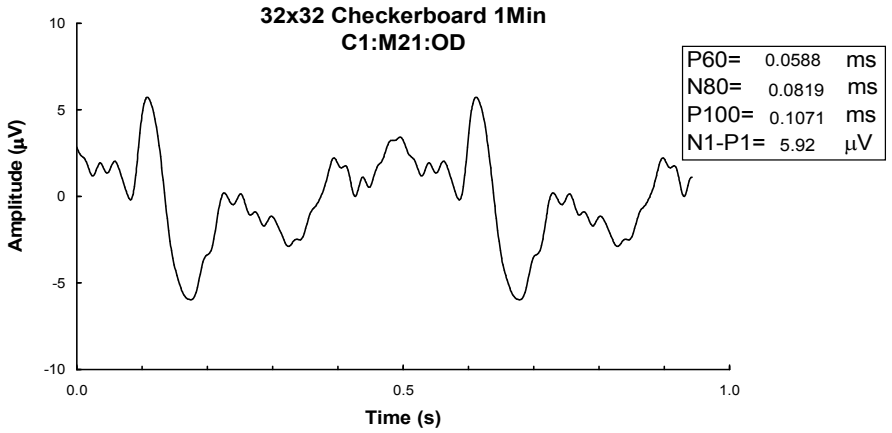

Figure 12: VEP trace from a control reflecting the normal amplitude and latency measurements elicited from the transient 32x32 contrast reversing checkerboard.

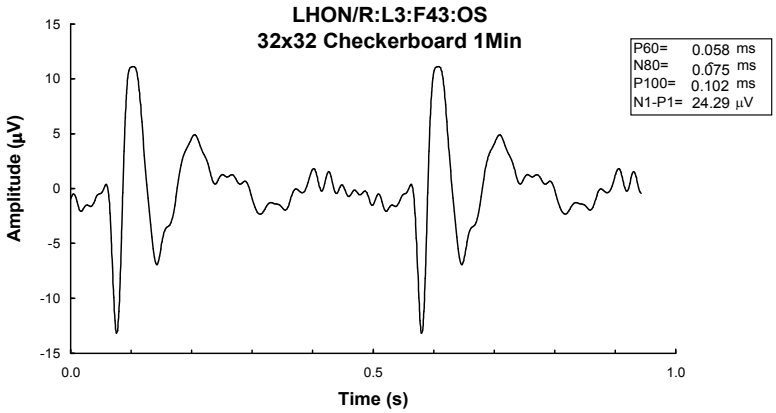

Figure 13: : VEP trace from an asymtomatic LHON individual reflecting amplitude and latency measurements elicited from the transient 32x32 contrast reversing checkerboard. Note the significantly higher amplitude and the normal latencies.

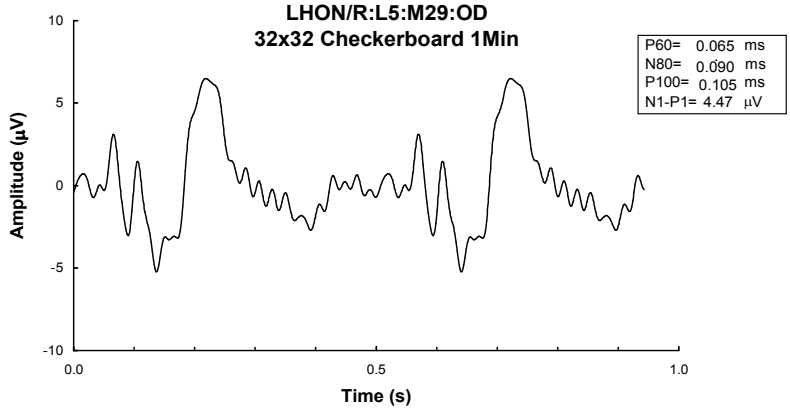

Figure 14: : VEP trace from an asymtomatic LHON individual reflecting amplitude and latency measurements elicited from the transient 32x32 contrast reversing checkerboard. Note the low P100 associated with magnocellular input to the cortex and the significantly higher amplitude of the subsequent positive wave associated with parvocellular input to the cortex.

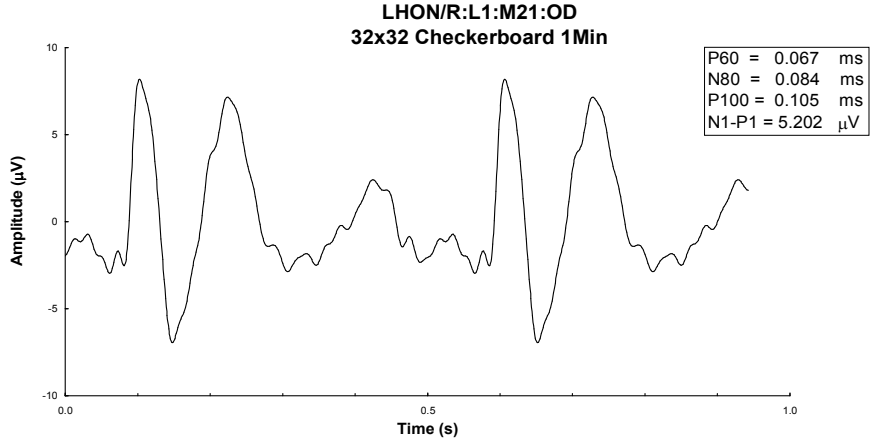

Figure 15: Decreased amplitude and increased latency measurements were obtained from the anomolous asymtomatic LHON individual from the transient 32x32 contrast reversing checkerboard.

Analysis of Individual MSC

Characteristic MSC plots indicating greater overall MSC values in the LHON participant as opposed to a normal control is depicted in figures 16 and 17 below. Note the greatest differential in the high frequency bands.

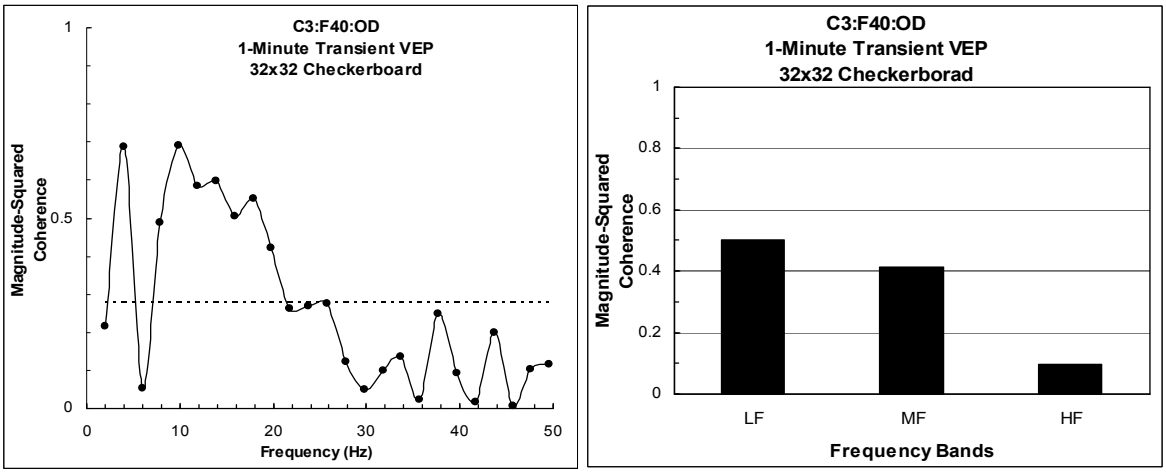

Figure 16a: MSC values plotted for even frequency components between 2 and 50 Hz. in a normal control. The critical value for individual harmonics is 0.28. Figure 15b: Pooled MSC values plotted for low, middle and high frequency components. Low frequencies include 4-12 Hz., middle frequencies include 14-26 Hz. and high frequencies include 28-42 Hz. The critical value 0.174 for low frequencies, 0.162 for middle frequencies and 0.158 for high frequencies.

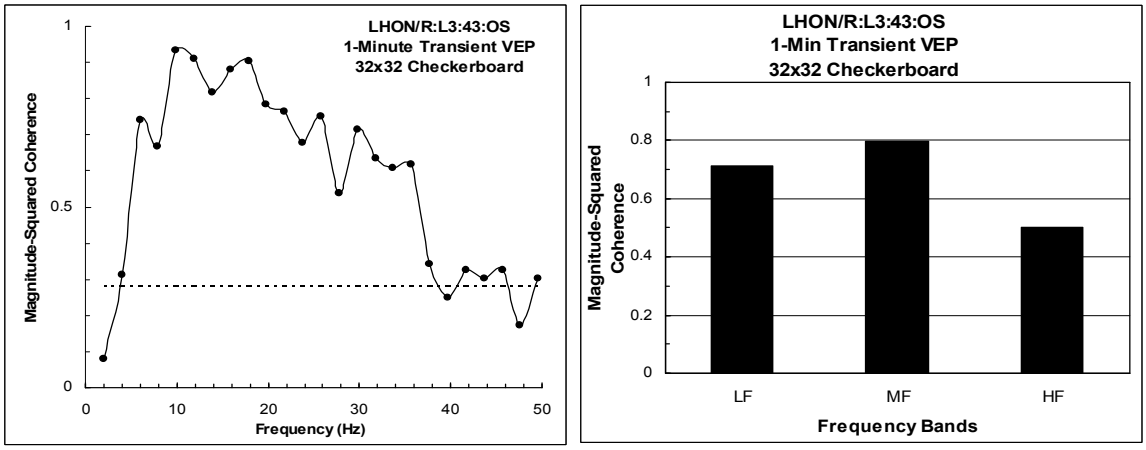

Figure 17a: MSC values plotted for even frequency components between 2 and 50 Hz. in an asymptomatic LHON individual. The critical value for individual harmonics was 0.28. Figure 16b: Pooled MSC values plotted for low, middle and high frequency components. Low frequencies included 4-12 Hz., middle frequencies included 14-26 Hz. and high frequencies included 28-42 Hz. The critical value was 0.174 for low frequencies, 0.162 for middle frequencies and 0.158 for high frequencies.

Analysis of Group Mean Amplitude

N1 –P1 amplitudes from this critical check condition were again higher in the LHON population as opposed to controls. Mean amplitudes given stimulation of the dominant eye were 7.904 μV and 13.852 μV for controls and LHON participants respectively and given stimulation of the nondominant eye, 7.384 μV and 12.463 μV for controls and LHON participants respectively.

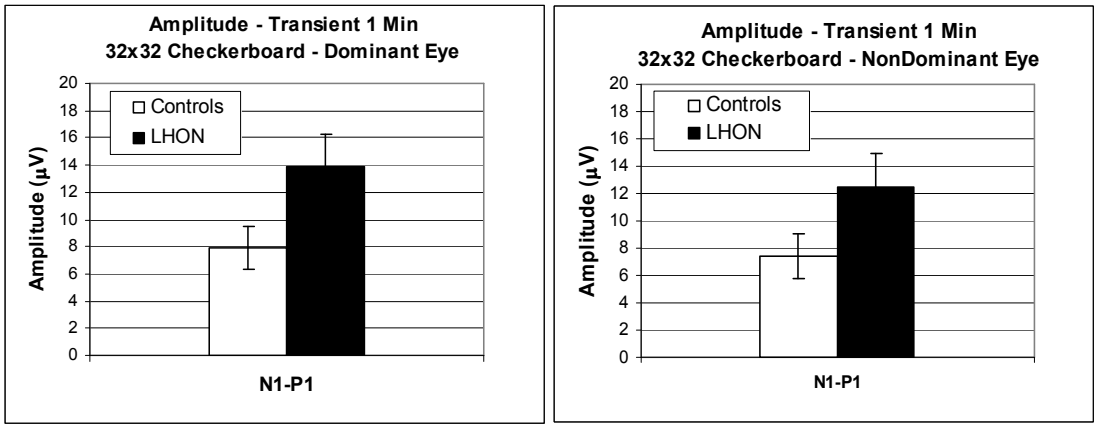

Figure 18: Mean amplitudes from the transient 32x32 contrast reversing checkerboard in the dominant (left) and nondominant (right) eyes in both asymptomatic LHON individuals and controls. Error bars indicate ± 1 SEM.

Analysis of Group Mean Latency

There were no significant latency differences in early and late positive and negative components given stimulation of both dominant and nondominant eyes between groups of participants. Latencies in both groups were close to population mean averages. Both controls and the LHON group elicited slightly early N2 (180 ms) latencies, although they were marginally more pronounced in the LHON population given stimulation of both dominant and nondominant eyes. Nominal increases in P0 (60 ms) latencies were also seen in the LHON group given stimulation of the nondominant eye.

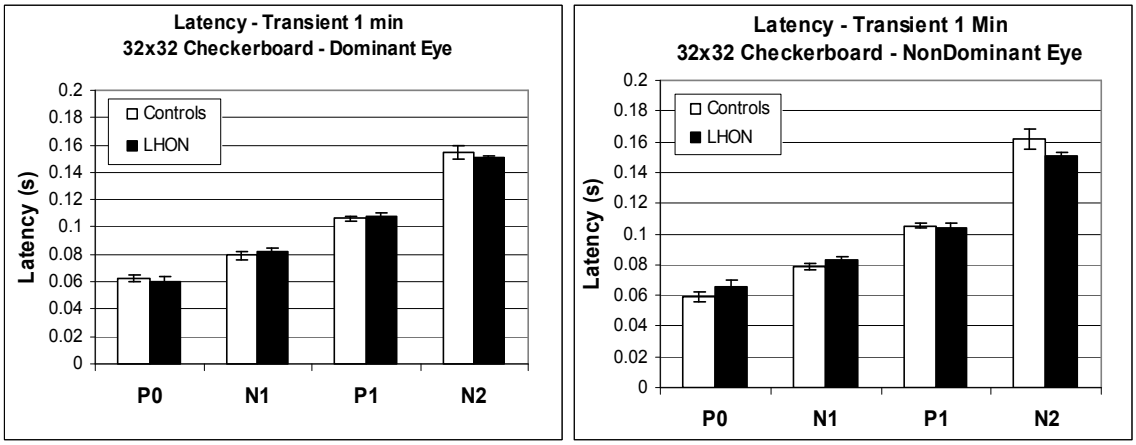

Figure 19: Mean latencies elicited from the transient 32x32 contrast reversing checkerboard in the dominant (left) and nondominant (right) eyes in asymptomatic LHON individuals and controls. Error bars indicate ± 1 SEM.

Analysis of Group Mean MSC

There were also no significant differences in MSC values from the low, middle or high spatial frequencies given stimulation of either the dominant or nondominant eye. Greater coherence was evidenced in all frequency bands for the LHON population given stimulation of both dominant and nondominant eyes. The largest differentials were in the middle frequency bands with MSC values of 0.512 and 0.347 in the given stimulation of the dominant eye and 0.477 and 0.288 given stimulation of the nondominant eye for LHON participants and controls respectively. All MSC values were significant, above critical value for each frequency band, except for a 0.136 MSC value, below the critical value of 0.158 given stimulation of the dominant eye in the high frequency band in controls, as compared to the LHON group with a 0.255 MSC value. Given stimulation of the dominant eye as well, the MSC value in the high frequency band was just above critical value for the controls at 0.179 as compared to 0.291 for the LHON group.

Furthermore, there is evidence to suggest that the low frequency bands correlate with later cortical activity, the middle frequency bands with P100 and the high frequency bands with P0. Greater coherence in the LHON population was seen in the high frequency band correlated with P0, input to the cortex, which is again consistent with the aforementioned findings of an increased afferent signal in LHON.

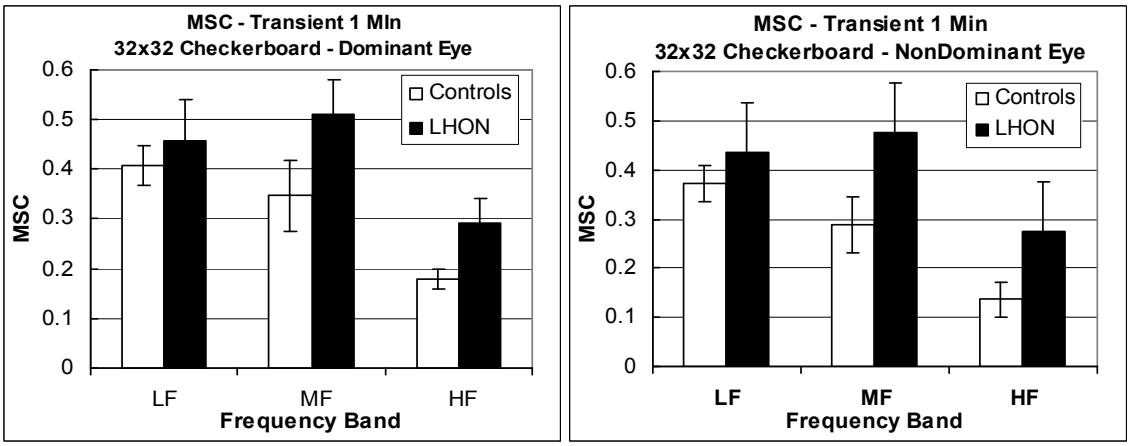

Figure 20: Mean magnitude squared coherence values for low, medium and high frequency bands elicited from the transient 32x32 contrast reversing checkerboard stimulus given stimulation of the dominant (left) and nondominant eyes (right) in asymptomatic LHON individuals and controls. Error bars indicate ± 1SEM.

Analysis of Transient VEPs to a Checkerboard Sweep

Analysis of Individual Amplitude and Latency Functions

Characteristic amplitude and phase functions for each checkerboard size in the transient sweep are presented. Note the greater amplitudes in the LHON individual as opposed to the control.

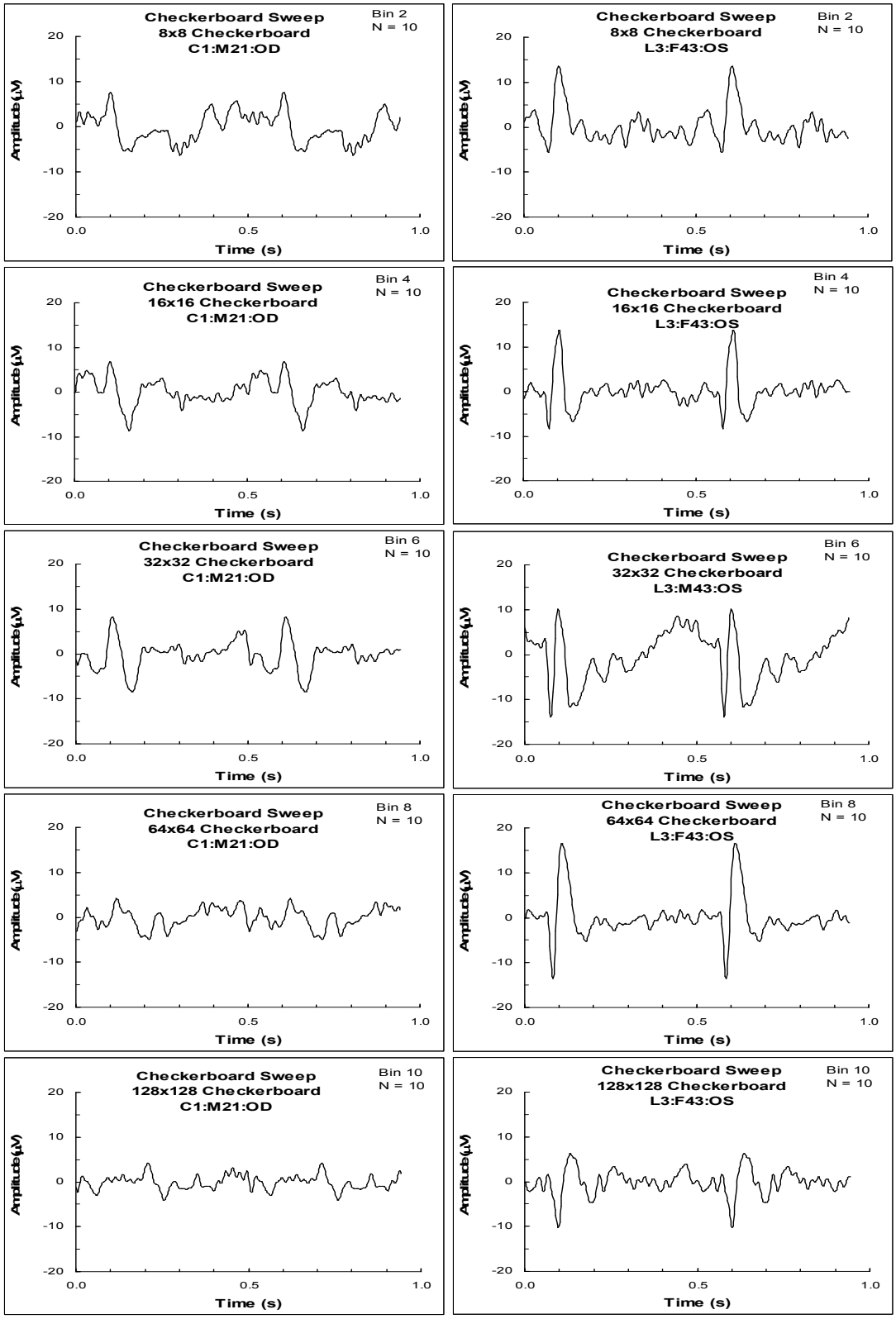

Figure 21: Individual amplitude and latency functions for each checkerboard size in the transient sweep for a control (left) and a LHON individual (right). Note the higher amplitudes in the LHON individual even at high spatial frequencies

Analysis of Individual MSC

As was evidenced in the group data, these characteristic MSC functions indicate greater overall coherence in the LHON individual as opposed to the control.

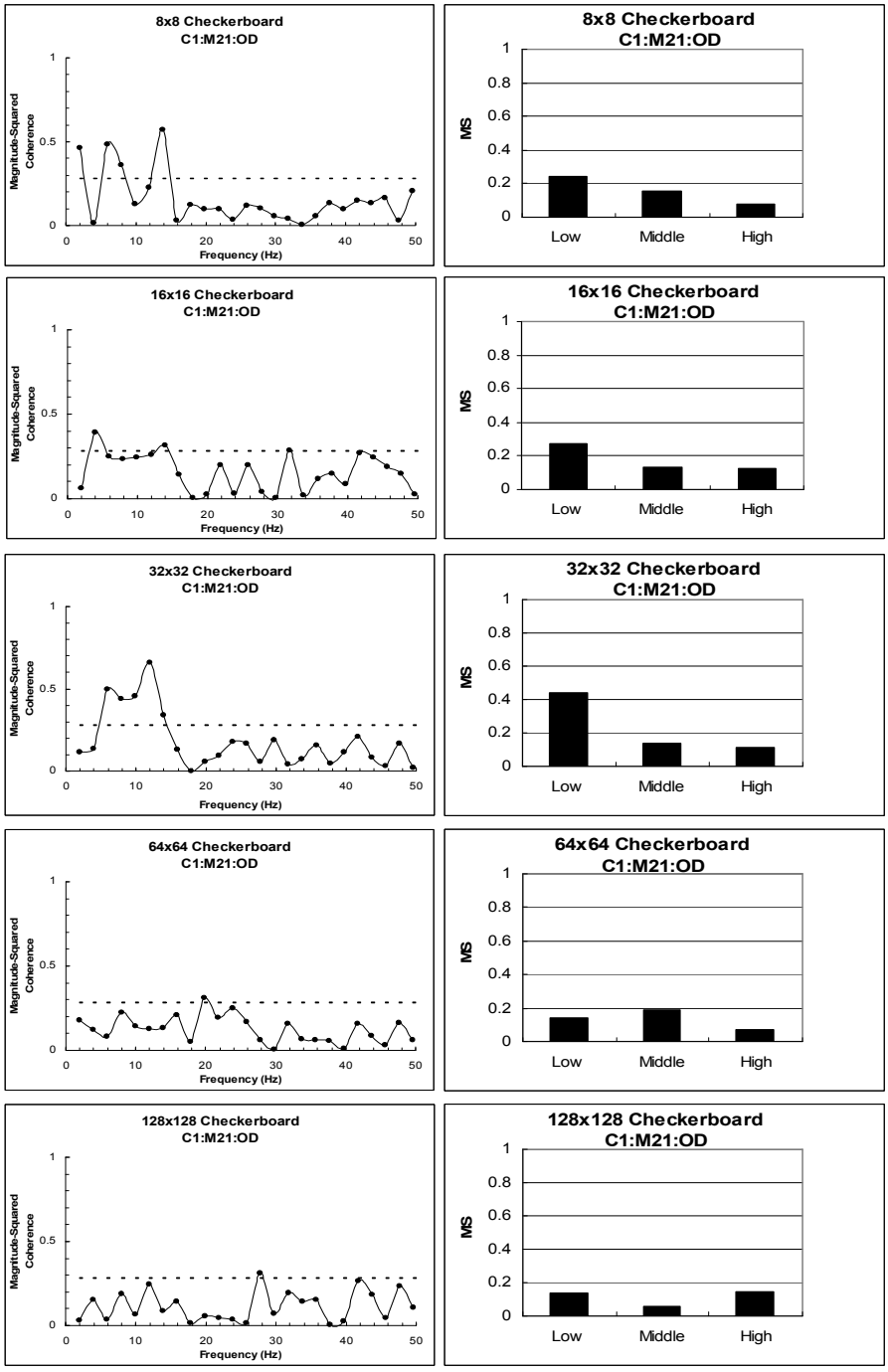

Figure 22: Magnitude squared coherence for a control (dominant eye) for each checkerboard size within the sweep. The left set of graphs plots MSC for each even harmonic until 50 Hz. The critical value for individual harmonics was 0.28. The right set of graphs pooled the low (4-12), middle (14-26) and high (28-42) frequency harmonics. The critical value was 0.174 for low frequencies, 0.162 for middle frequencies and 0.158 for high frequencies.

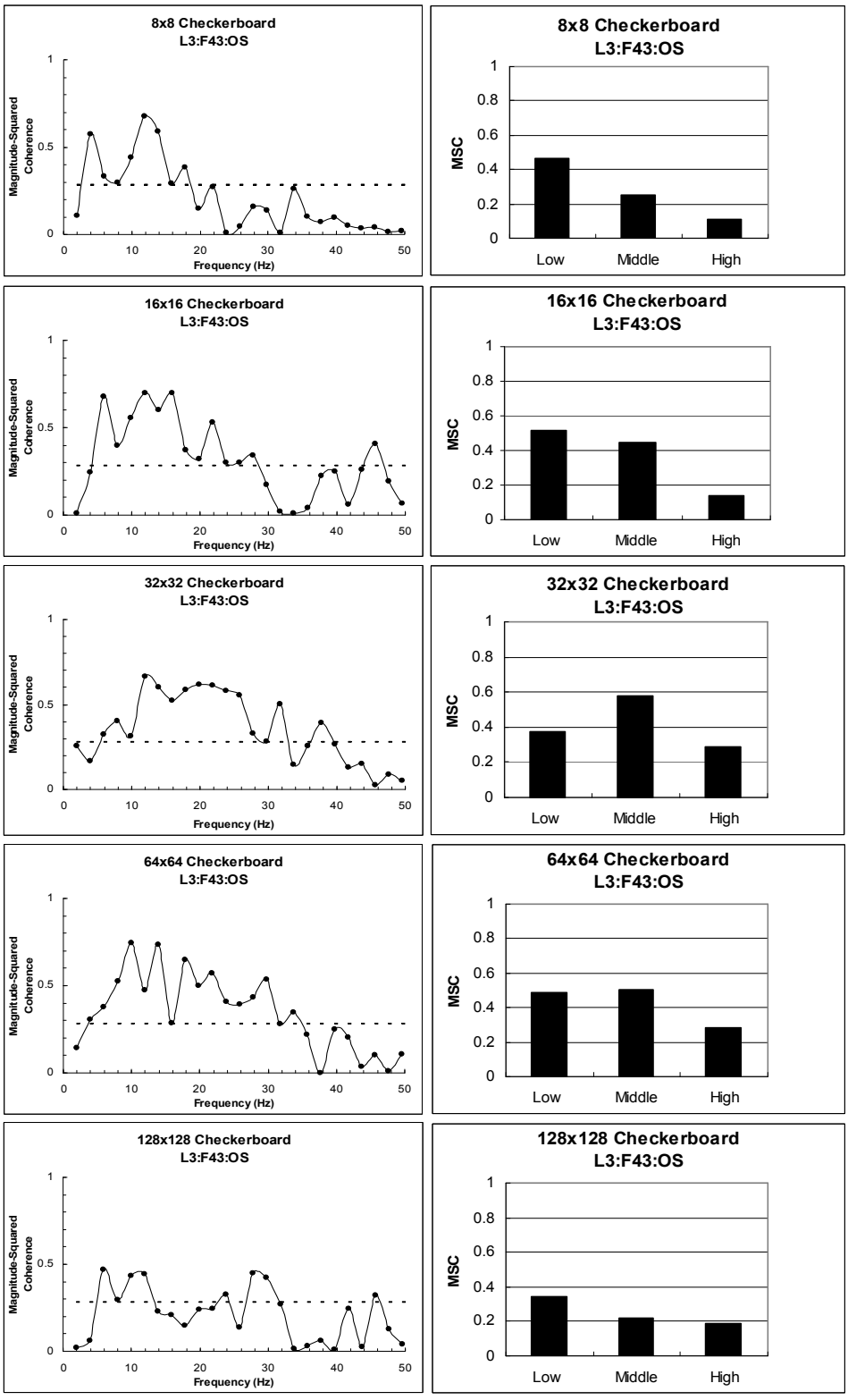

Figure 23: Magnitude squared coherence for a LHON individual (dominant eye) for each checkerboard size within the sweep. The left set of graphs plots MSC for each even harmonic until 50 Hz. The critical value for individual harmonics was 0.28. The right set of graphs pooled the low (4-12), middle (14-26) and high (28-42) frequency harmonics. The critical value was 0.174 for low frequencies, 0.162 for middle frequencies and 0.158 for high frequencies.

Analysis of Individual Checkerboard Acuity Estimates

Characteristic MSC functions with checkerboard acuity estimates are depicted below for both a control and a LHON individual. Note the higher estimates for the LHON individual.

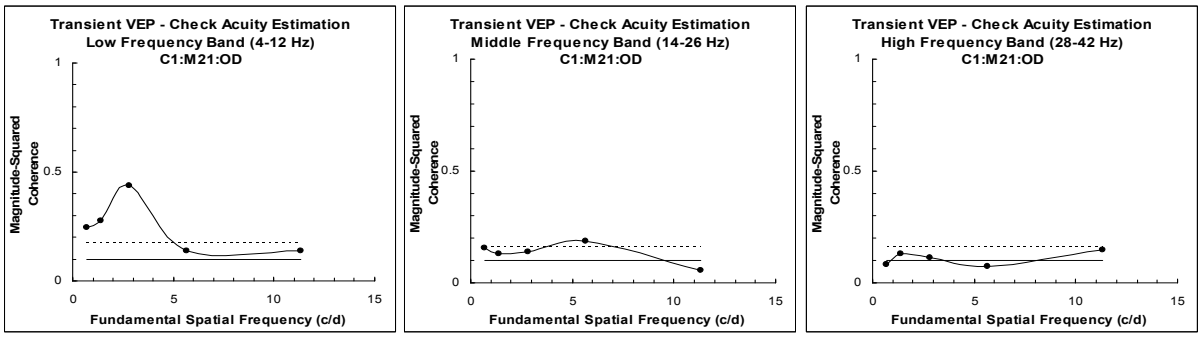

Figure 24: MSC values for a control (dominant eye) as a function of spatial frequency for low, middle and high frequencies. Checkerboard acuity estimates were calculated via extrapolation of the MSC function to the critical value. Bias (solid line) was 0.1 and the critical value (dashed line) was 0.174 for low frequencies, 0.162 for middle frequencies and 0.158 for high frequencies.

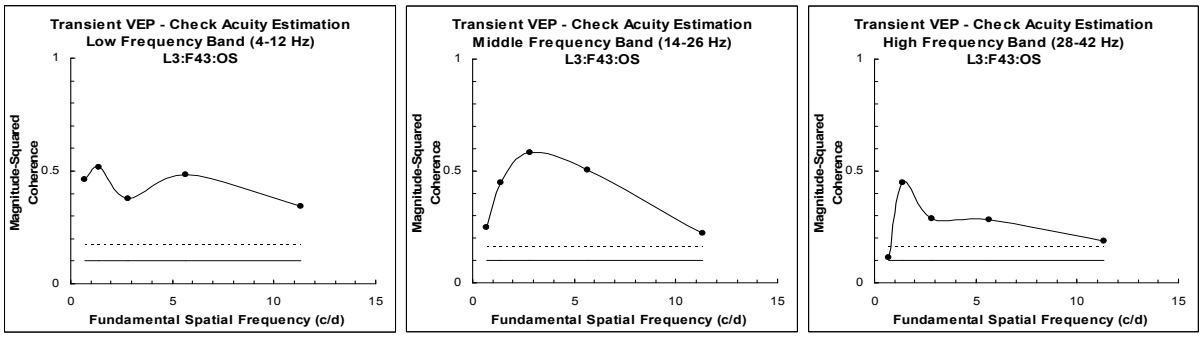

Figure 25: MSC values for a LHON individual (dominant eye) as a function of spatial frequency for low, middle and high frequencies. Checkerboard acuity estimates were calculated via extrapolation of the MSC function to the critical value. Bias (solid line) was 0.1 and the critical value (dashed line) was 0.174 for low frequencies, 0.162 for middle frequencies and 0.158 for high frequencies.

Analysis of Group Mean Amplitude

Greater N1-P1 and P1-N2 amplitude functions were evidenced in the LHON group across all check sizes in the transient sweep. The average differential amplitude

given stimulation of the dominant eye was of a magnitude of approximately 4 μV for N1-P1 and 3μV for P1-N2. For example, N1-P1 amplitudes were 7.76 μV and 12.14 μV and P1-N2 amplitudes were 12.21 μV and 15.27μV at the 8x8 check given stimulation of the dominant eye. The average differential amplitude given stimulation of the nondominant eye was of a magnitude of approximately 3 μV for N1-P1 and 1μV for P1-N2. Interestingly, however, the P1-N2 amplitude had the greatest differential given stimulation of the nondominant eye with amplitudes of 14.03 μV for the LHON group and 9.32 μV for controls. The smallest differentials overall were in the 128x128 check condition.

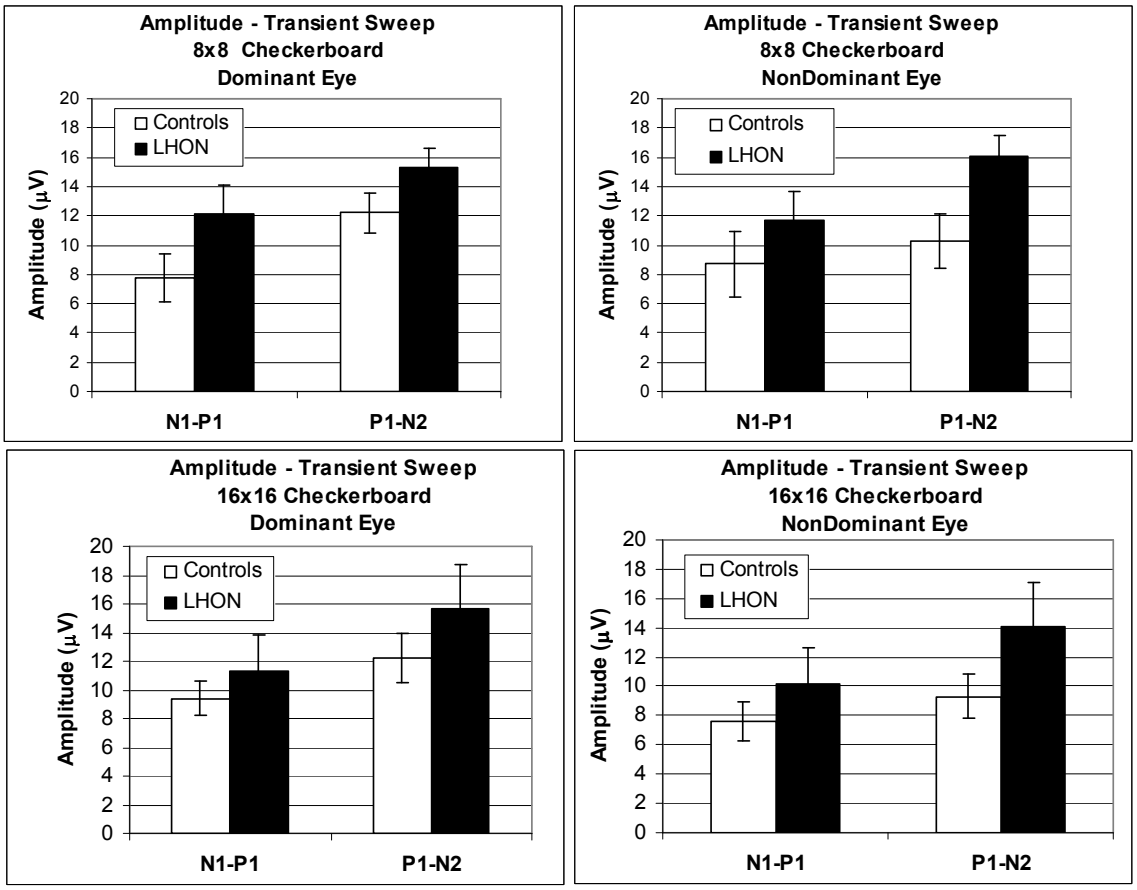

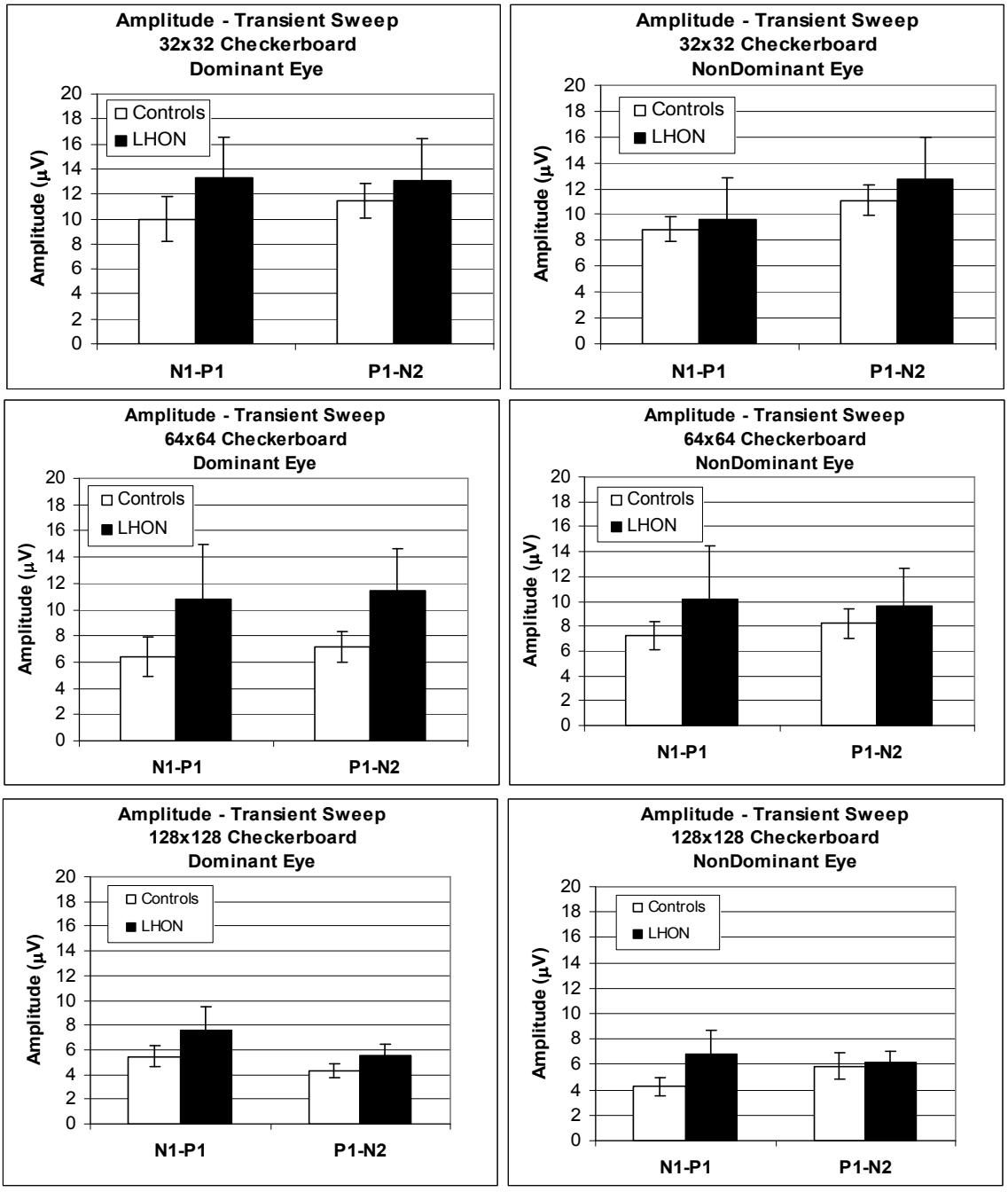

Figure 26: Amplitude measures from the transient checkerboard sweep through incremental check sizes given stimulation of the dominant (left) and nondominant eyes (right) in asymptomatic LHON individuals and controls. Error bars indicte ± 1 SEM.

Analysis of Group Mean Latencies

No significant differences were found between the groups in the latencies for both positive and negative early and late components. Overall, latencies increased with

smaller check sizes. However, for the most part, increased latencies were evidenced in both early and late components given stimulation of both dominant and nondominant eyes beginning with the 16x16 check and on for the remainder of the smaller check sizes given stimulation of the nondominant eye, and the 32x32 check and on for the remainder of the smaller check sizes given stimulation of the dominant eye. The increased P0 latencies evidenced in the transient sweep at the 32x32 check are consistent with the increased latencies evidenced in the LHON group in the transient 1 Min check stimulus given stimulation of the nondominant eye. The marginally increased N1 (80 ms) latencies evidenced in both eyes in the transient 1 Min checkerboard stimulus were again consistent with the increased latencies seen beginning with the 16x16 check and on for the remainder of the smaller check sizes given stimulation of the nondominant eye, and the 32x32 check and on for the remainder of the smaller check sizes given stimulation of the dominant eye. Whereas, early N2 latencies were seen in the transient 1 Min check in the LHON group in both eyes, this was not evidenced in the transient sweep stimulus at the 32x32 check condition. However, these early N2 latencies were seen in the LHON group in the transient sweep stimulus at the 8x8 check given stimulation of the nondominant eye and the 16x16 check given stimulation of the dominant eye.

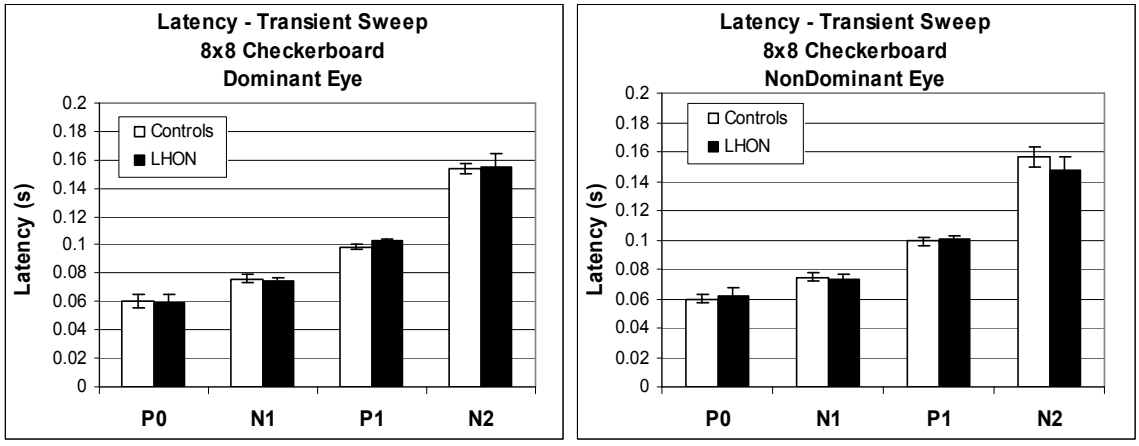

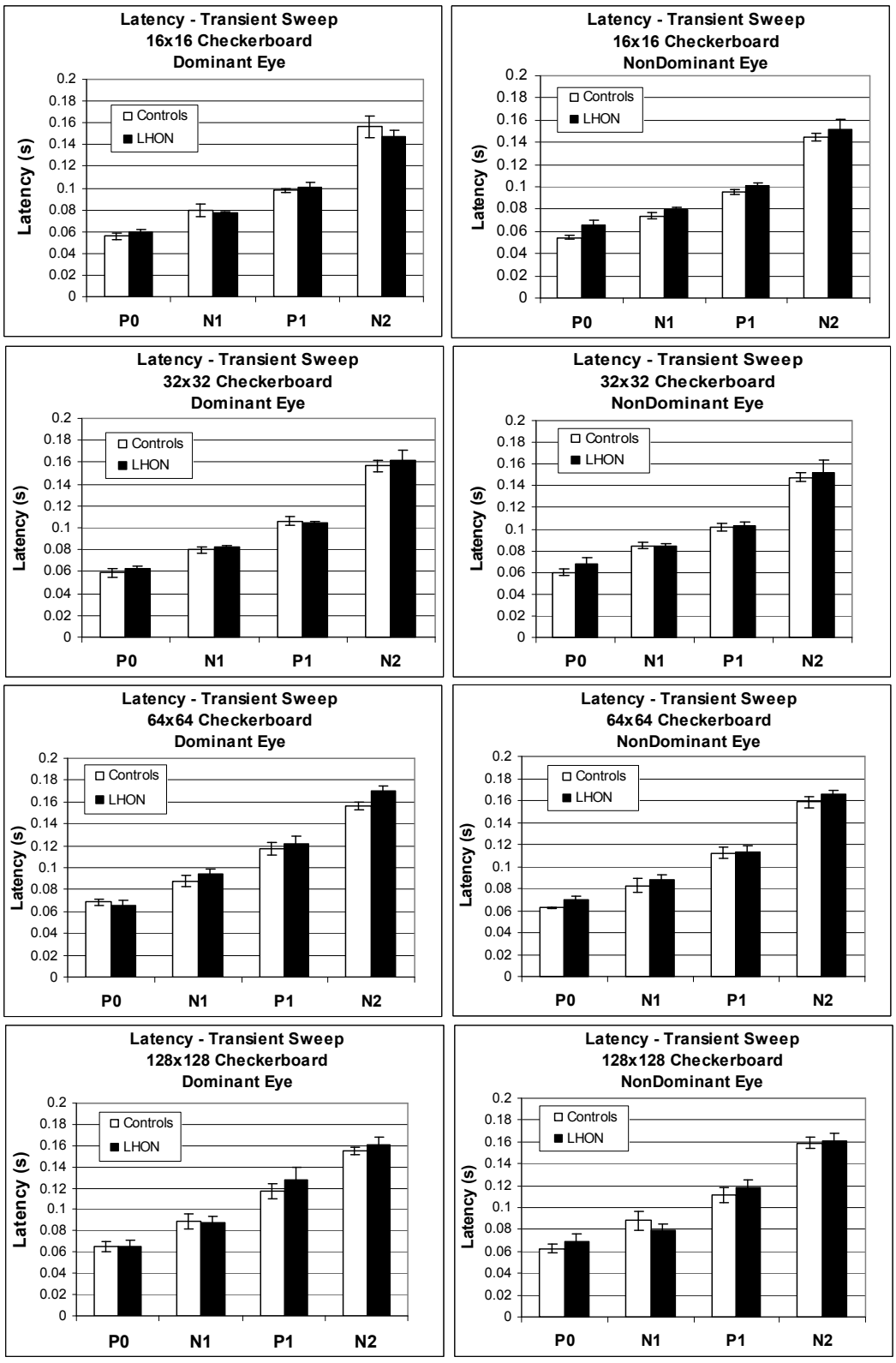

Figure 27: Mean latency values from the transient checkerboard sweep through incremental check size given stimulation of the dominant (left) and nondominant (right) eyes in asymptomatic: LHON individuals and controls. Error bars indicate ± 1SEM.

Analysis of Group Mean MSC Values

MSC values given stimulation of the dominant eye at both the 8x8 and 16x16 check conditions were significant in both the low and middle frequencies for both the LHON group and controls. The LHON group showed greater values for both frequencies in both conditions as well. The MSC for the high frequency did not reach the critical value of 0.158 in either condition for either group. At the 32x32 check, although the MSC for the high frequency rose in both groups, MSC did not surpass the critical value and MSC values were again only significant for both groups in the low and middle frequencies. MSC values were still greater for the LHON group in the middle frequencies (MSC=0.26) as opposed to controls (MSC=0.20), the MSC was slightly greater for controls at the low frequency (MSC= 0.21). At the 64x64 check condition, although both groups dip below the critical value of 0.174 at the low frequencies, the controls dip lower with MSC = 0.157 whereas the LHON group just loses significance with MSC = 0.170. At the middle frequencies, the controls are again below critical value (MSC = 0.136) while the LHON group is above (MSC = 0.205). MSC values are not significant at any frequency for both groups at the 128x128 check, even though MSC values for the LHON group are still greater than controls across all frequencies.

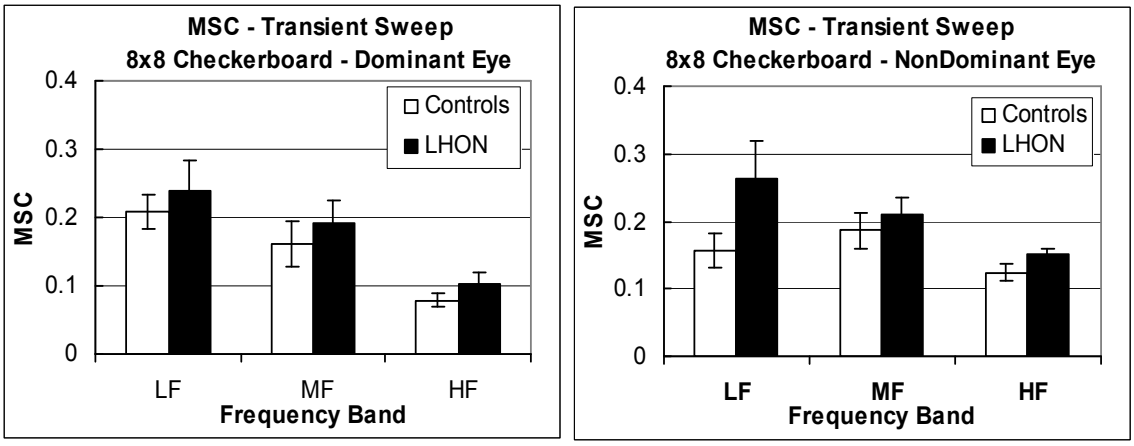

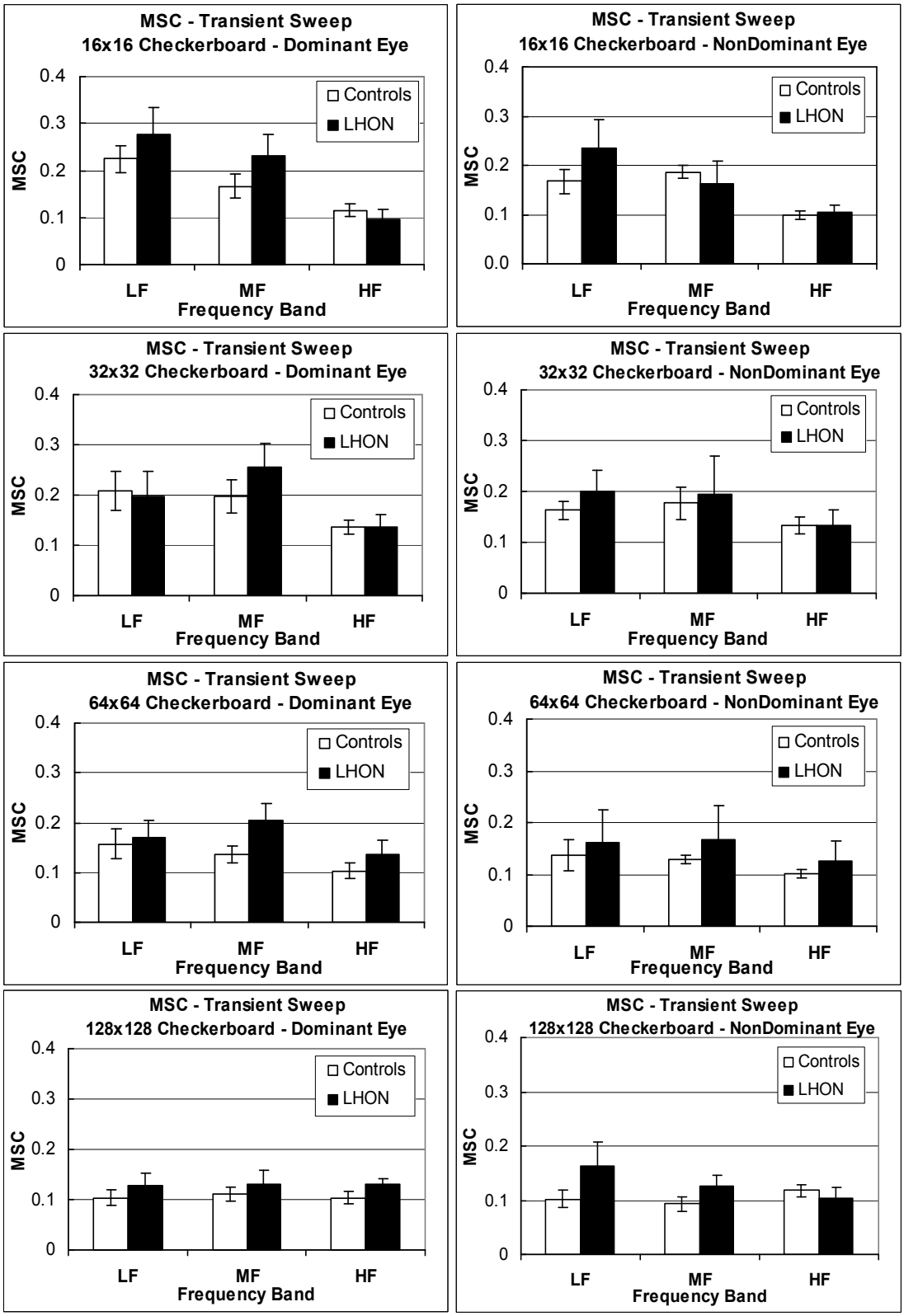

Figure 28: Mean magnitude squared coherence values of the low, middle and high frequency components from the transient checkerboard sweep through incremental check size given stimulation of both the dominant (left) and nondominant (right) eyes in asymptomatic LHON individuals and controls. Error bars indicate ± 1 SEM.

MSC values given stimulation of the nondominant eye at the 8x8 check were significant for both the LHON group and controls in the middle frequencies, with greater values again, for the LHON group (MSC = 0.210) as opposed to controls (MSC = 0.186). However, at the low frequencies, only the LHON group is significant (MSC = 0.263) as opposed to controls (0.157). Both groups did not surpass critical value at the high frequency band. At both the 16x16 and 32x32 check conditions, MSC values were significant again for the LHON population with MSC = 0.234 and 0.164 at the 16x16 check, and MSC = 0.200 and 0.195 at the 32x32 check condition for the low and high frequencies respectively. However, the MSC values were only significant at the middle frequencies for controls with MSC = 0.186 at the 16x16 check and 0.177 at the 32x32 check. Again, both groups did not reach critical value at high frequencies. At the 64x64 check condition, the LHON group only reached above critical value at the middle frequencies with MSC = 0.167. Still MSC values for the LHON group were greater than controls. At the 128x128 check condition, there were no significant MSC values in either group.

The repeated measures ANOVA indicated that in the contrast reversing checkerboard sweep, higher MSC values in the LHON population were nearly significant in the 8x8 checkerboard given stimulation of the dominant eye with $F(1, 12) = 4.44$, $p = 0.0567$.

Analysis of Group Mean Checkerboard Acuity Estimates

Checkerboard acuity from the contrast reversing checkerboard sweep, like Snellen acuity, generally indicated higher acuities for the controls. Interestingly, the greatest

differential was in the high frequencies given stimulation of the dominant eye with visual acuity estimation of 5.05 c/d for controls as opposed to 2.03 c/d for the LHON group and for low frequencies given stimulation of the nondominant eye with a visual acuity estimate of 5.44 c/d for controls and 2.65 c/d for the LHON participants. Moreover, controls had higher VA estimates overall given stimulation of the dominant eye with the greatest differential seen in the high frequencies. On the other hand, given stimulation of the nondominant eye, not only was the greatest differential in the low frequencies, but in both the middle and high frequencies the LHON group had higher VA estimates than controls with 4.62 c/d and 3.48 c/d estimates for the LHON group and 3.60 c/d and 2.76 c/d for controls in the middle and high frequencies respectively.

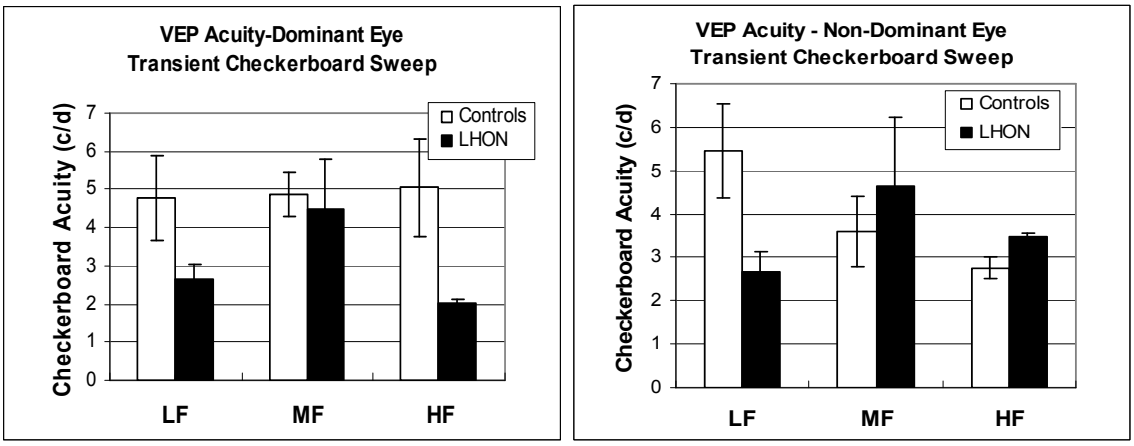

Figure 29: Checkerboard acuities measured in cycles/degree for low, medium and high frequency components, obtained from the transient checkerboard sweep in the dominant (left) and nondominant (right) eyes in asymptomatic LHON individuals and controls. Error bars indicate ± 1 SEM.

Analysis of Steady-State VEPs: Appearance-Disappearance of Isolated Checks

Analysis of Amplitude: Individual Functions

The sweep analysis of the isolated checks, depicted in Fig 30, revealed consistent

peak amplitudes at the 16x16 check, indicative of an intact magnocellular system. However, a consistent drop in the amplitude functions was noted across all four conditions between the 16x16 check and the 32x32 check in both the M bright and M dark conditions given stimulation of both dominant and nondominant eyes. For example, amplitudes were considerably high for L2 in the M bright condition given stimulation of both dominant and nondominant eyes with amplitudes of 7.40 μV and 6.16 μV respectively at the 16x16 condition, and 5.50 μV in the M dark condition given stimulation of the dominant eye. However, in the M bright condition given stimulation of the nondominant eye, the amplitude crashed at the32x32 check with an amplitude of 1.26 μV. Moreover, the aforementioned consistent declines and near dropout at the 32x32 check was evidenced in the M dark condition given stimulation of the nondominant eye in this same individual as well. Similarly, even in L6, an older female (age = 62), where one would expect lower amplitudes, considerably high amplitudes were evidenced. For example, an amplitude measure of 5.66 μV was obtained in the M bright condition given stimulation of the dominant eye in the 8x8 check, which then plummeted to 0.86 μV at the 32x32 check. Again, in the dark condition, an amplitude measure of 6.36 μV at the 16x16 check fell to 2.42 μV at the 32x32 condition. On the one hand, these cases are indicative of consistent increased signals at the 8x8 and 16x16 check sizes, whereas in these same individuals, amplitudes decreased considerably primarily at the 32x32 condition . These findings suggest an intact magnocellular pathway whose peak contrast is typically noted at the 16x16 check.

However, further analysis of the individual amplitude functions, revealed a drop in amplitude for L1 in the M bright condition given stimulation of the dominant eye,

beginning at check 8x8 with total dropout at check16x16 and only a 0.51 μV amplitude for check size 32x32. Two other participants, a mother and son (L6 and L5), showed a similar decline, beginning with the 8x8 check and falling to 0.86 μV and 0.61 μV, respectively at the 32x32 check. In the M dark condition given stimulation of the dominant eye as well, L1 indicated a similar drop in amplitude at the 8x8 and 16x16 check sizes, and although amplitude rose for L5 after the 4x4 check, his overall amplitude function was still low. Similarly, amplitude measures for L3 at the 8x8 and 16x16 checks were considerably low at 1.06 μV and1.57 μV respectively, and the amplitude only rose at the 32x32 and 64x64 check sizes. In the M dark condition, given stimulation of the nondominant eye, sharp declines for L1 were again seen with amplitudes of 2.0 μV and 0.57 μV for the 4x4 and 8x8 checks respectively. Similarly, another participant, L3 evidenced nearly identical amplitudes at those check sizes with 1.12 μV and 1.02 μV respectively. Consistent declines were evidenced for L2 until the 32x32 check with an amplitude measure of 0.66 μV and a modest rise afterward at the higher check sizes to only 0.84 μV at the 64x64 check and 1.06 μV at the 128x128 check. These findings implicate the middle check sizes and as such, suggest a magnocellular deficit. This seeming contradiction will be addressed in the discussion.

The magnitude of the amplitude measurements was always greatest for L4 given stimulation of both dominant and nondominant eyes in both the M bright and dark conditions. For example, amplitudes rose to 9.23 μV and 8.70 μV at the 16x16 check in the M dark condition given stimulation of both dominant eye and nondominant eyes respectively.

Low overall amplitudes in the spatial sweep were evidenced in the affected participant, LA (LHON affected), in both the M bright and dark conditions given stimulation of both dominant and nondominant eyes, consistent with the clinical expression of the disease. In the M bright condition in both eyes, the amplitude rose and fell, for the most part, albeit slightly, with each check. Given stimulation of the dominant eye, this pattern initiated with a rise from the 2x2 check to the 4x4 check, whereas given stimulation of the nondominant eye the pattern initiated with a decline from the 2x2 check to the 4x4 check. In the M dark condition, the amplitude was highest at the 8x8 check with amplitudes of 3.13 μV given stimulation of the dominant eye and 2.69 μV given stimulation of the nondominant eye whereafter the amplitude basically declined, with a slight rise after the 64x64 check given stimulation of the dominant eye and the 32x32 check given stimulation of the nondominant eye.

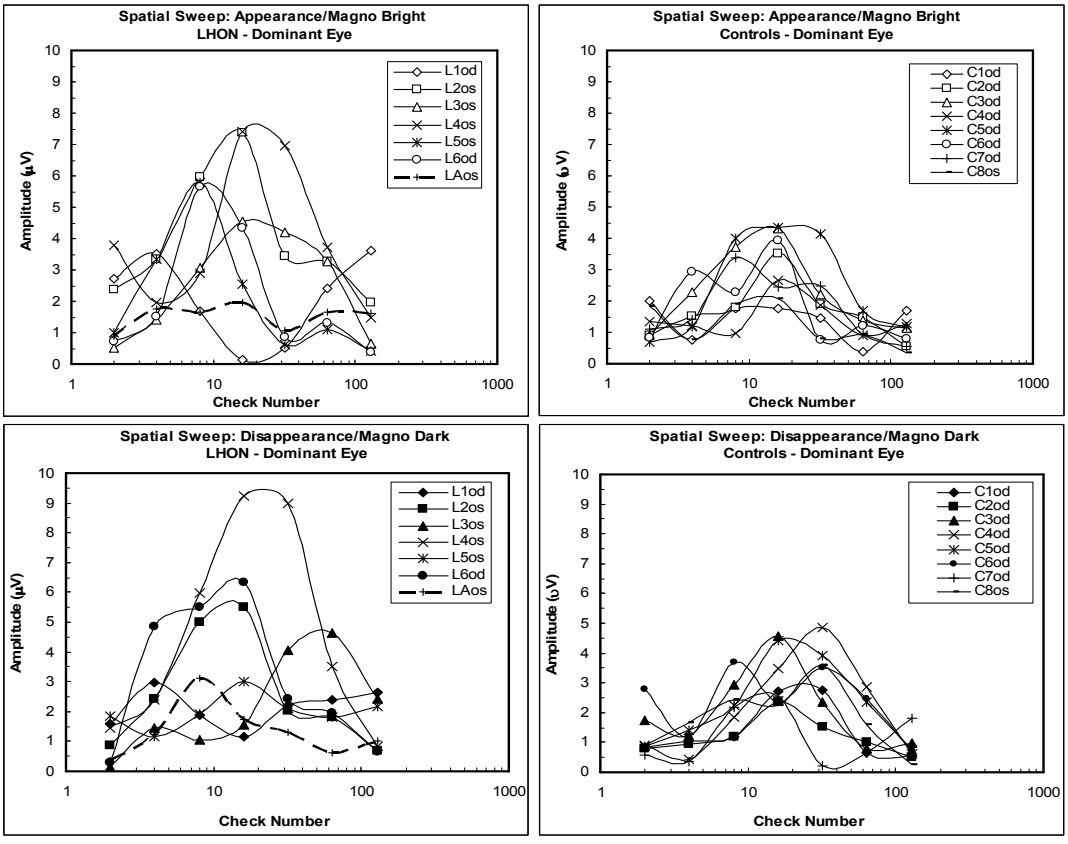

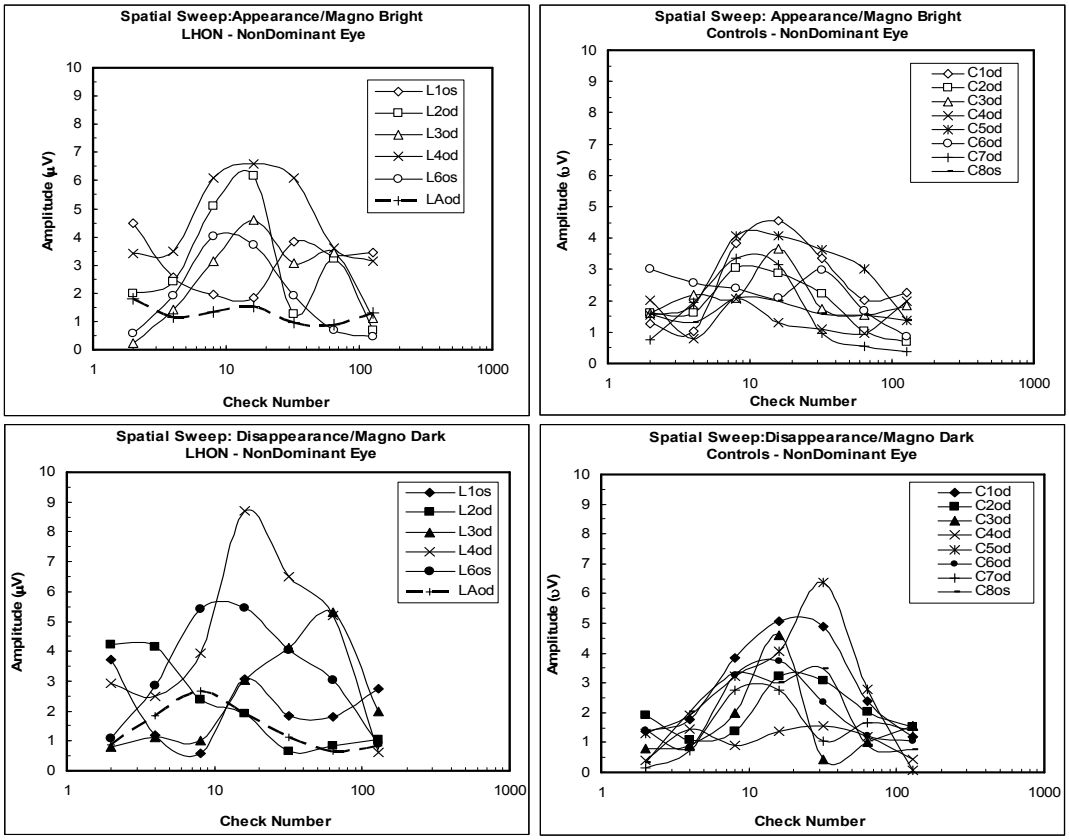

Figure 30: Individual amplitude plotted as a function of incremental check number from a spatial sweep of isolated bright and dark checks in the dominant (top 2 sets) and nondominant (bottom 2 sets) eyes of asymptomatic LHON individuals (left), controls (right), and one LHON affected individual with recovery of visual function (left). The amplitude function for the affected LHON individual is depicted in all graphs with a dashed line. Error bars indicate ± 1 SEM

Analysis of Amplitude: Group Mean Functions

The amplitude functions obtained from the fundamental frequency component of the VEP elicited by the isolated check sweep stimuli are depicted in Figure 31. These functions replicated the classic inverted U shape characteristic of this type of spatial function (Zemon et al., 1988). For the vast majority of check sizes under all conditions, the LHON group produced significantly larger amplitude responses than controls. All of these functions peaked at the 16x16 check for both normal controls and for LHON maternal relatives for both the appearance (M bright) and disappearance (M dark)

isolated check sweeps given stimulation of both dominant and nondominant eyes. However, the amplitude functions sharply declined, at the 32x32 check, albeit still higher in magnitude than controls, and then increased again at the 64x64 check in the M bright condition given stimulation of the dominant eye and the M bright and dark conditions given stimulation of the nondominant eye. Additionally, the peak tended to shift a little toward the smaller check sizes in the M dark condition given stimulation of both dominant and nondominant eyes with higher response amplitudes under the dark conditions overall. For controls, given stimulation of the dominant eye, in the M bright condition, the function fell to 1.10 μV at the 64x64 check, whereas in the M dark condition, the function was higher at 1.54 μV. The function fell in the M bright condition given stimulation of the dominant eye even at the 32x32 check to 1.95 μV, whereas in the M dark condition it was still higher at 2.84 μV. Similarly, given stimulation of the nondominant eye, in the M bright condition, the function fell to 2.20 μV at the 32x32 check, while it remained higher at 2.91 μV in the dark condition. These findings are consistent with the morphology and physiology of the visual system in that OFF cells are smaller than ON cells and therefore do not fall off as quickly at high spatial frequencies (Dacey &Peterson, 1992).

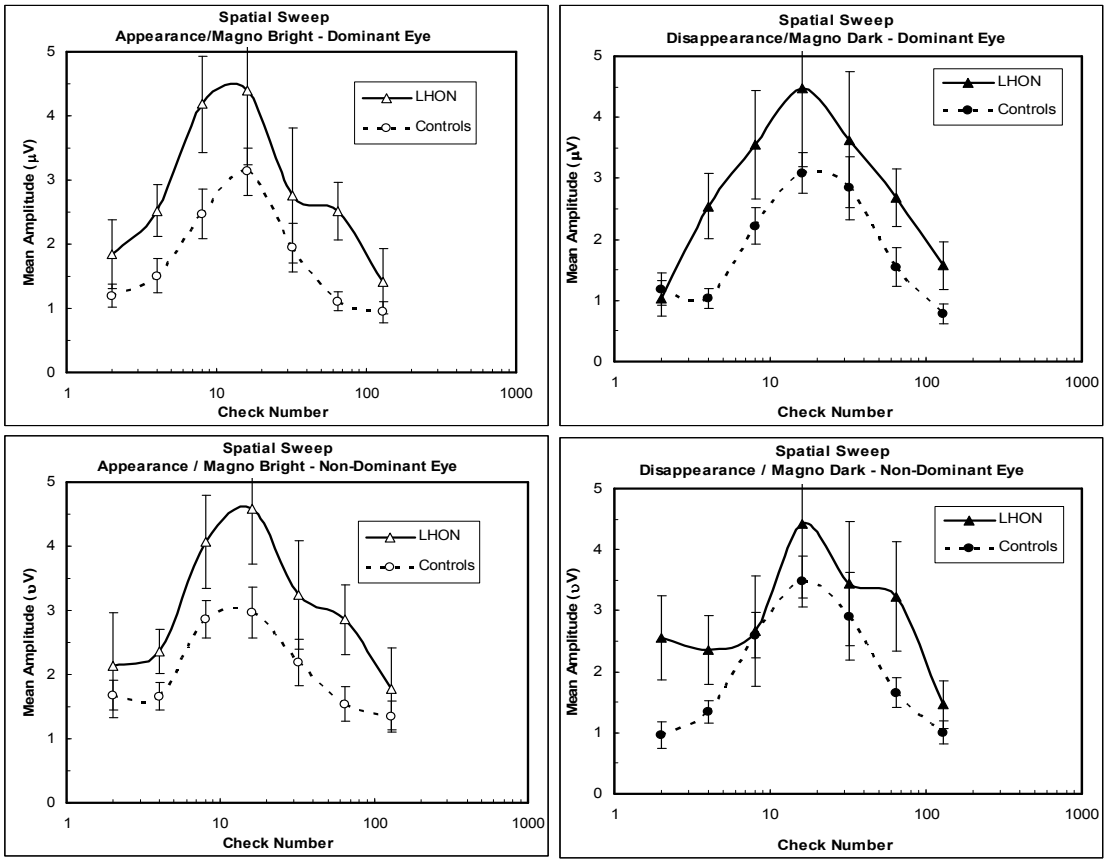

Figure 31: Mean amplitude as a function of incremental check number from a spatial sweep of isolated bright (left) and dark (right) checks in the dominant (top) and nondominant (bottom) eyes of asymptomatic LHON individuals and controls. Error bars indicate ± 1 SEM.

This basic waveform morphology was evidenced in the LHON population as well for both the M bright and dark conditions given stimulation of both dominant and nondominant eyes with average peaks at the 16x16 check. The most significant difference between the groups was in the magnitude of the functions, in that LHON amplitudes were higher at all check sizes in both the M bright and dark conditions given stimulation of both dominant and nondominant eyes reaching peaks, for example, at the 16x16 check of 4.47 μV in the dark condition given stimulation of the dominant eye and 4.58 μV in the bright and 4.42 μV in the dark condition given stimulation of the nondominant eye.

A repeated-measures, mixed-model ANOVA was used to analyze these data. Amplitude measures from the M bright condition, (including L1) showed significantly greater amplitudes for the LHON population across all check sizes with $F(1, 12) = 9.32$, $p = 0.0100$ given stimulation of the dominant eye, and $F(1, 11) = 6.40$, $p = 0.0279$ given stimulation of the nondominant eye. Pooling both dominance and nondominance, not used as a factor, significance was again reached with $F(1, 12) = 8.55$, $p = 0.0127$. Similarly, amplitude measures from the M dark condition also indicated significantly greater amplitudes for the LHON population as opposed to the normals given stimulation of both the dominant eye $F(1, 12) = 6.79$, $p = 0.0230$, the non dominant eye $F(11,1) = 4.91$, $p = 0.0486$ and when pooling dominance and nondominance together $F(1, 12) = 6.82$, $p = 0.0227$.

An anomalous participant from the LHON population was removed for further analysis based on evidence of early visual abnormalities. Amplitude measures from the contrast reversing checkerboard sweep for the M bright stimulus, (excluding L1) indicated an even stronger effect with significantly greater amplitudes for the LHON population across all check sizes with $F(1, 11) = 11.27$, $p = 0.0064$ given stimulation of the dominant eye, and significance as well given stimulation of the non dominant eye with $F(10, 1) = 4.96$, $p = 0.0501$. Pooling both dominance and nondominance, not used as a factor, significance was again reached with $F(1, 11) = 7.97$, $p = 0.0166$. Similarly, when removing the anomalous participant, an even greater effect was evidenced with amplitude measurements from the M dark condition indicating significantly greater amplitudes for the LHON population as opposed to the controls given stimulation of both the dominant eye $F(1, 11) = 7.92$, $p = 0.0168$, and the non dominant eye $F(10, 1) = 6.46$,

p=0.0293 and when pooling dominance and nondominance together F (1, 11) = 8.42, p=0.0144.

Analysis of Noise: Individual Functions

Although noise levels were highest for L1 across all check sizes in both M bright and dark conditions given stimulation of both dominant and nondominant eyes, his SNR ratios were almost totally below criterion or hovered right above the criterion in all four conditions. Specifically, in the M bright condition given stimulation of the dominant eye, the middle check sizes of 8x8, 16x16 and 32x32 were below criterion and given stimulation of the nondominant eye, check sizes of 8x8 and 16x16 were below criterion. In the M dark condition given stimulation of the dominant eye, all check sizes were below criterion except for check size 4x4 and given stimulation of the nondominant eye all were below criterion except for check sizes 2x2 and interestingly check size 16x16, which is inconsistent with an OFF pathway deficit. Overall, there was a consistent dropout at the middle check sizes for L1 indicative of a magnocellular deficit and the signal comes out of the noise at the higher checks indicative of an intact parvocellular system.

Noise levels were relatively low for the affected LHON participant, LA, in both M bright and dark conditions in both eyes. For example, the highest noise values obtained given stimulation of the dominant eye, was 1.3 at both the 64x64 check in the M bright condition and the 8x8 check in the M dark condition. Given stimulation of the nondominant eye, the highest levels obtained were 1.49 at the 32x32 check in the M bright condition and 1.8 at the 16x16 check in the M dark condition.

Analysis of Noise: Group Functions

Overall, no significant differences were found in noise functions as well. However, noise functions, elevated in the LHON population, approached significance in the M dark condition given stimulation of the dominant eye with $F(1, 12) = 4.38$, $p = 0.0583$ and when pooling both dominance and non dominance with $F(1, 12) = 4.50$, $p = 0.0554$. Given stimulation of the nondominant eye, slightly greater levels were also detected in the noise functions in the LHON population for both the M bright and M dark conditions. Noise for controls in the M bright condition ranged from 1.47 μV to 1.71μV given stimulation of the dominant eye and from 1.43 μV to 1.87 μV given stimulation of the nondominant eye, whereas the LHON group ranged from 1.75 μV to 2.10 μV given stimulation of the dominant eye and from 1.68 μV to 1.88 μV given stimulation of the nondominant eye. Similarly, in the M dark condition, noise for controls ranged from 1.46 to 1.76 given stimulation of the dominant eye and 1.47 μV to 1.76 μV given stimulation of the nondominant eye, whereas the LHON group ranged from 1.75 μV to 2.50 μV given stimulation of the dominant eye and from 1.67 μV to 2.24 μV given stimulation of the nondominant eye.

Analysis of SNR: Individual Functions

However, consistent with declines noted in the amplitude functions, similar overall declines were noted in SNR values between the 16x16 check and the 32x32 check across all four conditions. The high SNR value at the 16x16 check is again indicative of an intact magnocellular system, whereas the decline may represent either a faulty

parvocellular system or lateral inhibition at that check size due the magnified signal at the 16x16 check. Again, this seeming discrepancy will be addressed in the discussion.

In the isolated bright check condition, for L2 and L1 given stimulation of the dominant eye, and L2, L1, and L4 given stimulation of the nondominant eye, the data remained out of the noise until the highest check (128), whereas it dipped into the noise at that check size in the dark check condition, as opposed to controls whose data typically would stay out of the noise longer in the dark condition.

Furthermore, the evidence of signals out of the noise more consistently in the M bright conditions for the unaffected LHON relatives may be indicative of an intact ON system as opposed to more signals in the noise in the M dark conditions, which may reflect an OFF deficit. This is even more atypical given the normal findings of higher check sizes out of the noise in the M dark conditions.

SNR values for LA indicated the same rising and falling pattern as the noise levels in the M bright condition in both eyes. The SNR was at or below, yet near criterion, only at the 2x2 and 32x32 checks in the M bright condition given stimulation of the dominant eye, whereas it was at or below, yet mostly near criterion at the 4x4, 32x32, 64x64 and 128x128 check sizes given stimulation of the nondominant eye. In the M dark condition, the SNR was at or below, yet near criterion at the 2x2, 4x4, 64x64 and 128x128 check sizes given stimulation of the dominant eye, and the 2x2, 64x64 and 128x128 check sizes given stimulation of the nondominant eye. Except for the M bright condition given stimulation of the dominant eye, it would appear that the SNR data, implicate a low and a high check deficit as opposed to a middle check deficit in the affected LHON participant

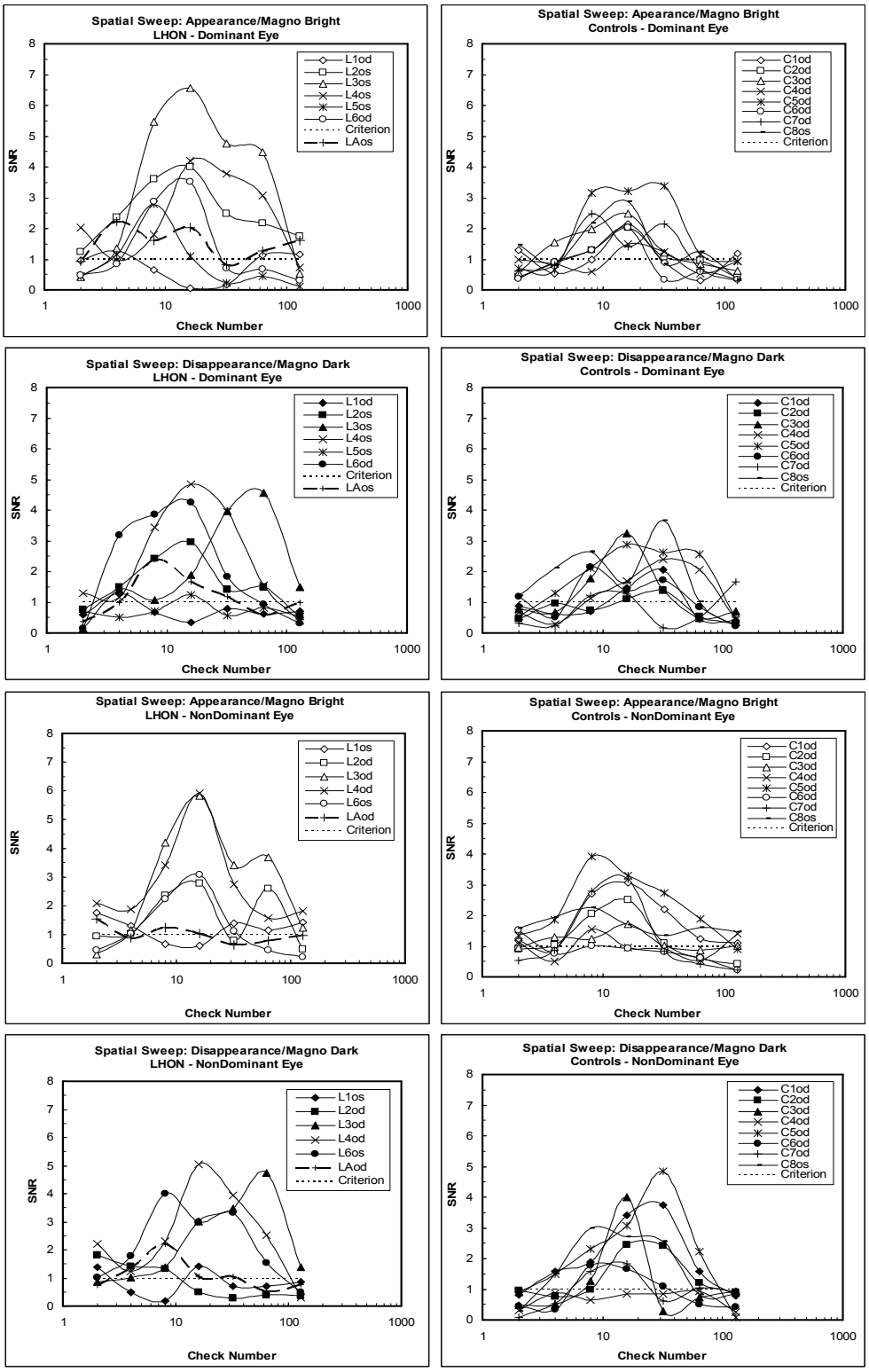

Figure 32: Individual signal-to-noise-ratios plotted as a function of incremental check number from a spatial sweep of isolated bright and dark checks in the dominant (top 2 sets) and nondominant (bottom 2 sets) eyes of asymptomatic LHON individuals (left), controls (right), and one LHON affected individual with recovery of visual function (left). The SNR function for the affected LHON individual is depicted in all graphs with a dashed line. SNR values below criterion indicate ratios indistinguishable from noise. Error bars indicate ± 1 SEM

Analysis of SNR: Group Functions

Mean signal-to-noise ratios were elevated in the LHON population in both the M bright and M dark condition given stimulation of the dominant eye. In both M bright and dark conditions in both eyes, the LHON group maintained SNR values above criterion up until the highest check of 128x128, except for the 2x2 check given stimulation of the dominant eye, whereas the controls were below or near criterion for the 2x2, 4x4, 64x64 and 128x128 check conditions. For example, in the M bright condition, given stimulation of the dominant eye, even at the 4x4 check size, the controls are below criterion with a SNR of 0.88 μV, while the SNR for the LHON population at the 4x4 check is above criterion at 1.32 μV. The differential persists with increased check sizes with SNR values for controls of 1.74 μV, 2.21 μV and 1.39 μV for the 8x8, 16x16 and 32x32 check sizes respectively as opposed to higher SNR values evidenced in the LHON population of 2.87 μV, 3.23 μV, and 2.02 μV. SNR dips below criterion at 0.79 μV for controls at the 64x64 check, while it remains well above the criterion at 2.00 μV in the LHON population. In the M dark condition as well, mean SNR was below criterion at 0.84 μV at the 4x4 check and above criterion at 1.50 μV in the LHON population. The greatest differential in this condition was noted at the 16x16 check with SNR of 1.83 μV for controls and 2.59 μV for the LHON population. This is consistent with peak amplitudes at the 16x16 check which then sharply declined at the 32x32 check. At the 64x64 check, controls were at criterion level, whereas in the LHON population, the SNR was 1.67 μV.

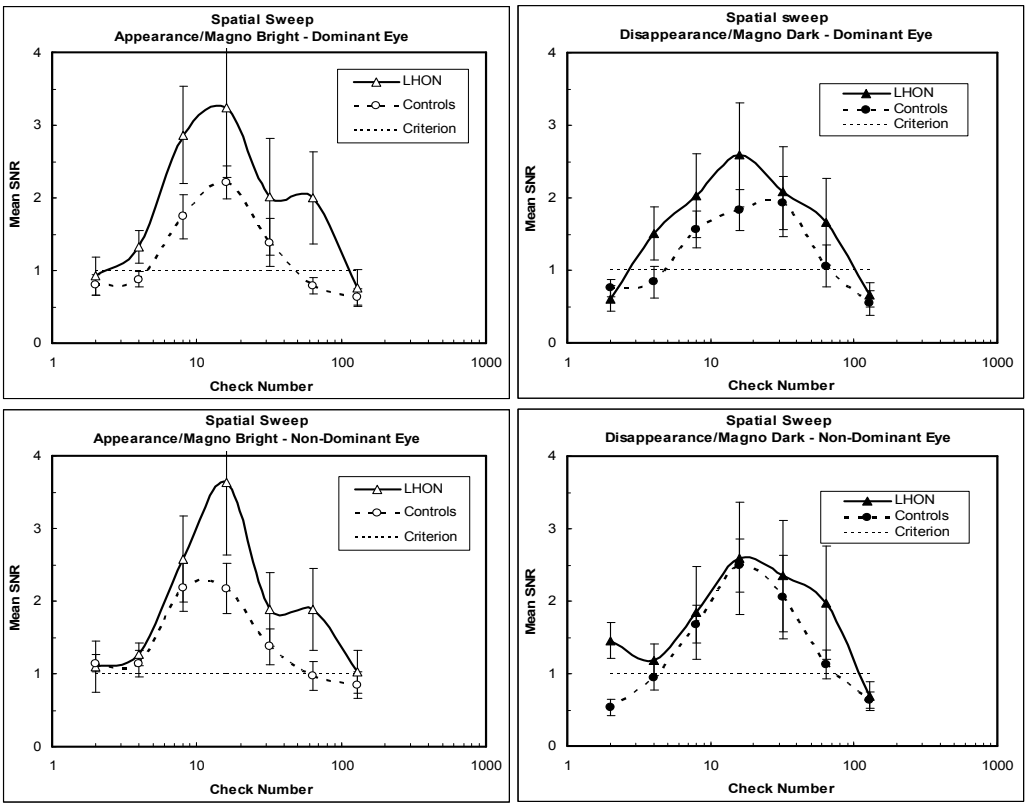

Figure 33: Mean signal-to-noise ratios as a function of incremental check number from a sweep employing isolated bright (left) and dark (right) checks given stimulation of both the dominant (top) and nondominant (bottom) eyes of asymptomatic LHON individuals and controls. SNR values below criterion indicate ratios indistinguishable from noise. Error bars indicate ± 1 SEM.

The greatest differential in SNR overall was evidenced in the M bright condition, given stimulation of the nondominant eye at the 16x16 check with a SNR of 2.17 for controls and 3.64 for the LHON group. This is again consistent with peak amplitude at the 16x16 check which sharply declined at the 32x32 check. Furthermore, at the 64x64 check, controls are at the criterion of 1, whereas the LHON group is still greatly above criterion with a SNR of 1.89. In the M dark condition as well, even at the 2x2 check, controls are considerably below criterion with a SNR of 0.54, whereas the LHON group is above criterion with a SNR of 1.46. Similarly at the 4x4 and 64x64 check conditions,

controls were near the criterion with SNR values of 0.95 and 1.13 respectively as opposed to the LHON group with SNR values of 1.19 and 1.98 respectively.

The mixed model ANOVA analysis revealed that differences in the signal-to-noise ratios were not significant in the initial analysis, with only a near significant finding in the M bright condition given stimulation of the dominant eye in the contrast sweep data with $F(1, 12) = 4.52$, $p = 0.0549$. However, when the anomalous participant was removed, signal-to-noise ratios obtained from the spatial frequency data were significantly elevated in the M bright condition given stimulation of the dominant eye with $F(1, 11) = 6.85$, $p = 0.0239$. Given stimulation of the nondominant eye, a trend level of significance was met with $F(10, 1) = 4.21$, $p = 0.0674$ and when pooling both dominance and nondominance, near significant findings were reached with $F(1, 11) = 4.57$, $p = 0.0558$. Trend levels of significance were obtained in the M dark conditions given stimulation of the dominant eye with $F(1, 11) = 4.30$, $p = 0.0624$, given stimulation of the nondominant eye with $F(10, 1) = 3.20$, $p = 0.1038$, and when pooling both dominance and nondominance with $F(1, 11) = 3.22$, $p = 0.1004$.

Analysis of Phase: Individual Functions

As per Figure 34, phase functions for both M bright and M dark conditions given stimulation of both the dominant and nondominant eyes for participant L1, indicated a more narrowly tuned phase function as compared to other maternal relatives and normal controls who generally expressed phase advance with increasing check size until approximately check 32x32 whereupon phase lag typically initiated. The phase functions for L1, however, were nearly identical in all four conditions expressing slight phase lag

until the 8x8 check except for the M dark condition given stimulation of the nondominant eye which indicated that lag until the 4x4 check., whereupon the function indicated a sharp phase advance until the 16x16 check whereafter it indicated the phase lag again, in all conditions except for the M dark condition given stimulation of the nondominant eye which fell after the 32x32 check.

The affected LHON participant evidenced relatively consistent phases throughout the conditions without extreme phase shifts that were evidenced in the unaffected LHON relatives. In the M bright condition, phase advance was evidenced until the 16x16 check given stimulation of the dominant eye and the 8x8 check given stimulation of the nondominant eye, whereupon phase lag ensued for the remainder of the function. In the M dark condition, given stimulation of the dominant eye, there was phase lag throughout the function with the sharpest lag between the 64x64 and 128x128 check sizes. Given stimulation of the nondominant eye, there was a relatively flat phase across check sizes until the 32x32 check with evidence of a phase advance at the 64x64 check, and a sharp phase lag, like that evidenced given stimulation of the dominant eye, at the 128x128 check.

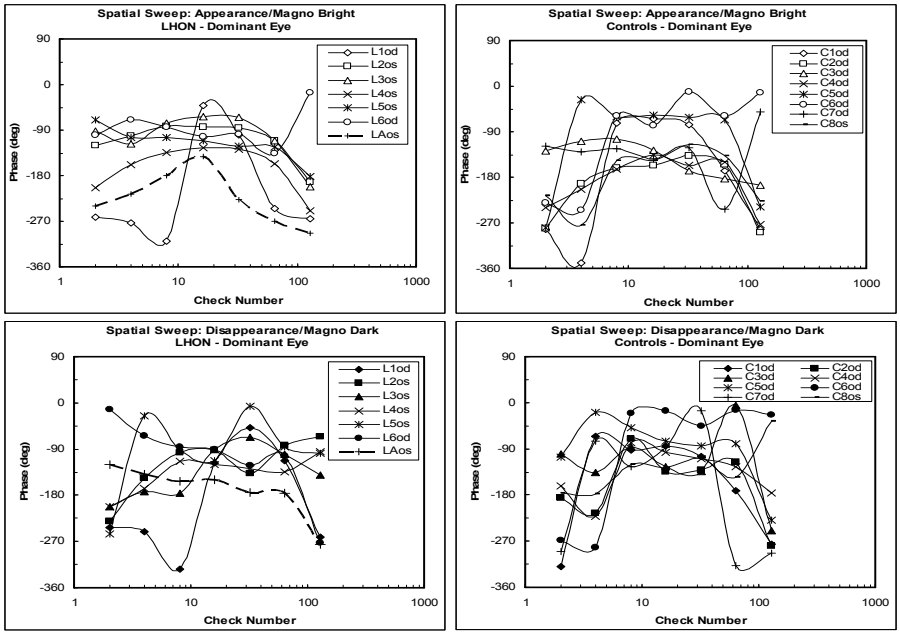

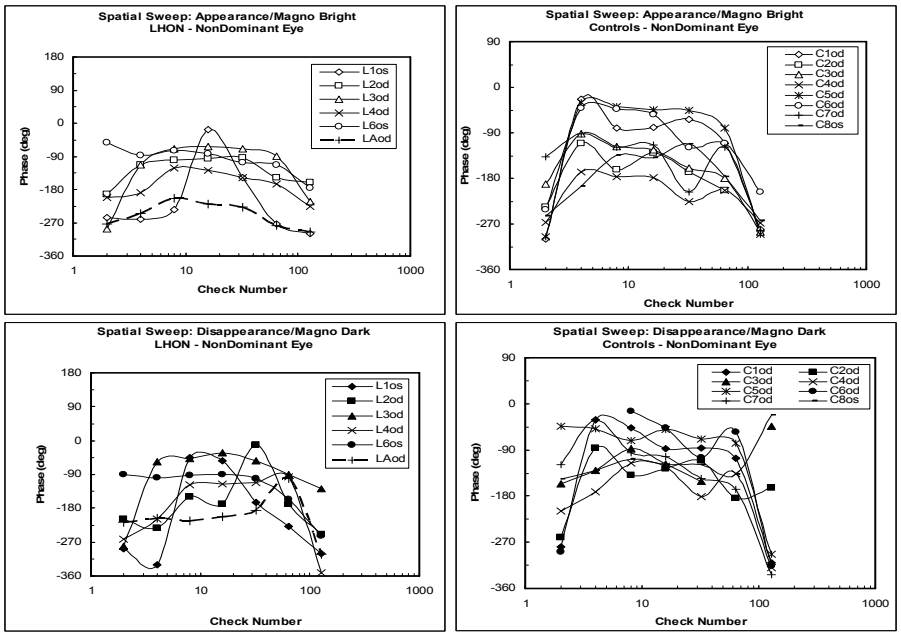

Figure 34: Individual phase plotted as a function of incremental check number from a spatial sweep of isolated bright and dark checks in the dominant (top 2 sets) and nondominant (bottom 2 sets) eyes of asymptomatic LHON individuals (left), controls (right), and one LHON affected individual with recovery of visual function (left). The phase function for the affected LHON individual is depicted in all graphs with a dashed line.

Analysis of Phase: Group Functions

Corresponding phase functions revealed the typical phase advance at the beginning of the function (larger checks) with increasing check sizes until the middle size checks, whereupon the phase shifts and begins to lag with increasing check size (smaller checks). Given stimulation of the dominant eye, this classic phase lag initiates primarily at the 32x32 check for both M bright and M dark conditions for both the LHON group and controls, whereas given stimulation of the nondominant eye, phase lag begins at the 16x16 check in the bright condition and at the 8x8 check in the dark condition for both the LHON group and controls. Furthermore, under all conditions in both eyes, except for the M bright condition given stimulation of the dominant eye where phase advances and phase lags for LHON group and controls were fairly synchronous, normals

tended to exhibit peak phases earlier, at larger check sizes of either the 4x4 or 8x8 check, whereas the LHON group tended to peak later at the 8x8, 16x16 or 32x32 check.

No significant differences were found in the phase functions in both bright and dark conditions given stimulation of both the dominant eye with F (1, 12) =2.07, p =0.1761 and the nondominant eye with F (1, 11) =0.09, p =0.7652, and when pooling both eyes together with F (1, 12) =1.11, p = 0.3135. Whereas phase differences were unremarkable in the first analysis, when the anomalous participant was removed, a significant positive shift in phase was observed in the LHON population as opposed to controls in the appearance (M bright) isolated check sweep given stimulation of the dominant eye with F (1, 11) = 7.64, p =0.0184. Although significance was not obtained given stimulation of the non dominant eye, when both dominance and nondominance were pooled, significance was again reached with F (1, 11) = 5.41, p =0.0402.

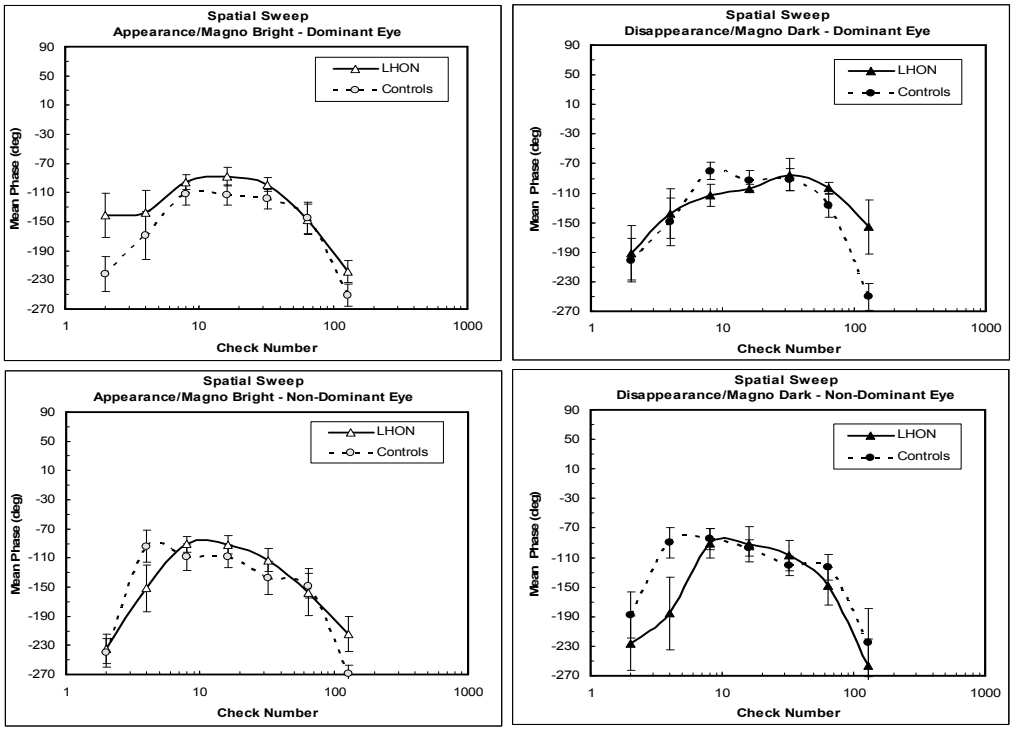

Figure 35: Mean phase as a function of incremental check number from a sweep employing isolated bright (left) and dark (right) checks in the dominant (top) and nondominant (bottom) eyes of asymptomatic LHON individuals and controls. Error bars indicate ± 1 SEM.

Analysis of Steady-State-Contrast VEPs: Appearance-Disappearance of Isolated Checks

Analysis of Amplitude: Individual Functions

The amplitude for L1 from the contrast response functions in the M bright and M dark conditions given stimulation of both the dominant and nondominant eyes shows increases in amplitude with increasing DOM like normal controls and for the most part, other maternal relatives. However, amplitude decreases sharply in the M bright and M dark conditions given stimulation of the dominant eye at the highest DOM suggesting significant hyperpolarizing inhibition at 32% DOM. Given stimulation of the nondominant eye, although the amplitude does not decrease sharply at 16% DOM, it plateaus and is comparably with other participants, at the lowest amplitude.

The low amplitude functions for the affected LHON participant indicated amplitude compression in all four conditions, especially in the M bright condition given stimulation of the nondominant eye with relatively flat amplitude measurements around 1μV throughout the function. In the other three conditions, modest increases in amplitude were evidenced with increasing DOM, yet the rise in amplitude was not commensurate with the rise in DOM. These low amplitudes and lack of contrast gain control is again consistent with the deficits described in the LHON visual system once a hypertoxic state ensues.

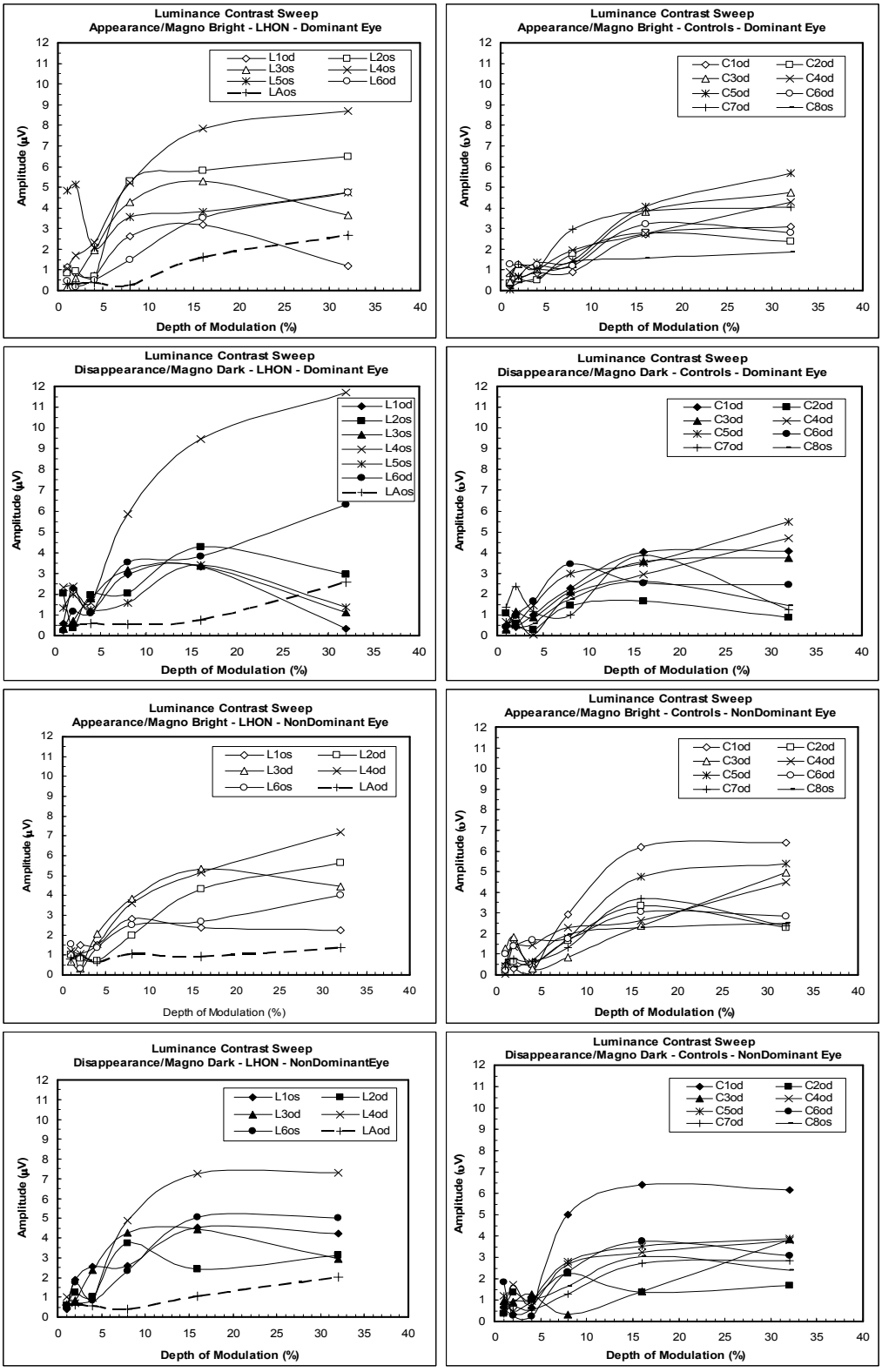

Figure 36: Individual amplitude plotted as a function of incremental depth of modulation (% contrast) from a contrast sweep of isolated bright and dark checks in the dominant (top 2 sets) and nondominant (bottom 2 sets) eyes of asymptomatic LHON individuals (left), controls (right), and one LHON affected individual with recovery of visual function (left). The amplitude function for the affected LHON individual is depicted in all graphs with a dashed line.

Hyperpolarizing inhibition may occur in other disease states with enhanced GABA in the brain. This is again consistent with my hypothesis of hypertoxicity. In normal probands positive for LHON mutations, once the supranormal, compensatory activity of a compromised oxidative system begins to fail, the byproducts of the oxidative stress would become toxic to the underlying system. This hypertoxicity is the proximate cause of the neural degeneration in the visual system.

Analysis of Amplitude: Group Functions

Consistent with the spatial function findings, amplitude measurements from the contrast response functions also indicated greater amplitudes in the LHON population as opposed to controls in both the M bright and M dark conditions given stimulation of both the dominant and nondominant eyes. For example, amplitudes rose from 3.73 μV at 8% DOM to 4.91 μV at 16%DOM in the M bright condition given stimulation of the dominant eye, whereas lower amplitudes were obtained for controls with 1.62 μV at 8% DOM and 3.11 μV at 16% DOM. The depth of modulation sweeps measuring contrast sensitivity for the M bright stimuli, indicated significantly greater amplitudes for the LHON population as opposed to controls given stimulation of the dominant eye with $F(1, 12) = 8.62$, $p = 0.0125$, and was nearly significant given stimulation of the non dominant eye with $F(11,1) = 4.47$, $p = 0.0582$. Nonetheless, when pooling both dominance and nondominance, not used as a factor, significance was again reached with $F(1, 12) = 9.09$, $p = 0.0108$. Whereas, significance was reached in the bright condition given stimulation of the dominant eye, significance was reached in the dark condition given stimulation of the non dominant eye with greater amplitude measures for the

LHON population as opposed to controls with F (11,1) = 6.39, p=0.0281. However, as in the bright condition, when pooling both dominance and nondominance, not used as a factor, significance was nearly reached with F (1, 12) = 4.41, p =0.0577.

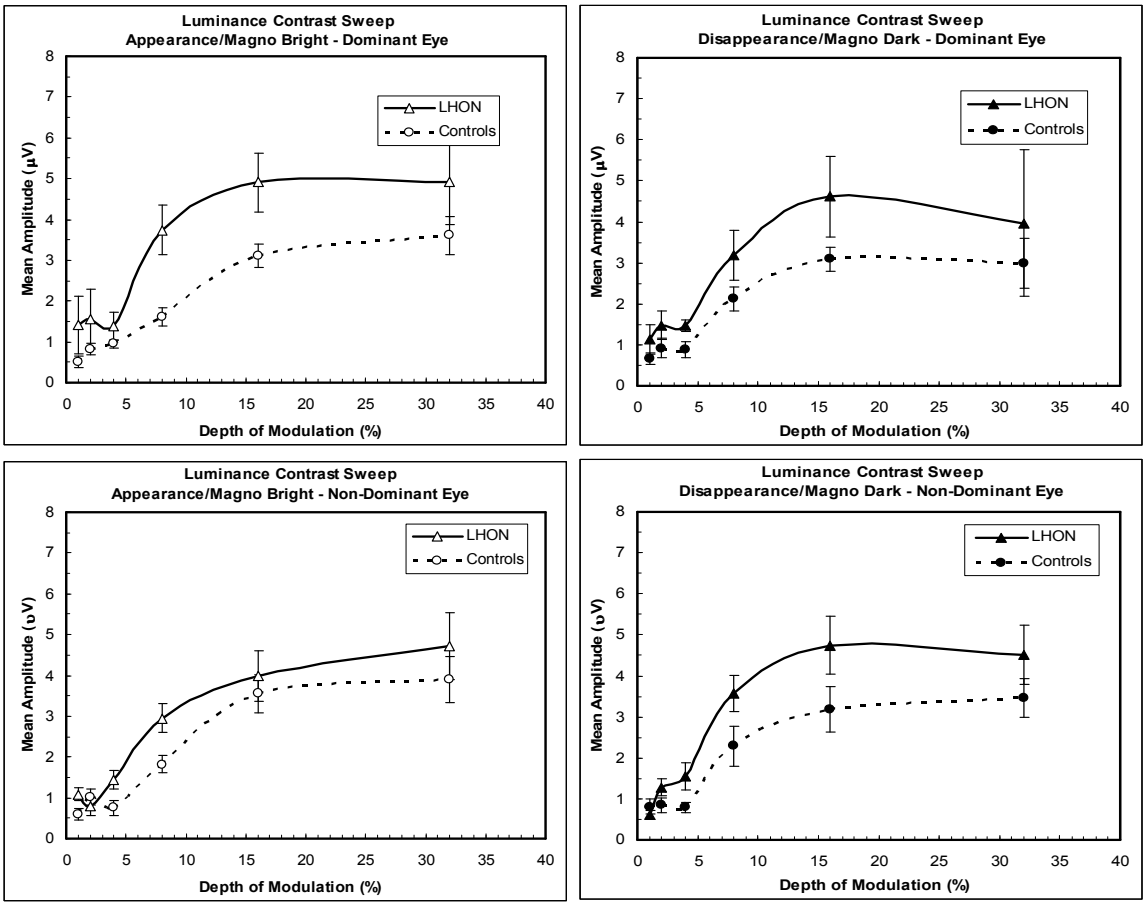

Figure 37: Mean amplitude as a function of incremental depth of modulation (% contrast) from a contrast sweep employing isolated bright (left) and dark (right) checks in the dominant (top) and nondominant (bottom) eyes of asymptomatic LHON individuals and controls. Error bars indicate ± 1 SEM.

For the most part, the greatest amplitudes were at 16% DOM for the LHON group and at 32%DOM for controls. Amplitude compression, where the slope decreases with increasing DOM, was evidenced in basically all conditions for both groups, except in the M bright condition given stimulation of the dominant eye for controls and in the M bright

condition given stimulation of the nondominant eye in the LHON group, where there was evidence of increased amplitude with increasing DOM.

Amplitude measurements in the contrast domain also indicated a more significant effect when the anomalous participant was removed. The luminance contrast sweeps for the M bright stimuli, again indicated significantly greater amplitudes for the LHON population as opposed to controls given stimulation of the dominant eye with $F(1, 11) = 14.83$, $p = 0.0027$, and reached significance given stimulation of the nondominant eye with $F(10, 1) = 6.81$, $p = 0.0261$ and pooling both dominance and nondominance with $F(1, 11) = 15.48$, $p = 0.0023$. However, even upon removal of the anomalous participant, in the contrast sensitivity sweep data in the dark condition, slightly less of an effect was seen when only trend significance was reached given stimulation of the dominant eye with $F(1, 11) = 3.77$, $p = 0.0781$ and significance was again only reached given stimulation of the nondominant eye, with greater amplitude measures for the LHON population as opposed to controls with $F(10, 1) = 5.18$, $p = 0.0460$. Again, as with the anomalous participant in the bright condition, when pooling both dominance and nondominance, significance was nearly reached with $F(1, 11) = 4.57$, $p = 0.0557$.

Analysis of Vector Mean Amplitudes: Group Functions

Significantly greater vector mean amplitudes were again evidenced in the LHON population as opposed to controls under both bright and dark conditions given stimulation of both the dominant and nondominant eyes. For example, the vector mean amplitude in the LHON population given stimulation of the dominant eye at 16% DOM was 4.73 μv and 4.39 μv in the bright and dark condition respectively, whereas it was 2.92 μv and

2.79 μv at 16% DOM for the controls. As in the mean amplitude functions, the vector mean amplitude functions also generally indicated amplitude compression with increasing DOM. The vector mean plots indicated the amplitude compression evidenced in the M dark condition for both the LHON group and controls given stimulation of the dominant eye and for the LHON group given stimulation of the nondominant eye. Amplitude compression was more severe in the LHON group. For example, amplitude decreased from 2.79 μV to 2.73 μV in controls, as opposed to 4.39 μV to 3.64 μV in the LHON group in the M dark condition given stimulation of the dominant eye with increases from16% to 32 % DOM.

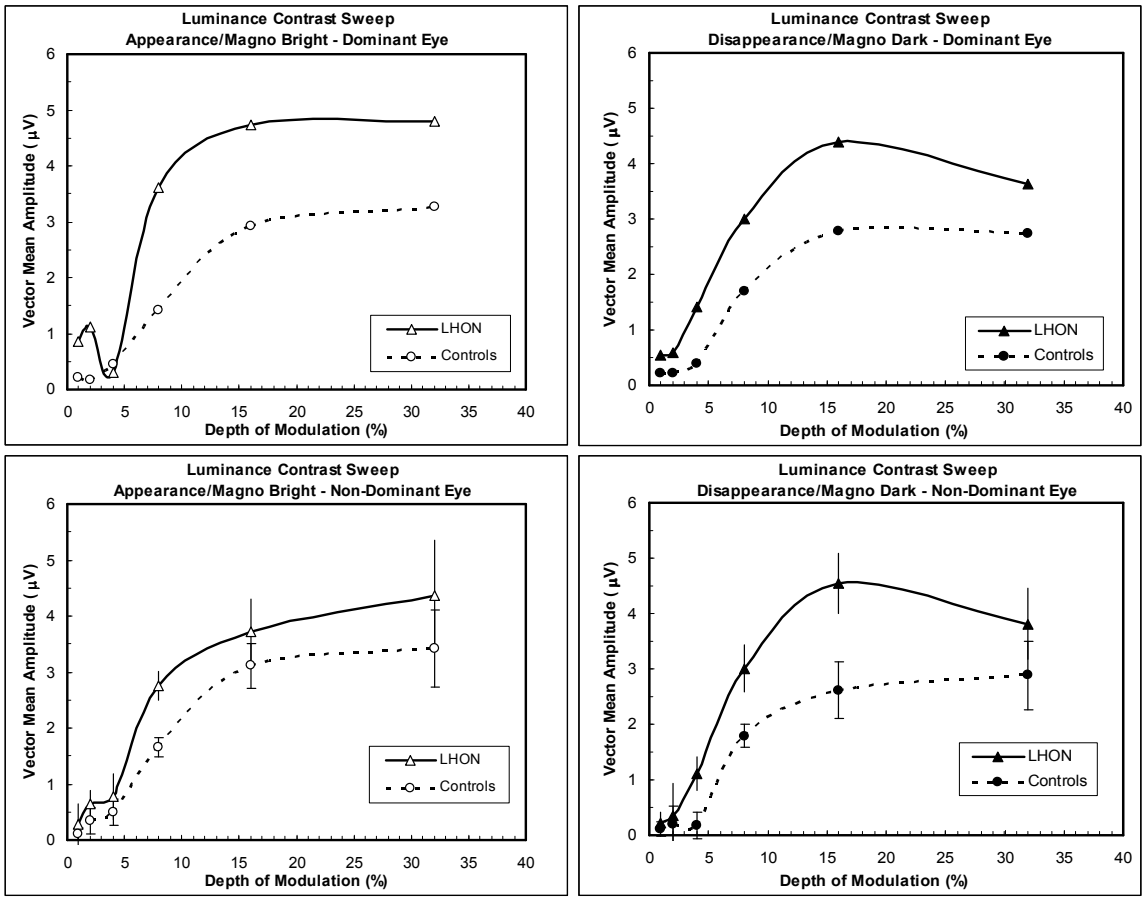

Figure 38: Vector mean amplitude as a function of incremental depth of modulation (% contrast) from a contrast sweep employing isolated bright (left) and dark (right) checks in the dominant (top) and nondominant (bottom) eyes of asymptomatic LHON individuals and controls. Error bars indicate ± 1 SEM.

Analysis of Noise and SNR: Individual Functions

Similarly, as in the SNR from the spatial sweeps, although noise levels were the highest for L1 across all check sizes in both M bright and dark conditions given stimulation of both the dominant and nondominant eyes, his SNR ratios were almost totally below criterion or hovered right above the criterion in all four conditions. Furthermore, the SNR data also rise and immediately drop in both the M bright and M dark conditions given stimulation of both the dominant and nondominant eyes, again, indicative of hyperpolarizing inhibition. Specifically, the SNR is above criterion at 8% DOM, at criterion at 16% DOM and below criterion at 32% DOM in the M bright conditions given stimulation of both the dominant and nondominant eyes. This drop in the SNR function is sharper in both eyes in the M bright condition as opposed to the M dark condition, and is consistent with other research showing this same effect in epilepsy and schizophrenia. Specifically, the SNR is at criterion at 8% and 16% DOM, and below criterion at 32% DOM in the M dark condition given stimulation of the dominant eye; and below criterion at 8% DOM and above criterion at 16% and 32% DOM given stimulation of the nondominant eye. These findings are nearly identical for L5 in the M bright and dark conditions given stimulation of the dominant eye. We cannot assess these attributes given stimulation of the nondominant eye for L5 due to the necessity to exclude his data from the nondominant eye due to inexplicable contamination of the VEP.

Noise levels for the affected LHON participant are low in all four conditions in the luminance contrast sweeps just as they were in the spatial sweeps. The SNR functions in the M bright condition indicate values below criterion until 16% DOM given

stimulation of the dominant eye and at criterion at 16% DOM given stimulation of the nondominant eye with SNR above criterion for both eyes at 32% DOM. In the M dark condition, SNR values were below criterion until 32% DOM given stimulation of the dominant eye and just above criterion at 1.15 at 32% DOM given stimulation of the nondominant eye.

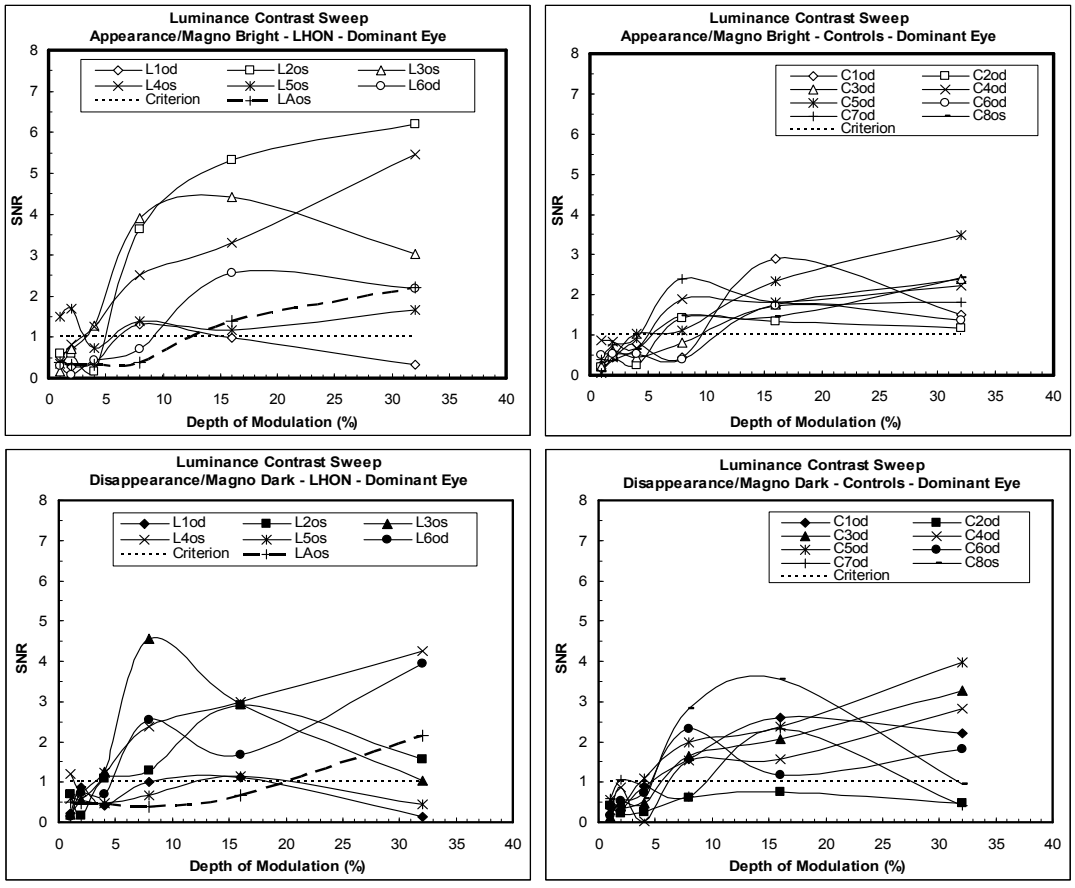

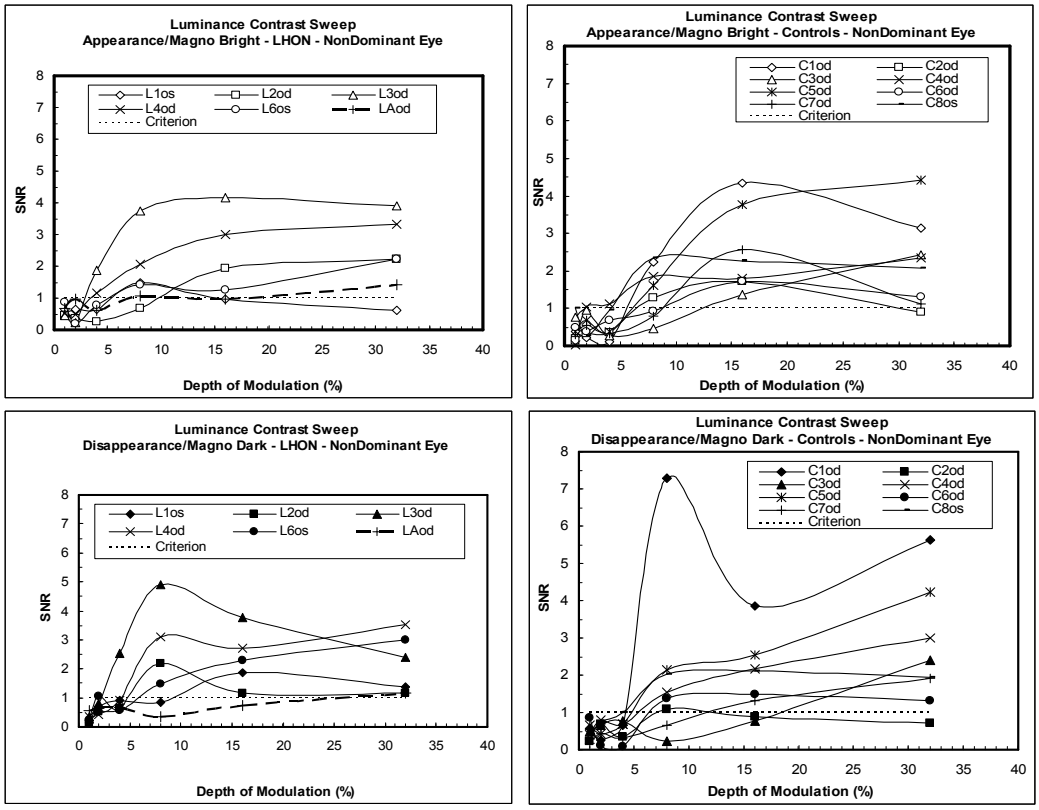

Figure 39: Individual signal-to-noise-ratios plotted as a function of incremental depth of modulation (% contrast) from a contrast sweep of isolated bright and dark checks in the dominant (top 2 sets) and nondominant (bottom 2 sets) eyes of asymptomatic LHON individuals (left), controls (right), and one LHON affected individual with recovery of visual function (left). The SNR function for the affected LHON individual is depicted in all graphs with a dashed line. SNR values below criterion indicate ratios indistinguishable from noise.

Analysis of Noise and SNR: Group Functions

Greater noise was seen in the LHON group as opposed to controls in the M bright condition given stimulation of the dominant eye and an even larger differential was seen in the M dark condition. Noise ranges were nearly identical to those evidenced in the spatial conditions. Noise for controls in the M bright condition ranged from 1.48 μV to 1.84 μV given stimulation of the dominant eye and from1.38 μV to 1.91 μV given stimulation of the nondominant eye, whereas the LHON group ranged from 1.88 μV to 2.26 μV given stimulation of the dominant eye and from 1.89 μV to 2.28 μV given

stimulation of the nondominant eye. Similarly, in the M dark condition, noise for controls ranged from 1.47 μV to 1.74 μV given stimulation of the dominant eye and 1.47 μV to 1.76 μV given stimulation of the nondominant eye, whereas the LHON group ranged from 1.88 μV to 2.37 μV given stimulation of the dominant eye and from1.58 μV to 2.60 μV given stimulation of the nondominant eye.

Furthermore, mean signal-to-noise ratios were elevated as well in the LHON population. In the M bright condition given stimulation of the dominant eye, both the controls (SNR = 0.66 μV) and LHON (SNR = 0.71μV) populations are nearly identical below criterion at 4% DOM, yet the SNR in the LHON population increases sharply to 2.24 μV at 8% DOM and 2.96 μV at 16% DOM and saturates thereafter, whereas SNR in the controls only reaches 1.25 μV at 8% DOM and 1.89 at 16% DOM and saturates thereafter. Interestingly, there was not as big a differential in SNR in the M dark condition given stimulation of the dominant eye. A rise in SNR was detectable in the LHON population again at 4% DOM with a SNR of 2.08 μV, whereas the controls only reached a SNR of 1.64 μV at 4% DOM. However, the remainder of the SNR function was nearly identical for both groups with increasing DOM.

Both groups were below criterion until 2% DOM in both the M bright and dark conditions given stimulation of the nondominant eye. At 4% DOM, the controls remained under criterion whereas the LHON group was right below criterion (SNR = 0.94) in the M bright condition and above criterion in the M dark condition (SNR = 1.11). The SNR for controls in the M bright condition rose until 16% DOM (SNR = 2.44), but then decreased with increasing contrast at 32% DOM (SNR = 2.22), whereas in the M dark condition, the SNR for controls decreased between 8% and 16% DOM from SNR =

2.04 to SNR =1.89, and then rose again with increasing contrast at 32% DOM with SNR =2.64. On the other hand, the SNR increased with increasing DOM for the LHON group in the M bright condition, and reached asymptote at 16% DOM in the M dark condition.

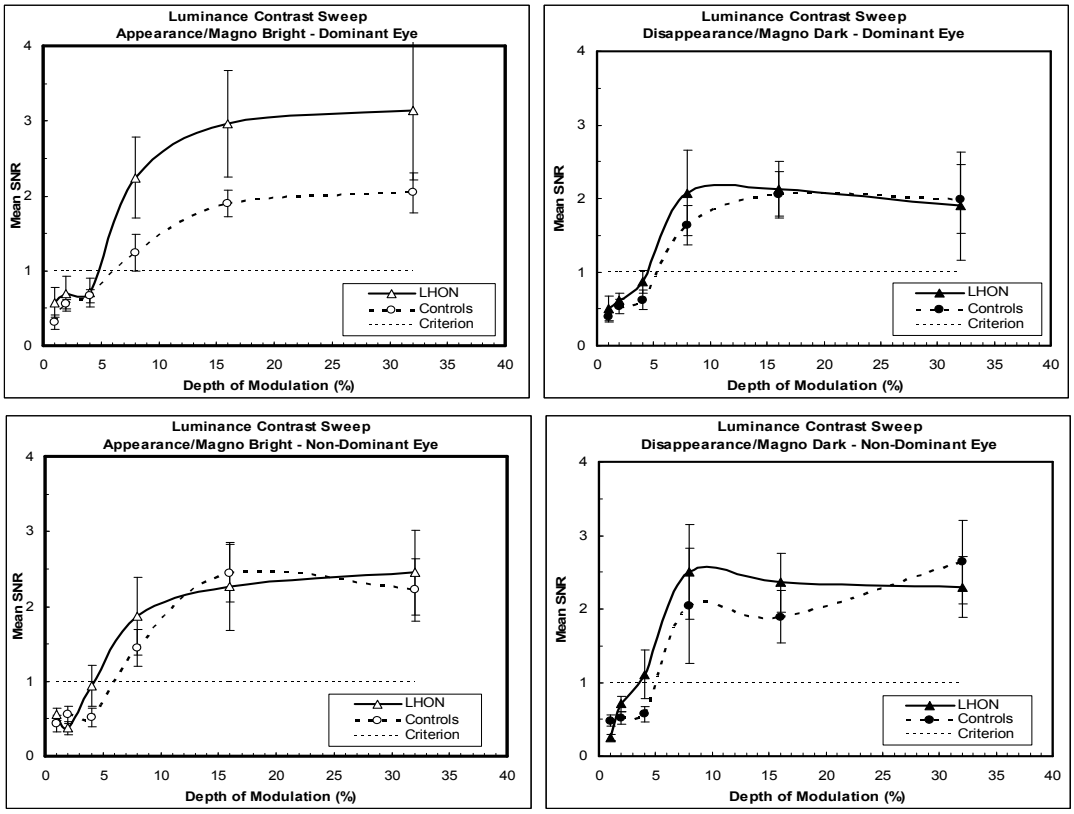

Figure 40: Mean signal-to-noise ratios as a function of incremental depth of modulation (% contrast) from a sweep employing isolated bright (left) and dark (right) checks in the dominant (top) and nondominant (bottom) eyes of asymptomatic LHON individuals and controls. SNR values below criterion indicate ratios indistinguishable from noise. Error bars indicate ± 1 SEM.

The mixed model ANOVA analysis revealed that differences in SNR from the contrast sweep data, were significantly elevated in the LHON population in the M bright condition given stimulation of the dominant eye with $F(1, 11) = 11.17$, $p = 0.0066$ and in the pooled data given stimulation of both the dominant and non dominant eyes with $F(1, 11) = 7.84$, $p = 0.0173$. This data indicates that the greater amplitudes evidenced in the

LHON population is not simply due to greater signal gain in the cortex contingent upon greater noise, but rather truly a more enhanced cortical signal. If there was simply greater noise, there would be a reduced ratio.

The morphology of these functions can sometimes hint at underlying physiology. The SNR in the LHON population given stimulation of the dominant eye appeared to rise more steeply in the M dark (OFF) condition, but then saturated with not as large a differential as controls. However, in the M bright condition (ON), the SNR function from the LHON population retained a greater differential throughout the range of check sizes and saturated with a higher asymptote than controls, again suggesting an ON/OFF difference in these populations.

Analysis of Phase: Individual Functions

In the contrast sweep conditions in the unaffected LHON sample, although the SNR indicated that the data generally remained out of the noise, the phase was flat, indicated a lag, or showed a slight phase advance which is consistent with weak contrast gain control and a faulty magnocellular input (Kaplan & Shapley, 1986). For example, L4, who consistently demonstrated the highest amplitudes across both M bright and dark conditions given stimulation of both the dominant and nondominant eyes (e.g. 11.70 μV at 32% DOM in the M dark condition given stimulation of the dominant eye), also demonstrated SNR ratios clearly above the critical value (e.g. SNR= 4.26 at 32% DOM in the M dark condition given stimulation of the dominant eye), and yet phase, in the same condition indicated only a moderate phase advance (from -136.23 at 16% DOM to -126.77 at 32%DOM). The bright contrast sweep data for L2 given stimulation of the

dominant eye indicates strong shunting inhibition because the data sharply jumps out of the noise at 8% contrast and the phase stays relatively flat, again supporting poor contrast gain control and weak magnocellular input. Similarly, the dark contrast sweep data for L2 in both eyes show a weak phase advance, again supporting a weak magnocellular input. Again, overall, these contrast functions show a definitive phase lag, whereas controls typically show phase advance. Once more, this is consistent with a dysfunctional magnocellular system with faulty contrast gain control and an intact parvocellular system.

The phase function for the affected LHON participant in the M bright condition indicated a steep phase lag from 4% to 16% DOM and a consequent steep phase advance from 8% to 16% DOM given stimulation of the dominant eye, and a phase lag from 2% to 8% DOM and mild phase advance from 8% to 16% DOM given stimulation of the nondominant eye. Thereafter, the phase functions indicated a phase lag given stimulation of the dominant eye and a flat phase given stimulation of the nondominant eye with increasing DOM from 16% to 32% DOM. In the M dark condition, given stimulation of the dominant eye, a sharp phase advance was noted from 2% to 8% DOM, a sharp phase lag from 8% to 16% DOM followed by another phase advance to 32% DOM. Given stimulation of the nondominant eye, a sharp phase lag was noted from 2% to 16% DOM with a subsequent phase advance to 32% DOM. It is interesting to note that overall in the M bright condition in both eyes, the phase was relatively flat with increasing DOM consistent with weak contrast gain control, and weak magnocellular input. However, in the M dark conditions in both eyes, the classic phase advance was noted with increasing DOM, suggesting perhaps an intact OFF as opposed to ON pathway.

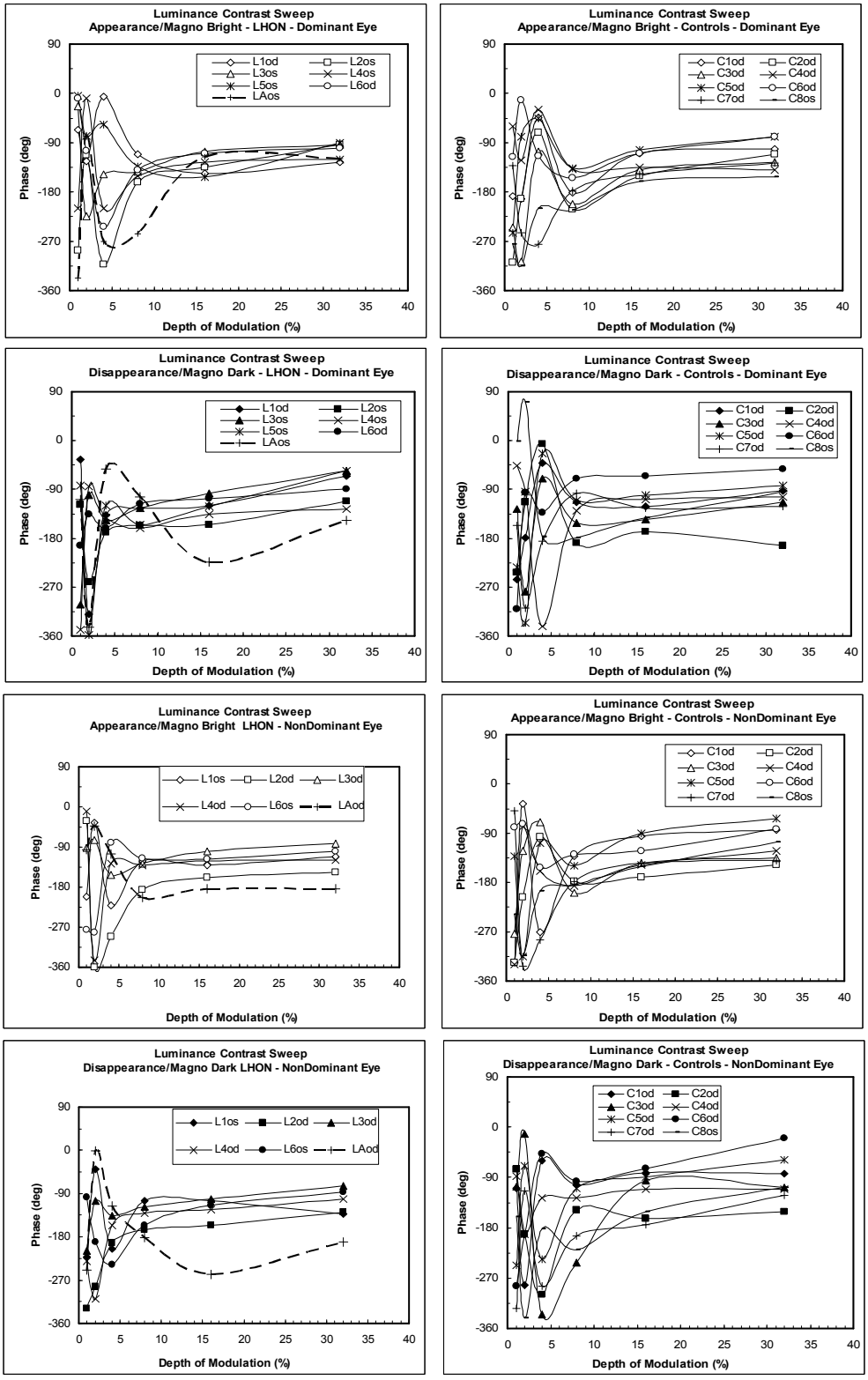

Figure 41: Individual phase plotted as a function of incremental depth of modulation (% contrast) from a contrast sweep of isolated bright and dark checks in the dominant (top 2 sets) and nondominant (bottom 2 sets) eyes of asymptomatic LHON individuals (left), controls (right), and one LHON affected individual with recovery of visual function (left). The phase function for the affected LHON individual is depicted in all graphs with a dashed line.

Analysis of Phase: Group Functions

Phase data in the M bright condition given stimulation of the dominant eye reveal a slight phase advance with increasing depth of modulation in both the LHON population and controls. Slightly more phase advance is noted for controls at low contrasts in the M bright condition and an overall phase advance is noted in the dark condition as well. In the M dark condition given stimulation of the nondominant eye, the LHON population exhibits a more drastic phase advance than controls between 4% and 8% DOM, but then exhibits a phase lag, whereas the controls are more consistent and express the typical phase advance with greater DOM.

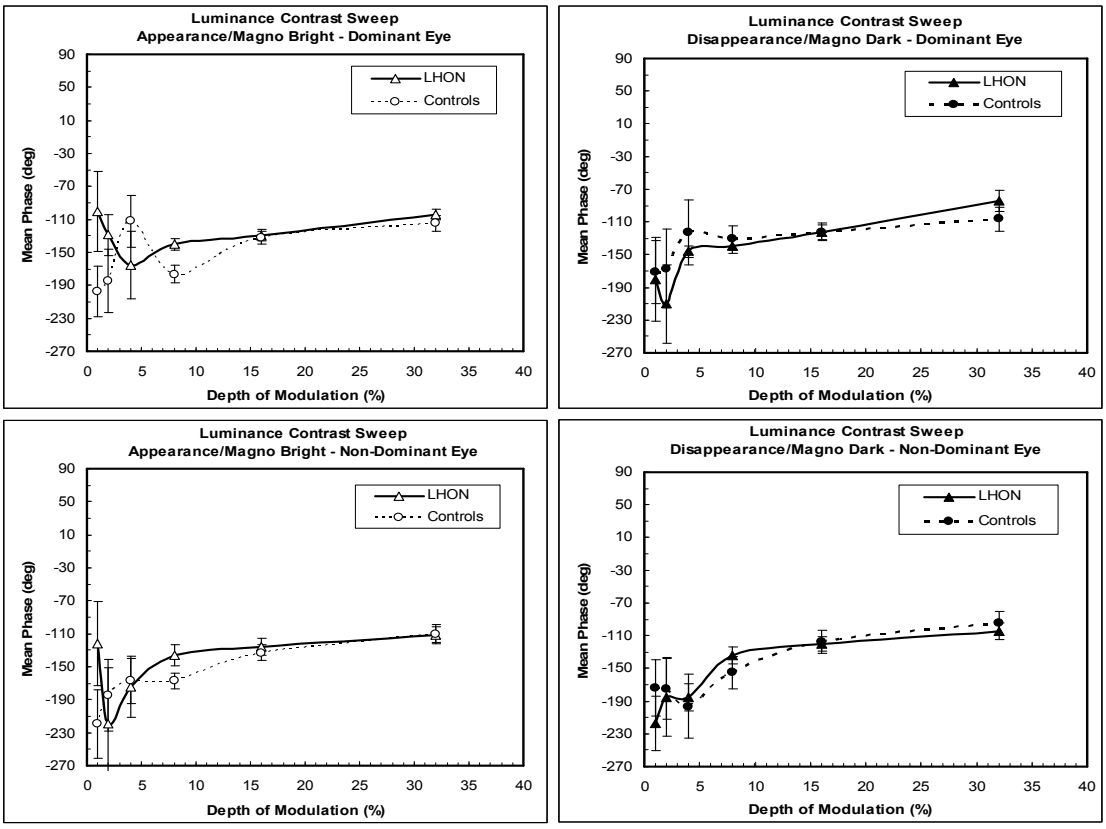

Figure 42: Mean phase as a function of incremental depth of modulation (% contrast) from a sweep employing isolated bright (left) and dark (right) checks in the dominant (top) and nondominant (bottom) eyes of asymptomatic LHON individuals and controls. Error bars indicate ± 1 SEM.

Similarly, greater phase advance in the controls was evidenced in the vector mean phase in both the M bright and M dark conditions given stimulation of both dominant and nondominant eyes. Typically, there is evidence of greater phase advance with increased DOM indicative of contrast gain control (Zemon &Ratliff, 1982; Zemon et al., 1987).

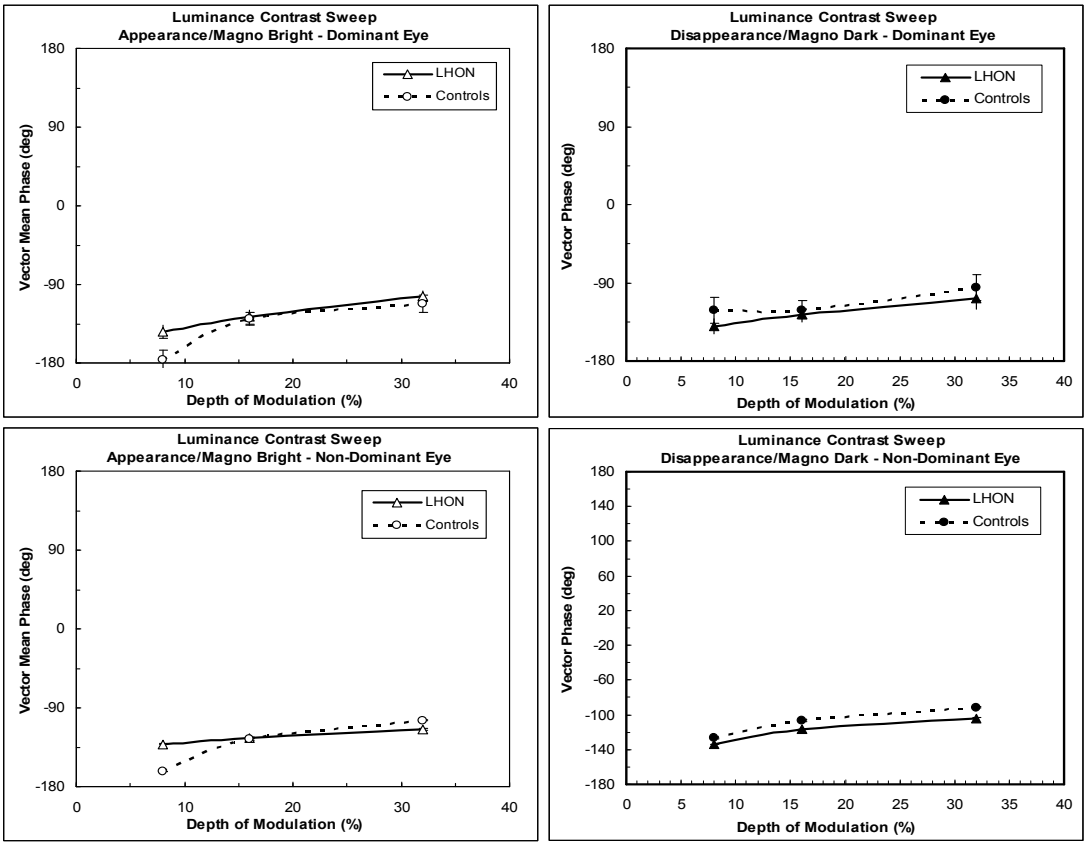

Figure 43: Vector mean phase as a function of incremental depth of modulation (% contrast) from a sweep employing isolated bright (left) and dark (right) checks in the dominant (top) and nondominant (bottom) eyes of asymptomatic LHON individuals and controls. Error bars indicate ± 1 SEM.

This research set out to determine which pathways, if any, might be selectively vulnerable to oxidative stress. Whereas asymptomatic LHON individuals express increased cortical signals with evidence of enhancement in both magnocellular, albeit perhaps specific spatial frequencies, and parvocellular pathways, data from the

anomalous participant and other individual functions support a magnocellular deficit as subclinically, selectively more vulnerable.

Chapter 9: Discussion

Summary of Overall Findings

Replication of Findings from Prior Experimentation

The data from the present set of experiments replicates the classic characteristics inherent in these functions. Specifically, the spatial functions replicate the amplitude compression in the M dark condition with increased check number (smaller checks) indicative of the inherent asymmetry in the ON/OFF pathways of the visual system (Zemon et al., 1988). Secondly, peak amplitudes in the spatial tuning functions were greater for smaller check sizes in the M dark conditions, again accentuating the asymmetry in the ON/OFF pathways of the smaller cell diameter of the OFF cell. Thirdly, some phase advance effects of contrast gain control were noted for controls in both M bright and M dark conditions given stimulation of both dominant and nondominant eyes in the contrast sweep.

Increased Cortical Signals

The most important finding was the consistently greater amplitudes and SNR values across all conditions implicating greater afferent signals in the LHON population as opposed to controls. Whereas Snellen, checkerboard and grating acuities were higher in controls (except for the mean grating acuity given stimulation of the dominant eye), significantly higher amplitudes were evidenced in the LHON population under both spatial and contrast stimuli, implicating increased afferent signals. Acuity, essentially a parvocellular test, measures resolving power at the highest spatial frequency, whereas the

other stimuli employed afford the requisite specificity for analyzing a broader range of visual function and selective pathway dysfunction.

Specifically, amplitudes in the LHON group were elevated as evidenced from mean amplitude measures from the transient 32x32 contrast reversing checkerboard and the spatial sweeps and mean amplitudes and vector mean amplitudes from the luminance sweeps. For the most part, SNR data and not just noise levels were consistently greater in the LHON population as opposed to controls, both in the spatial and contrast conditions, again suggesting an increased afferent signal in the LHON population.

Furthermore, greater coherence from the transient 32x32 contrast reversing checkerboard stimulus was seen in the LHON population in the high frequency band. There is evidence to suggest that the low frequency bands correlate with later cortical activity, the middle frequency bands with P100 and the high frequency bands with P0, input to the cortex. Greater coherence in the high frequency band is again consistent with the aforementioned findings of an increased afferent signal in LHON.

Selective Pathway Involvement

Enhanced M Pathway

The amplitudes, vector mean amplitudes, and SNR values from the luminance contrast sweeps were not only greater in magnitude in the LHON group but they also reflected greater contrast gain control as evidenced by greater saturation effects in nearly every condition. Specifically the function reached asymptote or turned down with increasing DOM in the LHON group as opposed to controls who were still showing increasing amplitudes with increasing DOM. Furthermore, the LHON group, in all

conditions, demonstrated a steep rise in slope at 4% DOM which has been shown to drive the magnocellular system exclusively, whereas controls demonstrated a smoother function indicating greater requisite DOM before rise in function. Although the SNR value was at or near criterion at 4% DOM except in the M bright condition given stimulation of the dominant eye, the controls were consistently below criterion in all four conditions at around 0.5 at 4% DOM. These findings, indicating greater contrast gain control is consistent with more enhanced magnocellular function in the LHON group.

Enhanced ON pathway

The evidence of signals out of the noise more consistently in the spatial sweep in the M bright conditions for the unaffected LHON relatives may be indicative of an intact ON system as opposed to more signals in the noise in the M dark conditions, which may reflect an OFF deficit. Similarly, the amplitudes from the contrast sweeps in the M bright conditions in both eyes indicated steeper slopes in the LHON group as opposed to controls perhaps indicative of a more enhanced ON response. The SNR from the contrast response functions in the LHON population appears to rise more steeply in the M dark (OFF) condition, but then saturates with not as significant a differential as controls. However, in the M bright condition (ON), the SNR function from the LHON population retains a greater differential throughout the range of check sizes and saturates with a higher asymptote than controls, again suggesting an enhanced ON pathway in LHON.

Enhanced P Pathway

Whereas the data from the luminance contrast sweeps were indicative of

enhanced magnocellular input, the data from the grating acuity sweeps indicated enhanced parvocellular input. Not only were the functions more consistently out of the noise at the higher spatial frequencies in the LHON group reflecting an intact parvocellular system, the checkerboard acuities were significantly greater for the asymptomatic LHON individuals as opposed to controls, perhaps reflecting enhanced P input.

M Pathway Deficits

The data from the anomalous LHON participant revealed rather striking magnocellular deficits in both transient and steady-state spatial conditions with marked dropout at the middle check sizes. Amplitude measurements from the contrast response functions may reflect hyperpolarizing inhibition at 32% DOM given the sharp decreases in amplitude at the highest DOM. The consistent dip in the function at 6 cpd which subsequently rises again at higher spatial frequencies in both dominant and nondominant eyes in asymptomatic LHON individuals from the grating sweep stimulus may similarly reflect hyperpolarizing inhibition due to hyperactivity from the enhanced cortical activity. Furthermore, it is perhaps the "notch" from the grating acuity functions, endemic to the asymptomatic LHON individuals, which may prove to be the most revealing as to the specific magnocellular spatial frequencies most vulnerable to hypertoxicty in LHON. "Notched" spatial frequency functions have been reported in normal controls (Tyler et al., 1978) albeit at lower spatial frequencies. The notch evidenced in LHON may thus reflect either a selective loss of narrow spatial frequency bandwidth within the middle spatial

frequencies or evidence of inhibitory processes canceling the supranormal, enhanced cortical EPSP activity evidenced in LHON.

Increased latencies from the transient contrast-reversing stimulus, dropout of the middle check sizes from the spatial sweep stimuli and low amplitudes and lack of contrast gain control from the contrast sweep stimuli in the affected LHON are also consistent with M pathway deficits.

Within-group variability

Although there was an attempt made to control for the inherent variability noted in this disease by selecting only the most common mutation for analysis, in essence, the only variable controlled for was genetic variability. It is not surprising that the within-group variability was greater in the LHON sample. Theoretically the construct of "asymptomatic" varies from no disease up until loss of vision. One would expect variability from individuals at different stages of a disease. In this study, significance was achieved despite the disadvantage of this within-group variability compounded with a small N. The within-subject variability, however, did induce a more cautious and conservative analysis of underlying etiological mechanisms. The small N did not afford the identification of potentially different subgroups within the asymptomatic group. Individual traces were distinctive as compared to the group mean, and yet were not only inherently consistent across conditions, but also consistent with other individual traces that although coerced recognition, did not obtain significance.

Transient 32x32 contrast reversing check

Significantly greater P100 amplitudes were evidenced in the LHON group. The P100 has been associated with a magnocellular gabaergic inhibitory contribution to the cortex (Previck et al., 1988). Again, these increased amplitudes are consistent with an enhanced M input to the cortex.

The greatest MSC differential was in the middle frequency bands in the transient 32x32 contrast reversing checkerboard stimulus given stimulation of both dominant and nondominant eyes, again consistent with the relative sparing or enhanced response of the M pathway. Furthermore, the MSC values in the LHON group at the 8x8 and 16x16 check sizes given stimulation of the dominant eye from the transient checkerboard sweep were significantly greater than controls at both the low and middle frequencies. MSC values overall indicated greater coherence in the LHON population at these frequencies.

Spatial Sweep

Peak amplitudes from the isolated check sweeps were at the 16x16 check in both the LHON group and controls given stimulation of both dominant and nondominant eyes. However, amplitude functions sharply declined in the LHON group, at the 32x32 check, albeit still higher in magnitude than controls, and then increased again slightly at the 64x64 check in the M bright condition given stimulation of the dominant eye and the M bright and M dark conditions given stimulation of the nondominant eye. The amplitude functions from the spatial sweeps not only indicated greater magnitudes, but this upswing magnified the differential in amplitude at the 64x64 check.

These findings are perhaps indicative of an enhanced magnocellular system since peak magnocellular responses have been correlated with the 16x16 check condition where there was evidence of a strong response in the LHON group. Furthermore, the sharp decline at the 32x32 check may reflect lateral inhibition suppressing that response due to the magnified response at the 16x16 check.

Similarly, SNR ratios from the isolated check sweep condition indicated the highest values and greatest differentials at the 16x16 check in the LHON group. The sharp decline evidenced in the amplitude plots was again evidenced in the M bright conditions given stimulation of both dominant and nondominant eyes. This is again consistent with either a relative sparing or increased sensitivity of the M pathway. The SNR data from the contrast response functions, although consistent with higher SNR values overall in the LHON group, do not maintain as consistent a differential over the whole contrast range in the M dark condition as was apparent in the M bright condition given stimulation of the dominant eye, indicative of an intact ON system.

Luminance Contrast Sweeps

The amplitudes and vector mean amplitudes from the luminance contrast sweeps were not only greater in magnitude in the LHON group but they also reflected steeper contrast gain control at lower DOM than controls and a greater saturation effect in every condition. Contrast gain control can be evaluated by the shape of these functions in terms of the slope of initial segment, and the asymptote of the function, or where the function saturates (Kaplan and Shapley, 1986). Research has implicated that contrast gain control was approximately eight to ten times greater in the M pathway as opposed to the P

pathway. The LHON group, in all conditions, demonstrated a steep rise in slope at 4% DOM, whereas controls demonstrated a smoother function indicating greater requisite DOM before rise in function. These findings, indicating greater contrast gain control for the LHON group is consistent with more enhanced magnocellular function in the LHON group.

Furthermore, the asymptote, or saturation of the function was higher in all conditions in the LHON group as opposed to controls as evidenced by the fact that the function either reached its asymptote or turned down with increasing DOM. Controls were still showing increasing amplitudes with increasing DOM. The semi-saturation constant, the DOM value at which the function reaches half the maximum contrast, was also higher in the LHON group as opposed to controls in all conditions. This may be indicative of hyperpolarization that was introduced at high contrasts due to the greater cortical input in the LHON group. These findings support more enhanced magnocellular function in the LHON group.

The amplitude in the M bright conditions in both eyes also indicated steeper slopes in the LHON group as opposed to controls perhaps indicative of a more enhanced ON response.

As with amplitude, the initial slope of the SNR function indicative of contrast gain control was steeper in the LHON group, for the most part at the critical value of 4% contrast, which has been shown to drive the magnocellular system exclusively. Similarly, although the SNR value was at or near criterion at 4% DOM except in the M bright condition given stimulation of the dominant eye, the controls were consistently below criterion in all four conditions at around 0.5 at 4% DOM. The SNR functions from

the LHON group indicated values that were larger in every condition and were nearly twice as large as controls at 8% DOM in the M bright condition given stimulation of the dominant eye. Similarly the asymptote, or saturation, of the functions were greater in the LHON group in the M bright condition given stimulation of the dominant eye and the M dark condition given stimulation of the nondominant eye, and was similar to controls in the M dark condition given stimulation of the dominant eye showing decreasing SNR with increasing DOM, all indicative of greater contrast gain control in the LHON group.

Furthermore, in the M dark conditions in both eyes, the fall in SNR begins at 8% DOM. Given that the spread of activation from parvocellular afferents is not evidenced until after 10% contrast (Tootell et al., 1988), this data strikingly represents again an enhanced magnocellular response and perhaps a weakened parvocellular input. These findings again are consistent with the clinical and histopathological evidence of the progression of the disease.

Clearly, the SNR differences were not as prominent in the M dark conditions as they were in the M bright conditions. However, taken in conjunction with the amplitude functions across all conditions, with overall steeper slopes in the initial segment and earlier saturation indicative of the requisite of less contrast to saturate and produce half the maximum response magnitude , one would still conclude that these findings support a more enhanced magnocellular input in LHON.

The phase data from the luminance functions given stimulation of the dominant eye indicating a slight phase advance in controls as opposed to the LHON group was counterintuitive. One would expect greater cortical contrast gain control with its associated greater phase shifts in a population that was exhibiting greater amplitudes.

This finding is indeed interesting given the significantly higher amplitudes elicited in the LHON population without the associated nonlinear phase shifts with increasing contrast. The derivative question is whether there was more contrast gain control, thought to be associated with shunting inhibition, in controls as opposed to the LHON population. The phase data from the affected LHON participant indicated mostly flat phases or phase lags in the M bright condition in both eyes consistent with weak contrast gain control and a faulty magnocellular input. However, the phase advance with increasing DOM in the M dark condition may bespeak an intact OFF as opposed to ON pathway which is inconsistent with the current hypothesis. Again, once the visual system succumbs to the hypertoxicity, the small cells, specifically OFF cells, should be more vulnerable to an apoptotic outcome.

Enhanced Magnocellular Response

This sparing of the M pathway is consistent with the histopathological evidence of a preferential loss of P fibers, about an 80% loss, in two patients with 11778A and 3460A mutations respectively (Win et al., 2002; Sadun et al., 2000). Atrophy of primarily the smaller axons is also consonant with the premise that the small fibers may require more energy for optimal intracellular ion pump functioning due to the larger surface area to volume ratio than the large fibers. Furthermore, the clinical presentation of central vision defects reflecting dysfunction of the papillomacular bundle which is mainly comprised of small P fibers. Moreover, research investigating neuroprotection of porcine retina in perfusion culture showed that fragmentation and destruction of the axons started in the center of the specimens at the optic nerve head after four days, whereas the axonal

structures in the periphery remained intact for up to nine days (Eckert et;. al., 2002).

Supranoramal ERG responses in optic nerve atrophy

It is interesting to note that supranormal amplitudes have been evidenced in the ERG in all types of optic nerve atrophy (Aurbach, E, 1962). The ERG has been shown to be centrally controlled by means of centrifugal fibers passing from the central nervous system via the optic nerve to the retina (Aurbach, E, 1962). Disruptions in these centrifugal fibers, which are inhibitory in nature, have been hypothesized as accounting for the supranormal ERG responses.

Furthermore, in siderosis retinae, the toxic effects of the metallic ions may be delayed for years (Karpe, 1948, 1956). If the foreign body is not removed, the increasing siderosis, is reflected in the ERG with a gradual decrease in the positive wave until near extinction and either a normal negative wave or a more slowly decaying negative wave. However, if the foreign body is removed during the stage when the ERG is supernormal, the ERG is reversible.

Enhanced cortical responses evidenced by increased amplitudes in the VEP in LHON are certainly different from enhanced retinal amplitudes from an ERG. However, substantiation of another, related system evidencing physiological enhancement prior to atrophy is important to recognize. Some aspects of the underlying etiological mechanisms may in fact be similar. Furthermore, dysfunction in the optic nerve, manifested in the centrifugal fibers may impact the VEP as well.

Hypothesized etiological determinants of the current findings

Nonetheless, results indicating greater amplitudes in the LHON population are surprising given the premise of oxidative compromise. One might have expected decreased amplitudes and other subclinical findings indicative of dysfunction as opposed to supranormal findings. Three hypotheses are offered for these findings:

Firstly, a compensatory process is hypothesized whereby the stressed cells produce additional mitochondria in an attempt to offset the inherent decrease in ATP productivity caused by the mitochondrial mutations and the subsequent decrease in oxidative phosphorylation (OXPHOS) efficiency. Increased cortical signals in LHON evidenced by greater amplitudes from VEP recordings in normal asymptomatic LHON maternal relatives may in fact be due to this increase in mitochondria and the derivative increase in net ATP impacting greater metabolic cellular activity.

Interestingly, there is no evidence of this type of compensatory process in other mitochondrial diseases such as MELAS, MERRF etc., where one might expect such a process due to the presence of ragged red fibers, ophthalmoplegia etc., where there might be more of a biological incentive to proliferate mitochondria.

Secondly, a lack of inhibition may contribute to the findings of increased cortical signals. Evidence from the transient contrast-reversing checkerboard stimuli revealed increased P_{60} signals with greater coherence than controls indicative of stronger excitatory input from the LGN prior to inhibitory input. The fall-off at high spatial frequencies is not inhibitory in nature, but rather due to degradation of EPSPs due to the physiological limitations of spatial summation at higher SF. Therefore one would expect inhibitory contributions at lower SFs, not in the middle frequencies where the “notched”

function occurred in the LHON group in the grating sweep stimuli. Furthermore, there were also increased P_{100} signals which have been associated with cortical gabaergic inhibition, which again would be in contradistinction to a normally functioning inhibitory contribution. Moreover, in the anomalous LHON individual, decreased P100 amplitudes are associated with a compromised magnocellular input. The increased latency in the P60 is also correlated with a deficiency in the initial cortical input.

The third explanation for the findings of increased cortical signals derives from the law of conservation of synaptic density. This presupposes the possibility of neuroplastic activity in regions of neural apoptosis, such that spared neurons will produce collateral branches into affected areas. In LHON, it is conceivable that M and ON pathways produce dendritic connections in P and OFF pathways respectively, indicating not only a sparing of that pathway but also, conceivably, a more enhanced M and ON response.

The confluence of mitochondrial and nuclear genetic and epigenetic variables impacting the biological system may at some point, render the system hypertoxic, whereby a threshold effect is reached which initiates the cascade of visual system demise. Research supports the notion of a chronic progressive disease, rather than as initially believed, an acute onset, based on indices of dysfunction in asymptomatic LHON individuals. Evidence of subclinical abnormalities in specific visual pathways, based upon their selective biochemical predisposition for neurotoxic damage, in asymptomatic individuals is consistent with this postulate of a compromised visual system in a chronic progressive disease state.

Arguments Supporting the Compensatory Model

Histopathological Evidence

The compensatory model is consistent with the histopathological evidence demonstrating supranormal densities of mitochondria in the extraocular muscles in LHON (Sadun et al., 1994). Specifically, there was an increase in mitochondria, approximately two-thirds of the cell mass, as opposed to a normal one-third, in the vicinity of the microtubules, and yet the microtubules themselves were depleted, perhaps the result of a deficiency in net ATP. Furthermore, a relative scarcity of microtubules as well as a small axon-to-fiber ratio was observed, suggesting axoplasmic stasis and axonal involution.

In normals, mitochondria are very abundant in the initial, unmyelinated part of the axons anterior to the lamina cibrosa, whereas their number suddenly decreases more posterior as the myelin sheath begins (Carelli & Sadun, 2004). Mitochondrial biogenesis occurs within the cellular somata of RGC in the retina. Mitochondria are then transported down the axons and accumulate where they are needed along the unmyelinated portion of the nerve anterior to the lamina cibrosa, under the Nodes of Ranvier in the retrobulbar nerve, and at the synaptic terminals in the vicinity of the sodium potassium (NaK) pumps. Anatomical differences in optic nerve axons, such as the asymmetric pattern of myelination, may correlate with differential distribution of mitochondrial populations in the different sections of the nerve based on differential bioenergetic requirements (Carelli et al., 2002). Different blood-brain barrier properties are also evidenced anterior and posterior to the lamina, possibly reflecting different metabolic needs of the optic nerve head (unmyelinated) and of the retrobulbar optic nerve (myelinated).

The accumulation of mitochondria occurs in LHON as well. Histopathological evidence of increased mitochondrial density was evidenced not only anterior in the optic nerve, in the unmyelinated axons but also posterior in the myelinated axons as well (Carelli & Sadun, 2004). Since the retina is unmyelinated, there is continuous depolarization of the membrane. Normals are able to repolarize all along the axons with normal functioning of the Na/K pumps and normal ATP production. In LHON, due to the OXPHOS compromise, individuals are incapable of producing the requisite ATP for normal repolarization. As such, they accumulate more mitochondria to offset the deficit. In fact, the stacking of mitochondria, perhaps reflecting the increased energy requirements for electrical conduction in the prelaminar and laminar optic nerve has also been associated with demyelinated axons (Barron et al., 2003). Furthermore, it is perhaps due to the physical nature of the narrow lamina cibrosa that ultimately causes the anoxic insult that initiates the threshold effect of clinical symptomology.

This hypothesis of overcompensation reflecting the increased stacking of mitochondria is also consistent with the aforementioned research implicating the NMDA receptor with metabolic compromise and excitotoxicity. When a system is metabolically compromised, there is insufficient neuronal ATP to sufficiently activate the membrane ion pumps, particularly the Na+, K+ -ATPase (Erecinska and Dagani, 1990; Haddad & Jiang, 1993). The resultant neuronal depolarization may relieve the voltage-dependent magnesium blockade of the NMDA receptor ion channel, leading to toxic receptor activation by ambient glutamate (Zeevalk & Nicklas, 1991, 1992; Albin & Greenamyre, 1992; Beal et al., 1993c). Furthermore, various in vitro and in vivo paradigms have shown that metabolic inhibition can lead to NMDA receptor-mediated ecitotoxic

neuronal death (Novelli et al., 1988; Zeevalk & Nicklas, 1990; Turski et al., 1991; Beal et al., 1992, 1993a).

Ophthalmoscopic Evidence

Observation of enlarged subsarcolemmal mitochondria in LHON probands (Nikoskelainen et al., 1984b, c) and the ophthalmoscopic evidence of telangiectatic microangiopathy and vascular tortuosity further substantiated this compensatory postulate. Increased vascular perfusion may be another venue for the biological system to compensate for the oxidative compromise, which would also yield an increase in net ATP. The ophthalmoscopic evidence of a relative opacity of the NFL in the acute phase of LHON (Nikoskelainen et al., 1994), further substantiates this premise. This opacity perhaps reflects increased mitochondrial density which creates the opacity as opposed to a more transparent normal fundus.

Retinal Nerve Fiber Layer

Significant thickening of temporal retinal nerve fiber layer (RNFL), as measured by optical coherence tomography (OCT), was detected in asymptomatic members with the 11778 mtDNA mutation whereas trend significance was reached with the 3460 mtDNA mutation (Savini et al., 2005). OCT has also shown RNFL to be thicker in affected LHON patients where the duration of the disease was shorter than six months and severely thinned in patients whose illness was longer than six months (Barboni et al., 2005). Furthermore, thicker RNFL was evidenced in LHON patients with disease duration under six months and visual recovery. Consistent with clinical (centrocecal

scotoma) and histopathological evidence (preferential small fiber (P) loss), the temporal fibers (papillomacular bundle) are the first and most severely affected.

Advanced serial analysis (ASA) of GDx data (Sherman, unpublished data) revealed thickened RNFL in an asymptomatic 11778 carrier with 20/20 VA in both eyes four months prior to initial vision loss of 20/40 OD and 20/60 OS. The GDx is a nerve fiber analyzer using scanning laser polarimetry to analyze the birifringent properties of the NFL. This optical imaging technique indirectly computes a thickness correlate based on the linear relationship between the retardation of monochromatic reflected light and histologically measured RNFL thickness. Mitochondria, which have birifringent qualities, would impact this measure.

Thicker RNFL was demonstrated in this 11778 patient inferior temporally with evidence of a thickened superior papillomacular bundle (PMB) as well in the left eye where vision loss was manifest first. Two weeks later, the inferior temporal bundle demonstrated further increased thickening, most dramatically depicted with ASA by a narrow arcuate bundle, corresponding to a total increase of more than 40u when contrasted with the baseline. On the same scan, the previously thickened superior PMB and inferior nasal bundle was thinner. A GDx performed six months later revealed highly significant thinning of nearly all of the RNFL

Similarly, GDx data from the right eye indicated that the entire temporal zone was statistically thicker than the baseline measured six months prior. Furthermore, the inferior temporal bundle corresponded to about a 40u increase in thickness relative to the baseline. Scans obtained one year after disease onset demonstrated a thinning of the

RNFL both inferiorly and superiorly as well as a persistent thickening of a few smaller zones, relative to baseline.

These findings further substantiate the present hypothesis of a compensatory process that may cascade into devastating clinical symptomology if hypertoxicity of the visual system prevails. Thicker RNFL, correlated with the increase in mitochondria, may reflect the attempt to subvert a compromised system by generating extra proteins and microtubules for the axoplasmic transport necessary to surpass the oxidative compromise. These derivative thicker axons may in fact be responsible for the enhanced cortical signals evidenced in the LHON population. In an early stage of acute disease, there is evidence of thicker than baseline RNFL indicative of the increased mitochondria. With progression into a more acute phase there is further thickening of the pappillomacular bundle and other zones again implicating this overcompensatory process. When the cycling effects of this compromised OXPHOS process become hypertoxic, the compensatory process fails and the chronic progressive stage of vision loss ensues with the eventual associated loss of most of the PMD followed by loss of most of the RNFL. It is during the early part of this chronic progressive stage, that the selective subclinical abnormalities are hypothesized.

Furthermore, the rationale underlying the eventual failure of the compensatory process is contingent upon inadequate volume, specifically in the lamina cibrosa sclera, the exit point of the optic nerve, to accommodate this influx of mitochondria. Axonal stasis due to faulty motoric motors, confounded with the small diameter of the lamina cibrosa sclera, may in fact be the causative anoxic insult which is the threshold effect whereupon clinical symptomology is expressed.

Arguments against the Compensatory Model

There are two philosophical arguments against the first proposition of a compensatory process. Firstly, the increased mitochondrial density in the extra ocular muscles may in fact represent stacking of the mitochondria due to axoplasmic stasis, as opposed to a compensatory hyperproduction of mitochondria. Protein synthesis, occurring within the cell body, is transported via microtubules, in conjunction with the molecular motors kinesin and dynein, down the axon via axonal transport mechanisms. Axonal stasis or constipation occurs when insufficient ATP interferes with normal functioning of the axonal transport system. The accumulation of large numbers of mitochondria in the vicinity of the microtubules, and yet the depletion of the microtubules themselves in conjunction with the excess debris evidenced in the histopathological data (Sadun et al., 1994) may represent the axonal stasis endemic to this system of oxidative compromise.

Secondly, increased mitochondrial densities evidenced in the extra ocular muscles, are independent of evoked responses measured from V1 from the occipital cortex. On the other hand, one has to also recognize that the ocular tissue obtained from the affected 11778 individual was indicative of massive neuronal atrophy and negative findings of supranormal densities of mitochondria in optic nerve, for example, does not negate its existence in the chronic progressive stages of the disease, where there may have been such increases in an attempt to overcompensate for the inherent oxidative compromise. Furthermore, the convergent ophthalmoscopic and RNFL evidence of mitochondria within the fundus and RNFL lend credence to the postulate of the increase

in net ATP from supranormal mitochondrial density directly impacting cortical responses from V1.

Hypertoxicity and Selective Pathway Involvement

Decreased amplitude measures from both the spatial and contrast stimuli were elicited from the affected LHON participant indicating weak cortical signals. This is again consistent with the hypothesis that initially the biological system attempts to overcompensate for the inherent oxidative compromise evidenced with increased amplitudes indicating greater afferent signals. However, when the hypertoxicity prevails, the visual system does not have the extra resources, i.e. increased mitochondria to produce even normal amplitudes and the overtaxed, damaged system can produce only weak signals. Alternatively, decreased amplitudes are indicative of the clinical progression of the disease with its apoptotic neural correlate.

Furthermore, evidence of weak contrast gain in the anomalous participant as compared with the relative enhancement evidenced in the contrast sweep data from the other asymptomatic LHON participants is consistent with the excitotoxicity hypothesis. Specifically, research has shown that the administration of NMDA antagonists into the visual system produces a specific reduction in contrast gain and plateau response both cortically (Fox et al., 1990) and in the LGN (Kwon et al., 1992). As previously mentioned, the unique status of the NMDA receptor as both a ligand and a voltage-dependent ion channel has led many researchers to hypothesize that neuronal membrane potential is a critical variable in modulating excitotoxicity (Zeevalk & Nicklas, 1992; Beal et al., 1993c). Impaired energy metabolism may enhance excitotoxic damage by

several mechanisms including decreases in ATP levels, reduced sodium-potassium ATPase activity, partial cell-membrane depolarization, and relief of the voltage-dependent Mg^{2+} block of NMDA receptors (Beal, 1992). NMDA receptor activation may then generate reactive oxygen species further impairing the functioning of many macromolecules (Bowling & Beal, 1994) thus enhancing the excitotoxicity and derivative apoptosis.

In the affected LHON participant, in the spatial sweep data, there were more regular phases throughout the functions, consistent with the lower amplitudes obtained and a faulty visual system. The SNR data from the spatial functions, implicate a low and a high check deficit as opposed to a middle check deficit in the affected LHON participant except for the M bright condition given stimulation of the dominant eye.

The difference in deficits between the asymptomatic and affected individuals and even the seeming discrepancy in the asymptomatic LHON sample is perhaps contingent upon the quantitative differential of magnocellular vs. parvocellular inputs. The current research investigated function in asymptomatic maternal relatives, not the structural damage manifest in patients with onset of symptomology. Like many CNS disorders, there is not necessarily a clear chronological progression from structural abnormality to functional abnormality.

Evidence of centrocecal scotomas in LHON can only provide magnitude differentials in terms of M and P pathway involvement due to the heterogeneous morphology of midget and parasol cells throughout the retina. First, magnocellular ganglion cells comprise only 10% of all fibers in the primate optic nerve. Second, the spatial density of midget bipolars matches the cone density to an eccentricity of about

10mm, whereas the ratio drops to about 60% of cone density with eccentricity. This suggests convergence of several cones to individual midget bipolars in peripheral retina, and as such, the peripheral as well as the central retina, could provide chromatically specific input to the P pathway.

Thus, an analysis of selectivity of M and P pathway pathology is complicated by the necessary speculation as to the mathematical correlates of the ratio of physiological atrophy to functional compromise. One might expect that the relative density of the P input may afford more resistance to visual compromise as opposed to the relative sparsity of the M input such that earlier functional compromise may occur from oxidative stress in fewer M cells. Alternatively, the M fibers may be more sensitive functionally to oxidative stress because they are more metabolically active.

As previously mentioned, the inherent oxidative compromise may elicit a compensatory process due to either increased mitochondrial density or increased M and/or ON afferents. However, a hypertoxic milieu may create a threshold whereupon the overcompensation would begin to fail and the chronic progression of the disease would initiate. At this threshold, a nondiscriminating disease process may clinically manifest in the M cells first such based upon the lower number of M cells. However, with progressive atrophy, a parvocellular deficit would manifest as well. In fact, the histopathology data support a more pronounced parvocellular deficit and a relative sparing of the M pathway (Win et al., 2002; Sadun et al., 2000). With recovery of function, as with EM, the affected LHON patient in the present study, a parvocellular deficit may be sustained due to the fact that there is to date, no reversal of neuronal atrophy. As such, the midget cells with small cell diameter, comprising the parvocellular

pathway, may be more susceptible to apoptosis, whereas the larger diameter cells, like the parasol cells, comprising the magnocellular pathway, although they may be compromised, are less susceptible to an apoptotic outcome. As such, with recovery of function, only those cells, compromised, but not apoptotic, can recover.

Summary of Hypothesized Etiological Progression

Evidence of enhanced cortical signals is consistent with the hypothesis of either increased mitochondrial activity or increased afferents in the visual system impacting the magnocellular and ON pathways selectively. Conversely, when the supranormal compensatory activity would begin to fail, abnormalities in the magnocellular and OFF systems would be detected first – consistent with individual VEP functions including the anomalous participant.

Perhaps in any given population of normal maternal relatives the distribution is not unimodal but at the very least, bimodal. Some individuals before the expression of overt symptomology may produce supranormal responses due to the overcompensation of the biological system, whereas the other subset, once the overstressed system reaches critical levels of hypertoxicity, subclinical, selective pathway deficits would initiate until overt symptoms manifested as well.

In LHON, in theory, at the present time, one cannot prove hyperproduction of mitochondria or neuroplastic production of afferents, as opposed to a stacking problem due to axoplasmic stasis. Nonetheless, clinically speaking, this lack of etiological clarity is purely philosophical, in terms of asymptomatic diagnostic criteria of increased signals.

In conclusion, the hypothesized etiological determinant of the present findings is that normals positive for an LHON mutation may express enhanced cortical responses due to either increased mitochondrial density or neuroplasticity of the M and/or On afferents. The biological system is either attempting to compensate for a compromised oxidative system, or this is simply a manifestation of the axonal stasis. Nonetheless, those individuals who progress into an active state of disease would evidence subclinical abnormalities similar to the anomalous participant in the M and OFF domain. If the disease process was not arrested via some prophylactic intervention, the disease would reach a threshold whereby symptomology would chronically progress to a state of near or complete vision loss.

Limitations of the Current Study

The obvious flaw in the current investigation is the small sample. Understanding that this is an orphan disease, I believed that families of an affected family member would be eager to volunteer their time to research that would potentially shed light on this devastating illness. Yet, recruitment was surprisingly difficult. Despite the small N, the differences obtained were statistically significant indicative of robust findings.

The small N, as previously mentioned however, did preclude a subgroup analysis to detect bimodality. Furthermore, the prolonged latencies in the LHON group from the present investigation did not reach significance like other research indicating prolonged latencies in asymptomatic carriers (Lam et al., 2003, Solomeo et al., 2003). A larger sample may have afforded the requisite power to corroborate these findings.

Nonetheless, in order to compensate for a small sample and attempt to still have meaningful data, the data was analyzed both with and without the anomalous participant. The data was analyzed with both means and medians and there were no substantive and significant differences between the two analyses.

Furthermore, after initial analysis with the mixed model ANOVA, significance was only reported after establishing that there were no interactions between the group and the within subject factor (i. e. check size, DOM, etc.). Only then was least square means results reported on that factor. A t value and 95% confidence interval was computed for the significant differences between the two groups for the gradations specific to each within subject factor. Furthermore, nonsignificant data was also evaluated via confidence intervals to evaluate the likelihood of positive findings given a larger N. It has been proposed that clinical trials of nonsignificance should state a confidence interval rather than a post hoc power analysis (Levine & Ensom, 2001), which indeed has become American Psychological Association policy for all journal submissions once a study is analyzed (Wilkinson, 1999).

Another limitation of the study is the fact that the LHON unaffected participants had a corrected Snellen VA of 0.8 as opposed to normal controls with a Snellen acuity of 1.25. One of the requirements of the study was that all participants should be visually normal or corrected to normal. However, since the population was so sparse, participants who did not meet this specific criterion could not be excluded. On the other hand, the lower VA could only have undermined the current hypothesis with a lack of significant findings. The fact that signals were greater in the LHON population, despite their visual compromise strengthens, not weakens the given hypothesis. Nonetheless, it would have

been preferable had the control and experimental group been more consistent across all variables so as not to introduce any confounds.

Future Research

1. *VEP Analyses of Other LHON Mutations.*

VEP protocols investigating other LHON mutations are critical to see whether the subclinical abnormalities evidenced in the VEP with the 11778 mutation would be consistent with other mutations. This would help clarify whether the oxidative stressors in LHON are more global or whether the neurotoxicity inherent in one mutation is exclusive of the neutotoxicity inherent in another. Selectivity in hypertoxic etiology would necessitate investigations of therapeutic selectivity.

2. *Association of LHON and MS.*

Abnormal VEP recordings are evidenced in MS patients after recovery from acute optic neuritis. As such, VEP records from the affected LHON patient after recovery of visual function is perhaps even more difficult to decipher based on the assumption of an overall lack of neurological coherence after neurological dysfunction.

Research implicating excess female transmission of multiple sclerosis and the incidence of MS-like illness in patients with LHON has led researchers to postulate that mtDNA mutations contributes to the genetic susceptibility to MS. The histopathological evidence of increased mitochondrial density both anterior to the lamina cibrosa in the unmyelinated axons and posterior in the optic nerve, in the myelinated axons, where there is generally a sparsity of mitochondria (Carelli &

Sadun, 2004) should be evaluated within this context as well.

Future VEP studies should be conducted to specifically assess latency differentials in both affected and unaffected LHON participants as well as affected and unaffected MS participants. Analyzing these latencies in individuals positive for both a LHON mtDNA mutation as well as MS-like symtomology may shed light on the interaction between the two disorders with respect to myelinated and unmyelinated axons and the implications thereof with respect to a potential prophylactic intervention.

3. ***Association with DOA and Other Optic Atrophies***

Identification of mutations in the nuclear gene OPA1 as the causative factor in DOA has confirmed the nuclear encoding of a mitochondrial protein (Cardaioli et al., 2005). This finding may have similar etiological consequence in LHON. Interestingly, as postulated in LHON, research employing Opa1 mRNA isoforms in whole retina and in isolated retinal ganglion cells (RGCs) has revealed greater aggregation of the mitochondrial network induced by the downregulation of Opa1 in RGCs than in control cerebellar granule cells (Kamei et al., 2005).

LHON is considered the paradigm of mitochondrial optic neuropathies with its maternal inheritance and association with specific mutations in mtDNA. The variety of optic neuropathies associated with vitamin depletion, toxic exposures, alcohol and tobacco abuse, and use of certain drugs may in essence represent clinical phenocopies of this pathology. Therefore, ascertaining the

etiological pathogenesis of this disease and potential prophylaxis, may have ramifications not only in LHON, but in its phenotypic correlates as well.

4. ***Longitudinal Analysis***

Replication of the current protocol with larger N in both adults and children longitudinally should yield baseline indices of asymptomatic norms under the different VEP conditions. As such, deviation from that established norm, or the patient's own personal baseline measurements, may be a preclinical indicator of disease onset. It is possible that this technology may in fact shed light on the heretofore lack of predictability between asymptomatic carriers and clinical expression.

Furthermore, replication with a larger N, with more specific hypotheses of bimodality in the distribution, may help clarify the confusing evidence of intact and perhaps enhanced M and ON pathways in some asymptomatic LHON individuals and evidence of abnormal M pathways in other asymptomatic individuals, most notably the anomalous participant. More substantive evidence of this bimodality may be critical in the understanding of the predictability of onset of disease in asymptomatic carriers.

Quantitative measurements from GDX data could also be used to correlate with specific supranormal or attenuated VEP responses. Baseline GDX data of RNFL thickness and VEP data should be collected in an attempt to establish norms in both children and adults positive for LHON mutations. Deviations from either an established norm or from one's own personal baseline may indicate disease onset.

Interestingly, even normal RNFL thickness or normal EP recordings, may in fact be indicative of subclinical disease onset in individuals positive for LHON mutations.

5. ***Inclusion of Parvocellular Specific Stimuli***

Due to the complexity in the progression of selective pathway involvement, both magnocellular and parvocellular specific VEP stimuli should be included in the longitudinal study. Evidence of the high incidence of rare tritan defects in asymptomatic LHON individuals reflecting S-cone dysfunction, may be assessed via isoluminant blue-on yellow off chromatic VEP stimuli aimed at probing koniocellular pathway involvement. Further clarification of enhancements and deficits is critical in order to demystify the evidence of not only enhanced parvocellular function reflected in significantly higher grating acuities, but also enhanced magnocellular function reflected in increased amplitudes, vector mean amplitudes, and SNR functions from the spatial stimuli and increased contrast gain control from the contrast stimuli confounded by evidence of magnocellular deficits reflected in the "notched" spatial frequency functions from the grating sweeps.

Perhaps clarification of the progression of selective pathway enhancements and subsequent deficits could more clearly identify those at greater or more imminent risk of losing vision. Identification of different subgroups within the asymptomatic classification may provide a more defined period for prophylactic intervention. Furthermore, as with the case of siderosis retinae, there may be a critical period of cortical enhancement beyond which prophylactic intervention would have no effect.

6. *Prophylactic Intervention Protocols*

Future longitudinal research may establish the potential of these VEP baseline measurements as biomarkers which may then afford the possibility of investigating neuroprotective agents in asymptomatic LHON carriers before the disease becomes irreversible. Prophylactic intervention protocols, employing cyanide detoxification agents like hydroxycobalamine, metabolic bypass therapies like idebenone, coenzyme Q_{10}, and ALC, MS therapies employing immunosuppressors like cyclosporine and beta interferon, minoxidil, neurotrophins such as brain-derived neurotrophic factor (BDNF), neurotrophin-4 or 5 (NT-4/5), 2-deoxy-D-glucose (2DG), tetanus neurotoxin (TeNT), bradykinin and diazoxide (Mit. K(ATP) channel agonists), brimonidine (BMD), cytokines, fibroblast growth factor(FGF-2), gene therapies etc., that could be administered if an individual, on repeated examination, deviated from his/her original baseline measurements. For more detailed information about the premises underlying these prophylactic protocols see appendix 6.

The current investigation indicated that even normal amplitude measurements in unaffected LHON maternal relatives, may be indicative of an abnormality. As such it is critical to establish baseline measurements and note deviations off that baseline. This VEP biomarker provides a means to analyze individuals at risk for disease expression. Serial VEP records repeated after a course of treatment would assess whether there was no change, a return to baseline, or an exacerbation of the asymptomatic abnormal VEP records. This protocol, besides potentially shedding light on the etiological determinants of the disease, provides a quantitative measure of

the efficacy of the intervention protocol under investigation. Perhaps most important, is its ability to evaluate those intervention protocols in the absence of clinical disease.

Appendix 1: Association between LHON and MS

In one study, eighteen Italian patients presenting with sporadic, bilateral, or sequential optic neuritis (ON) were evaluated for 14 mtDNA base changes associated with LHON (Sartore et al., 1995). During a 36-month follow-up, 11 ON patients developed symptoms that afforded a clinical diagnosis of MS. No patient was positive for any of the primary LHON mutations, however, ON and ON-MS patients were both positive for single or multiple secondary mutations at nts 4216/ND1, 4917/ND2 and 13708/ND5. On the other hand, normal controls as well as MS controls without visual failure also harbored these mtDNA base changes at similar frequencies. Coexistence of three sequence changes was found in two cases (1 ON-MS and 1 MS control patient) as well as two neutral sequences in the ND4 gene. Thus, the researchers concluded that these secondary mutations do not contribute to MS susceptibility, but merely represent neutral mtDNA polymorphisms.

In a similar study, the protein and RNA coding sequences were analyzed in nine patients with MS with a positive family history (Chalmers et al., 1996). Nine alterations in amino acid sequence and an additional 18 silent base changes were detected. No significant variation was evidenced in tRNA of rRNA sequences. Mutations at bps 4216 and 4917, both considered LHON secondary mutations, were identified. Two other mutations at bps 11447 and 14766 were found in all MS patients sequenced. However, RFLP analysis of 175 unrelated MS patients and 233 normal controls revealed these changes at similar frequencies in the MS patients as in the controls. Furthermore, the mutations at bps 4216 and 4917 were noted at higher frequencies in the north European

controls than previously documented. These researchers also concluded that mtDNA variability is unlikely to contribute to MS susceptibility.

On the other hand, there is research that still maintains that the association between LHON and MS is significant based upon both an extensive literature search and on the clinical analysis of 55 LHON pedigrees (103 patients) and 40 MS patients (Vanopdenbosch et al., 2000). All three primary LHON mutations occurring in the European and North American populations have been associated with an MS-like syndrome and therefore carrying a primary LHON mutation is a risk factor for developing MS. Furthermore, a recent MRI study revealed white matter lesions in a LHON patient with the 3460 mutation (Lev et al., 2002).

Appendix 2: Secondary LHON mtDNA Mutations

Analysis of the mitochondrial ND3, ND4L, and ND4 genes did not reveal any mutations that could have been etiologic determinants of the biochemical and clinical abnormalities present in the Queensland pedigree (Howell & McCullough, 1990). Subsequent analysis of the ND1, ND2, ND5, and ND6 genes revealed two homoplasmic mutations. The first mutation (ND1/L285P) involved a T-to-C transition at nucleotide 4160 of the ND1 gene, which causes the highly conserved leucine residue to be replaced with proline at amino acid position 285 of the ND1 protein (Howell et al., 1991a). Secondary structure analysis of the ND1/L285P posits that there is a disruption in a small *alpha* helix spanning residues 282-291 in a hydrophilic loop that is directly related to the proline replacement, rendering this region as a hydrophilic random coil. The second mutation, identified in only one branch of the pedigree, involved an A-to-G transition at nucleotide position 4136, which resulted in the substitution of cysteine for tyrosine at amino acid residue 277. Screening for the ND1/Y277C is of relative ease for the nucleotide change at position 4136 generates an easily detectable new *Sph*I site.

One postulate implicates the ND1/Y277C as an intragenic suppressor mutation which ameliorates the neurological abnormalities and complex I deficiency (Howell et al., 1991). Support for this hypothesis stems from two pieces of observational data. Firstly, among the five members of the pedigree carrying both ND1 mutations, only two of the males were clinically abnormal. Their dysfunction was completely within the visual domain and did not include any history of infantile encephalopathy, or any other neurological complication. In contrast, these complications were present in other members of the pedigree who only carried one ND1 mutation. Secondly, preliminary

biochemical studies indicated that the complex I defect was less severe in the two family members carrying the ND1/Y277C substitution (Parker et al., 1989).

Even with confirmation of an intragenic suppressor, the clinical variability and evidence of neurological discordance within the pedigree cannot be explained (Wallace, 1970). For example, a clinically normal individual within the Queensland LHON pedigree carried only the L285P mutation. Furthermore, the mother of an asymptomatic male, both carriers of the L285P mutation, had normal vision, yet displayed neurological abnormalities. Another member had recovered from infantile encephalopathy as a child, yet was a clinically normal adult. Thus, heteroplasmy could not be implicated in this Queensland pedigree for the variability in phenotypic presentation, and as such, one mitochondrial mutation may be deemed necessary, but not sufficient for the expression of the disease.

Several other mutations have been identified that appear to be of secondary importance with regard to not only the probability and severity of LHON symptomology, but also to later prognosis and recovery of function. These include mutations at nucleotide positions 4216 of the ND1 gene (Johns et al., 1992), 4917 of the ND2 gene (Johns et al., 1992), 5244 of the ND2 gene (Anderson et al., 1981), 13708 of the ND5 gene (Johns et al., 1991; Anderson et al., 1981), and 15812 of the apocytochrome b gene (Johns et al., 1991; Anderson et al., 1981).

In an attempt to identify pathogenetically significant mtDNA mutations in LHON probands not carrying any of the three primary mutations, another mutation was isolated at nt 14484C, altering methionine-64 to valine in a highly conserved region of the ND6 gene (Johns et al., 1992). This nt 14484C mutation has been identified with a high

correlative significance in probands harboring the mtDNA haplotype carrying the 13708 secondary mutation. A silent T-to-C transition at nt 14485 was identified in multiple samples. Consistent sequence differences were noted at nt 14199 with a C-to-A conversion, at nt 14272 with a G-to-C conversion, and at nt 14368 with a G-to-C conversion.

The 14484C mutation was found to be associated with an mtDNA haplotype containing four missense mutations found also in controls, ranging from 5% with the 13708 mutation to 42% with the 10398 mutation. Data support the present hypothesis, suggesting that the coincidence of the 14484C mutation with this mtDNA haplotype, may either create a synergistic, deleterious effect on mitochondrial oxidative phosphorylation, or the 14484C mutation may be linked to another pathogenic mutation that is primarily responsible for LHON symptomology. Data has confirmed that 14484C positive LHON probands, have harbored both the nt 15257 in apocytochrome b, and the nt 15812 (Johns et al., 1992).

Novel mitochondrial DNA nucleotide transversions at C14482A (M641) and C14482G (M641) were found to cause LHON with visual recovery in an Italian pedigree (Valentino et al., 2002). These mutations confirm that that the ND6 gene of Complex I is a mutational hot spot suggesting that different amino acid substitutions at residue 64, including the more common T14484C (M64V), are associated with visual recovery.

A novel mitochondrial mutation at C4171A/ND1 was identified in two Korean families with LHON where all affected members spontaneously recovered after variable suffering of months to years of initial vision loss (Kim et al., 2002). This mutation replaces leucine with methionine in a conserved extramembrane loop of the ND1 gene.

Appendix 3: Clinical Case Histories of LHON Secondary mtDNA Mutations

Two bizarre clinical case histories have been reported with the ultimate discovery of two LHON mutations upon mitochondrial analysis at nts 4216 and 4917, which are both class II mutations that produced symptomology in the absence of a class I mutation. The first case involved a 46 year old patient who was asymptomatic, yet the optic disc from his right eye was markedly pale (Sherman et al., 1993). Although the patient was positive for both the nt 4216 and nt 4917 mutation, a diagnosis of a non-Leber's mitochondrial optic neuropathy was given based upon the fact that the patient did not exhibit any of the symptomology classically associated with this disease. Although mild peripheral vision loss was detected within several months of the initial consultation, with indications of subsequent deterioration, the esoteric, noncommittal, elusive diagnosis remained intact due to the absence of any correlative symptomology to that which Leber himself had described.

The second case involved a patient who had lost his left globe in WWII, and visual deterioration began in his right eye in the late 1960's (Sherman et al., 1992). By 1970, visual acuity had dropped to below 20/400, yet funduscopic evaluation revealed only a questionable temporal pallor. After visual deterioration below 10/400 with eccentric viewing, the patient was forced to learn Braille and aided his motility by sensing the direction of air currents. A dermatologist prescribed minoxidil to enhance the hair growth on his arms so that his ability to detect even the most subtle air currents would improve. After a regimen with minoxidil for approximately one year, the patient began to regain vision such that by 1988 the patient discontinued use of minoxidil for he no longer needed to sense air currents. Within a few months the patient's vision began to

deteriorate and minoxidil was restarted. At a recent exam, visual acuity was measured at 20/15 and his optic disc was pink and healthy. Mitochondrial analysis of the patient's blood revealed LHON mutations at nts 4216 and 4917.

Appendix 4: Homoplasmy vs. Heteroplasmy

Segregation and transmission analysis in LHON have yielded controversial results with respect to the influence of selection. A longitudinal study of eight family members positive for the primary nt 3460A mutation, showed no change in the mutant-allele frequency over a period of 3.5 years (Ghosh et al., 1996). Constant values were obtained irrespective of both the ratio of mutant to wild type alleles and the age of the individual. Hence, the lack of evidence supporting selection pressures operating over this time period led to the conclusion of random drift occurring in these cell populations.

Positive selection favoring the replication and/or segregation of the mtDNA molecules carrying the mutant allele has been evidenced in heteroplasmic nt 11778A pedigrees in which the frequency of the mutant allele increased in successive generations (Smith et al., 1993; Howell et al., 1994). However, instances of transmission to a lower mutant-allele frequency have been noted to occur in other LHON pedigrees (Vilkki et al., 1990; Zhu et al., 1992; Ghosh et al., 1996), indicating transmission data that are inconsistent with pristine selection processes.

It has been hypothesized that a bias due to incomplete ascertainment has supported conclusions of positive selection based on the available evidence of an overall increase in the mutant-allele frequency in successive generations of heteroplasmic LHON pedigrees (Howell et al., 1994). Matrilineal pedigrees positive for a LHON mtDNA mutation, but who have not had any family members exhibit visual deficits, have not been identified and analyzed, hence underestimating their prevalence in the LHON population at large. Hence this constraint limits analysis to pedigrees where the high threshold of the mutant-allele necessary for disease expression has been actualized,

indicating that the drift toward the homoplasmic state is nearly complete. This is consistent with the finding that the nt 11778A mutation, the most pervasive of the primary LHON mtDNA mutations, has been noted to be generally homoplasmic mutant (Brown et al., 1992; Newman et al., 1991). This suggestion is limited to primary LHON mutations due to evidence supporting positive selection in other pathogenic mitochondrial mutations (Poulten and Morten, 1993; Matthews et al., 1995).

Although a high proportion of LHON patients carry the 11778A mutation, derivative symptomology is inconsistent within the pedigree itself. Originally, phenotypic variability was not considered the product of the segregation of mixed mutant and wild type mtDNAs, as the nt 11778A mutation was originally found to be homoplasmic in all LHON pedigrees (Carducci et al., 1991; Wallace et al., 1988). However, slow mitochondrial gene segregation, or persistent heteroplasmy, had been posited as an explanation for the variable expression in other mtDNA disorders such as myoclonic epilepsy and ragged red fiber (MERRF) disease (Wallace, 1992; Shoffner et al., 1990). Thus, this hypothesis was not discounted as a possible etiologic determinant for the phenotypic variability evidenced in LHON pedigrees (Lott et al., 1990).

Positive selection maintaining heteroplasmy (Koehler et al., 1991) is a logical premise in diseases involving mtDNA deletions such as myoclonic epilepsy and MERRF, for the virulence of the homoplasmic mutant state would be mitigated with replications of the mitochondrial deletions (Holt et al., 1988). However, it has been argued that it is illogical to presume selection for persistent heteroplasmy in mitochondrial diseases such as LHON that involve a point mutation and in general a mild clinical presentation (Howell et al., 1992).

Clinical statistics substantiate this contention with evidence of both homoplasmic and heteroplasmic LHON probands and asymptomatic relatives with direct maternal lineage. Studies analyzing restriction fragment patterns in leukocyte mt DNA indicate no significant difference between affected and unaffected individuals within the same matrilineal pedigree (Holt et al., 1988). In actuality, the incidence of heteroplasmy has been reported to be significantly lower than homoplasmy (Newman et al., 1991). These findings have been consistent with all LHON mitochondrial mutations.

However, data from an analysis of peripheral blood from many LHON pedigrees with the 11778A mutation indicates a trend suggesting that heteroplasmic individuals have a greater chance of remaining visually asymptomatic than individuals who are homoplasmic mutant. However, no evidence of clinical differences in disease severity exists between symptomatic heteroplasmic or homoplasmic individuals. Furthermore, the percentage of mtDNA mutations increases in subsequent generations indicating a significant progression toward homoplasmy. The underlying genetic process producing this unidirectional drift remains unclear. Postulates of oxidative stress caused by one or more mtDNA mutations which by some unknown mechanism potentiates gene replication have been offered (Smith et al., 1993).

The proportion of mutant mtDNA in the optic nerves and/or their vasculature has recently been postulated as possibly affecting the likelihood of developing the disease (Harding, 1991). Histopathological data from a female positive for the ND4/11778A mutation substantiates the aforementioned postulate of heteroplasmy, specifically of the optic nerve, as a possible determinant of disease severity (Sadun et al., 1994). Nearly homoplasmic DNA was found in the optic nerve (20/21), retina (22/22), sclera (13/13),

and eye muscle (20/21), whereas heteroplasmic DNA was found in white blood cells and platelets (18/55).

Meiotic segregation, resulting in the differential proportions of mutant and wild type mtDNA in tissue such as the optic nerve, can possibly account for the differential in genetic propensity for vision loss amongst members of the same pedigree. Mitotic segregation, resulting in mtDNA genotypic variability between tissues in the same individual, may render the classic blood sample nonrepresentative of the mitochondrial genotype in the optic nerve. Thus, in order to increase the reliability of genetic diagnosis, not only must many individuals within a pedigree be tested, but also many tissues within an individual.

Research previously utilized to support systemic heteroplasmy as a determinant of disease severity is not wholly inconsistent with the findings of homoplasmy within the optic nerve. A drastic shift across generations was documented with regard to both tissue variability and the proportion of mutant mtDNA (Lott et al., 1990). For example, one unaffected mother showed 65% mutant mtDNA, whereas her affected son showed 100% mutant mtDNA. Two affected individuals were shown to have predominantly mutant mtDNA in their blood, yet essentially normal mtDNA in their hair. Similarly, evidence from an LHON family with four affected individuals has been documented in which only one of the probands had a positive *Sfa*NI restriction pattern, whereas the other three affected individuals tested negative in both blood and muscle samples (Cormier et al., 1991). Thus, this demonstrated rapidity in both meiotic and mitotic segregation, which originally yielded the hypothesis of heteroplasmy, is not inconsistent with the aforementioned histopathological findings which suggest that heteroplasmy or

homoplasmy of the optic nerve is the only genetic variable of etiological importance with regard to disease severity.

This premise presupposes the reduction in the respiratory complex I efficiency, due to the presence of mutant type mtDNA. The heteroplasmic genotype, specific to the optic nerve, may only express phenotypically when the ATP production of the wild type mtDNA is no longer sufficient for adequate cell maintenance. This threshold effect implies a consonant functioning of the tissue with respect to both the proportion of wild and mutant type DNA present and its inherent respiratory needs. Hence, the likelihood of exhibiting symptoms should be mitigated in those individuals whose optic nerve cells are heteroplasmic (Wallace, 1989, 1986; Zeviani et al., 1989).

Appendix 5: Excitatory amino acids

Glutamate is believed to be the major excitatory neurotransmitter in the retina, and is used in the synthesis of proteins, other amino acids, and even other neurotransmitters (Stryer, 1988). Although glutamate is present in all neurons, only a few are glutamatergic, releasing glutamate as their neurotransmitter. Neuroactive glutamate is stored in synaptic vesicles in presynaptic axon terminals, and is incorporated into the vesicles by a glutamate transporter located in the vesicular membrane (Fykse & Fonnum, 1996). This transporter selectively accumulates glutamate through a sodium-independent, ATP-dependent process (Naito &Ueda, 1983; Tabb & Ueda, 1991), resulting in a high concentration of glutamate in each vesicle.

Physiological research has shown that the application of glutamate or aspartate (EAAs) to the retina mimicked the action of the endogenous photoreceptor transmitter (Murakami et al., 1975). On the other hand, the exogenous application of two broad spectrum EAA receptor antagonists, PDA (piperazine dicarboxylic acid) and kynurenic acid, blocked the light-evoked responses of OFF-bipolar, horizontal, amacrine and ganglion cells (Slaughter & Miller, 1983a,b). Conversely, APB (L-2-amino-4-phosphonobutyrate) selectively blocked ON-bipolar cells, with little effect on horizontal or OFF-bipolar cells (Slaughter & Miller, 1981; Shiells et al., 1981). Inhibition of amacrine and ganglion cell light responses, therefore, is due to a decrease in the input from ON-bipolar cells, not a direct effect on postsynaptic receptors. Since the light responses of all third-order neurons were blocked by the broad spectrum antagonists PDA and kynurenic acid, Slaughter and Miller (1983a-c) postulated that both photoreceptors and bipolar cells released an EAA such as glutamate. Studies monitoring the released

neurotransmitter of depolarized photoreceptors and bipolar cells with EAA-sensitive patches (Tachibana & Okada, 1991; Copenhagen & Jahr, 1989) have confirmed this postulate. Furthermore, immunocytochemical studies indicate that most, if not all, photoreceptors, bipolar cells and ganglion cells appear immunoreactive using antibodies directed against glutamate (Ehinger et al., 1988; Marc et. al, 1990; Massey, 1990; Jojich & Pourcho, 1996).

Glutamate receptors

Multiple glutamate receptor types have been identified, each characterized by its specific sensitivity to glutamate analogues and by the features of the glutamate-elicited current. Two classes of glutamate receptors have been identified; ionotropic glutamate receptors, which directly gate ion channels and metabotropic glutamate receptors, which may be coupled to an ion channel or other cellular functions via an intracellular second messenger cascade. These receptor types are similar in that they both bind glutamate and glutamate binding can influence the permeability of ion channels.

Iionotropic Glutamate Receptors

Ionotropic receptors (iGluRs) mediate fast synaptic transmission as they directly influence ion channel activity since the receptor and ion channel form one complex. There are two major classes of EAA receptors that directly gate ionotropic channels existing in the retina (Cohen & Miller, 1994). The NMDA receptor class is singularly activated by the EAA agonist N-methyl-D-aspartate. The non-NMDA receptor class, also known as the Kainate/AMPA class, is activated by a heterogeneous group of EAA agonists including kainic acid (KA), quisqualic acid (QQ), and the potent agonist AMPA (α-amino 3-hydroxy 5-methyl 4-isoxazolepropionic acid).

The kinetics of the non-NMDA, ligand-gated currents differ such that AMPA and quisqualate elicited currents rapidly desensitize, whereas kainite-gated currents do not (Connaughton, 1997). Glutamate binding onto NMDA receptors opens non-selective cation channels, resulting in a conductance increase. However, the high conductance channel associated with these receptors is more permeable to Ca+2 than Na+ ions (Mayer & Westbrook, 1987) and NMDA-gated currents typically have slower kinetics than kainite and AMPA-gated channels.

Metabotropic Receptors

Unlike ionotropic receptors, which are directly linked to an ion channel, metabotropic receptors (mGluRs) are coupled to their associated ion channel through a second messenger pathway. Ligand (glutamate) binding activates a G-protein and initiates an intracellular cascade (Nestler & Duman, 1994). MGluRs are classified into three groups based on structural homology, agonist selectivity and their associated second messenger cascade.

In the retina, non-NMDA receptors have been identified on horizontal cells, OFF-bipolar cells, amacrine cells, and ganglion cells. NMDA receptors are present in the inner retina, yet are thought to be absent in the outer retina (Slaughter & Miller, 1983c; Massey & Miller, 1987, 1988). The retina also contains the APB receptor, a metabotropic (G-protein gated) receptor which is activated by the APB agonist (Slaughter & Miller, 1981; Nawy & Jahr, 1990). In contrast to non-NMDA and NMDA receptors, a conductance decrease is elicited with glutamate binding onto an APB receptor (Nawy & Copenhagen, 1987, 1990) due to the closure of cGMP-gated non-selective cation channels (Nawy & Jahr, 1990).

Different EAA receptor classes are expressed by retinal neurons on their dendrites. For example, only ON-center depolarizing (mixed) bipolar cells possess L-APB receptors (Slaughter & Miller, 1981). Yet, APB application selectively blocks the ON-pathway in the retina specifically the ON-bipolar cell responses, the ON-responses in amacrine cells (Taylor & Wassle, 1995) and the ON-responses in ganglion cells (Cohen & Milller, 1994). Therefore, the inhibition noted in amacrine and ganglion cell responses is due to a decrease in the input from ON-bipolar cells, not a direct effect on postsynaptic receptors.

Retinal ganglion cells and some amacrine cells express both functional NMDA receptors and non-NMDA receptors (Massey & Miller, 1988; Cohen & Miller, 1994). The currents elicited through these different iGluR types can be distinguished pharmacologically such that non-NMDA receptor antagonists block a transient component of the ganglion cell response, whereas NMDA receptor antagonists block a sustained component (Mittman et al., 1990; Diamond & Copenhagen, 1993; Cohen & Miller,1994).

Electrophysiological recordings have identified ionotropic glutamate receptors on the neurons comprising the OFF-pathway in both higher and lower vertebrates. In the distal retina, OFF-bipolar cells (Sasaki & Kaneko, 1996) and horizontal cells (Yang & Wu, 1991; Zhou et al., 1993) respond to kainate, AMPA and quisqualate application, but not NMDA nor APB.

Appendix 6: Metabolic Inhibition and Membrane Potential

The finding that modulation of membrane potential affects malonate induced excitotoxicity in vivo supports the hypothesis that membrane depolarization is a critical variable in the manifestation of NMDA receptor damage induced by metabolic inhibition. The finding that slight elevations of extracellular K+ levels have enhanced NMDA receptor activation in rat hippocampus, through a probable impairment of neuronal repolarization (Poolos & Kocsis, 1990) further substantiates the hypothesized involvement of membrane depolarization in neuronal death.

It has been hypothesized that the reduction of anoxia-induced depolarization by potassium channel activators decreases presynaptic glutamate release (Ben-Ari, 1990), but this type of release has been shown to be short-lived (Kauppinen et al., 1988). As such, the excessive release of endogenous glutamate is not hypothesized as the etiologic determinant in the initiation of toxicity caused by metabolic inhibitors in vivo (Beal et al., 1993a; Greene & Greenamyre, 1995b). In fact, although a delayed increase in extracellular concentrations of glutamate and other amino acids were measured following striatal malonate injection, this increase was largely blocked by dizocilipine (MK-801), suggesting that the increase may be a result, rather than a cause, of NMDA receptor activation (Messam et al., 1995). Similar glutamate release results were evidenced in chick retina following mild metabolic inhibition (Zeevalk & Nicklas, 1992). Furthermore, in vivo experimentation has been inefficient in producing neurotoxicity with elevated glutamate levels as a univariate variable (Massieu et al., 1995). On the other hand, although delayed release of EAAs following metabolic inhibition may not be

a precipitating variable, it is nonetheless considered a metabolic condition that can exacerbate the degree and consequences of neurotoxicity.

Alternatively, the effects of membrane potential on malonate toxicity may be due to the release of endogenous glutamate as a result of membrane potential modulation. Indeed, in vitro experimentation has shown that ATP depletion, ouabain, or increased extracellular potassium levels can increase glutamate release, either by decreasing or reversing glutamate uptake (Barbour et al., 1988; Szatkowski et al., 1990; Madl & Burgesser, 1993), and that these mechanisms can be synergistic (Madl & Burgesser, 1993).

Similarly, the activity of cGMP-gated channels from carp cone photoreceptors has been shown to be modulated by at least two opposing mechanisms mediated by ATP which both increases and decreases the apparent agonist affinity (Watanabe & Shen, 1997). In the photoreceptor outer segment, cGMP is the second messenger working at the final stage of phototransduction both in the rod and the cone. The activity of rod cGMP-gated channels has been shown to be modulated by nucleoside triphosphates (Filatov et al., 1989), by phosphorylation (Gordon et al., 1992), by calmodulin or other calcium-dependent mechanisms (Hsu & Molday, 1993; 1994; Chen et al., 1994; Gordon et al., 1995b), and by diacylglycerol analogs (Gordon et al., 1995a). These modulation mechanisms interact with the calcium dependent modulation mechanisms involved in light adaptation of photoreceptors (Kawamura & Murakami, 1991; Koch, 1992; Koutalos & Yau, 1996).

Appendix 7: Consent Forms

10/2004 Participant Initials _____ID # _____

ROCKLAND PSYCHIATRIC CENTER
NATHAN S. KLINE INSTITUTE FOR PSYCHIATRIC RESEARCH

INFORMED CONSENT FORM FOR CONTROLS FOR RELATIVES OF LHON PATIENTS ADULTS (AGES 18-65)

Title: Visual Processing in Schizophrenia

Principal Investigator: Dr. Pamela D. Butler (845) 398-6537
Co-Investigators: Dr. Daniel Javitt (845) 398-6534
Dr. Isaac Schechter (845) 398-6617
Dr. Charles Schroeder (845) 398-6539
Ms. Gail Silipo (845) 398-6536

Name of Participant:_____

Purpose of Study: The purpose of this research is to learn more about the possible causes of Lebers Hereditary Optic Neuropathy (LHON) and to understand more about visual dysfunction. In order to gain more information about abnormalities of brain function that may be associated with LHON, both behavioral and electrophysiological (i.e., brain waves) measures will be tested. Specifically, you have been asked to participate as a control in this research to study your responses to visual patterns.

Description of Study Procedures: This protocol consists of two parts: 1) a diagnostic interview and brief psychological tests, and 2) visual cognitive tasks.

For the purposes of this study, we will take your medical and psychiatric history and you will be asked about social factors, such as your education, family background, marital status, employment history, and drug and alcohol history. You will take some brief psychological tests, for example, paper and pencil tests, looking at pictures or answering questions involving reasoning or other thinking abilities.

If you agree to participate in this study, you will begin by having a vision test. For the behavioral tasks, you will be asked to look at letters or shapes presented on a screen. You will be asked to report, either verbally or with a simple key press, your responses to the visual stimuli. All together, these tests and interviews will take between two and four hours, but they may be completed in several shorter sessions if you wish.

You will be asked to perform these visual tasks while your brain waves are recorded using an electrical recording device known as an electroencephalograph (EEG). Three electrodes will be placed on your head or a state of the art, comfortable electrode cap will be placed on your head, and several electrodes placed on your face. Each recording session will take approximately 1-3 hours. Breaks will be provided automatically every 20 minutes, and you will be allowed to take additional breaks whenever you ask.

Participant Initials_____ ID#_____

Title: Visual Processing in Schizophrenia
Principal Investigator: Dr. Pamela D. Butler

You will provide your own transportation to the Nathan Kline Institute in Orangeburg, New York.

Expected Risks and Benefits:

No adverse effects are expected. However, you may experience some minimal discomfort while putting on the electrodes or electrode cap. It is not expected that having the brain wave test will have any immediate effect.

You understand that this study is being done for research purposes only and that you will not benefit directly. While the procedures in this study may have some similarity to procedures done for clinical purposes, they are not designed for clinical interpretation and will not receive such an interpretation. It is hoped, however, that the knowledge gained from this study will be of benefit to others in the future.

Payment for Participation:

You will not receive payment for participation in this study.

Research Standards and Rights of Participants:

The nature of this study has been clearly explained to you both in writing and orally. You understand that your right to privacy and the confidentiality of your participation in this project, should you choose to participate, will be safeguarded to the extent permitted by law. The researchers in this project guarantee that with two exceptions the information you give us will be held in the strictest confidence. The two exceptions are if you tell us that you are planning to hurt yourself or someone else. All information obtained in this study will be kept in a locked office and will be kept strictly confidential. The only people who will be allowed access to the information will be the research staff, the staff who are treating you, the Institutional Research Review Boards for the Protection of Participants at the Nathan Kline Institute, and the Rockland County Department of Mental Health, also the quality assurance monitors of the study sites, and the National Institute of Mental Health. Under state law, certain legal advocacy organizations (groups that support participant's rights) have authority to obtain confidential participant records. Therefore, we could be required to give copies of your study records to one of these organizations if they request them. However, they would not be allowed to reveal your identifying information to anyone else without your permission. When the research findings are published or presented, no individual identifying information will be used. Individual confidentiality is protected by the use of assigned code numbers, and by reporting only the group results.

In the event that you experience an injury at the Nathan Kline Institute as a direct result of participating in this research, the facility will provide emergency medical care within its capabilities, arrange such other emergency medical care as may be necessary and assist you in arranging follow up care. Neither the facility nor the Research Foundation for Mental Hygiene makes any commitment to pay for medical care, nor do they have programs to provide you with financial compensation for such injury. By agreeing to participate in this research and signing this consent form, you do not waive any legal rights nor do you release the research staff, the Nathan Kline Institute, Rockland Psychiatric Center or the Research Foundation for Mental Hygiene from liability for negligence.

Participant Initials_____ ID#_____

Title: Visual Processing in Schizophrenia
Principal Investigator: Dr. Pamela D. Butler

If you have any questions about this study, you may contact Dr. Pamela D. Butler at (845) 398-6537. If you have any question about your rights as a participant in this study, you may contact Carole Roth JD, NKI/RPC IRB Director at (845) 398-5492 or Erna Ostrom, NKI/RPC Coordinator at (845) 398-5493.

Agreement to Participate:

By signing this form, you agree to participate in a medical research study entitled: Visual Processing in Schizophrenia, to be carried out under the supervision of Dr. Pamela D. Butler, telephone number (845) 398-6537.

You have been told by the doctor or other persons conducting this research that your participation is voluntary, and that you may withdraw from the study at any time.

You voluntarily consent to participate in this research study conducted under the supervision of Dr. Pamela D. Butler. You will be given a copy of this consent form and a copy may be sent to the Department of Quality Assurance of Rockland Psychiatric Center for monitoring purposes.

_____ _____
Participant Signature Date

_____
Print Name

PERSON OBTAINING CONSENT

I believe that this consent is freely given, by a participant with sufficient capacity to consent, and the participant has been given all of the information deemed necessary by the IRB or requested by the participant.

_____ _____
Signature of person obtaining consent (Research Staff) Date

_____ _____
Print name Title

10/2004 Participant Initials _____ID # _____

ROCKLAND PSYCHIATRIC CENTER/
NATHAN S. KLINE INSTITUTE FOR PSYCHIATRIC RESEARCH

INFORMED CONSENT FORM FOR LHON PATIENTS OR RELATIVES

ADULTS (AGES 18-65)

Title: Visual Processing in Schizophrenia

Principal Investigator: Dr. Pamela D. Butler (845) 398-6537
Co-Investigators: Dr. Daniel Javitt (845) 398-6534
Dr. Isaac Schechter (845) 398-6617
Dr. Charles Schroeder (845) 398-6539
Ms. Gail Silipo (845) 398-6536
Ms. Lisa Kleiner (914) 636-5289

Name of Participant:_____

Purpose of Study: The purpose of this research is to learn more about the possible causes of Lebers Hereditary Optic Neuropathy (LHON) and to understand more about visual dysfunction. In order to gain more information about abnormalities of brain function that may be associated with LHON, both behavioral and electrophysiological (i.e., brain waves) measures will be tested. Specifically, you have been asked to participate in this research to study how persons with LHON or relatives or these individuals respond to visual patterns.

Description of Study Procedures: This protocol consists of two parts: 1) a diagnostic interview and brief psychological tests, and 2) visual cognitive tasks.

For the purposes of this study, we will take your medical and psychiatric history and you will also be asked about social factors, such as your education, family background, marital status, employment history, and drug and alcohol history. You will take some brief psychological tests, for example, paper and pencil tests, looking at pictures or answering questions involving reasoning or other thinking abilities.

If you agree to participate in this study, you will begin by having a vision test. For the behavioral tasks, you will be asked to look at letters or shapes presented on a screen. You will be asked to report, either verbally or with a simple key press, your responses to the visual stimuli. All together, these tests and interviews will take between two and four hours, but they may be completed in several shorter sessions if you wish.

You will be asked to perform these visual tasks while your brain waves are recorded using an electrical recording device known as an electroencephalograph (EEG). Three electrodes will be placed on your head or a state of the art, comfortable electrode cap will be placed on your head, and several electrodes placed on your face. These electrodes and cap will be put on with gel. No hair will be shaved and it does not hurt when the electrodes or cap are removed. Each recording session will take approximately 1-3 hours. Breaks will be provided automatically every 20 minutes, and you will be allowed to take additional breaks whenever you ask.

Participant Initials_____ ID#_____

Title: Visual Processing in Schizophrenia
Principal Investigator: Dr. Pamela D. Butler

You will provide your own transportation to the Nathan Kline Institute in Orangeburg, New York.

Expected Risks and Benefits:

No adverse effects are expected. However, you may experience some minimal discomfort while putting on the electrodes or electrode cap.

This research study will give you no direct benefits. While the procedures in this study may have some similarity to procedures done for clinical purposes, they are not designed for clinical interpretation and will not receive such an interpretation. It is hoped, however, that the knowledge gained from this study will be of benefit to others in the future.

Payment for Participation:

You will not receive payment for participation in this study.

Research Standards and Rights of Participants:

The nature of this study has been explained to you both in writing and orally. Your right to privacy and the confidentiality of your participation in this project, should you choose to participate, will be safeguarded to the extent permitted by law. The researchers in this project will keep your information strictly confidential in a locked office. There are a few exceptions to this confidentiality. If you tell us that you are planning to hurt yourself or someone else we must contact someone who will help. The only people who will be allowed access to the information will be the research staff, the staff who are treating you, the Institutional Research Review Boards for the Protection of Participants at the Nathan Kline Institute, and the Rockland County Department of Mental Health, also the quality assurance monitors of the study sites, and the National Institute of Mental Health. Under state law, certain legal advocacy organizations (groups that support participant's rights) have authority to obtain confidential participant records. Therefore, we could be required to give copies of your study records to one of these organizations if they request them. However, they would not be allowed to reveal your identifying information to anyone else without your permission. When the research findings are published or presented, no individual identifying information will be used. Individual confidentiality is protected by the use of assigned code numbers, and by reporting only the group results.

In the event that you experience an injury at the Nathan Kline Institute as a direct result of participating in this research, the facility will provide emergency medical care within its capabilities, arrange such other emergency medical care as may be necessary and assist you in arranging follow up care. Neither the facility nor the Research Foundation for Mental Hygiene makes any commitment to pay for medical care, nor do they have programs to provide you with financial compensation for such injury. By agreeing to participate in this research and signing this consent form, you do not waive any legal rights nor do you release the research staff, the Nathan Kline Institute, Rockland Psychiatric Center or the Research Foundation for Mental Hygiene from liability for negligence.

Participant Initials_____ ID#_____

Title: Visual Processing in Schizophrenia
Principal Investigator: Dr. Pamela D. Butler

If you have any question about this study, you may contact Dr. Pamela D. Butler at (845) 398-6537. If you have any question about your rights as a participant in this study, you may contact Carole Roth JD, NKI/RPC IRB Director at (845) 398-5492 or Erna Ostrom, NKI/RPC Coordinator at (845) 398-5493.

Patient Agreement to Participate:

By signing this form, you agree to participate in a medical research study entitled: Visual Processing in Schizophrenia, to be carried out under the supervision of Dr. Pamela D. Butler, telephone number (845) 398-6537.

You have been told by the doctor or other persons conducting this research that your participation is voluntary, and that you may withdraw from the study at any time.

You voluntarily consent to participate in this research study conducted under the supervision of Dr. Pamela D. Butler. You will be given a copy of this consent form and a copy may be sent to the Department of Quality Assurance of Rockland Psychiatric Center for monitoring purposes.

_____ _____
Participant Signature Date

_____
Print Name

PERSON OBTAINING CONSENT

I believe that this consent is freely given, by a participant with sufficient capacity to consent, and the participant has been given all of the information deemed necessary by the IRB or requested by the participant.

_____ _____
Signature of person obtaining consent (Research Staff) Date

_____ _____
Print name Title

Appendix 8: Future Research

Metabolic Bypass Therapies

Ubiquinone or coenzyme Q_{10} is a mitochondrial respiratory chain component and as such is an integral member of the mitochondrial electron transport chain. Cells receive energy from the transfer of electrons between flavoproteins to the cytochromes via reversible reduction/oxidation. Coenzyme Q_{10} is essential for proper functioning of the mitochondria; it decreases free radical accumulation within the cell membrane and blocks lipid peroxidation (Folkers et al., 1991). Patients with Kearns-Sayre syndrome have been successfully treated with coenzyme Q_{10}, with evidence of an improved biochemical and clinical condition, especially ECG (Ogasahara et al., 1986).

Other cofactors for enzymes responsible for oxidative phosphorylation have been suggested due to their reported clinical efficacy. Successful treatment with riboflavine has been reported in a complex-I deficient patient with NADH-CoQ reductase deficient myopathy (Arts et al., 1983). Ascorbate and menadione (K3), prescribed in a patient with a deficiency in a cytochrome b-containing complex-III displayed minor functional, but greater biochemical improvement in the electron transport capabilities and the ATP synthesis rate via NMR examinations of skeletal muscle at rest (Eleff et al., 1984). Menadione is believed to be capable of bridging complex-I activity by mediating electron transport from NADH to electron acceptors further down the electron transport chain, namely coenzyme Q or cytochrome c (Przyrembel, 1987). *In vitro* experimentation has indicated that respiration can be restored with menadione in mitochondria blocked by the complex-I inhibitor amytal (Conover & Ernster, 1962). Similarly, menadione added to cultured fibroblasts treated with rotenone, a Complex-I inhibitor, normalized the lactate

to pyruvate ratio after incubation with glucose and increased the intracellular concentration of ATP (Wijburg et al., 1990). Furthermore, increased NADH-oxidation was observed in both complex-I and complex-III inhibited fibroblasts when menadione was added to the incubation medium (Wijburg et al., 1991). Whereas, muscle creatine levels took seven times longer to return to normal as compared with controls in individuals with a defect in the NADH-CoQ reductase (Complex I) after exercise (Clark et al., 1984), subjective improvement with increased exercise tolerance was reported in an elderly patient taking menadione with complex-I deficiency (Land et al., 1981) and remarkable improvement was reported in an infant diagnosed with a complex-I deficiency exhibiting a multisystem disorder with severe congenital lactic acidosis (Wijburg et al., 1989). However, there have also been reports of no improvement (Przyrembel, 1987; Morgan-Hughes et al., 1984).

An electron-shuttle molecule, idebenone (CV-2619), was used at the Keio University in Japan to bypass metabolic blocks in the electron transport chain (Mashima et al., 1992). Idebenone, an antioxidant, has been shown to readily enter rat brain, localizing in the mitochondria (Torii et al., 1985) and to decrease quisqualate toxicity (Miyamoto & Coyle, 1990). Idebenone is a quinol responsible for not only stimulating net ATP formation in cerebral metabolism, but also for inhibiting lipid peroxidation in the mitochondrial membrane and by the reduction of non-respiratory oxygen consumption in cerebral metabolism (Sugiyama & Fujita, 1985; Sugiyama et al., 1985).

Research investigating treatment with idebenone combined with vitamin B2 and vitamin C in LHON patients revealed that although there was no significant difference in the number of eyes with visual recovery, there was a significant difference in the mean

interval between onset of LHON symptomology and visual recovery in the treated group (Mashima et al., 2000).

Similarly, acetyl-levo-carnitine (ALC), a drug currently available only in Europe, may also be effective in bypassing mitochondrial defects with the restoration of normal ATP production. Research has shown that ALC exhibits a partial protection effect against 1-methyl, 4-phenyl-1,2,3,6-tetrahydropyridine (MPTP)- induced toxicity in nonhuman primates. Monkeys pretreated with ALC did not show signs of parkinsonism or electroretinographic changes typical of the MPTP induced dopaminergic deficiency (Bodis-Wollner et al., 1991, 1990a; Burlina et al., 1989). The underlying supposition implicates ALC protection in mitochondrial respiration, target of the toxic metabolite MPP+, and as such presents as a prospective therapeutic strategy in neurodegenerative diseases.

The promising results obtained with metabolic bypass therapies such as idebenone, coenzyme Q_{10}, and ALC require further investigation. Reports of a successful cocktail therapy, implementing both idebenone and coenzyme Q_{10} in the treatment of MELAS (Ihara et al., 1989), may inspire other cocktail therapy protocols for treatment in LHON, which may prove to be more effective than a singular approach.

Progress in the molecular mechanics of axonal transport, has yielded a correlation between OXPHOS and ATP requirements in transport. The proteins and organelles necessary for neuronal integrity are synthesized in the cell body and then transported down the axon via axonal transport mechanisms. Microtubules, in conjunction with the proteins kinesin and dynein which act as molecular motors, are integral to the process of axonal transport. Axonal stasis, or constipation, occurs when ATP production is

insufficient to maintain axonal transport (Brady, 1991; Brady et al., 1985, 1982). Extruded axoplasm preparations have provided for the direct evaluation of the molecular mechanics of fast axonal transport (Brady et al., 1985). Research investigating the effects of OXPHOS inhibitors and/or various agents that deplete ATP concentrations on organelle motility has revealed a complete cessation of movement (Brady et al., 1985, 1982). For example, perfusion of AMP-PNP (Adenylyl-imidodiphosphate), a weak competitive inhibitor of both myosin and dynein, into axoplasm preparations indicate a relatively immediate cessation of both anterograde and retrograde axonal transport, even in the presence of stoichometric concentrations of ATP (Brady et al., 1985; Lasek & Brady, 1985, 1984). Research must be initiated to investigate possible etiological correlates of axonal transport inhibition to OXPHOS related diseases, such as Lebers.

Minoxidil

The aforementioned anecdotal evidence indicating a gradual improvement in visual acuity after a longstanding blindness of fourteen years with the spurious use of minoxidil must be investigated further (Sherman et al., 1992). Certainly, at the very least, this case history is the quintessential example of a non-textbook diagnosis with an even more non-textbook therapy, reminding us all very quietly to maintain a non-textbook approach to clinical cases, namely to retain an open-mind.

Neuroprotective Agents

Newer research is investigating the potential use of neuroprotective agents in the treatment of LHON. Neurotrophic factors, such as brain-derived neurotrophic factor

(BDNF) and neurotrophin-4 or 5 (NT-4/5) have been shown to be effective in rescuing RGCs from retrograde apoptosis and promote growth of intraretinal axons in rodent and cat models (Watanabe et al., 1997). On the other hand, although upregulation of the neurotrophin receptor TrkB in combination with its ligand, BDNF, has been shown to promote extensive survival of adult rat RGCs *in vivo*, it has not been shown to enhance adult RGC regeneration and in fact appears to have an inhibitory effect on RGC axon growth (Pernet & Di Polo, 2003).

Pretreatment with 2-deoxy-D-glucose (2DG), a non-metabolizable glucose analog that mimics caloric restriction, has also been shown to ameliorate the loss of neurons (15%) in the RGC after a 44% NMDA-induced excitotoxic loss (Lan et al., 2003).

Research has shown that the increase in nitric oxide synthesis in monocularly deprived (MD) newborn rats which causes apoptosis in the contralateral LGN can be reversed by glutamate receptor antagonists (Nucci et al., 1997; 2000). Intravitreal injection of tetanus neurotoxin (TeNT) blocks neurotransmitter release (Schiavo et al., 2000) and prevents MD-induced apoptosis in the LGN (Nucci et al., 2002). On the other hand, nitric oxide has been shown to protect against ATP-induced cell death in retinal microvasculature by a mechanism that involves neither cGMP nor inhibition of the ATP-evoked rise in Ca^{2+} (Kobayashi et al., 2003).

Glutamate neurotoxicity is suppressed by opening the ATP dependent potassium channels of mitochondria (Mit. K(ATP) channel). Research has shown the protective effects of bradykinin and diazoxide (Mit. K(ATP) channel agonists) against glutamate neurotoxicity. These protective effects were inhibited by the simultaneous application of

5-HD (a Mit. K(ATP) channel antagonist) against bradykinin and chelerythrine (a PKC inhibitor) against 5-HD (Yamauchi et al., 2002).

Topically administered brimonidine (BMD), a selective alpha-2 agonist, has been shown to increase growth factor expression and apoptosis cascade inhibition. In a recent study (Villegas-Perez et al., 2002), transient ischemia was induced in rats by ligature of the ophthalmic vessels (LOV). Retrograde axonal transport investigated 7 or 14 days after LOV in vehicle-treated rats (left eye treated with two 5υl of saline alone), revealed that the densities of Fluorogold (FG)-labeled RGCs in the left retinas had diminished to 40% or 27%, respectively of their contralateral non-ischemic retinas. FG-labeled RGCs in the left retinas of the BMD treated rats, measured 7 or 14 days after LOV, showed densities that were comparable to those found in their right control non-ischemic retinas. Analysis of anterograde axonal transport indicated areas devoid of the tracer cholera toxin subunit b (CTB)-labeled RGC terminals in the visual layers of the contralateral superior colliculi in the vehicle treated rats. These areas were larger and more numerous 60 -days after LOV than 30 days after LOV. On the other hand, the BMD treated rats showed a normal density of CTB-labeled RGC terminals spanning the visual layers of the contralateral superior colliculi both 30 and 60 days after LOV.

A similar 24 hour study also demonstrated that Brimonidine was effective in ameliorating cellular apoptosis two and a half fold induced by TNF-α, a primary inflammatory cytokine detected in many neurodegenerative diseases of the CNS (Cruz et al., 2002). In addition, this study found that Nitroxide Ester or ETOPS (ethyl-2,2',6,6'-tetramethylpiperidylidene-1-oxyl-succinate), a novel caged nitroxide shown to decrease

reactive oxygen species toxicity in selective challenge systems, was even more effective with an approximate four fold decrease in cell death .

Even topical application of the purite formulation of brimonidine, Alphagan-P, was shown to be effective in protecting ganglion cells in chronically ocular hypertensive (COHT) rats (Banaskiewicz et al., 2003). Laser-induced elevations in intraocular pressure (IOP) decreased by 33% (day 1 of treatment) and by 25% (day 15 of treatment). Furthermore, there was a 17% decrease in RGCs 10 days after IOP elevation remaining relatively constant at a 16% decrease after 21 days, as opposed to the vehicle treated group with a 41% decrease after 21 days.

Unfortunately, human research employing Brimonidine in patients with retinal dystrophies has not yielded impressive results (Merin et al., 2003). Visual acuity, color vision and contrast sensitivity were similar in treated and control eyes. Although a trend toward smaller visual field loss was evidenced in the treated eyes when assessing absolute visual field loss, this difference disappeared when evaluating percent of visual field loss.

Research has also established that not only neurotrophins, but also cytokines enhance RGC survival in vitro. The synergistic effect of combined treatments using both neurotrophins and cytokines was found to further improve RGC neuroprotection (Yip et al., 2002). Current research is also investigating different doses and formulations of topically applied brimonidine to evaluate optimal neuroprotective effects (LaFuente et al., 2002; WoldeMussie et al., 2002).

Research has even investigated the use of the psychotropic cannabinoid, Δ 9-tetrahydroxycannabinol (THC), 4-hydroxy-2,2,6,6-tetramethylpiperidine-n-oxyl

(TEMPOL) and N-omega-nitro-D-arginine methyl ester (L-NAME) in rat retina where intravitreal injection of NMDA induced a hypertoxic milieu which caused a dose-dependent apoptosis and loss of inner retinal neurons (Liou et al., 2003). Both L-NAME and THC protected retinal neurons by either scavenging or attenuating accumulation of NO, superoxide anion and peroxynitrite, whereas TEMPOL protected retinal neurons by either scavenging or attenuating accumulation of superoxide anion and peroxynitrite.

Additionally, fibroblast growth factor (FGF-2) has been implicated not only in retinal ganglion cell (RGC) survival, but also as a trophic factor upregulating the expression of GAP-43, a protein correlated with axonal growth, and stimulating the regeneration of injured RGC axons (Sapieha et al., 2003; Soto et al, 2002). Lomerizine, a diphenylmethylpiperazine calcium antagonist, has also been shown to enhance retinal ganglion cell survival induced by optic nerve damage (Sawada et al., 2003).

Calpain-mediated proteolysis has been suggested in the pathogenesis of neuronal cell death associated with excitotoxicity and ischemia. Research has shown that the inhibition of calcium-activated neutral cysteine proteases by the calpain inhibitor MDL 28170 reduced RGC loss in a model of acute excitotoxic stimulation and as such provides neuroprotection from cerebral ischemia and NMDA excitotoxicity (Pallas et al., 2003).

Gene Therapy

Hammerhead ribozymes designed to degrade mRNA of the NDUFA1 gene encoding the Complex I precursor MWFE polypeptide and the manganese superoxide dismutase (MnSOD) gene were then cloned into recombinant adeno-associated virus (rAAV) vector and tested in cell lines (Qi et al., 2002). Mouse ocular tissues infected

with ribozymes against mRNA for mitochondrial proteins expressed similar histopathological features as optic nerve tissues from autopsied LHON patients, suggesting a potential animal model of mitochondrial failure. This technique has been employed to further show the rescue of cell lines employing genes, such as superoxide dismutase (SOD2), to detoxify reactive oxygen species which have been shown to contribute to cellular death in experimentally induced complex I deficiencies such as LHON (Qi, et al., 2003). Murine cell lines infected with Adeno associated virus (AAV) expressing ribozymes, RzM338 and RzM217, designed to reduce expression of the nuclear encoded NDUFA1 subunit gene of complex I, induced massive cell death in vitro and Leber-like optic neuropathy in vivo. Introducing AAV expressing the human SOD2 gene had a protective effect against hydrogen peroxide and increased cell survival by 17% and 54% in cells co-infected with ribozyme RzM338 and RzM217, respectively.

Similarly, human osteosarcoma cell lines were infected with AAV expressing a ribozyme against cytochrome oxidase subunit II (COX II), chosen as a ribozyme target because reductions in COX activity are resistant to cyanide poisoning, thus increasing cell survival in KCN media (Lewin et al., 2003). After four days of KCN selection, there was a four-fold increase in cell survival, a 70% reduction in cytochrome oxidase activity and at least a 50% reduction in COX II expression in RzCOX II transfected cells as opposed to mock infection.

A synthetic, tagged ND4 gene, compatible with the universal genetic code, was inserted in an AAV vector and then imported into the mitochondria of cybrids harboring the G11778A mutation. Not only did the mitochondrial survival rate increase threefold under restrictive conditions that coerced the cells to rely primarily on OXPHOS to

produce ATP, but the G11778A cybrids showed a threefold increase in ATP synthesis to a level indistinguishable from cybrids containing normal mitochondrial DNA (Guy, et al., 2002). These studies indicating the restoration of respiration by allotopic expression are promising for the application of gene therapy in LHON.

However, a follow-up study investigating the administration of Complex II substrates that bypass the mutated Complex I did not significantly improve LHON cybrid cell survival (Guy et al., 2003). Cybrid cells coerced into predominantly relying on OXPHOS to produce ATP by placing them in a galactose medium containing either the Complex II substrate succinate or the Complex I substrate pyruvate as the main carbon source for glycolysis, dwindled 67% and 73% respectively. Furthermore, superoxide levels doubled in LHON cybrids placed in galactose media as compared to transmitochondrial LHON cybrids grown in glucose media, and mitochondrial defenses using the AAV as a vector to deliver the human gene SOD2 to LHON cybrids increased cell survival by only 25% relative to mock infection with AAV expressing GFP. Despite increased superoxide levels contributing to cellular death and potential optic neuropathy, the levels of antioxidant gene protection did not result in the aforementioned threefold increase in cell survival using allotropic ND4 rescue. These findings are consistent with the complexity in the clinical and biochemical etiology of LHON and suggest that other reactive oxygen species or reduced ATP synthesis may also play a role in cellular injury and optic neuropathy.

REFERENCES

Abele, A. E., and Miller, R. J. (1990) Potassium channel activators abolish excitotoxicity in cultured hippocampal pyramidal neurons. *Neuroscience Letters* **115**, 195-200.

Adams, J. H., Blackwood, W., and Wilson, J. (1966) Further clinical pathological observations on Leber's optic atrophy. *Brain* **89**, 15-26.

Adrian, F. D., and Mathews, B. H. C. (1934) The Berger rhythm: potential changes from the occipital lobes of man. *Brain* **57**, 355-385.

Aizenman, E., Frosch, M. P., and Lipton S. A. (1988) Responses mediated by excitatory amino acid receptors in solitary retinal ganglion cells from rat. *Journal of Physiology (London)* **396**, 75-91.

Ajax, E T., & Kardon, R. (1998) Late-onset Leber's hereditary optic neuropathy. *Journal of Neuroophthalmology* **18**, 30-31.

Alexander, K. R., Fishman, G. A., Peachey, N. S., Marchese, A. L., and Tso, M. O. (1992). 'On' response defect in paraneoplastic night blindness with cutaneous malignant melanoma. *Investigative Ophthalmology and Vision Science* **33**, 477-483.

Alexander, K. R., Rajagopalan, A. S., Seiple, W., Zemon, V. M., and Fishman G. A. (2005) Contrast response properties of magnocellualr and parvocellular pathways in retinistis pigmentosa assessed by the visual evoked potential. *Investigative Ophthalmology and Vision Science* **46**, 2967-2973.

Albin, R. L., and Greenamyre, J. T. (1992) Alternative excitotoxic hypothesis. *Neurology* **42**, 733-738.

Anderson, S., Bankier, A. T., Barrell, B. G., de Bruijn, M. H., Coulson, A. R., Douin, J., Eperon, I. C., Nierlich, D. P., Roe, B. A., Sanger, F., Schreier, P. H., Smith, A. J., Staden, R., and Young, I. G. (1981) Sequence and organization of the human mitochondrial genome. *Nature* **90**, 457-465.

Ara, F., Hotta, Y., Hayakawa, M., Yanashima, K., Kanai, A., and Fujiki, K. (1991) A trial of molecular diagnosis in Leber's optic neuropathy. *Nippon Ganka Gakkai Zasshi - Acta Societatis Ophthalmologicae Japonicae* **95**, 715-720.

Arden, G. B., Gunduz, K., and Perry, S. (1988a) Colour vision testing with a computergraphics system: preliminary results. *Documenta Ophthalmologica* **69**, 167-174.

Arden, G. B., Gunduz, K., and Perry, S. (1988b) Colour vision testing with a computergraphics system. *Clinical Vision Sciences* **2**, 303-320.

Arnason, B. G. W. (1993) Interferon beta in multiple sclerosis. *Neurology* **43**, 641-643.

Arts, W. F. M., Scholte, H. R., Boggard, J. M., Kerrebijn, K. F., and Luyt-Houwen, I. E. (1983) NADH-CoQ reductase deficient myopathy: successful treatment with riboflavin. *Lancet* **2**, 581-582.

Asseman, R., Hemery, B., Puech, B., and Castier, P. (1989) Leber's optic neuropathy: Future prospects. *Bulletin Des Societes D Ophtalmologie De France* **89**, 1235-1237.

Aurbach, E. (1962) Clinical application of bioelectrical tests. In: A. J. Ballantyne, and I. C. Michaelson, (Eds.), *Textbook of the Fundus of the Eye* (pp. 533-542). Baltimore: The Williams & Wilkins Co.

Banaskiewicz, R., Vorwerk, C. K., Ruiz, G., Wheeler, L. A., and WoldeMussie, E. (2003) Neuroprotective effect of topical administration of Alphagan-P in rats with laser-induced chronic ocular hypertension. Poster session presented at the annual meeting of the Association for Research in Vision and Ophthalmology, Sarasota, Florida.

Banerjee, A.K., MacSweeney, J. E., Hykin, P. G., and Sanders, M. D. (1990) Leber's optic neuropathy and mitral valve prolapse. *Journal of the Royal Society of Medicine* **83**, 55-56.

Barber, C., and Galloway, N. R. (1977) Adaptation effects in the transient visual evoked potential. In D. Lehman & E. Callaway (Eds.), *Human Evoked Potentials: Applications and Problems* (pp. 17-30). New York: Plenum Press.

Barboni, P., Mantovani, V., Montagna, P., Bragliani, M., Cortelli, P., Lugaresi, E., Puddu, P., Caramazza, R. (1992) Mitochondrial DNA analysis in Leber's hereditary optic neuropathy. *Ophthalmic Paediatric Genetics* **13**, 219-226.

Barboni, P., Savini, G., Valentino, M. L., Montagna, P., Cortelli, P., De Negri, A. M., Sadun, F., Bianchi, S., Longneck, L., Zanini, M., de Vivo, A., and Carelli, V. (2005) Retinal nerve fiber layer evaluation by optical coherence tomography in Leber's hereditary optic neuropathy. *Ophthalmology* **112(1)**:120-6.

Barbour, B., Brew, H., and Attwell, D. (1988) Electrogenic glutamate uptake in glial cells is activated by intracellular potassium. *Nature* **335**, 433-435.

Barlow, H. B., and Levick, W. R. (1965) The mechanism of directionally selective units in rabbit's retina. *Journal of Physiology* **178**, 477-504.

Barron, M. J., Griffiths, P. G., Turnbull, D. M., Bates, D., and Nichols, P. P. (2003, May) Na+ channels co-localise with mitochondrial enzyme activity in the unmyelinated part of the human optic nerve head. Poster session presented at the annual meeting of the Association for Research in Vision and Ophthalmology, Sarasota, Florida.

Beal, M. F. (1992a) Does impairment of energy metabolism result in excitotoxic neuronal death in neurodegenerative illnesses? *Annals of Neurology* **31**, 119-130.

Beal, M. F. (1992b) Mechanisms of excitotoxicity in neurologic diseases. *FASEB Journal* **6**, 3338-3344.

Beal, M. F. (1992c) Role of excitotoxicity in human neurological disease. *Current Opinion in Neurobiology* **2**, 657-662.

Beal, M. F., Brouillet, E., Jenkins, B. G., Ferrante, R. J., Kowall, N. W., Miller, J. M., Storey, E., Srivastava, R., Rosen, B. R., and Hyman, B. T. (1993a) Neurochemical and histological characterization of striatal excitotoxic lesions produced by the mitochondrial toxin 3-nitropropionic acid. *Journal of Neuroscience* **13**, 4181-4192.

Beal, M. F., Brouillet, E., Jenkins, B. G., Henshaw, R., Rosen, B. R., and Hyman, B. T. (1993b) Age-dependent striatal excitotoxic lesions produced by the endogenous mitochondrial inhibitor malonate. *Journal of Neurochemistry* **61**, 1147-1150.

Beal, M. F., Hyman, B. T., and Koroshetz, W. (1993c) Do defects in mitochondrial energy metabolism underlie the pathology of neurodegenerative disease? *Trends in Neuroscience* **16**, 125-131.

Beal, M. F., Matson, W. R., Storey, E., Milbury, P., Ryan, E. A., Ogawa, T., and Bird, E. D. (1992) Kynurenic acid concentrations are reduced in Huntington's disease cerebral cortex. *Journal of Neurological Science* **108,** 80-87.

Beal, M. F., Swartz, K. J., Hyman, B. T., Storey, E., Finn, S. F., and Koroshetz, W. (1992) Aminooxyacetic acid results in excitotoxic lesions by a novel indirect mechanism. *Journal of Neurochemistry* **57**, 1068-1073.

Beck, R. W., and Smith, C. H. (1988) *Neuro-Ophthalmology: A Problem Oriented Approach.* Boston: Little, Brown.

Beckman, J. S., and Crow, J. P. (1993) Pathological implications of nitric oxide, superoxide and peroxynitrite formation. *Biochemistry Society Transactions* **21**, 330-334.

Ben-Ari, Y. (1990) Modulation of ATP sensitive K+ channels: a novel strategy to reduce the deleterious effects of anoxia. In Y. Ben-Ari (Ed.), *Excitatory Amino Acids and Neuronal Plasticity* (pp. 481-489). New York: Plenum Press.

Ben-Ari, Y., Krnjevic, K., and Crepel, V. (1990) Activators of ATP sensitive K+ channels reduce anoxic depolarization in CA3 hippocampal neurons. *Neuroscience* **37**, 55-60.

Bendat, J. S., and Piersol, A. G. (1986) Random data: analysis and measurement procedures. (2nd ed.) New York: Wiley.

Berger, H. (1932) Ober das Elektroenzephalogramm des Menschen. *Archiv Die Psychiatria* **97**, 6-26.

Berninger, T. A., and Schuurmans, R. P. (1985) Spatial tuning of the pattern ERG across temporal frequency. *Documenta Ophthalmologica* **61**, 17-25.

Berninger, T. A., Bird, A. C., and Arden, G. B. (1989a) Leber's hereditary optic atrophy. *Ophthalmic Paediatrics and Genetics* **10**, 211-227.

Berninger, T. A., von Meyer, L., Siess, E., Schon, O., and Goebel, F. D. (1989b) Leber's hereditary optic atrophy: further evidence for a defect of cyanide metabolism? *British Journal of Ophthalmology* **73**, 314-316.

Berridge, M. J., and Irvine, R. F. (1984) Inositol triphosphate, a novel second messenger in cellular signal transduction. *Nature* **312**, 315-321.

Berson, E. L., and Lessell, S. (1988). Paraneoplastic night blindness with malignant melanoma. *American Journal of Ophthalmology* **106**, 307-311.

Besch, D., Leo-Kottler, B., Zrenner, E., and Wissinger, B. (1999) Leber's hereditary optic neuropathy: clinical and molecular genetic findings in a patient with a new mutation in the ND6 gene. *Graefes Archives of Clinical and Experimental Ophthalmology* **237**, 745-752.

Besch, D., Wissinger, B., Zrenner, E., and Leo-Kottler, B. (2000) A case of Leber optic neuropathy with a new point mutation in the cytochrome b gene. *Ophthalmologe* **97**, 22-26.

Bird, A. M. D., and McEachern, D. (1949) Leber's hereditary optic atrophy in a Canadian family. *Canadian Medical Association Journal* **61**, 376-383.

Bird, T. D., and Crill, W. B. (1981) Pattern reversal visual evoked potentials in the hereditary ataxias and spinal degenerations. *Annals of Neurology* **9**, 243-250.

Black, G. C., Craig, I, W., Oostra, R. J., Norby, S., Rosenberg, T., Morten, K., Laborde, A., and Poulton, J. (1995) Leber's hereditary optic neuropathy: implications of the sex ratio for linkage studies in families with the 3460 ND1 mutation. *Eye*. **9**, 513-516.

Bodis-Wollner, I. (1990) Physiological effects of acetyl-levo-carnitine in the central nervous system. *International Journal of Clinical Pharmacological Research* **10**, 109-114.

Bodis-Wollner, I., and Yahr, M. D. (1978) Measurements of visual evoked potential in Parkinson's disease. *Brain* **101**, 661-671.

Bodis-Wollner, I., Chung, E., Ghilardi, M. F., Glover, A., Onofrj, M., Pasik, P., and Samson, Y. (1991) Acetly-levo-carnitine protects against MPTP-induced parkinsonism in primates. *Journal of Neural Transmission* **3**, 63-72.

Bolhuis, P. A., Bleeker-Wagemakers, E. M., Ponne, N. J., Van Schooneveld, M. J., Westerveld, A., Van den Bogert, C., and Tabak, H. F. (1990) Rapid shift in genotype of human mitochondrial DNA in a family with Leber's hereditary optic neuropathy. *Biochemical and Biophysical Research Communications* **170**, 994-997.

Boos, R., Muller, F., and Wassle, H. (1990) Actions of excitatory amino acids on brisk ganglion cells in the cat retina. *Journal of Neurophysiology* **65**, 1368-1379.

Borg, D. C. (1993) *Oxygen Free Radicals and Tissue Injury.* In M. Tarr & F. Samson (Eds), (pp. 12–53). Boston: Birkhauser.

Borruat, F. X., Green, W. T., Graham, E. M., Sweeney, M. G., Morgan-Hughes, J. A., and Sanders, M. D. (1992) Late onset Leber's optic neuropathy: a case confused with ischaemic optic neuropathy. *British Journal of Ophthalmology* **76**, 571-573.

Borruat, F. X., Hirt, L., & Regli, F. (1994) Optic neuropathy caused by alcoholism and smoking: a diagnostic pitfall of Leber's optic neuropathy. *Review Neurology (Paris)* **150**, 799-801.

Boulet, L., Karpati, G., and Shoubridge, E. A. (1992) Distribution and threshold expression of the tRNA(Lys) mutation in skeletal muscle of patients with myoclonic epilepsy and ragged-red fibers (MERRF). *American Journal of Human Genetics* **51**, 1187-1200.

Boveris, B., and Chance, B. (1973) The mitochondrial generation of hydrogen peroxide. General properties and effect of hyperbaric oxygen. *Journal of Biochemistry* **134**, 707-716.

Bower, S. P., Hawley, I., and Mackey, D. A. (1992) Cardiac arrhythmia and Leber's hereditary optic neuropathy. *Lancet* **339**, 1427-1428.

Bowling, A. C., Barkowski, E. E., McKenna-Yasek, D., Sapp, P., Horvitz, H. R., Beal, M. F. and Brown, R. H. (1995) Superoxide dismutase concentration and activity in familial amyotrophic lateral sclerosis. *Journal of Neurochemistry* **64**, 2366-2369.

Bowling, A. C., and Beal, M. F. (1995) Bioenergetic and oxidative stress in neurodegenerative diseases. *Life Sciences* **56**, 1151-1171.

Bowling, A. C., Mutisya, E. M, Walker, L. C., Price, D. L., Cork, L. C., and Beal, M. F. (1993) Age-dependent impairment of mitochondrial function in primate brain. *Journal of Neurochemistry* **60**, 1964-1967.

Bowling, A. C., Schulz, J. B., Brown, R. H. and Beal, M. F. (1993) Superoxide dismutase activity, oxidative damage, and mitochondrial energy metabolism in familial and sporadic amyotrophic lateral sclerosis. *Journal of Neurochemistry* **61**, 2322-2325.

Boycott, B. B., and Hopkins, J. M. (1991) Cone bipolar cells and cone synapses in the primate retina. *Visual Neuroscience* **6**, 49-60.

Boycott, B. B., and Hopkins, J. M. (1993) Cone synapses of a flat diffuse cone bipolar cell in the primate retina. *Journal of Neurocytology* **22**, 765-778.

Boycott, B. B., and Wassle, H. (1974) The morphological types of ganglion cells of the domestic cat's retina. *Journal of Physiology* **240**, 397-419.

Boycott, B. B., and Wassle, H. (1991) Morphological classification of bipolar cells of the primate retina. *European Journal of Neuroscience* **3**, 1069-1088.

Boycott, B. B., Hopkins, J. M., and Sperling, H. G. (1987) Cone connections of the horizontal cells of the rhesus monkey's retina. *Proceedings of the Royal Society of London B* **229**, 345-379.

Brady, S. T. (1991) Molecular motors in the nervous system. *Neuron* **7**, 521-533.

Brady, S. T., Lasek, R. J., and Allen, R. D. (1982) Fast axonal transport in extruded axoplasm from squid giant axon. *Science* **218**, 1129-1131.

Brady, S. T., Lasek, R. J., and Allen, R. D. (1985) Video microscopy of fast axonal transport in isolated axoplasm: a new model for study of molecular mechanisms. *Cell Motility* **5**, 81-101.

Brandstatter, J. H., Hartveit, E., Sassoe-Pognetto, M., and Wassle, H. (1994) Expression of NMDA and high-affinity kainate receptor subunit mRNAs in the adult rat retina. *European Journal of Neuroscience* **6**, 1100-1112.

Breitmeyer, B. G., and Ganz, L. (1976) Implications of sustained and transient channels for theories of visual pattern masking, saccadic suppression, and information processing. *Psychological Review* **83**, 1-36.

Breitmeyer, B. G., and Ganz, L. (1977) Temporal studies with flashed gratings: inferences about human transient and sustained channels. *Vision Research* **17**, 861-865.

Bremner, F. D., Shallo-Hoffmann, J., Riordan-Eva, P., and Smith, S. E. (1999) Comparing pupil function with visual function in patients with Leber's hereditary optic neuropathy. *Investigative Ophthalmology and Visual Science* **40**, 2528-2534.

Brew, H., & Attwell, D. (1987) Electrogenic glutamate uptake is a major current carrier in the membrane of axolotl retinal glial cells. *Nature* **327**, 707-709.

Brown, M. D., Trounce, I. A., Jun, A. S., Allen, J. C., & Wallace, D. C. (2000) Functional analysis of lymphoblast and cybrid mitochondria containing the 3460, 11778, or 14484

Leber's hereditary optic neuropathy mitochondrial DNA mutation. *Journal of Biological Chemistry* **275**, 39831-39836.

Brown, M. D., Voljavec, A. S., Lott, M. T., MacDonald, I., and Wallace, D.C. (1992a) Leber's hereditary optic neuropathy: a model for mitochondrial neurodegenerative diseases. *Faseb Journal* **6**, 2791-2799.

Brown, M. D., Voljavec, A. S., Lott, M. T., Torroni, A., Yang, C. C., and Wallace, D. C. (1992b) Mitochondrial DNA complex I and III mutations associated with Leber's hereditary optic neuropathy. *Genetics* **130**, 163-173.

Brown, M. D., Yang, C. C., Trounce, I., Torroni, A., Lott, M. T., and Wallace, D. C. (1992c) A mitochondrial DNA variant identified in Leber's hereditary optic neuropathy patients which extends the amino acid sequence of cytochrome *c* oxidase subunit I. *American Journal of Human Genetics* 51, 378-385.

Brown, M. D., and Wallace, D. C. (1994) Spectrum of mitochondrial DNA mutations in Leber's hereditary optic neuropathy. *Clinical Neuroscience* **2**, 138-145.

Browne, S. E., Bowling, A. C., MacGarvey, U., Baik, M. J., Berger, S. C., Muqit, M. M., Bird, E. D., and Beal, M. F. (1997) Oxidative damage and metabolic dysfunction in Huntington's disease: selective vulnerability of the basal ganglia. *Annals of Neurology* **41**, 646-653.

Brunette, J. R., and Bernier, R. G. (1969) Study of a family of Leber's optic atrophy with recuperation. In J. R. Brunette & A. Barbeau (Eds.), *Progress in Neuro-ophthalmology* (pp. 91-95). Amsterdam: Excerpta Medica.

Brunette, J. R., and Bernier, R. G. (1970) Diagnostic et prognostic de la maladie de Leber: Incidence de la recuperation totale spontanee. *Union Medicale Du Canada* **99**, 643-652.

Bruyn, G. W., and Went, L. N. (1964) A sex-linked heredodegenerative neurological disorder, associated with Leber's optic atrophy. Part 1, Clinical studies. *Journal of the Neurological Sciences* **1**, 59-80.

Bruyn, G. W., Vielvoye, G. J., and Went, L. N. (1991) Hereditary spastic dystonia: a new mitochondrial encephalopathy? Putaminal necrosis as a diagnostic sign. *Journal of the Neurological Sciences* **103**, 195-202.

Bu, X. D., and Rotter, J. I. (1992) Leber hereditary optic neuropathy: estimation of number of embryonic precursor cells and disease threshold in heterozygous affected females at the X-linked locus. *Clinical Genetics* **42**, 143-148.

Bu, X. D., and Rotter, J. I. (1991) X chromosome-linked and mitochondrial gene control of Leber hereditary optic neuropathy: evidence from segregation analysis for dependence on X chromosome inactivation. *Proceedings of the National Academy of Sciences of the United States of America* **88**, 8198-8202.

Burlina, A. P., Sershen, H., Debler, E. A., and Lajtha, A. (1989) Uptake of acetylcarnitine in the brain. *Neurochemical Research* **14**, 489-493.

Butler, P. D., Schechter, I, Zemon, V, Schwartz, S. G., Greenstein, V. C., Gordon, J., Schroeder, C. E., and Javitt, D. C. (2001) Dysfunction of early stage visual processing in schizophrenia. *American Journal of Psychiatry* **158**, 1126-1133.

Butler, P. D., Zemon, V, Schechter, I., Saperstein, A., Hoptman, M., Lim, K., Revheim, N., Silipo, G., and Javitt, D. C. (2005) Early-stage visual processing and cortical amplification deficits in schizophrenia. *Archives of General Psychiatry* **62**, 495-504.

Cagianut, B., Schnebli, H. P., Rhyner, K., and Furrer, J. (1984) Decreased thiosulfate sulfur transferase (rhodanese) in Leber's hereditary optic atrophy. *Klinische Wochenschrift* **62**, 850-854.

Cardaioli, E., Gallus, G. N., Da Pozzo, P., Rufa, A., Franceschini, R., Motolese, E., Caporossi, A., Dotti, M. T., and Federico, A. (2005) A novel mutation producing premature termination codon at the OPA1 gene causes autosomal dominant optic atrophy. *Journal of Neurology* [Epub ahead of print]

Carelli, V., Ghelli, A., Bucchi, L., Montagna, P., De Negri, A., Leuzzi, V., Carducci, C., Lenaz, G., Lugaresi, E., and Degli Esposti, M. (1999) Biochemical features of mtDNA 14484 (ND6/M64V) point mutation associated with Leber's hereditary optic neuropathy. *Annals of Neurology* **45**, 320-328.

Carelli, V., Ghelli, A., Ratta, M., Bacchilega, E., Sangiorgi, S., Mancini, R., Leuzzi, V., Cortelli, P., Montagna, P., Lugaresi, E., and Degli Esposti, M. (1997) Leber's hereditary optic neuropathy: biochemical effect of 11778/ND4 and 3460/ND1 mutations and correlation with the mitochondrial genotype. *Neurology* **48**, 1623-1632.

Carelli, V., Ross-Cisneros, F. N., and Sadun, A. A. (2002) Optic nerve degeneration and mitochondrial dysfunction: genetic and acquired optic neuropathies. *Neurochemistry International* **40**, 573-584.

Carelli, V., Ross-Cisneros, F. N., and Sadun, A. A (2004) Mitochondrial dysfunction as a cause of optic neuropathies. *Progress in Retina and Eye Research* **23**, 53-89.

Carelli, V., Vergani, L., Bernazzi, B., Zampieron, C., Bucchi, L., Valentino, M., Rengo, C., Torroni, A., and Martinuzzi, A. (2002) Respiratory function in cybrid cell lines carrying European mtDNA haplogroups: implications for Leber's hereditary optic neuropathy. *Biochimica et Biophysica Acta* **1588**, 7-14.

Carelli, V., Wang, K., Valentino, M. L., Shankar, S. P., Salomao, S. S., Belfort, R., Sadun, A. A., and Stone, E. M. (2003) Segregation analysis of a large LHON pedigree is consistent

with the existence of a nuclear modifying gene. Poster session presented at the annual meeting of the Association for Research in Vision and Ophthalmology, Sarasota, Florida.

Carroll, F. D. (1966) Nutritional amblyopia. *Archives of Ophthalmology* **76**, 406-411.

Carroll, W. M., and Mastaglia, F. L. (1979) Leber's optic neuropathy: A clinical and visually evoked potential study of affected and asymptomatic members of a six generation family. *Brain* **102**, 559-580.

Carvalho, M. R., Muller, B., Rotzer, E., Berninger, T., Kommerell, G., Blankenagel, A., Savontaus, M. L., Meitinger, T., and Lorenz, B. (1992) Leber's hereditary optic neuroretinopathy and the X-chromosomal susceptibility factor: no linkage to DXs7. *Human Heredity* **42**, 316-320.

Caton, R. (1875) The electric currents of the brain. *British Medical Journal* **278**, 28.

Celesia G. G., and Daly, R. F. (1977) Effects of aging on visual evoked responses. *Archives of Neurology* **34**, 403-407.

Chalmers, R. M., Davis, M. B., Sweeney, M. G., Wood, N. W., and Harding A. E. (1996) Evidence against an X-linked visual loss susceptibility locus in Leber hereditary optic neuropathy. *American Journal of Human Genetics* **59**, 103-108.

Chalmers, R. M., Robertson, N., Compston, D. A. S., Harding, A. E. (1996b) Sequence of Mitochondrial DNA in patients with multiple sclerosis. *Annals of Neurology* **40**, 239-243.

Chan, C., Mackey, D. A., and Byrne, E. (1996) Sporadic Leber hereditary optic neuropathy in Australia and New Zealand. *Australian and New Zealand Journal of Ophthalmology* **24,** 7-14.

Chang, H. (1959) The Evoked Potentials. In J. Field, H. W. Magoun, & V. E. Hall (Eds.), *Handbook of Physiology, Section I: Neurophysiology, Vol. I.* Washington, D. C.: American Physiological Society.

Chen, J. D., Cox, I., and Denton, M. J. (1989) Preliminary exclusion of an X-linked gene in Leber optic atrophy by linkage analysis. *Human Genetics* **82**, 203-207.

Chen, T. Y., Illing, M., Molday, L. L., Hsu, Y. T., & Yau, K. W., & Molday, R. S. (1994) Subunit 2 (or beta) of retinal rod cGMP-gated cation channel is a component of the 240-kDa channel-associated protein and mediates Ca(2+)-calmodulin modulation. *Proceedings of the National Academy of Sciences of the United States of America* **91**, 11757-11761.

Chew, S. J. (1990) Leber's hereditary optic atrophy: an atypical case with response to hydroxycobalamine therapy. *Singapore Medical Journal* **31**, 293-294.

Chomyn A, Lai ST, Shakeley R, Bresolin N, Scarlato G, Attardi G. (1994) Platelet-mediated transformation of mtDNA-less human cells: analysis of phenotypic variability among clones from normal individuals--and complementation behavior of the tRNALys mutation causing myoclonic epilepsy and ragged red fibers. *American Journal of Human Genetics* **54,** 966-974.

Chomyn, A., Mariottini, P., Cleeter, M.W., Ragan, C.I,, Matsuno-Yagi, A., Hatefi, Y., Doolittle, R.F., and Attardi, G. (1985) Six unidentified reading frames of human mitochondrial DNA encode components of the respiratory-chain NADH dehydrogenase. *Nature* **314**, 592-597.

Chomyn, A., Martinuzzi, A., Yoneda, M., Daga, A., Hurko, O., Johns, D., Lai, S. T., Nonaka, I., Angelini, C., and Attardi, G. (1992) MELAS mutation in mtDNA binding site for transcription termination factor causes defects in protein synthesis and in respiration but no change in levels of upstream and downstream mature transcripts. *Proceedings of the National Academy of Sciences of the United States of America* **89**, 4221-4225.

Ciafaloni, E., Ricci, E., Servidei, S., Shanske, S., Silvestri, G., Manfredi, G., Schon, E. A., and DiMauro, S. (1991) Widespread tissue distribution of a tRNALeu(UUR) mutation in the mitochondrial DNA of a patient with MELAS syndrome. *Neurology* **41**, 1663-1664.

Clark, J. B., Hayes, D. J., Morgan-Hughes, J. A., & Byrne, E. (1984) Mitochondrial myopathies: disorders of the respiratory chain and oxidative phosphorylation. *Journal of Inherited Metabolic Diseases* **7**, 62-68.

Cleland, B. G., and Levick, W. R. (1974a) Brisk and sluggish concentrically organized ganglion cells in the cat's retina. *Journal of Physiology* **240**, 421-456.

Cleland, B. G., and Levick, W. R. (1974b) Properties of rarely encountered types of ganglion cells in the cat's retina and an overall classification. *Journal of Physiology* **240**, 457-492.

Cock, H. R., Cooper, J. M., and Schapira, A. H. (1999) Functional consequences of the 3460-bp mitochondrial DNA mutation associated with Leber's hereditary optic neuropathy. *Journal of Neurological Science* **165**, 10-17.

Cock, H. R., Tabrizi, S. J., Cooper, J. M., and Schapira, A. H. (1998) The influence of nuclear background on the biochemical expression of 3460 Leber's hereditary optic neuropathy. *Annals of Neurology* **44**, 187-193.

Cohen, E. D., and Miller, R. F. (1994) The role of NMDA and non-NMDA excitatory amino acid receptors in the functional organization of primate retinal ganglion cells. *Visual Neuroscience* **11**, 317-332.

Cohen, S. N., Syndulko, K., Tourtellote, W. W., and Potvin, A. R. (1980) Critical frequency of photic driving in the diagnosis of multiple sclerosis: A comparison to pattern evoked responses. *Archives of Neurology* **37**, 80-83.

Colenbrander, M. C. (1962) Observations on the heredity of Leber's disease. O*phthalmologica* **144**, 446-450.

Connaughton, V. P. (2003, August). Glutamate and glutamate receptors in the vertebrate retina. Available Webvision: Hostname: med.utah.edu Directory: http://webvision.med.utah.edu/GLU.html#General%20overview%20of%20synaptic%20transmission.

Connolly, M., and Van Essen, D. (1984) The representation of the visual field in parvicellular and magnocellular layers of the lateral geniculate nucleus in the macaque monkey. *Journal of Comparative Neurology* **226**, 544-564.

Conover, T. E., and Ernster, L. (1962) DT diaphorase: Relation to respiratory chain of intact mitochondria. *Biochimica et Biophysica Acta* **58**, 189-200.

Constantine, E. F. (1955) Leber's disease with recovery. *Archives of Ophthalmology* **53**, 608-609.

Copenhagen, D. R., & Jahr C. E. (1989) Release of endogenous excitatory amino acids from turtle photoreceptors. *Nature* **341**, 536-539.

Cormier, V., Rotig, A., Geny, C., Cesaro, P., Dufier, J. L., Munnich, A. (1991) mtDNA heteroplasmy in Leber hereditary optic neuroretinopathy. *American Journal of Human Genetics* **48,** 813-814.

Corral-Debrinski, M., Horton, T., Lott, M. T., Shoffner, J. M., Beal, M. F., and Wallace, D. C. (1992a) Mitochondrial DNA deletions in human brain: regional variability and increase with advanced age. *Nature Genetics* **2**, 324-329.

Corral-Debrinski, M., Shoffner, J. M., Lott, M. T., and Wallace, D. C. (1992b) Association of mitochondrial DNA damage with aging and coronary atherosclerotic heart disease. *Mutation Research* **275,** 169-80.

Cortelli, P., Montagna, P., Avoni, P., Sangiorgi, S., Bresolin, N., Moggio, M., Zaniol, P., Mantovani, V., Barboni, P., Barbiroli, B., and Lugaresi, E. (1991) Leber's hereditary optic neuropathy: genetic, biochemical, and phosphorus magnetic resonance spectroscopy study in an Italian family. *Neurology* **41**, 1211-1215.

Cortelli, P., Montagna, P., Pierangeli, G., Lodi, R., Barboni, P., Liguori, R., Carelli, V., Iotti, S., Zaniol, P., Lugaresi, E., and Barbiroli, B. (1997) Clinical and brain bioenergetics improvement with idebenone in a patient with Leber's hereditary optic neuropathy: a clinical and 31P-MRS study. *Journal of Neurological Science* **148**, 25-31.

Cotton, P. (1993) Cause of Cuban outbreak neuropathologic puzzle. *Journal of the American Medical Association* **270,** 421-423.

Cox, T. A. (1986) Pupillography of a relative afferent pupillary defect. *American Journal of Ophthalmology* **101**, 320-324.

Cox, T. A., Thompson, H. S., and Corbett, J. J. (1981) Relative afferent pupillary defects in optic neuritis. *American Journal of Ophthalmology* **92**, 685-690.

Crabb, D. W., Edenberg, H. J., Bosron, W. F., and Li, T. K. (1989) Genotypes for aldehyde dehydrogenase deficiency and alcohol sensitivity. The inactive ALDH2(2) allele is dominant. *Journal of Clinical Investigation* **83**, 314-316 **.**

Creutzfeldt, O. D., and Kuhnt, U. (1973) Electrophysiology and topographical distribution of visual evoked potentials in animals. In R. Jung (Ed.), *Handbook of Sensory Physiology* (Vol, 7, Part 3, pp. 595 - 646). Berlin: Springer-Verlag.

Crooks, J., and Kolb, H. (1992) Localization of GABA, glycine, glutamate and tyrosine hydroxylase in the human retina. *Journal of Comparative Neurology* **315**, 287-302.

Cruz, M. M., Ornelas Walker, S., Kolostyak, K. P., Ross-Cisneros, F. N., Sebag, J., Hsia, C. J. C., and Sadun, A. A. (2002, May) Influence of Brimonidine (alpha-2 agonist) and Nitroxide Ester (ETOPS) on retinal cell survival following apoptotic stimulus. Poster session presented at the annual meeting of the Association for Research in Vision and Ophthalmology, Sarasota, Florida.

Cullom, M. E., Heher, K. L., Miller, N. R., Savino, P. J., and Johns, D. R. (1993) Leber's hereditary optic neuropathy masquerading as tobacco-alcohol amblyopia. *Archives of Ophthalmology* **111**, 1482-1485.

Dacey, D. M. (1994) Physiology, morphology and spatial densities of identified ganglion cell types in primate retina. *Ciba Found Symposium* **184**, 12-28; discussion 28-34, 63-70.

Dacey, D. M. (1993a) Morphology of a small-field bistratified ganglion cell type in the macaque and human retina. *Visual Neuroscience* **10**, 1081-1098

Dacey, D. M. (1993b) The mosaic of midget ganglion cells in the human retina. *Journal of Neuroscience* **13**, 5334-5355.

Dacey, D. M., and Lee, B. B. (1994) The 'blue-on' opponent pathway in primate retina originates from a distinct bistratified ganglion cell type. *Nature* **367**, 731-735.

Dacey, D. M. and Petersen, M. R. (1992) Dendritic field size and morphology of midget and parasol ganglion cells of the human retina. *Proceedings of the National Academy of Sciences of the United States of America* **89**, 9666-9670.

Danielson, S. R., Wong, A., Carelli, V., Martinuzzi, A., Schapira, A. H., and Cortopassi, G. A. (2002) Cells bearing mutations causing Leber's hereditary optic neuropathy are sensitized to Fas-induced apoptosis. *Journal of Biological Chemistry* **277**, 5810-5815.

Davanger, S., Ottersen, O. P., and Storm-Mathisen, J. (1991) Glutamate, GABA, and glycine in the human retina: an immunocytochemical investigation. *Journal of Comparative Neurology* **311**, 483-494.

Daw, N. W., Brunken, W. J., and Parkinson, D. (1989) The function of synaptic transmitters in the retina. *Annual Review of Neuroscience* **12**, 205-225.

Degli-Esposti, M., Carelli, V., Shelli, A., Ratta, M., Crimi, M., Sangiorgi, S., Montagna, P., Lenaz, G., Lugaresi, E., and Cortelli, P. (1994) Functional alterations of the mitochondrially encoded ND4 subunit associated with Leber's hereditary optic neuropathy. *FEBS Letters* **352**, 375-379.

Degli-Esposti, M., Ngo, A., Ghelli, A., Benelli, B., Carelli, V., McLennan, H., and Linane, A. W. (1996) The interaction of Q analogs, particularly hydroxydecyl benzoquinone (idebenone), with the respiratory complexes of heart mitochondria. *Archives of Biochemistry and Biophysics* **330**, 395-400.

de Gottrau, P., Buchi, E. R., and Daicker, B. (1992) Distended optic nerve sheaths in Leber's hereditary optic neuropathy. *Journal of Clinical Neuro-Ophthalmology* **12**, 89-93.

Denny-Brown, D. E. (1947) Neurological conditions resulting from prolonged and severe dietary restriction. *Medicine* **26**, 41-113.

Devasagayam, T. P. A., Steenken, S., Obendorf, M. S. W., Schulz, W. A., and Sies, H. (1991) Formation of 8-hydroxy(deoxy)guanosine and generation of strand breaks at guanine residues in DNA by singlet oxygen. *Biochemistry* **30**, 6283-6289.

Diamond, J. A., and Copenhagen, D. R. (1993) The contribution of NMDA and non-NMDA receptors to the light-evoked input-output characteristics of retinal ganglion cells. *Neuron* **11**, 725-738.

Diggle, P. J., Lian, K. Y., and Zeger, S. L. (1994) *Analysis of longitudinal data.* Oxford: Oxford Science Publications, Claredon Press.

Dixon, D. B., and Copenhagen, D. R. (1992) Two types of glutamate receptors differentially excite amacrine cells in the tiger salamander retina. *Journal of Physiology (London)* **449**, 589-606.

Dizdaroglu, M. (1991) Chemical determination of free radical-induced damage to DNA. *Free Radical Biology and Medicine* **10**, 225-242.

Dobie, R. A., and Wilson, M. J. (1989) Analysis of auditory evoked potentials by magnitude-squared coherence. *Ear and hearing* **10**, 2-13.

Dobie, R. A., and Wilson, M. J. (1993) Optimal smoothing of coherence estimates. *Electroencephalography and Clinical Neurophysiology* **80**, 194-200,

Dorfman, L. F., Nikoskelainen, E. K., Rosenthal, A. R., and Sogg, R. L. (1977) Visual evoked potentials in Leber's hereditary optic neuropathy. *Annals of Neurology* **1**, 565-568.

Dotti, M. T., Caputo, N., Signorini, E., and Federico, A. (1992) Magnetic resonance imaging findings in Leber's hereditary optic neuropathy. *European Neurology* **32**, 17-19.

Dowling, J. E., and Boycott, B. B. (1966) Organization of the primate retina: electron microscopy. *Proceedings of the Royal Society of London. Series B: Biological Sciences* **166**, 80-111.

DuBois, L. G., and Feldon, S. E. (1992) Evidence for a metabolic trigger for Leber's hereditary optic neuropathy: A case report. *Journal of Clinical Neuro-Ophthalmology* **12**, 15-16.

Duke-Elder, Sir S. (1971) Leber's Hereditary Optic Atrophy. In Sir S. Duke-Elder (Ed.), *System of Ophthalmology* (pp. 108–116). St. Louis: C. V. Mosby.

Dykens, J. A., Stern, A., Trenkner, E. (1987) Mechanism of kainate toxicity to cerebellar neurons in vitro is analogous to reperfusion tissue injury. *Journal of Neurochemistry* **49**, 1222-1228.

Eckert, E., Kobuch, K. A., Aigner, L., and Spiegel, D. (2002, May) Preservation of ganglion cells in adult retinal tissue cultures – an in vitro- model for neuroprotection. Poster session presented at the annual meeting of the Association for Research in Vision and Ophthalmology, Sarasota, Florida.

Egger, J., and Wilson J. (1983) Mitochondrial inheritance in a mitochondrially mediated disease. *New England Journal of Medicine* **309**, 142-146.

Ehinger, B., Otterson, P., Storm-Mathisen, J., and Dowling, J. (1988) Bipolar cells in the turtle retina are strongly immunoreactive for glutamate. *Proceedings of the National Academy of Sciences of the United States of America* **85**, 8321-8325.

Eleff, S., Kennaway N. G., Buist, N. R. M., Darley-Usmar, V. M., Capaldi, R. A., Bank, W. J., and Chance, B. (1984) ^{31}P NMR study of improvement in oxidative phosphorylation by vitamins K_3 and C in a patient with a defect in electron transport at Complex III in skeletal muscle. *Proceedings of the National Academy of Sciences of the United States of America* **81**, 3529-3533.

Enroth-Cugell, C. and Robson, J. G. (1966) The contrast sensitivity of retinal ganglion cells of the cat. *Journal of Physiology* **187**, 517-552.

Erecinska, M., and Dagani, F. (1990) Relationships between the neuronal sodium/potassium pump and energy metabolism. *Journal of General Physiology* **95**, 591-616.

Erickson, R. P. (1972) Leber's optic atrophy, a possible example of maternal inheritance. *American Journal of Human Genetics* **23**, 348-349.

Famiglietti, E. V., Kaneko, A., & Tachibana, M. (1977) Neuronal architecture of ON and OFF pathways to ganglion cells in carp retina. *Science* **198**, 1267-1269.

Famiglietti, E. V. Jr., and Kolb, H. (1976) Structural basis for ON-and OFF-center responses in retinal ganglion cells. *Science* **194**, 193-195.

Federico, A., Manneschi, L., Meloni, M., Alessandrini, C., Bardelli, A. M., Dotti, M. T., and Sabatelli P. (1988) Histochemical, ultrastructural and biochemical study of muscle mitochondria in Leber's hereditary optic atrophy. *Journal of Inherited Metabolic Diseases* **11**, 193-197.

Ferguson, F. R., and Critchley, M. (1928) Leber's optic atrophy and its relationship with the heredo-familial ataxias. *Journal of Neurological Psychiatry* **9**, 120-132.

Ferrante, R. J., Browne, S. E., Shinobu, L. A., Bowling, A. C., Baik, M. J., MacGarvey, U., Kowall, N. W., Brown, R. H. Jr, and Beal, M. F. (1997) Evidence of increased oxidative damage in both sporadic and familial amyotrophic lateral sclerosis. *Journal of Neurochemistry* **69**, 2064-2074.

Filatov, G. N., Jainazarov, A.B., Kolesnikov, S. S., Lyubarsky, A. L., & Fesenko, E. E. (1989) The effect of ATP, GTP and cAMP on the cGMP-dependent conductance of the fragments from frog rod plasma membrane. *FEBS Lett* **245**, 185-188.

Fine, P. E. M. (1977) Analysis of family history data for evidence of non-mendelian inheritance. *Journal of Medical Genetics* **14**, 399-407.

Fine, P. E. M. (1978) Mitochondrial inheritance and Leber's disease. *Lancet* **2**, 659-661.

Flanagan., J. G., and Harding, G. F. A. (1986) The visual evoked potential and the "scotomatous negativity" in pre-chiasmal lesions. *Investigative Ophthalmology and Visual Science* **27** (Supp), 104.

Fletcher EJ, Johnston GA. (1991) Regional heterogeneity of L-glutamate and L-aspartate high-affinity uptake systems in the rat CNS. *Journal of Neurochemistry* **57**, 911-914.

Folkers, K., Hanioka, T., Xia, L.-J., McRee, J. T. Jr., and Langsjoen, P. (1991) Coenzyme Q_{10} increase T4/T8 ratios of lymphocytes in ordinary subjects and relevance to patients having the AIDS related complex. *Biochemical and Biophysical Research Communications* **176**, 786-791.

Foulds, W. S., and Pettigrew, A. R. (1977) The biochemical basis of the toxic amblyopia. In E. S. Perkins & W. W. Hill (Eds.), *Scientific Foundation of Ophthalmology* (pp. 50-54). London, UK: Wm. Heinemann.

Fox, K., Sato, H., and Daw, N. (1990) The effect of varying stimulus intensity on NMDA-receptor activity in cat visual cortex. *Journal of Neurophysiology* **64**, 1413-1428.

Francois, J. (1968) Hereditary optic atrophy. *International Ophthalmology Clinics* **8**, 1016-1054.

Franks, W. A., and Sanders, M. D. (1990) Leber's hereditary optic neuropathy in women. *Eye* **4**, 482-485.

Freed, M. A. (1992) GABAergic circuits in the mammalian retina. In R. R. Mize, R. E. Marc, & A. M. Sillito (Eds.), *Progress in Brain Research: GABA in the Retina and Central Nervous System* (Vol. 90, pp. 107-132). Amsterdam: Elsevier.

Frumkes, T. E., and Nelson, R. (1995) Functional role of GABA in cat retina: I. Effects of $GABA_A$ agonists. *Visual Neuroscience* **12**, 641-650.

Frumkes, T. E., Nelson, R., and Pflug, R. (1995) Functional role of GABA in cat retina: II. Effects of $GABA_A$ antagonists. *Visual Neuroscience* **12**, 651-661.

Funakawa, I., Kato, H., Terao, A., Ichihashi, K., Kawashima, S., Hayashi, T., Mitani, K., & Miyazaki, S. (1995) Cerebellar ataxia in patients with Leber's hereditary optic neuropathy. *Journal of Neurology* **242**, 75-77.

Funalot B, Ranoux D, Mas JL, Garcia C, Bonnefont JP. (1996) Brainstem involvement in Leber's hereditary optic neuropathy: association with the 14,484 mitochondrial DNA mutation. *Journal of Neurology Neurosurgery and Psychiatry* **61**, 533-534.

Fykse, E. M., & Fonnum, F. (1996) Amino acid neurotransmission: dynamics of vesicular uptake. *Neurochem Res* **21**, 1053-1060.

Gal, A., Schinzel, A., Orth, U., Fraser, N. A., Mollica, F., Craig, I. W., Kruse, T., Machler, M., Neugebauer, M., and Bleeker-Wagemakers, L. M. (1989) Gene of X-chromosomal congenital stationary night blindness is closely linked to DXS7 on Xp. *Human Genetics* **81**, 315-318.

Gass, A., Barker, G. J., MacManus, D., Sanders, M., Riordan-Eva, P., Tofts, P. S., Thorpe, J., McDonald, W. I., Moseley, I. F., and Miller, D. H. (1995) High resolution magnetic resonance imaging of the anterior visual pathway in patients with optic neuropathies using fast spin echo and phased array local coils. *Journal of Neurology Neurosurgery and Psychiatry* **58**, 562-569.

Gerbitz, K. D., Paprotta, A., Obermaier-Kusser, B., Rietschel, M., and Zerres, K. (1992) No genetic differences between affected and unaffected members of a German family with Leber's hereditary optic neuropathy (LHON) with respect to ten mtDNA point mutations associated with LHON. *FEBS Letters* **314**, 251-255.

Gevins, A. S., Zeitlin, G. M., Doyle, J. C., Yingling, C. D., Schaffer, R. E., Callawa, E., and Yeager, C. L. (1979) Electroencephalogram correlates of higher cortical functions. *Science* **203**, 665-668.

Ghelli, A., Degli Esposti, M., Carelli, V., and Lenaz, G. (1997) Changes in mitochondrial complex I activity and coenzyme Q binding site in Leber's hereditary optic neuropathy (LHON). *Molecular Aspects of Medicine* **18 Suppl**., S263-267.

Ghelli, A., Zanna, C., Porcelli, A. M., Schapira, A. H., Martinuzzi, A., Carelli, V., and Rugolo, M. (2002) Leber's hereditary optic neuropathy (LHON) pathogenic mutations induce mitochondrial-dependent apoptotic death in transmitochondrial cells incubated with galactose medium. *Journal of BiologicalChemistry* **18**, S263-267.

Ghosh, S. S., Fahy, E., Bodis-Wollner, I., Sherman, J., and Howell, N. (1996) Longitudinal study of a heteroplasmic 3460 Leber hereditary optic neuropathy family by multiplexed primer-extension analysis and nucleotide sequencing. *American Journal of Human Genetics* **58**, 325-334.

Giles, R. E., Blanc, H., Cann, H. M., and Wallace, D. C. (1980) Maternal inheritance of mitochondrial DNA. *Proceeding of the National Academy of Sciences USA* **77,** 6715-6719.

Gilman, S. C., Bonner, M. J., and Pellmar, T. C. (1994) Free radicals enhance basal release of D-[3H]aspartate from cerebral cortical synaptosomes. *Journal of Neurochemistry* **62**, 1757-1763.

Gittinger, J. W., Keltner, J. L., Miller, N. R., and Burde, R. M. (1979) Progressive visual loss associated with peculiar disc swelling. *Survey of Ophthalmology* **24**, 117-121.

Glaser, J. S. (1988) Topical diagnosis: prechiasmal visual pathways. In T. D. Duane & E. A. Jaeger (Eds.), *Duane's Clinical Ophthalmology* (Vol. II, pp. 37-39). Philadelphia, PA: JB Lippincott.

Goadsby, P. J., and Fine, R. D. (1988) Leber's optic atrophy and "rhodanese" activity. *Medical Journal of Australia* **149**, 110-111.

Gold, G. H., and Dowling, J. E. (1979) Photoreceptor coupling in retina of the toad, Bufo marinus. I. Anatomy. *Journal of Neurophysiology* **42**, 292-310.

Gordon, S. E., Brautigan, D. L., & Zimmerman, A. L. (1992) Protein phosphatases modulate the apparent agonist affinity of the light-regulated ion channel in retinal rods. *Neuron* **9**, 739-748.

Gordon, S. E., Downing-Park, J., Tam, B., & Zimmerman A. L. (1995a) Diacylglycerol analogs inhibit the rod cGMP-gated channel by a phosphorylation-independent mechanism. *Biophysiology Journal* **69**, 409-417.

Gordon, S. E., Downing-Park, J., & Zimmerman, A. L. (1995b) Modulation of the cGMP-gated ion channel in frog rods by calmodulin and an endogenous inhibitory factor. *Journal of Physiology* **486**, 533-546.

Govan, G. G., Smith, P. R., Kellar-Wood, H., Schapira, A. H., and Harding, A. E. (1994) HLA class II genotypes in Leber's hereditary optic neuropathy. *Journal of Neurological Science* **126**, 193-196.

Grant, G. B., and Dowling J. E. (1995) A glutamate-activated chloride current in cone-driven ON bipolar cells of the white perch retina. *Journal of Neuroscience* **15**, 3852-3862.

Grant, G. B., and Dowling J. E. (1996) ON bipolar cell responses in the teleost retina are generated by two distinct mechanisms. *Journal of Neurophysiology* **76**, 3842-3849.

Greene, J. G., and Greenamyre, J. T. (1995a) Characterization of the excitotoxic potential of the reversible succinate dehydrogenase inhibitor malonate. *Journal of Neurochemistry* **64**, 430-436.

Greene, J. G., and Greenamyre, J. T. (1995b) Exacerbation of NMDA, AMPA, and L-glutamate excitotoxicity by the succinate dehydrogenase inhibitor malonate. *Journal of Neurochemistry* **64**, 2332-2338.

Greene, J. G., and Greenamyre, J. T. (1996) Manipulation of membrane potential modulates malonate-induced striatal excitotoxicity in vivo. *Journal of Neurochemistry* **66**, 637-643.

Greene, J. G., Porter, R. H. P., Eller, R. V., and Greenamyre, J. T. (1993) Inhibition of succinate dehydrogenase by malonic acid produces an "excitotoxic" lesion in rat striatum. *Journal of Neurochemistry* **61**, 1151-1154.

Greenstein, V.C., Seliger, S., Zemon, V., and Ritch, R. (1998) Visual evoked potential assessment of the effects of glaucoma on visual subsystems. *Vision Research* **38**, 1901-1911.

Grunert, U., Greferath, U., Boycott, B. B., and Wassle, H. (1993) Parasol (P alpha) ganglion-cells of the primate fovea: immunocytochemical staining with antibodies against GABAA-receptors. *Vision Research* **33**, 1-14.

Grunert, U., and Wassle, H. (1990) GABA-like immunoreactivity in the macaque monkey retina: a light and electron microscopic study. *Journal of Comparative Neurology* **297**, 509-524.

Guy, J., Qi, X., Carelli, V., Martinuzzi, A., Hauswirth, W. W. and Lewin, A. S. (2003, May) Evaluation of potential treatment strategies for Leber hereditary optic neuropathy. Poster session presented at the annual meeting of the Association for Research in Vision and Ophthalmology, Sarasota, Florida.

Guy, J., Qi, X., Pallotti, F., Schon, E. A., Manfredi, G., Carelli, V., Martinuzzi, A., Hauswirth, W. W. and Lewin, A. S. (2002) Rescue of a mitochondrial deficiency causing Leber hereditary optic neuropathy. *Annals of Neurology* **52**, 534-542.

Haddad, G. G., and Jiang, C. (1993) Mechanisms of anoxia-induced depolarization in brainstem neurons: in vitro current and voltage clamp studies in the adult rat. *Brain Research* **625**, 261-268.

Hagemoser, K., Weinstein, J., Bresnick G., Nellis R., Kirkpatrick, S., and Pauli R. M. (1989) Optic atrophy, hearing loss, and peripheral neuropathy. *American Journal of Medical Genetics* **33**, 61-65.

Halliday, A. M. (1976) Visually evoked response in optic nerve disease. *Transactions of the Ophthalmological Societies of the United Kingdom* **96**, 372-376.

Halliday, A. M. (1982) *Evoked potentials in clinical testing.* (pp. 221-222) Edinburgh: Churchill Livingstone.

Halliday, A. M., Barrett, G., Blumhardt, L. D., and Kriss, A. (1979) The macular and paramacular subcomponents of the pattern evoked response. In D. Lehmann & E. Callaway (Eds.), *Human Evoked Potentials: Applications and Problems* (pp. 135-151). New York: Plenum Press.

Halliwell, B. (1987) Oxidants and human disease: some new concepts. *FASEB Journal* **1**, 358-364.

Handoko, H. Y., Wirapati, P. J., Sudoyo, H. A., Sitepu, M., and Marzuki, S. (1998) Meiotic breakpoint mapping of a proposed X linked visual loss susceptibility locus in Leber's hereditary optic neuropathy. *Journal of Medical Genetics* **35**, 668-671.

Hanefeld, F. A., Ernst, B. P., Wilichowski, E., Christen, H. J. (1994) Leber's hereditary optic neuropathy mitochondrial DNA mutations in childhood multiple sclerosis. *Neuropediatrics* **25**, 331.

Harding, A. E. (1991) Neurological disease and mitochondrial genes. *Trends in Neuroscience*. **14**, 132-138.

Harding, A. E. (1989) The mitochondrial genome--breaking the magic circle. *New England Journal of Medicine* **320**, 1341-1343.

Harding, A. E., Sweeney, M. G., Govan, G. G., and Riordan-Eva, P. (1995) Pedigree analysis in Leber hereditary optic neuropathy families with a pathogenic mtDNA mutation. *American Journal of Human Genetics* **57**,77-86.

Harding, A. E., Sweeney, M. G., Miller, D. H., Mumford, C. J., Kellar-Wood, H., Menard, D., McDonald, W. I., and Compston, D. A. (1992) Occurrence of a multiple sclerosis-like illness in women who have a Leber's hereditary optic neuropathy mitochondrial DNA mutation. *Brain* **115**, 979-989.

Harding, G. F. A. (1974) The visual evoked response. *Advances in Ophthalmology* **28**, 2-28.

Harding, G. F. A., and Crews, S. J. (1982) The VER in hereditary optic atrophy of the dominant type. In J. Courjon, F. Mauguiere, & M. Revol (Eds.), *Clinical Applications of Evoked Potentials in Neurology* (pp. 21-30). New York: Raven Press.

Harper, P. S. (1977) Mendelian inheritance or transmissible agent? The lesson of Kuru and the Australia antigen. *American Journal of Medical Genetics* **14**, 389-398.

Hartline, H. K. (1938) The response of single optic nerve fibers of the vertebrate eye to illumination of the retina. *American Journal of Physiology* **121**, 400-415.

Hatefi, Y. (1985) The mitochondrial electron transport and oxidative phosphorylation system. *Annual Review of Biochemistry* **54**, 1015-1069.

Heinzel, B., John, M., Klatt, P., Bohme, E., and Mayer, B. (1992) Ca2+/calmodulin-dependent formation of hydrogen peroxide by brain nitric oxide synthase. *Biochemical Journal* **281**, 627--630.

Hendrickson, A. E., Koontz, M. A., Pourcho, R. G., Sarthy, P. V., and Goebel, D. J. (1988) Localization of glycine-containing neurons in the macaque monkey retina. *Journal of Comparative Neurology* **273**, 473-487.

Hendry, S. H. C., and Reid, C. R. (2000) The koniocellular pathway in primate vision. *Annual Review of Neuroscience* **23**, 127-153.

Henshaw, R., Jenkins, B. G., Schulz, J. B., Ferrante, R. J., Kowall, N. W., Rosen, B. R., and Beal, M. F. (1994) Malonate produces striatal lesions by indirect NMDA receptor activation. *Brain Research* **647**, 161-166.

Hiida, Y., Mashima, Y., Oguchi, Y., Uemura, Y., Kudoh, J., Sakai, K., and Shimizu, N. (1991) Mitochondrial DNA analysis of Leber's hereditary optic neuropathy. *Japanese Journal of Ophthalmology* **35**, 102-106.

Holloway, T. B. (1933) Leber's disease. *Archives of Ophthalmology* **9**, 789.

Holt, I. J., Miller, D. H., and Harding, A. E. (1989) Genetic heterogeneity and mitochondrial DNA heteroplasmy in Leber's hereditary optic neuropathy. *Journal of Medical Genetics* **26**, 739-743.

Holt, I. J., Harding, A. E., and Morgan-Hughes, J. A. (1988) Deletions of muscle mitochondrial DNA in patients with mitochondrial myopathies. *Nature* **331**, 717-719.

Horvath, R., Abicht, A., Shoubridge, E. A., Karcagi, V., Rozsa, C., Komoly, S., & Lochmuller, H. (2000) Leber's hereditary optic neuropathy presenting as multiple sclerosis-like disease of the CNS. *Journal of Neurology* **247**, 65-67.

Hotta,Y., Fujiki, K., Hayakawa, M., Nakajima, A., Kanai, A., Mashima, Y., Hiida, Y., Shinoda, K., Yamada, K., Oguchi, Y., et al. (1995) Clinical features of Japanese Leber's hereditary optic neuropathy with 11778 mutation of mitochondrial DNA. *Japanese Journal of Ophthalmology* **39**, 96-108.

Howell, N. (1994) Primary LHON mutations: Trying to separate "Fruyt" from "Chaf". *Clinical Neuroscience* **2**, 130-137.

Howell, N., Bindoff, L. A., McCullough, D. A., Kubacka, I., Poulton, J., Mackey, D., Taylor, L., and Turnbull, D. M. (1991a) Leber hereditary optic neuropathy: identification of the same mitochondrial ND1 mutation in six pedigrees. *American Journal of Human Genetics* **49**, 939-950.

Howell, N., Ghosh, S. S., Fahy, E., and Bindoff, L. A. (2000) Longitudinal analysis of the segregation of mtDNA mutations in heteroplasmic individuals. *Journal of Neurological Science* **172**, 1-6.

Howell, N., Kubacka, I., Xu, M., and McCullough, D. A. (1991b) Leber hereditary optic neuropathy: involvement of the mitochondrial ND1 gene and evidence for an intragenic suppressor mutation. *American Journal of Human Genetics* **48**, 935-942.

Howell, N., Kubacka, I., Halvorson, S., and Mackey, D. A. (1993) Leber's hereditary optic neuropathy: the etiological role of a mutation in the mitochondrial cytochrome *b* gene. *Genetics* **133**, 133-136.

Howell, N., Kubacka, I., McDonough, B., Hodess, A. B., & Harter, D. H. (2001) mtDNA analysis of Leber hereditary optic neuropathy associated with spondyloepiphyseal dysplasia. *American Journal of Medical Genetics* **100**, 219-222.

Howell, N., and McCullough, D. A. (1990) An example of Leber hereditary optic neuropathy not involving a mutation in the mitochondrial ND4 gene. *American Journal of Human Genetics* **47**, 629-634.

Howell, N., McCullough, D. A., and Bodis-Wollner, I. (1992a) Molecular genetic analysis of a sporadic case of Leber hereditary optic neuropathy. *American Journal of Human Genetics* **50**, 443-446.

Howell, N., McCullough, D. A., Kubacka, I., Halvorson, S., and Mackey, D. A. (1992b) The sequence of human mitochondrial DNA: The question of errors versus polymorphisms. *American Journal of Human Genetics* **50**, 1333-1337.

Howell, N., Xu, M., Halverson, S., Bodis-Wollner, I. and Sherman, J. (1994) A heteroplasmic LHON family: tissue distribution and transmission of the 11778 mutation. *American Journal of Human Genetics* **48**, 935-942.

Hsu, Y. T., & Molday, R. S. (1993) Modulation of the cGMP-gated channel of rod photoreceptor cells by calmodulin. *Nature* **361**, 76-79.

Hsu, Y. T., & Molday, R. S. (1994) Interaction of calmodulin with the cyclic GMP-gated channel of rod photoreceptor cells. Modulation of activity, affinity purification, and localization. *Journal of Biological Chemistry* **269**, 29765-29770.

Hubel, D. H. , and Wiesel, T. N. (1959) Receptive fields of single neurons in the cat's striate cortex. *Journal of Physiology of London* **148**, 574-591.

Hubel, D. H. , and Wiesel, T. N. (1962) Receptive fields, binocular interaction, and functional architecture in the cat's visual cortex. *Journal of Physiology* **160**, 106-154.

Hubel, D. H. , and Wiesel, T. N. (1972) Laminar and columnar distribution of geniculo-cortical fibers in the macaque monkey. *Journal of Comparative Neurology* **146**, 421-450.

Hubel, D. H. , and Wiesel, T. N. (1977) Ferrier lecture. Functional architecture of macaque monkey visual cortex. *Proceedings of the Royal Society of London B Biological Science* **198**, 1-59.

Huoponen, K., Lamminen, T., Juvonen, V., Aula, P., Nikoskelainen, E., and Savontaus, M. L. (1993) The spectrum of mitochondrial DNA mutations in families with Leber hereditary optic neuroretinopathy. *Human Genetics* **92**, 379-384.

Huoponen, K., Vilkki, J., Aula, P., Nikoskelainen, E. K., and Savontaus, M. L. (1991) A new mtDNA mutation associated with Leber hereditary optic neuroretinopathy. *American Journal of Human Genetics* **48**, 1147-1153.

Huoponen, K., Vilkki, J., Savontaus, M. L., Aula, P., and Nikoskelainen, E. K. (1990) Analysis of mitochondrial ND4 gene DNA sequence in Finnish families with Leber hereditary optic neuroretinopathy. *Genomics* **8**, 583-585.

Hwang, J. M., & Park, H. W. (1996) Carbon monoxide poisoning as an epigenetic factor for Leber's hereditary optic neuropathy. *Korean Journal of Ophthalmology* **10**, 122-123.

Ihara, Y., Namba, R., Kuroda, S., Sato, T., and Shirabe, T. (1989) Mitochondrial encephalomyopathy (MELAS): pathological study and successful therapy with coenzyme Q10 and idebenone. *Journal of the Neurological Sciences* **90**, 263-271.

Imachi, J. (1967) Neuro-surgical treatment of Leber's optic atrophy and its pathogenetic relationship to arachnoiditis. In *Progress in Ophthalmology, Proceedings of the Second International Congress of Neuro-Genetics and Neuro-Ophthalmology* (Vol II, pp. 121-127). Montreal: Excerpta Medica.

Imachi, J. (1973) Leber's disease: its genetics, clinical pictures, therapy and histopathology (author's translation). *Nihon Ganka Gakkai Zasshi (Acta Sociologica Ophthalmologica Japan)* **77**, 1658-1685.

Imai, Y., and Moriwaki, D. (1936) A probable case of cytoplasmic inheritance in man: A critique of Leber's disease. *Journal of Genetics* **33**, 163-167.

Inglese, M., Rovaris, M., Bianchi, S., Comi, G., and Fillippi, M. (2001a) Magnetization transfer and diffusion tensor MR imaging of the optic radiations and calcarine cortex from patients with Leber's hereditary optic neuropathy. *Journal of Neurological Science* **188**, 33-36.

Inglese, M., Rovaris, M., Bianchi, S., La Mantia, L., Mancardi, G. L., Ghezzi, A., Montagna, P., Salvi, F., and Fillippi, M. (2001b) Magnetic resonance imaging, magnetisation transfer imaging, and diffusion weighted imaging correlates of optic nerve, brain, and cervical cord damage in Leber's hereditary optic neuropathy. *Journal of Neurology Neurosurgery and Psychiatry* **70**, 444-449.

Isashiki, Y., and Nakagawa, M. (1991) Clinical correlation of mitochondrial DNA heteroplasmy and Leber's hereditary optic neuropathy. *Japanese Journal of Ophthalmology* **35**, 259-267.

Isashiki, Y., Tabata, Y., Kamimura, K., and Ohba, N. (1997) Genotypes of aldehyde dehydrogenase and alcohol dehydrogenase polymorphisms in patients with Leber's hereditary optic neuropathy. *Japanese Journal of Human Genetics* **42**, 187-191.

Ishikawa, S., Ichibe, Y., Yokoe, J., and Wakakura, M. (1995) Leber's hereditary optic neuropathy among Japanese. *Muscle Nerve* **3**, 85-89.

Jaeger, W. (1954) Dominant vererbte Optikusatrophie. *Albrecht Von Graefes Archiv fur Ophthalmologie* **155**, 457-484.

Jaeger, W. (1978) Dominant hereditary optic atrophies and Leber's disease. *Documenta Ophthalmologica Proc. Series* **17**, 91-115.

Jacobson, D. M., and Stone, E. M. (1991) Difficulty differentiating Leber's from dominant optic neuropathy in a patient with remote visual loss. *Journal of Clinical Neuro-Ophthalmology* **11**, 152-157.

Jacobson, D. M., Stone, E. M., Miller, N. R., Pollock, S. C., Fletcher, W. A., McNussen, P. J., and Martin, T. J. (1998) Relative afferent pupillary defects in patients with Leber hereditary optic neuropathy and unilateral visual loss. *American Journal of Ophthalmology* **126**, 291-295.

Jansen, P. H., van der Knaap, M. S., & de Coo, I. F. (1996) Leber's hereditary optic neuropathy with the 11778 mtDNA mutation and white matter disease resembling multiple sclerosis: clinical, MRI and MRS findings. *Journal of Neurological Science* **135**, 176-180.

Jasper, H. H. (1958) The ten twenty electrode system of the International Federation. *Electroencephalography Journal* **10**, 371-375.

Jay, B. (1990) Leber's hereditary optic neuropathy. *Eye* **4**, vii.

Jeffreys, D. (1977) The physiological significance of pattern visual evoked potentials. In J. E. Desmedt (Ed.), *Visual evoked potentials in man: New developments* (pp. 134-167). Oxford: Clarendon Press.

Johns, D. R. (1990a) Improved molecular-genetic diagnosis of Leber's hereditary neuropathy. *New England Journal of Medicine* **323**, 1488-1489.

Johns, D. R. (1990b) The molecular genetics of Leber's hereditary neuropathy. *Archives of Ophthalmology* **108**, 1405-1407.

Johns, D. R., and Berman, J. (1991) Alternative simultaneous complex I mitochondrial DNA mutations in Leber's hereditary optic neuropathy. *Biochemical and Biophysical Research Communications* **174**, 1324-1330.

Johns, D. R., and Neufeld, M. J. (1991) Cytochrome *b* mutations in Leber's hereditary optic neuropathy. *Biochemical and Biophysical Research Communications* **181**, 1358-1364.

Johns, D. R., Heher, K. L., Smith, K. H., and Miller, N. R. (1993a) Leber's hereditary optic neuropathy: Clinical manifestations of the 14484 mutation. *Archives of Ophthalmology* **111**, 495-498.

Johns, D. R., and Sadun, A. A. (1994) Cuban epidemic optic neuropathy. Mitochondrial DNA analysis. *Journal of Neuroophthalmology* **14**, 130-134.

Johns, D. R., Smith, K. H., and Miller, N. R., Sulewski, M. E., Bias, W. B. (1993b) Identical twins who are discordant for Leber's hereditary optic neuropathy. *Archives of Ophthalmology* **111**, 1491-1494.

Johns, D. R., Smith, K. H., Savino, P. J., and Miller, N. R. (1993c) Leber's hereditary optic neuropathy: Clinical manifestations of the 15257 mutation. *Ophthalmology* **100**, 981-986.

Johns, D. R., Neufeld, M. J., and Park, R. D. (1992a) An ND-6 mitochondrial DNA mutation associated with Leber hereditary optic neuropathy. *Biochemical and Biophysical Research Communications* **187**, 1551-1557.

Johns, D. R., Smith, K. H., and Miller, N. R. (1992b) Leber's hereditary optic neuropathy: Clinical manifestations of the 3460 mutation. *Archives of Ophthalmology* **110**, 1577-1581.

Jojich, L., and Pourcho, R. G. (1996) Glutamate immunoreactivity in the cat retina: a quantitative study. *Visual Neuroscience* **13**, 117-133.

Jun, A. S., Brown, M. D., and Wallace, D. C. (1994) A mitochondrial DNA mutation at nucleotide pair 14459 of the NADH dehydrogenase subunit 6 gene associated with maternally inherited Leber hereditary optic neuropathy and dystonia. *Proceedings of the National Academy of Sciences of the United States of America* **91**, 6206-6210.

Juvonen, V., Vilkki, J., Aula, P., Nikoskelainen, E., and Savontaus, M. L. (1993) Reevaluation of the linkage of an optic atrophy susceptibility gene to X-chromosomal markers in Finnish families with Leber hereditary optic neuroretinopathy (LHON). *American Journal of Human Genetics* **53**, 289-292.

Kaas, J. H., and Krubitzer, L. A. (1991) The organization of extrastriate visual cortex. In: B.. Dreher & S. R. Robinson (Eds.), *Neuroanatomy of the visual pathways and their development. (Vision and visual dysfunction,* **Vol 3***).* (pp.302-323). Boca Raton, FL: CRC Press.

Kalman, B., Lublin, F. D., and Alder, H. (1995) Mitochondrial DNA mutations in multiple sclerosis. *Multiple Sclerosis* **1**, 32-36.

Kamei, S., Chen-Kuo-Chang, M., Cazevieille, C., Lenaers, G., Olichon, A., Belenguer, P., Roussignol, G., Renard, N., Eybalin, M., Michelin, A., Delettre, C., Brabet, P., and Hamel, C. P. (2005) Expression of the Opa1 mitochondrial protein in retinal ganglion cells: its downregulation causes aggregation of the mitochondrial network. *Investigative Ophthalmology and Visual Science* **46**, 4288-4294.

Kanai, Y., Smith, C. P., & Hediger, M. A. (1994) A new family of neurotransmitter transporters: the high-affinity glutamate transporters. *FASEB Journal* **8**, 1450-1459.

Kaneko, A. (1971) Electrical connections between horizontal cells in the dogfish retina. *Journal of Physiology* **213**, 95-105.

Kaplan, E (1991) The receptive field structure of retinal ganglion cells in cat and monkey. In A. G. Leventhal (Ed.), *Vision and Visual Dysfunction* (pp. 10-40). Boston: CRC Press.

Kaplan, E (2003) The M, P and K pathways of the primate visual system. In L. M. Chalupa & J. S. Werner (Eds.), *The Visual Neurosciences* (pp. 481-493). Rhode Island: MIT Press.

Kaplan, E., Lee, B. B., and Shapley, R. M. (1990) New views of primate retinal function. In N. N. Osborne & G. J. Chader (Eds.), *Progress in Retinal Research* (Vol. 9, pp. 273-335). New York: Pergamon Press.

Kardon, R. H., Haupert, C. L., and Thompson, H. S. (1993) The relationship between static perimetry and the relative afferent pupillary defect. *American Journal of Ophthalmology* **115**, 351-356.

Karpe, G. (1957) The electroretinogram in siderosis bulbi. *Biblica Ophthalmologica* **48,** 182-190.

Kaupp, U. B., and Koch, K. W. (1992) Role of cGMP and Ca2+ in vertebrate photoreceptor excitation and adaptation. *Annual Review of Physiology* **54**, 153-175.

Kauppinen, R. A., McMahon, H. T., and Nicholls, D. G. (1988) Ca^{2+} dependent and Ca^{2+} independent glutamate release, energy status and cytosolic Ca^{2+} concentration in isolated nerve terminals following metabolic inhibition: possible relevance to hypoglycemia and anoxia. *Neuroscience* **27**, 175-182.

Kawamura, S.,Murakami, M. (1991) Calcium-dependent regulation of cyclic GMP phosphodiesterase by a protein from frog retinal rods. *Nature* **349**, 420-423.

Kellar-Wood, H., Robertson, N., Govan, G. G., Compston, D. A., and Harding, A. E. (1994) Leber's hereditary optic neuropathy mitochondrial DNA mutations in multiple sclerosis. *Annals of Neurology* **36,** 109-112.

Kermode, A. G., Moseley, I. F., Kendall, B. E., Miller, D. H., MacManus, D. G., and McDonald, W. I. (1989) Magnetic resonance imaging in Leber's optic neuropathy. *Journal of Neurology, Neurosurgery & Psychiatry* **52**, 671-674.

Kerrison, J. B., Howell, N., Miller, N. R., Hirst, L., and Green, W. R. (1995) Leber hereditary optic neuropathy. Electron microscopy and molecular genetic analysis of a case. *Ophthalmology* **102**, 1509-1516.

Kerrison, J. B., Miller, N. R., Hsu, F., Beaty, T. H., Maumenee, I. H., Smith, K. H., Savino, P. J., Stone, E. M., and Newman, N. J. (2000) A case-control study of tobacco and alcohol

consumption in Leber Hereditary Optic Neuropathy. *American Journal of Ophthalmology* **130**, 803-812.

Kerrison, J. B., and Newman N. J. (1997) Clinical spectrum of Leber's hereditary optic neuropathy. *Clinical Neuroscience* **4**, 295-301.

Kim, J. Y., Hwang, J. M., & Park, S. S. (2002) Mitochondrial DNA C4171A/ND1 is a novel primary causative mutation of Leber's hereditary optic neuropathy with a good prognosis. *Annals of Neurology* **51**, 630-634.

Kirkham, T. H., and Coupland, S. G. (1981) An electroretinal and visual evoked potential study in Friedreich's ataxia. *Canadian Journal of Neurological Sciences* **8**, 289-294.

Klivenyi, P., Karg, E., Rozsa, C, Horvath, R., Komoly, S., Nemeth, I, Turi, S., and Vecsei, L. (2001) alpha-Tocopherol/lipid ratio in blood is decreased in patients with Leber's hereditary optic neuropathy and asymptomatic carriers of the 11778 mtDNA mutation. *Journal of Neurology Neurosurgery and Psychiatry* **70**, 359-362.

Knierim, J. J., and Van Essen, D. C. (1992) Visual cortex: Cartography,connectivity, and concurrent processing. *Current Opinion in Neurobiology* **2**, 150-155.

Kobayashi, M., Kawamura, H., Sugiyama, T., and Puro, D. G. (2003, May) Nitric oxide prevents ATP-induced cell death in retinal microvessels. Poster session presented at the annual meeting of the Association for Research in Vision and Ophthalmology, Sarasota, Florida.

Kobayashi, M., Ichiki, T., Sugiyama, N., Sano, T., Ban, K., Tsuboi, T., Inagaki, H., Okajima, K., Sobajima, H., Suzuki, S., et al. (1992) Multiple enzyme defects in mitochondria of a case with congenital lactic acidosis and hyperammonaemia. *Journal of Inherited Metabolic Disease* **15**, 809-814.

Koch, K. W. (1992) Biochemical mechanism of light adaptation in vertebrate photoreceptors. *Trends in Biochemical Science* **17**, 307-311.

Kolb, H. (1970) Organization of the outer plexiform layer of the primate retina: Electron microscopy of Golgi-impregnated cells. *Philosophical Transactions of the Royal Society of London B* **258**, 261-283.

Kolb, H., and DeKorver, L. (1991) Midget ganglion cells of the parafovea of the human retina: a study by electron microscopy and serial section reconstructions. *Journal of Comparative Neurology* **303**, 617-636.

Kolb, H., Boycott, B. B., and Dowling, J. E. (1969) A second type of midget bipolar cell in the primate retina. *Philosophical Transactions of the Royal Society of London B* **255**, 177-184.

Kolb, H., Nelson, R. and Mariani, A. (1981) Amacrine cells, bipolar cells and ganglion cells of the cat retina: a Golgi study. *Vision Research* **21**, 1081-1114.

Kormann, B, A., Schuster, H., Berninger, T. A., and Leo-Kottler, B. (1991) Detection of the G to A mitochondrial DNA mutation at position 11778 in German families with Leber's hereditary optic neuropathy. *Human Genetics* **88**, 98-100.

Kothe, A. C., Lovasik, J. V., Pace, R., Hrynchak, P. K., and Flanagan, J. G. (1990) Visual and neural function in Leber's optic neuropathy. *Optometry and Vision Science* **67**, 138-147.

Koutalos, Y., & Yau, K. W. (1996) Regulation of sensitivity in vertebrate rod photoreceptors by calcium. *Trends in Neuroscience* **19**, 73-81.

Kuffler, S. W. (1953) Discharge patterns and functional organization of mammalian retina. *Journal of Neurophysiology* **16**, 37-68.

Krill, A. E. (1977) Primary hereditary optic neuropathies. In A. E. Krill & D. B. Archer (Eds.), *Krill's Hereditary Retinal and Choroidal Diseases: Clinical Characteristics* (Vol II, pp. 1111-1117). Hagerstown: Harper & Row.

Kulikowski, J. J. and Tolhurst, D. J. (1973) Psychophysical evidence for sustained and transient detectors in human vision. *Journal of Physiology* **232**, 149-162.

Kupersmith, M. J., Shakin, E., Siegel, I. M., and Lieberman, A. (1982) Visual system abnormalities in patient's with Parkinson's disease. *Archives of Neurology* **39**, 284-286.

Kwittken, J., and Barest, H. D. (1958) The neuropathology of hereditary optic atrophy (Leber's disease): the first complete anatomic study. *American Journal of Pathology* **34**, 185-207.

Kwon, Y. H., Nelson, S. B., Toth, L. J., and Sur, M. (1992) Effect of stimulus contrast and size on NMDA receptor activity in cat lateral geniculate nucleus. *Journal of Neurophysiology* **68,** 182-196.

Lafon- Cazal, M., Culcasi, M., Gaven, F., Pietri, S., and Bockaert, J. (1993a) Nitric oxide, superoxide, and peroxynitrite: putative mediators of NMDA-induced cell death in cerebellar granule cells. *Neuropharmacology* **32**, 1259-1266.

Lafon- Cazal, M., Pietri, S., Culcasi, M., and Bockaert, J. (1993b) NMDA-dependent superoxide production and neurotoxicity. *Nature* **364**, 535-537.

LaFuente, M. P., Villegas-Perez, M. P., Mayor-Torroglosa, S., Aguilera, M. E., Miralles de Imperial, J., & Vidal-Sanz, M. (2002, May) Dose-dependent neuroprotective effects of Brimonidine against ischemia-induced retinal ganglion cell death. Poster session presented at the annual meeting of the Association for Research in Vision and Ophthalmology, Sarasota, Florida.

Lam, T. T., Carelli, V., Salomao, S., Belfort, R., Berezovsky, A., Quiros, P., Sadun, F. DeNegri, A. M., Sherman, J., and Sadun, A. A. (2003, May) Circulating antioxidants, lipid peroxidation products, cytokines and neuron-specific enolase in Leber's hereditary optic neuropathy (LHON) patients. Poster session presented at the annual meeting of the Association for Research in Vision and Ophthalmology, Sarasota, Florida.

Lan, Y. W., Kwong, J. M. K., Ishii, Y., Caprioli, J. (2003, May) 2-deoxy-D-glucose protects retinal ganglion cells against N-methyl-D-aspartate mediated excitotoxicity. Poster session presented at the annual meeting of the Association for Research in Vision and Ophthalmology, Sarasota, Florida.

Land, J. M., Hockaday, J. M., Trevor Hughes, J., and Ross, B. D. (1981) Childhood mitochondrial myopathy with ophthalmoplegia. *Journal of the Neurological Sciences* **51**, 371-382.

Larsson, N. G., Andersen, O., Holme, E., Oldfors, A., and Wahlstrom, J. (1991) Leber's hereditary optic neuropathy and complex I deficiency in muscle. *Annals of Neurology* **30**, 701-708.

Lasek, R. J., and Brady, S.T. (1984) Adenylyl imidodiphosphate (AMPPNP), a nonhydrolyzable analogue of ATP, produces a stable intermediate in the motility cycle of fast axonal transport. *Biological Bulletin* **167**, 503-506.

Lasek, R. J., and Brady, S.T. (1985) Attachment of transported vesicles to microtubules in axoplasm is facilitated by AMP-PNP. *Nature* **316**, 645-647.

Leber, T. (1871) Ueber hereditare und congenital-angelegte Sehnervenleiden. *Graefes Archives of Ophthalmology* **2**, 249-291.

Leo-Kottler, B., and Christ-Adler, M. (1999) Leber optic neuropathy in women and children. *Ophthalmologe* 96, 698-701.

Lesell, S., Gise, R. L., and Krohel, G. B. (1983) Bilateral optic neuropathy with remission in young men. Variation on a theme by Leber? *Archives of Ophthalmology* **40**, 2-6.

Lettvin, J. Y., Maturana, H. R., McCulloch, W. S., and Pitts, W. H. (1959) What the frog's eye tells the frog's brain. *Proceedings of the Institute of Radio Engineers* **47**, 1940-1951.

Lev, D., Yanoov-Sharav, M., Watemberg, N., Leshinsky-Silver, E., and Lerman-Sagie, T. (2002) White matter abnormalities in Leber's hereditary optic neuropathy due to the 3460 mitochondrial DNA mutation. *European Journal of Paediatric Neurology* **6**, 121-123.

Leventhal, A. G., Rodieck, R. W., and Dreher, B. (1981) Retinal ganglion cell classes in the Old World monkey: Morphology and central projections. *Science* **213**, 1139-1142.

Levick, W. R. (1967) Receptive fields and trigger features of ganglion cells in the visual streak of the rabbits retina. *Journal of Physiology* **188**, 285-307.

Levine, M., and Ensom, M. H. H. (2001) Post hoc power analysis: an idea whose time has passed? *Pharmacotherapy* **21**, 405-409.

Levine, R. L., Garland, D., Oliver, C. N., Amici, A., Climent, I., Lenz, A. G., Ahn, B. W., Shaltiel, S., and Stadtman, E. R. (1990) Determination of carbonyl content in oxidatively modified proteins. *Methods in Enzymology* **186**, 464-478.

Lewin, A. S., Qi, X., and Guy, J. (2003, May) Reduction in expression of a gene encoded by mtDNA: A potential model system for LHON. Poster session presented at the annual meeting of the Association for Research in Vision and Ophthalmology, Sarasota, Florida.

Lieberman, A., Levidow, L., and Korein, J. (1972) The EEG, the visually evoked responses, and the reaction time in Parkinson's disease during treatment with levodopa. *Neurology* **22**, 452.

Linasley, D. B., and Wicke, J. D. (1974) The electroencephalogram: Autonomous electrical activity in man and animals. In R. F. Thompson & M. M. Patterson (Eds.), *Bioelectric Recording Techniques* (Vol. 1) New York: Academic Press.

Lincoff, N. S., Odel, J. G., and Hirano, M. (1993) 'Outbreak' of optic and peripheral neuropathy in Cuba? *Journal of the American Medical Association* **270**, 511-518.

Linnane, A. W., Marzuki, S., Ozawa, T., and Tanaka, M. (1989) Mitochondrial DNA mutations as an important contributor to ageing and degenerative diseases. *Lancet* **1**, 642-645.

Liou, G. I., Matragoon, S., El-Remessy,A. B., Khalil, I. E., Abou-Mohamed, G., Tsai, N.-T., Caldwell, R. W., and Caldwell, R. B. (2003) Neuroprotective effect of (-) & Delta_upper; ^{9}-Tetrahydrocannabinol in NMDA-induced apoptosis in rat retina. *ARVOAbstracts*.

Lipton, S. A., Choi, Y. B., Pan, Z. H., Lei, S. Z., Chen, H. S., Sucher, N. J., Loscalzo, J., Singel, D. J., and Stamler, J. S. (1993) A redox-based mechanism for the neuroprotective and neurodestructive effects of nitric oxide and related nitroso-compounds. *Nature* **364**, 626-632.

Littell, R. C., Stroup, W. W, and Wolfinger, R. D. (1996) *SAS System for Mixed Models*. Cary, NC: SAS Institute Inc.

Livingstone, I. R., Mastaglia, F. L., Howe, J. W. (1980) Leber's hereditary optic neuropathy. Clinical and visual evoked response studies in asymptomatic and symptomatic members of a 4-generation family. *British Journal of Ophthalmology* **64**, 751-757.

Lodi, R., Carelli, V., Cortelli, P., Iotti, S., Valentino, M.L., Barboni, P., Pallotti, F., Montagna, P., & Barbiroli, B. (2002) Phosphoros MR spectroscopy shows a tissue specific in vivo distribution of biochemical expression of the G3460A mutation in Leber's hereditary optic neuropathy. *Journal of Neurology Neurosurgery and Psychiatry* **72**, 805-807.

Lodi, R., Taylor, D. J., Tabrizi, S. J., Kumar, S., Sweeney, M., Wood, N. W., Styles, P., Radda, G. K., and Schapira, A. H. (1997) In vivo skeletal muscle mitochondrial function in Leber's hereditary optic neuropathy assessed by 31P magnetic resonance spectroscopy. *Annals of Neurology* **42**, 573-579.

Lopez, P. F., and Smith, J. L. (1986) Leber's optic neuropathy- new observations. *Journal of Clinical Neuro-ophthalmology* **6**, 144-152.

Lott, M. T., Voljavec, A. S., and Wallace, D. C. (1990) Variable genotype of Leber's hereditary optic neuropathy patients. *American Journal of Ophthalmology* **109**, 625-631.

Lovegrove, W. (1991) Spatial frequency processing in dyslexic and normal readers. In J. F. Stein (Ed.), *Vision and Visual Dysfunction* (pp. 148-154).

Loveland, B. E., Wang, C. R., Yonekawa, H., Hermel, E., Fischer-Lindahl, K. (1990) Maternally transmitted histocompatibility antigen of mice: a hydrophobic peptide of a mitochondrially encoded protein. *Cell* **60**, 971-980.

Ludtke, H., Kriegbaum, C., Leo-Kottler, B., and Wilhelm, H. (1999) Pupillary light reflexes in patients with Leber's hereditary optic neuropathy. *Graefes Archives of Clinical and Experimental Ophthalmology* **237**, 207-211.

Lundsgaard, R. (1944) Leber's disease: a genealogic, genetic, and clinical study of 101 cases of retrobulbar optic neuritis in 20 Danish families (thesis). *Acta Ophthalmologica* **21**, 1-306.

MacKay, D. M. (1977) Adaptation of evoked potentials by patterns of texture-contrast. *Experimental Brain Research* **29**, 149-153.

Mackey D. A. (1994) Three subgroups of patients from the United Kingdom with Leber hereditary optic neuropathy. *Eye* **8**, 431-436.

Mackey, D. A., and Buttery, R. G. (1992) Leber hereditary optic neuropathy in Australia. *Australian and New Zealand Journal of Ophthalmology* **20**, 177-184.

Madl J. E., and Burgesser, K. (1993) Adenosine triphoshate depletion reverses sodium-dependent, neuronal uptake of glutamate in rat hippocampal slices. *Journal of Neuroscience* **13**, 4429-4444.

Maffei, L., and Fiorentini, A. (1981) Electroretinographic responses to alternating gratings before and after section of the optic nerve. *Science* **211**, 953-955.

Majander, A., Huoponen, K., Savontaus, M.-L., Nikoskelainen, E., and Wikstrom, M. (1991) Electron transfer properties of NADH:ubiquinone reductase in the ND1/3460 and the ND4/11778 mutations of Leber hereditary optic neuroretinopathy (LHON). *FEBS Letters* **292**, 289-292.

Malik, S., Sudoyo, H., & Marzuki, S. (2000) Microphotometric analysis of NADH- tetrazolium reductase deficiency in fibroblasts of patients with Leber hereditary optic neuropathy. *Journal of Inherited Metabolic Diseases* **23**, 730-744.

Malpeli, J. G., Lee, D., & Baker, F. H. (1996) Laminar and retinotopic organization of the macaque lateral geniculate nucleus: magnocellular and parvocellular magnification functions. *Journal of Comparative Neurology* **375**, 363-377.

Marc, R. E. (1992) Structural organization of GABAergic circuitry in ectotherm retinas. In R. R. Mize, R. E. Marc, & A. M. Sillito (Eds)., *Progress in Brain Research, Vol 90: GABA in the Retina and Central Nervous System* (pp. 61-92). Amsterdam: Elsevier.

Marc, R. E., & Lam, D. M. K. (1981) Uptake of aspartic and glutamic acid by photoreceptors in goldfish retina. *Proceedings of the National Academy of Sciences of the United States of America* **78**, 7185-7189.

Marc, R. E., Liu, W.-L. S., Kalliontis, M., Raiguel, S. F., and Van Haesendonck, E. (1990) Patterns of glutamate immunoreactivity in the goldfish retina. *Journal of Neuroscience* **10**, 4006-4034.

Mariani, A. P. (1981) A diffuse, invaginating cone bipolar cell in primate retina. *Journal of Comparative Neurology* **197**, 661-671.

Marr, D. (1982) Vision: A computational investigation into the human representation and processing of visual information. San Francisco, CA: Freeman.

Martin, P. R., and Grunert, U. (1992) Spatial density and immunoreactivity of bipolar cells in the macaque monkey retina. *Journal of Comparative Neurology* **323**, 269-287.

Mashima, Y., Hiida Y., and Oguchi Y. (1992) Remission of Leber's hereditary optic neuropathy with idebenone. *Lancet* **340**, 368-369.

Mashima, Y., Imamura, Y., and Oguchi Y. (1997) Dissociation of damage to spatial and luminance channels in early Leber's hereditary optic neuropathy manifested by the visual evoked potential. *Eye* **11**, 707-712.

Mashima, Y., Kigasawa, K., Hasegawa, H., Tani, M., and Oguchi, Y. (1996) High incidence of pre-excitation syndrome in Japanese families with Leber's hereditary optic neuropathy. *Clinical Genetics* **50**, 535-537.

Mashima Y., Kigasawa, K., Wakakura, M., and Oguchi Y. (2000) Do idebenone and vitamin therapy shorten the time to achieve visual recovery in Leber hereditary optic neuropathy? *Journal of Neuroophthalmology* **20**, 166-170.

Mashima, Y., Oshitari, K., Imamura, Y., Momoshima, S., Shiga, H., and Oguchi, Y. (1998) Orbital high resolution magnetic resonance imaging with fast spin echo in the acute stage of Leber's hereditary optic neuropathy. *Journal of Neurology Neurosurgery and Psychiatry* **64**, 124-127.

Mashima, Y., Saga, M., Hiida, Y., Oguchi, Y., Wakakura, M., Kudoh, J., and Shimizu, N. (1995) Quantitative determination of heteroplasmy in Leber's hereditary optic neuropathy by single-strand conformation polymorphism. *Investigative Ophthalmology and Visual Science* **36**, 1714-1720.

Massey, S. C. (1990) Cell types using glutamate as a neurotransmitter in the vertebrate retina. In N. Osborne & G. Chader (Eds.), *Progress in Retinal Research* (Vol 10, pp. 399-425). Oxford, England: Pergamon Press.

Massey, S. C., and Miller, R. F. (1987) Excitatory amino acid receptors of rod- and cone-driven horizontal cells in the rabbit retina. *Journal of Neurophysiology* **57**, 645-659.

Massey, S. C., and Miller, R. F. (1988) Glutamate receptors of ganglion cells in the rabbit retina: Evidence for glutamate as a bipolar transmitter. *Journal of Physiology (London)* **405**, 635-655.

Massey, S. C., and Miller, R. F. (1990) *N*-methyl-*D*-aspartate receptors of ganglion cells in rabbit retina. *Journal of Neurophysiology* **63**, 16-30.

Massey, S. C., and Redburn, D. A. (1987) Transmitter circuits in the vertebrate retina. *Progress in Neurobiology* **28**, 55-96.

Massieu, L., Morales-Villagran, A., and Tapia R. (1995) Accumulation of extracellular glutamate by inhibition of its uptake is not sufficient for inducing neuronal damage: an in vivo microdialysis study. *Journal of Neurochemistry* **64**, 2262-2272.

Mast, J., and Victor, J. D. (1991) Fluctuations of steady-state VEPs: Interaction of driven evoked potentials and the EEG. *Electroencephalography and Clinical Neurophysiology*, **78**, 389-401.

Matsumoto, M., Hayasaka, S., Kadoi, C., Hotta, Y., Fujiki, K., Fujimaki, T., Takeda, M., Ishida, N., Endo, S., and Kanai, A. (1999) Secondary mutations of mitochondrial DNA in Japanese patients with Leber's hereditary optic neuropathy. *Ophthalmic Genetics* **20**, 153-160.

Matthews, P. M., Brown, R. M., Morten, K., Marchington, D., Poulton, J., and Brown, G. (1995) Intracellular heteroplasmy for disease-associated point mutations in mtDNA:

implications for disease expression and evidence for mitotic segregation of heteroplasmic units of mtDNA. *Human Genetics* **96**, 261-268.

Matthews, P. M., Hopkin, J., Brown, R. M., Stephenson, J. B., Hilton-Jones, D, and Brown, G. K. (1994) Comparison of the relative levels of the 3243 (A-->G) mtDNA mutation in heteroplasmic adult and fetal tissues. *Journal of Medical Genetics* **31**, 41-44.

Mayer, M. L., and Westbrook, G. L. (1987a) Permeation and block of *N*-methyl-*D*-aspartic acid receptor channels by divalent cations in mouse cultured central neurons. *Journal of Physiology (London)* **394**, 501-527.

Mayer, M. L., and Westbrook, G. L. (1987b) The physiology of excitatory amino acids in the vertebrate central nervous system. *Progress in Neurobiology* **28**, 197-276.

McCluskey, D. J., O'Connor, P. S., and Sheehy, J. T. (1986) Leber's optic neuropathy and Charcot-Marie-Tooth disease. Report of a case. *Journal of Clinical Neuro-Ophthalmology* **6**, 76-81.

McGuire, B. A., Stevens, J. K., and Sterling, P. (1986) Microcircuitry of beta ganglion cells in cat retina. *Journal of Neuroscience* **6**, 907-918 **.**

McLeod, J. G., Low, P. A., and Morgan-Hughes, J. A. (1978) Charcot-Marie-Tooth disease with Leber optic atrophy. *Neurology* **28**, 179-184.

Meire, F. M., Van Coster, R., Cochaux, P., Obermaier-Kusser, B., Candaele, C., and Martin, J. J. (1995) Neurological disorders in members of families with Leber's hereditary optic neuropathy (LHON) caused by different mitochondrial mutations. *Opthalmic Genetics* **16**, 119-126.

Merigan, W. H., and Maunsell, J. H. (1993) How parallel are the primate visual pathways? *Annual Review of Neuroscience* **16**, 369-402.

Merin, S. C., Obelensky, A., Chowers, I., and Banin, E. (2003, May) A pilot study of topical treatment with an □$_2$-agonist in patients with retinal dystrophies. Poster session presented at the annual meeting of the Association for Research in Vision and Ophthalmology, Sarasota, Florida.

Messam, C. A., Greene, J. G., Greenamyre, J. T., and Robinson, M. B. (1995) Intrastriatal injections of the succinate dehydrogenase inhibitor, malonate, cause a rise in extracellular amino acids. *Brain Research* **684**, 221-224.

Mignard, M and Malpeli, J. G. (1991) Paths of information flow through visual cortex. *Science* **251**, 1249-1251.

Milam, A. H., Dacey, D. M., and Dizhoor, A. M. (1993) Recoverin immunoreactivity in mammalian cone bipolar cells. *Visual Neuroscience* **10**, 1-12.

Miller, N. R. (1982) The hereditary optic neuropathies. Monosymptomatic hereditary optic neuropathies. Leber's optic neuropathy, In N. R. Miller (Ed.), *Walsh and Hoyt's Clinical Neuro-Ophthalmology* (4th ed., pp. 311-317) Baltimore: Williams and Wilkins.

Miller, R. F., and Dacheux, R. F. (1976) Synaptic organization and ionic basis of on and off channels in mudpuppy retina. I. Intracellular analysis of chloride-sensitive electrogenic properties of receptors, horizontal cells, bipolar cells, and amacrine cells. *Journal of General Physiology* **67**, 639-659.

Miller, R. F., and Slaughter, M. M. (1986) Excitatory amino acid receptors of the retina: Diversity of subtypes and conductance mechanisms. *Trends in Neuroscience* **11**, 211-218.

Miquel, J. (1991) *Archives of Gerontological Geriatrics* **12**, 99-117.

Mittman, S., Taylor, W. R., and Copenhagen, D. R. (1990) Concomitant activation of two types of glutamate receptor mediates excitation of salamander retinal ganglion cells. *Journal of Physiology (London)* **428**, 175-197.

Miyamoto, M., and Coyle, J. T. (1990) Idebenone attenuates neuronal degeneration induced by intrastriatal injection of excitotoxins. *Experimental Neurology* **108**, 38-45.

Mojon, D. S., Fujihara, K., Hirano, M., Miller, C., Lincoff, N. S., Jacobs, L. D., and Greenberg, S. J. (1999a) Leber's hereditary optic neuropathy mitochondrial DNA mutations in familial multiple sclerosis. *Graefes Archives of Clinical and Experimental Ophthalmology* **237**, 348-350.

Mojon, D. S., Herbert, J., Sadiq, S. A., Miller, J. R., Madonna, M., and Hirano, M. (1999b) Leber's hereditary optic neuropathy mitochondrial DNA mutations at nucleotides 11778 and 3460 in multiple sclerosis. *Ophthalmologica* **213**, 171-175.

Moncada, S., and Higgs, A. (1993) The L-arginine-nitric oxide pathway. *New England Journal of Medicine* **329**, 2002-2012.

Mondelli, M., Rossi, A., Scarpini, C., Dotti, M. T., and Federico, A. (1991) Leber's optic atrophy: VEP and BAEP changes in 16 asymptomatic subjects. *Acta Neurologica Scandinavia* **84**, 366.

Mondelli, M., Rossi, A., Scarpini, C., Dotti, M. T., and Federico, A. (1990) BAEP changes in Leber's hereditary optic atrophy: further confirmation of multisystem involvement. *Acta Neurologica Scandinavia* **81**, 349-353.

Mondelli, M., Rossi, A., Scarpini, C., Dotti, M. T., and Federico, A. (1991) Leber's optic atrophy: VEP and BAEP changes in 16 asymptomatic subjects. *Acta Neurologica Scandinavia* **84**, 366.

Montgomery, R. D. (1965) The medical significance of cyanogen in plant foodstuffs. *American Journal of Clinical Nutrition* **17**, 103-113.

Morgan-Hughes, J. A., Hayes, D. J., Clark, J. B., and Cooper, J. M. (1984) Results of exploratory therapeutical trials. In K. Folkers & Y. Yamamura (Eds.), *Biochemical and Clinical Aspects of Coenzyme Q*. (Vol. 4 , pp. 417-424). Amsterdam: Elsevier Science Publishers.

Mueller-Jensen, A., Bushart, W., Steidinger, J., Funk, M., and Hellner, K. A. (1978) Die Lebersche Optikusatrophie (Ein interdisziplinare studie). *Klinische Monatsblaetter fuer Augenheilkunde Kmaua* **172**, 831-842.

Murakami, M., Ohtsuka, T., and Shimazaki, H. (1975) Effects of aspartate and glutamate on the bipolar cells in the carp retina. *Vision Research* **15**, 456-458.

Murakami, T., Mita, S., Tokunaga, M., Maeda, H., Ueyama, H., Kumamoto, T., Uchino, M., & Ando, M. (1996) Hereditary cerebellar ataxia with Leber's hereditary optic neuropathy mitochondrial DNA 11778 mutation. *Journal of Neurological Science* **142**, 111-113.

Mutisya, E. M., Bowling, A. C., and Beal, M. F. (1994) Cortical cytochrome oxidase activity is reduced in Alzheimer's disease. *Journal of Neurochemistry* **63**, 2179-2184.

Naito, S., and Ueda, T. (1983) Adenosine triphosphate-dependent uptake of glutamate into Protein I-associated synaptic vesicles. *Journal of Biological Chemistry* **258**, 696-699.

Nagy, I. (1990) Chemistry, toxicology, pharmacology, and pharmacokinetics of idebenone: a review. *Archives of Gerontological Geriatrics* **11**, 177-186.

Naka, K. (1977) Functional organization of catfish retina. *Journal of Neurophysiology* **40**, 26-43.

Nakamura M. (1993) Genetic analysis of Japanese pedigrees with Leber's hereditary optic neuropathy. *Kobe Journal of Medical Science* **39**, 171-182.

Nakamura, M., Fujiwara, Y., and Yamamoto, M. (1993) The two locus control of Leber hereditary optic neuropathy and a high penetrance in Japanese pedigrees. *Human Genetics* **91**, 339-341.

Nakamura, M., andYamamoto, M. (1994) Genetic characteristics of Japanese pedigrees with Leber's hereditary optic neuropathy. *Nippon Ganka Gakkai Zasshi* **98**, 319-326.

Nawy, S., and Copenhagen, D. R. (1987) Multiple classes of glutamate receptor on depolarizing bipolar cells in retina. *Nature* **325**, 56-58.

Nawy, S., and Copenhagen, D. R. (1990) Intracellular cesium separates two glutamate conductances in retinal bipolar cells of goldfish. *Vision Research* **30**, 967-972.

Nawy, S., and Jahr, C. E. (1990) Suppression by glutamate of cGMP-activated conductance in retina bipolar cells. *Nature* **346**, 269-271.

Nelson, R., and Kolb, H. (1983) Synaptic patterns and response properties of bipolar and ganglion cells in the cat retina. *Vision Research* **23**, 1183-1195.

Nelson, J. I., Seiple, W. H., Kupersmith, M. J., and Carr, R. E. (1984) A rapid evoked potential index of cortical adaptation. *Electroencephalography and Clinical Neurophysiology* **59**, 454-464.

Nestler, E. J., and Duman, E. S. (1994) G proteins and cyclic nucleotides in the nervous system. In G. J. Siegel, B. W. Agranoff, R. W. Albers, & P. B. Molinoff (Eds.), *Basic Neurochemistry* (5th ed., pp.429-448). New York: Raven Press.

Newman, N. J. (1991) Leber's hereditary optic neuropathy. *Ophthalmology Clinics of North America* **4**, 431-447.

Newman, N. J. (1993a) Neuro-ophthalmology: the afferent visual system. *Current Opinion in Neurology* **6**, 738-746.

Newman, N. J. (1993b) Leber's hereditary optic neuropathy. New genetic considerations. *Archives of Neurology* **50**, 540-548.

Newman, N. J. (1997) The hereditary optic neuropathies. In N. R. Miller & N. J. Newman (Eds.) Walsh & Hoyt's Clinical Neuroophthalmology, 5th Ed. Baltimore: Williams & Wilkins.

Newman, N. J., Lott, M. T., and Wallace, D. C. (1991) The clinical characteristics of pedigrees of Leber's hereditary optic neuropathy with the 11778 mutation. *American Journal of Ophthalmology* **111**, 750-762.

Ngo, J. T., Bateman, J. B., Cortessis, V., Sparkes, R. S., Mohandas, T., Inana, G., and Spence, M. A. (1989) Norrie disease: linkage analysis using a 4.2-kb RFLP detected by a human ornithine aminotransferase cDNA probe. *Genomics* **4**, 539-545.

Nikoskelainen, E. K. (1984a) Leber hereditary optic neuropathy. *Current Opinion in Ophthalmology* **2**, 531-537.

Nikoskelainen, E. K. (1984b) New aspects of the genetic, etiologic, and clinical puzzle of Leber's disease. *Neurology* **34**, 1482-1484.

Nikoskelainen, E. K. (1985) The clinical findings in Leber's hereditary optic neuroretinopathy. Leber's disease. *Transcripts of the Ophthalmological Society of the United Kingdom* **104**, 845-852.

Nikoskelainen, E. K. (1994) Clinical picture of LHON. *Clinical Neuroscience* **2**, 115-120.

Nikoskelainen, E. K., Hassinen, I. E., Paljärvi, L., Lang, H., and Kalimo, H. (1984a) Leber's hereditary optic neuroretinopathy, a mitochondrial disease? *Lancet* **2**, 1474.

Nikoskelainen, E. K,. Hoyt, W. F., and Nummelin, K. U. (1982) Ophthalmoscopic findings in Leber's hereditary optic neuropathy. I. Fundus findings in asymptomatic family members. *Archives of Ophthalmology* **100**, 1597-1602.

Nikoskelainen, E. K., Hoyt, W. F., and Nummelin, K. U. (1983) Ophthalmoscopic findings in Leber's hereditary optic neuropathy. II. The fundus findings in the affected family members. *Archives of Ophthalmology* **101**, 1059-1602.

Nikoskelainen, E. K., Hoyt, W. F., and Nummelin, K. U. (1984b) Fundus findings in Leber's hereditary optic neuropathy. III. Fluorescein angiographic studies. *Archives of Ophthalmology* **102**, 981-989.

Nikoskelainen, E. K., Huoponen, K., Juvonen, V., Lamminen, T., Nummelin, K., and Savontaus, M. L. (1996) Ophthalmologic findings in Leber hereditary optic neuropathy, with special reference to mtDNA mutations. *Ophthalmology* **103**, 504-514.

Nikoskelainen, E. K., Marttila, R. J., Huoponen, K., Juvonen, V., Lamminen, T., Sonninen, P., and Savontaus, M. L. (1995) Leber's "plus": neurological abnormalities in patients with Leber's hereditary optic neuropathy. *Journal of Neurology Neurosurgery and Psychiatry* **59**, 160-164.

Nikoskelainen, E. K., Nummelin, K., and Savontaus, M.-L. (1988) Does sporadic Leber's disease exist? *Journal of Clinical Neuro-Ophthalmology* **8**, 225-229.

Nikoskelainen, E. K., Paljärvi, L., Lang, H., and Kalimo, H. (1984c) Leber's hereditary optic neuropathy. A mitochondrial disease? *Acta Neurologica Scandinavia*, **69**, 172-173.

Nikoskelainen, E. K., Savontaus, M. L., Huoponen, K., Antila, K., & Hartiala, J. (1994) Pre-excitation syndrome in Leber's hereditary optic neuropathy. *Lancet* **344**, 857-858.

Nikoskelainen, E. K., Savontaus, M.-L., Wanne, O. P., Katila, M., and Nummelin, K. (1987) Leber's hereditary optic neuroretinopathy, a maternally inherited disease. A genealogic study in four pedigrees. *Archives of Ophthalmology* **105**, 665-671.

Nikoskelainen, E. K., Sogg, R. L., Rosenthal, A. R., Friberg, T. R., and Dorfman, L. J. (1977) The early phase in Leber's hereditary optic atrophy. *Archives of Ophthalmology* **95**, 969-978.

Nikoskelainen, E. K., Vilkki, J., Huoponen, K., and Savontaus, M.-L. (1991) Recent advances in Leber's hereditary optic neuroretinopathy. *Eye* **5**, 291-293.

Nikoskelainen, E. K., Wanne, O. P., and Dahl, M. (1985) Pre-excitation syndrome and Leber's hereditary optic neuroretinopathy. *Lancet* **1**, 696.

Ninomiya, T., Yamazaki, H., Munakata, S., Yoshino, H., and Sato, T. (1997) A case of Leber's hereditary optic neuropathy with elevated blood levels of lactate and pyruvate. *British Journal of Ophthalmology* **81**, 422.

Nishimura, M., Obayashi, H., Ohta, M., Uchiyama, T., Hao, Q., and Saida T. (1995) No association of the 11778 mitochondrial DNA mutation and multiple sclerosis in Japan. *Neurology* **45**, 1333-1334.

Nohl, H., and Jordan, W. (1986) *Biochemical and Biophysical Research Communications* **138**, 533-539.

Nohl, H., Breuninger, V. and Hegner, D. (1978) Influence of mitochondrial radical formation on energy-linked respiration. *European Journal of Biochemistry* **90**, 385-390.

Norby S, Lestienne P, Nelson I, Rosenberg T. (1991) Mutation detection in Leber's hereditary optic neuropathy by PCR with allele-specific priming. *Biochemical and Biophysical Research Communication* **175**, 631-636.

Norcia, A. M. (1992) Vision testing by visual evoked potential techniques. In S. J. Isenberg (Ed.), *The eye in infancy* (2nd ed., pp. 157-173). St. Louis: Mosby.

Norcia, A. M., and Tyler, C. W. (1985) Spatial frequency sweep VEP: Visual acuity during the first year of life. *Vision Research* **25**, 1399-1408.

Norcia, A. M., Tyler, C. W., Hamer, R. D., and Wesemann, W. (1989) Measurement of spatial contrast sensitivity with the swept contrast VEP. *Vision Research* **29**, 627-637.

Novelli, A., Reilly, J. A., Lysko, P. G., and Henneberry, R. C. (1988) Glutamate becomes neurotoxic via the NMDA receptor when intracellular energy levels are reduced. *Brain Research* **451**, 205-212.

Novotny, E. J., Singh, G., and Wallace, D. C. (1986) Leber's disease and dystonia: A mitochondrial disease. *Neurology* **36**, 1053-1060.

Nucci, C., Piccirilli, S., Bagetta, G., Nistico, R., and Cerulli, L., (1997) N-methyl-D-aspartate (NMDA) and non-NMDA glutamate receptor antagonists protect from apoptosis induced in the lateral geniculate nucleus of rabbits exposed to the dark. *Neuroscience Letters* **229**, 185-188.

Nucci, C., Piccirilli, S., Nistico, R., Cerulli, L., and Bagetta, G. (2002, May) Neuroprotective effects of intravitreal Tetanus Neurotoxin (TeNT) injection in the lateral geniculate nucleus (LGN) of monocularly deprived (MD) new-born rats. Poster session presented at the annual meeting of the Association for Research in Vision and Ophthalmology, Sarasota, Florida.

Nucci, C., Piccirilli, S., Rodino, P., Nistico, R., Grandinetti, M., Cerulli, L., Leist, M., Nicotera, P., & Bagetta, G. (2000) Apoptosis in the dorsal lateral geniculate nucleus after monocular deprivation involves glutamate signaling, NO production, and PARP activation. *Biochemical and Biophysical Research Communication* **278**, 360-367.

Ogasahara, S., Nishikawa, Y., Yorifuji, S., Soga, F., Nakamura, Y., Takahashi, M., Hashimoto, S., Kono, N., and Tarui, S. (1986) Treatment of Kearns-Sayre syndrome with coenzyme Q_{10}. *Neurology* **36**, 45-53.

Ohlenbusch, A., Wilichowski, E., and Hanefeld, F. (1998a) Characterization of the mitochondrial genome in childhood multiple sclerosis. I. Optic neuritis and LHON mutations. *Neuropediatrics* **29**, 175-179.

Ohlenbusch, A., Wilichowski, E., and Hanefeld, F. (1998b) Characterization of the mitochondrial genome in childhood multiple sclerosis. III. Multiple sclerosis without optic neuritis and the non-LHON-associated genes. *Neuropediatrics* **29**, 313-319.

Olsen, N. K., Hansen, A. W., Norby, S., Edal, A. L., Jorgensen, J. R., and Rosenberg, T. (1995) Leber's hereditary optic neuropathy associated with a disorder indistinguishable from multiple sclerosis in a male harbouring the mitochondrial DNA 11778 mutation. *Acta Neurologica Scandinavia* **91**, 326-329.

Onsuntokun, B. O. (1973) Ataxic high cassava diets in West Africa. In B. Nestel, & R. Maclutyre (Eds.), *Chronic Cassava Toxicity* (pp. 127-138). Ottawa: International Development Research Center.

Oostra, R. J., Kemp, S., Bolhuis, P. A., and Bleeker-Wagemakers, E. M. (1996) No evidence for 'skewed' inactivation of the X-chromosome as cause of Leber's hereditary optic neuropathy in female carriers. *Human Genetics* **97**, 500-505.

Ott, J., Bhattacharya, S., Chen, J. D., Denton, M. J., Donald, J., Dubay, C., Farrar, G. J., Fishman, G. A., Frey, D., Gal, A., Humphries, P, Jay, B., Jay, M., Litt, M., Machler, M., Musarella, M., Neugebauer, M., Naussbaum, R. L., Terwilliger, J. G., Weleber, R. G., Wirth, B., Wong, F., Worton, R. G., and Wright, A. F. (1990) Localizing multiple X chromosome-linked retinitis pigmentosa loci using multilocus homogeneity tests. *Proceedings of the National Academy of Sciences U S A* **87,** 701-704.

Ortiz, R. G., Newman, N. J., Manoukian, S. V., Diesenhouse, M. C., Lott, M. T., and Wallace, D. C. (1992) Optic disk cupping and electrocardiographic abnormalities in an American

pedigree with Leber's hereditary optic neuropathy. *American Journal of Ophthalmology* **113**, 561-566.

Palan, A., Stehouwer, A., and Went, L. N. (1989) Studies on Leber's optic neuropathy III. *Documenta Ophthalmologica* **71**, 77-87.

Pallas, M., Knop, C., Behrens-Baumann, W., and Vorwerk, C. K. (2003, May) Neuroprotective effects of calpain inhibitor MDL 28170 in a model of intravitreal excitotoxicity. Poster session presented at the annual meeting of the Association for Research in Vision and Ophthalmology, Sarasota, Florida.

Pallini, R., Dotti, M. T., Di Natale, P., Alessandrini C., Guazzi, G. C., and Federico, A. (1988) Leber's hereditary optic atrophy: rhodanese activity and ultrastructural findings in liver biopsy. *Brain Disfunction* 1, 331-334.

Parker, W. D. Jr., Oley, C. A., and Parks, J. K. (1989) A defect in mitochondrial electron-transport activity (NADH-coenzyme Q oxido-reductase) in Leber's hereditary optic neuropathy. *New England Journal of Medicine* **320**, 1331-1333.

Paulus, W., Straube, A., Bauer, W., Harding, A. E. (1993) Central nervous system involvement in Leber's optic neuropathy. *Journal of Neurology* **240**, 251-253.

Pellegrini-Giampietro, D. E., Cherici, G., Alesiani, M., Carla, V. and Moroni, F. (1988) Excitatory amino acid release from rat hippocampal slices as a consequence of free-radical formation. *Journal of Neurochemistry* **51**, 1960-1963.

Peng, Y. W., Blackstone, C. D., Huganir, R. L., and Yau, K. W. (1995) Distribution of glutamate receptor subtypes in the vertebrate retina. *Neuroscience* **66**, 483-497.

Perkin, G. D., and Rose, F. C. (1979) *Optic neuritis and its differential diagnosis* (pp. 136-141). Oxford: Oxford University Press

Pernet, V., and Di Polo, A. (2003, May) BDNF promotes robust survival of retinal ganglion cells but not axon regeneration within the adult rat optic nerve. Poster session presented at the annual meeting of the Association for Research in Vision and Ophthalmology, Sarasota, Florida.

Perry, V. H., Oehler, R., and Cowey, A. (1984) Retinal ganglion cells that project to the dorsal lateral geniculate nucleus in the macaque monkey. *Neuroscience* **12**, 1101-1123.

Pfurtscheller, G., and Aranibar, A. (1977) Event-related cortical desynchronization detected by power measurements of scalp EEG. *Electroencephalography and Clinical Neurophysiology* **42**, 817-826.

Pfurtscheller, G., and Cooper, R. (1975) Frequency dependence of the transmission of the EEG from cortex to scalp. *Electroencephalography and Clinical Neurophysiology* **38**, 93-96.

Phillips, C. I. and Gosden, C. M. (1991) Leber's hereditary optic neuropathy and Kearns-Sayre syndrome: mitochondrial DNA mutations. *Survey of Ophthalmology* **35**, 463-472.

Picaud, S. A., Larsson, H. P., Grant, G. B., Lecar, H., & Werblin, F. (1995b) Glutamate-gated chloride channel with glutamate-transporter-like properties in cone photoreceptors of the tiger salamander. *Journal of Neurophysiology* **74**, 1760-1771.

Picaud, S., Larsson, H. P., Wellis, D. P., Lecar, H., & Werblin, F. (1995a) Cone photoreceptors respond to their own glutamate release in the tiger salamander. *Proceedings of the National Academy of Sciences of the United States of America* **92**, 9417-9421.

Pin, J. P., and Duvoisin, R. (1995) Review: Neurotransmitter receptors I. The metabotropic glutamate receptors: Structure and functions. *Neuropharmacology* **34**, 1-26.

Polyak, S. L. (1941) *The retina.* Chicago, Illinois: Chicago University Press.

Poole, C. J. M., and Kind, P. R. N. (1986) Deficiency of thiosulfate sulfurtransferase (rhodanese) in Leber's hereditary optic neuroretinopathy. *British Medical Journal* **292**, 1229-1230.

Poolos, N. P., and Kocsis, J. D. (1990) Elevated extracellular potassium concentration enhances synaptic activation of N-methyl-D-aspartate receptors in hippocampus. *Brain Research* **508**, 7-12.

Pou, S., Pou, W. S., Bredt, D. S., Snyder, S. H., and Rosen, G. M. (1991) Generation of superoxide by purified brain nitric oxide synthase. *Journal of Biological Chemistry* **267**, 24173-24176.

Poulton J. (1992) Mitochondrial DNA and genetic disease. *Bioessays* **14**, 763-768.

Poulton, J., Deadman, M. E., and Gardiner R. M. (1989) Duplications of mitochondrial DNA in mitochondrial myopathy. *Lancet* **1**, 236-239.

Poulton, J., Deadman, M. E., Bronte-Stewart, J., Foulds, W.S., and Gardiner R. M. (1991) Analysis of mitochondrial DNA in Leber's hereditary optic neuropathy. *Journal of Medical Genetics* **28**, 765-770.

Poulton, J., and Morten, K. (1993) Noninvasive diagnosis of the MELAS syndrome from blood DNA. *Annals of Neurology* **34**, 116.

Przyrembel, H. (1987) Therapy in mitochondrial disorders. *Journal of Inherited Metabolic Disease* **10** (supp), 129-146.

Puro D. G., Hwang, J. J., Kwon, O. J., and Chin, H. (1996a) Characterization of an L-type calcium channel expressed by human retinal Muller (glial) cells. *Brain Research. Molecular Brain Research* **37**, 41-48.

Puro D. G., Yuan, J. P., and Sucher, N. J. (1996b) Activation of NMDA receptor-channels in human retinal Muller glial cells inhibits inward-rectifying potassium currents. *Visual Neuroscience* **13**, 319-326.

Purpura, K., Tranchina, D., Kaplan, E., and Shapley, R. M. (1990) *Visual Neuroscience* **4**, 75-93.

Puttfarcken, P. S., Getz, R. L., and Coyle, J. T. (1993a) Kainic acid-induced lipid peroxidation: protection with butylated hydroxytoluene and U78517F in primary cultures of cerebellar granule cells. *Brain Research* **624**, 223-232.

Puttfarcken, P. S., Handen, J. S., Montgomery, D. T., Coyle, J. T., and Werling, L. L. (1993b) N-acetyl-aspartylglutamate modulation of N-methyl-D-aspartate-stimulated [3H]norepinephrine release from rat hippocampal slices. *Journal of Pharmacology and Experimental Therapeutics* **266**, 796-803.

Qi, X., Lewin, A. S., & Guy, J. (2002, May) Creating an animal model of optic neuropathy using ribozymes to deplete mitochondrial enzymes. Poster session presented at the annual meeting of the Association for Research in Vision and Ophthalmology, Sarasota, Florida.

Qi, X., Lewin, A., & Guy, J. (2003, May) Oxidative injury induced by Complex I deficiency is protected with AAV mediated gene transfer of human SOD2. Poster session presented at the annual meeting of the Association for Research in Vision and Ophthalmology, Sarasota, Florida.

Quiros, P. A., Torres, R. J., Salomao, S., Berezovsky, A., Carelli, V., Sherman, J., Sadun, F., De Negri, A., Belfort, R., and Sadun, A. A. (2003, May) Color vision defects in asymptomatic carriers of the Lebers hereditary optic neuropathy (LHON) MtDNA 11778 mutation from a giant Brazilian LHON pedigree: A case control study. Poster session presented at the annual meeting of the Association for Research in Vision and Ophthalmology, Sarasota, Florida.

Regan, D. (1973) Evoked potentials specific to spatial patterns of luminance and colour. *Vision Research* **13**, 2381-2402.

Regan, D. (1979) Electrical responses evoked from the human brain. *Scientific American* **241**, 134-146.

Regan, D. (1989*) Human brain electrophysiology: Evoked potentials and evoked magnetic fields in science and medicine*. New York: Elsevier Science Publishing.

Rehsteiner, K. (1930) Die erste anatomische Untersuchung eines Falles von geschlechtsgebunden-hereditarer Sehnervenatrophie (Leberscher Krankheit). *Graefe's Archives of Ophthalmology* **125**, 14-28.

Reichman, N., Porteous, C. M., and Murphy, M. P. (1994) Cyclosporin A blocks 6-hydroxydopamine-included efflux of Ca2+ from mitochondria without inactivating the mitochondrial inner-membrane pore. *Biochemical Journal* **297**, 151-155.

Reid, R. C., & Shapley, R. M. (1992) Spatial structure of cone inputs to receptive fields in primate lateral geniculate nucleus. *Nature* **356**, 716-718.

Riordan-Eva, P., Sanders, M. D., Govan, G. G., Sweeney, M. G., Da Costa, J., and Harding, A. E. (1995) The clinical features of Leber's hereditary optic neuropathy defined by the presence of a pathogenic mitochondrial DNA mutation. *Brain* **118**, 319-337.

Rizzo, J. F. III. (1995) Adenosine triphosphate deficiency: A genre of optic neuropathy. *Neurology* **45**, 11-16.

Rodieck, R. W. (1979) Visual pathways. *Annual Review of Neuroscience* **2**, 193-225.

Rodieck, R. W. (1988) The primate retina. In H. D. Steklis & J. Brown (Eds.), *Comparative primate biology*, (Neurosciences Vol. 4, pp. 203-278). New York: Liss.

Rodieck RW. (1991) The density recovery profile: a method for the analysis of points in the plane applicable to retinal studies. *Visual Neuroscience* **6**, 95-111.

Rodieck, R. W., & Stone, J. (1965) Analysis of receptive fields of cat retinal ganglion cells. *Journal of Neurophysiology* **58**, 833-849.

Rodieck, R. W., and Watanabe, M. (1993) Survey of the morphology of macaque retinal ganglion cells that project to the pretectum, superior colliculus, and parvicellular laminae of the lateral geniculate nucleus. *Journal of Comparative Neurology* **338**, 289-303.

Rogers, J. (1977) Leber's disease. *Australian Journal of Ophthalmology* **5**, 111-119.

Ronne, H. (1944) The inheritance of Leber's disease (cytoplasmic inheritance). *Acta Ophthalmologica* **22**, 203-236.

Rose, F. C., Bowden, A. N., and Bowden, P. M. A. (1970) The heart in Leber's optic atrophy. *British Journal of Ophthalmology* **54**, 388-393.

Ryan, S., and Arden, G. B. (1988) Electrophysiological discrimination between retinal and optic nerve disorders. *Documenta Ophthalmologica* **68**, 247-255.

Saadati, H. G., Hsu, H. Y., Heller, K. B., and Sadun, A. A. (1998) A histopathologic and morphometric differentiation of nerves in optic nerve hypoplasia and Leber hereditary optic neuropathy. *Archives of Ophthalmology* **116**, 911-916.

Saito, H. A. (1983) Pharmacological and morphological differences between X- and Y-type ganglion cells in the cat's retina. *Vision Research* **23**, 1299-1308.

Sadun, A. (1998) Acquired mitochondrial impairment as a cause of optic nerve disease. *Transactions of the American Ophthalmological Society* **96**, 881-923.

Sadun, A. A., Johnson, B. M., and Schaechter, J. D. (1986) Neuroanatomy of the human visual system: part III. Three retinal projections to the hypothalamus. *Journal of Clinical Neuroopthalmology* **6**, 371-379.

Sadun, A. A., Schaechter, J. D., and Smith, L. E. H. (1984) A retinohypothalamic pathway in man: light mediation of circadian rhythms. *Brain Research* **302**, 371-377.

Sadun, A. A., Carelli, V., Salomao, S., Berezovsky, A., Quiros, P., Sadun, F., DeNegri, A., Sherman, J., Lam, T., and Belfort, R. (2003) Leber's hereditary optic neuropathy (LHON) as a chronic disease: evidence in carriers and affected in a giant Brazilian pedigree. Poster session presented at the annual meeting of the Association for Research in Vision and Ophthalmology, Sarasota, Florida.

Sadun, A. A., Carelli, V., Bose, S., Ross-Cisneros, F. N., Barboni, P. and Ahrens, E. T. (2002) First application of extremely high-resolution magnetic resonance imaging to study microscopic features of normal and LHON human optic nerve. *Ophtalmology* **109**, 1085-1091.

Sadun, A. A., Kashima, Y., Wurdeman, A. E., Dao, J., Heller, K., and Sherman, J. (1994a) Morphological findings in the visual system in a case of Leber's hereditary optic neuropathy. *Clinical Neuroscience* **2**, 165-172.

Sadun, A. A., Martone, J. F., Muci-Mendoza, R., Reyes, L., DuBois, L., Silva, J. C., Roman, G., and Caballero, B. (1994b) Epidemic optic neuropathy in Cuba. Eye findings. *Archives of Ophthalmology* **112,** 691-699.

Sadun, A. A., Martone, J. F., Reyes, L., Du Bois, L., Roman, G. C., and Caballero, B. (1994c) Optic and peripheral neuropathy in Cuba. *Journal of the American Medical Association* **271,** 663-664.

Sadun, A. A., Win, P. H., Ross-Cisneros, F. N., Walker, S. O. & Carelli, V. (2000) Leber's hereditary optic neuropathy differentially affects smaller axons in the optic nerve. *Transactions of the American Opthalmological Society* **98**, 223-232.

Salmaggi, A., Carrara, F., and Zeviani, M. (1994) Remarkable recovery of visual function in a patient with Leber's hereditary optic neuropathy and multiple mutations of mitochondrial DNA. *International Journal of Neuroscience* **77,** 261-266.

Salomao, S., Berezovsky, A., Andrade, R. E., Belfort Jr., R., Kjaer, P. K., Carelli, V., and Sadun, A. A. (2002) Electrophysiologic findings in patients with 11778 Lebers hereditary optic Neuropathy (LHON). Poster session presented at the annual meeting of the Association for Research in Vision and Ophthalmology, Sarasota, Florida.

Salomao, S. R., Carelli, V., Sacai, P. Y., Berezovsky, A., Andrade, R. E., Chicani, C. F., Pereira, J. M., Moraes, M. N., Belfort Jr., R., and Sadun, A. A. (2003) Pattern-reversal visually evoked potential (VEP) in asymptomatic carriers from an extensive Brazilian pedigree with 11778 Leber's hereditary optic neuropathy (LHON). Poster session presented at the annual meeting of the Association for Research in Vision and Ophthalmology, Sarasota, Florida.

Santiesteban-Freixas, R., Rodriguez-Hernandez, M., Hirano, M., Francisco-Plasencia, M., Mendoza-Santiesteban, C., Carrero-Salgado, M., Mendez-Larramendi, I., Serrano-Verdura, C., and Luis-Gonzalez, S. (1999) Lebers hereditary optic neuropathy and its possible relation to a recent epidemic in Cuba. *Review in Neurology* **29**, 289-296.

Sapieha, M., Peltier, M., Manning, W. C., and Di Polo, A. (2003, May) Fibroblast growth factor-2 gene delivery stimulates extensive axonal regeneration of adult retinal ganglion cells *in vivo*. Poster session presented at the annual meeting of the Association for Research in Vision and Ophthalmology, Sarasota, Florida.

Sartore, M., Grasso, M., Piccolo, G., Fasani, R., Bergamaschi, R., Malaspina, A., Ceroni, M., Kobayashi, M., Semeraro, A., Arbustini, E., Surrey, S. and Fortina, P. (1995) Leber's hereditary optic neuropathy (LHON)-related mitochondrial DNA sequence changes in italian patients presenting with sporadic bilateral optic neuritis. *Biochemicaland Molecular Medicine* **56**, 45-51.

Sasaki, T., and Kaneko, A. (1996) L-glutamate-induced responses in OFF-type bipolar cells in the cat retina. *Vision Research* **36**, 787-795.

Savini, G., Barboni, P., Valentino, M. L., Montagna, P., Cortelli, P., De Negri, A. M., Sadun, F., Bianchi, S., Longneck, L., Zanini, M., de Vivo, A., and Carelli, V. (2005) Retinal nerve fiber layer evaluation by optical coherence tomography in unaffected carriers with Leber's hereditary optic neuropathy mutations. *Ophthalmology* **112(1)**:127-31

Sawada, A., Karim, M., and Taniguchi, T. (2003, May) Lomerizine, a novel diphenylmethylpiperazine calcium antagonist, enhances retinal ganglion cell survival induced by optic nerve damage. Poster session presented at the annual meeting of the Association for Research in Vision and Ophthalmology, Sarasota, Florida.

Schaechter, J. D., and Sadun, A. A. (1985) A second hypothalamic nucleus receiving retinal input in man: the paraventricular nucleus. *Brain Research* **340**, 243-250.

Schafer, L., and Thorling, E. B. (1990) Lipid peroxidation and antioxidant supplementation in old age. *Scandinavian Journal of Clinical and Laboratory Investigation* **50**, 69-75.

Schein, S. J., & DeMonasterio, F. M. (1987) The mapping of retinal and geniculate neurons onto striate cortex of macaque. *Journal of Neuroscience* **7**, 996-1009.

Schiavo, G., Matteoli, M., & Montecucco, C. (2000) Neurotoxins affecting neuroexocytosis. *Physiology Review* **80**, 717-766.

Schlegel, J., Schweizer, M., and Richter, C. (1992) 'Pore' formation is not required for the hydroperoxide-induced Ca2+ release from rat liver mitochondria. *Biochemical Journal* **285**, 65-69.

Scholes, J. H. (1975) Colour receptors, and their synaptic connexions, in the retina of a cyprinid fish. *Philosophical Transactions of the Royal Society of London B Biological Sciences* **270**, 61-118.

Seedorf, T. (1985) The inheritance of Leber's disease: A genealogical follow-up study. *Acta Ophthalmologica* **63**, 135-145.

Seedorff, T. (1968) Leber's Disease. II. *Acta Ophthalmologica* **46**, 4-25.

Seedorff, T. (1970) Leber's Disease. V. *Acta Ophthalmologica* **48**, 186-213.

Seiple, W. H., Kupersmith, M. J., Nelson, J. I., and Carr, R. E. (1984) The assessment of evoked potential contrast threshold using real-time retrieval. *Investigative Ophthalmology and Visual Science* **25**, 627-631.

Shapley, R., and Perry, V. H. (1986) *Trends in Neuroscience* **9**, 229-235.

Sheardown, M. J., Nielsen, E. O., Hansen, A. J., Jacobsen, P., and Honore, T. (1990) 2,3-Dihydroxy-6-nitro-7-sulfamoyl-benzo-(*f*)quinoxaline: a neuroprotectant for cerebral ischemia. *Science* **247**, 571-574.

Sherman, J. (1982) Simultaneous pattern-reversal electroretinograms and visual evoked potentials in diseases of the macula and optic nerve. *Annals of the New York Academy of Science* **382**, 214.

Sherman, J. (1984) Visual Evoked Potential (VEP). In J. E. Terry (Ed.) *Ocular Disease: Detection, Diagnosis, and Treatment* (pp. 495-527). Springfield, Illinois: Charles C. Thomas Publishers.

Sherman, J. (1986) ERG and VEP as supplemental aids in the differential diagnosis of retinal versus optic nerve disease In R. Cracco and I. Bodis-Wollner (Eds.), *Evoked Potentials* (pp. 343-353). New York: Alan R. Liss.

Sherman, J. (1992) Patient management: A cure for blindness as well as baldness? (Minoxidil for optic neuropathy). *Optometric Management* **26**,

Sherman, J. (1996) Can minoxidil restore vision? *Optometric Management* , 45-46.

Sherman, J., and Kleiner, L. (1994) Visual system dysfunction in Leber's hereditary optic neuropathy. *Clinical Neuroscience* **2**, 121-129.

Sherman, J., Bass, S. J., Noble, K. G., Nath, S., and Sutija, V. (1986) Visual evoked potential delays in central serous choroidopathy. *Investigative Ophthalmology and Visual Science* **2**, 214-221.

Sherman, J., Roth, J. M., Quiros, P., Carelli, V., Berezovsky, A., Salomao, S., Sadun, F., DeNegri, A., Belfort, R., and Sadun, A. (2003, May) Retinal nerve fiber layer (RNFL) assessment and patterns of RNFL loss in 200 members of a LHON Brazilian pedigree. Poster session presented at the annual meeting of the Association for Research in Vision and Ophthalmology, Sarasota, Florida.

Shiells, R. A., and Falk, G. (1992a) The glutamate-receptor linked cGMP cascade of retinal ON-bipolar cells is Pertussis and cholera toxin-sensitive. *Proceedings of the Royal Society of London, Biology* **247**, 17-20.

Shiells, R. A., and Falk, G. (1992b) Properties of the cGMP-activated channel of retinal ON-bipolar cells. *Proceedings of the Royal Society of London, Biology* **247**, 21-25.

Shiells, R. A., Falk, G., and Naghshineh, S. (1981) Action of glutamate and aspartate analogs on rod horizontal and bipolar cells. *Nature* **294**, 592-594.

Shigenaga, M. K., and Ames, B. N. (1991) Assays for 8-hydroxy-2'-deoxyguanosine: a biomarker of in vivo oxidative DNA damage. *Free Radical Biology and Medicine* **10**, 211-216.

Shoffner, J. M., Brown, M. D., Stugard, C., Jun, A. S., Pollock, S., Haas, R. H., Kaufman, A., Koontz, D., Kim, Y., Graham, J. R., Smith, E., Dixon, J., and Wallace, D. C. (1995) Leber's hereditary optic neuropathy plus dystonia is caused by a mitochondrial DNA point mutation. *Annals of Neurology* **38**, 163-169.

Shoffner, J. M., Lott, M. T., Lezza, A. M., Seibel, P., Ballinger, S. W., and Wallace, D. C. (1990) Myoclonic epilepsy and ragged-red fiber disease (MERRF) is associated with a mitochondrial DNA tRNA(Lys) mutation. *Cell*. **61,** 931-937.

Shoffner, J. M. IV, and Wallace, D. C. (1990) Oxidative phosphorylation diseases: Disorders of two genomes. *Advances in Human Genetics* **19**, 267.

Shoffner, J. M., and Wallace, D. C. (1992) Mitochondrial genetics: principles and practice. *American Journal of Human Genetics* **51**, 1179-1186.

Silveira, L. C. L., and Perry, V. H. (1991) The topography of magnocellular projecting ganglion cells (M-ganglion cells) in the primate retina. *Neuroscience* **40**, 217-237.

Simon, D. K., Mayeux, R., Marder, K., Kowall, N. W., Beal, M. F., and Johns, D. R. (2000) Mitochondrial DNA mutations in complex I and tRNA genes in Parkinson's disease. *Neurology* **54**, 703-709.

Simon, D. K., Pulst, S. M., Sutton, J. P., Browne, S. E., Beal, M. F., and Johns, D. R. (1999) Familial multisystem degeneration with parkinsonism associated with the 11778 mitochondrial DNA mutation. *Neurology* **53**, 1787-1793.

Singh, G., Lott, M. T., and Wallace, D. C. (1989) A mitochondrial DNA mutation as a cause of Leber's hereditary optic neuropathy *New England Journal of Medicine* **320,** 1300-1305.

Slaughter, M. M., and Miller, R. F. (1981) 2-amino-4-phosphonobutyric acid: A new pharmacological tool for retina research. *Science* **211**, 182-185.

Slaughter, M. M., and Miller, R. F. (1983*a*) Bipolar cells in the mudpuppy use an excitatory amino acid neurotransmitter. *Nature* **303**, 537-538.

Slaughter, M. M., and Miller, R. F. (1983*b*) An excitatory amino acid antagonist block cone input to sign-conserving second-order retinal neurons. *Science* **219**, 1230-1232.

Slaughter, M. M., and Miller, R. F. (1983*c*) The role of excitatory amino acid transmitters in the mudpuppy retina: An analysis with kainic acid and N-methyl aspartate. *Journal of Neuroscience* **3**, 1701-1711.

Smith, C. D., Carney, J. M., Starke-Reed, P. E., Oliver, C. N., Stadtman, E. R., Floyd, R. A., and Markesbery, W. R. (1991) Excess brain protein oxidation and enzyme dysfunction in normal aging and in Alzheimer disease. *Proceedings of the National Academy of Sciences of the United States of America* **88**, 10540-10543.

Smith, J. L., Hoyt, W. F., and Susac, J. O. (1973) Ocular fundus in acute Leber optic neuropathy. *Archives of Ophthalmology* **90**, 349-354.

Smith, J. L., Tse, D. T., Byrne, S. F., Johns, D. R., and Stone, E. M. (1990) Optic nerve sheath distention in Leber's optic neuropathy and the significance of the "Wallace mutation". *Journal of Clinical Neuro-Ophthalmology* **10**, 231-8.

Smith, K.H., Johns, D. R., Heher, K. L., Miller, N. R. (1993) Heteroplasmy in Leber's hereditary optic neuropathy. *Archives of Ophthalmology* **111**, 1486-1490.

Smith, P. R., Cooper, J. M., Govan, G. G., Harding, A. E., and Schapira, A. H. (1994) Platelet mitochondrial function in Leber's hereditary optic neuropathy. *Journal of Neurological Science* **122**, 80-83.

Smith, P. R., Cooper, J. M., Govan, G. G., Riordan, P. E., Harding, A. E., Schapira, A. H. V. (1995) Antibodies to human optic nerve in Leber's hereditary optic neuropathy. *Journal of the Neurological Sciences* **130**, 134-138.

Smith, V. C., Pokorny, J., and Ernest, J. T. (1977) Primary hereditary optic atrophies. In A. E. Krill (Ed.), *Hereditary Retinal and Choroidal Diseases Vol. II. Clinical Characteristics*. Hagerstown, Md.: Harper & Row Publishers.

Sokol, S. (1990) The visual evoked cortical potential: Clinical use of the VECP in children. In G. A. Fischman & S. Sokol (Eds.), *Electrophysiological testing in disorders of the retina, optic nerve and visual pathway*. American Academy of Ophthalmology.

Soto, I., del Cueto, C., & Blanco, R. E. (2002, May) FGF-2 enhances adult retinal ganglion cell regeneration after axotomy. Poster session presented at the annual meeting of the Association for Research in Vision and Ophthalmology, Sarasota, Florida.

Stacy, R. W. (1960) Biological and medical electronics. New York: McGraw Hill.

Stell, W. K., Ishida, A. T., and Lightfoot, D. O. (1977) Structural basis for on-and off-center responses in retinal bipolar cells. *Science* **198,** 1269-1271.

Sterling, P. (1983) Microcircuitry of the cat retina. *Annual Review of Neuroscience* **6**, 149-185.

Stone, J., and Fukuda, Y. (1974) Properties of cat retinal ganglion cells: a comparison of W-cells with X- and Y-cells. Journal of Neurophysiology 37, 722-748.

Stone, J., and Hoffman, K. P. (1971) Conduction velocity as a parameter in the organization of the afferent relay in the cat's lateral geniculate nucleus. *Brain Research* **32**, 454-459.

Stone, E. M., Newman, N. J., Miller, N. R., Johns, D. R., Lott, M. T., and Wallace, D. C. (1992) Visual recovery in patients with Leber's hereditary optic neuropathy and the 11778 mutation. *Journal of Clinical Neuro-Ophthalmology* **12**, 10-14.

Stone, S., and Schutte, M. (1991) Physiological and morphological properties of OFF- and ON-center bipolar cells in the *Xenopus* retina: effects of glycine and GABA. *Visual Neuroscience* **7**, 363-376.

Stryer, L. (1988) Biochemistry (3rd ed.), New York: W. H. Freeman.

Sudoyo, H., Marzuki, S., Mastaglia, F, and Carroll, W. (1992) Molecular genetics of Leber's hereditary optic neuropathy: study of a six-generation family from Western Australia. *Journal of Neurological Science* **108**, 7-17.

Sugiyama, Y., and Fujita, T. (1985) Stimulation of the respiratory and phosphorylating activities in rat brain mitochondria by idebenone (CV-2619), a new agent improving cerebral metabolism. *FEBS (Federation of European Biomedical Societies) Letters* **184**, 48-51.

Sugiyama, Y., Fujita, T., Matsumoto, M., Okamoto, K., & Imada, I. (1985) Effects of idebenone (CV-2619) and its metabolites on respiratory activity and lipid peroxidation in brain mitochondria from rats and dogs. *Journal of Pharmacobiodynamics* **8**, 1006-1017.

Sun, A. Y., Cheng, Y., and Sun, G. Y. (1992a) Kainic acid-induced excitotoxicity in neurons and glial cells. *Progress in Brain Research* **94**, 271-280.

Sun, A. Y., Cheng, Y., Bu, Q., and Oldfield, F. (1992b) The biochemical mechanism of the excitotoxicity of kainic acid. Free radical formation. *Molecular and Chemical Neuropathology* **17**, 51-63.

Sur, M., and Sherman, S. M. (1982) Linear and nonlinear W-cells in C-laminae of the cat's lateral geniculate nucleus. *Journal of Neurophysiology* **47**, 869-884.

Sweeney, M. G., Davis, M. B., Lashwood, A., Brockington, M., Toscano, A., and Harding, A. E. (1992) Evidence against an X-linked locus close to DXS7 determining visual loss susceptibility in British and Italian families with Leber hereditary optic neuropathy. *American Journal of Human Genetics* **51**, 741-748.

Syme, I. G., Bronte-Stewart, J., Foulds, W. S., McClure, E., Logan, R., and Stansfield, M. (1983) Clinical and biochemical findings in Leber's hereditary optic atrophy. *Transcripts of the Ophthalmological Society of the United Kingdom.* **103**, 556-559.

Szatkowski, M., Barbour, B., and Attwell, D. (1990) Non-vesicular release of glutamate from glial cells by reversed electrogenic glutamate uptake. *Nature* **348**, 443-446.

Tabb, J. S., & Ueda, T. (1991) Phylogenetic studies on the synaptic vesicle glutamate transporter. *Journal of Neuroscience* **11**, 1822-1828.

Tachibana, M., and Kaneko, A. (1988) L-glutamate-induced depolarization in solitary photoreceptors: a process that may contribute to the interaction between photoreceptors in situ. *Proceedings of the National Academy of Sciences of the United States of America* **85**, 5315-5319.

Tachibana, M., and Okada, T. (1991) Release of endogenous excitatory amino acids from ON-type bipolar cells isolated from the goldfish retina. *Journal of Neuroscience* **11**, 2199-2208.

Tanaka, A., Kiyosawa, M., Mashima, Y., and Tokoro, T. (1998) A family with Leber's hereditary optic neuropathy with mitochondrial DNA heteroplasmy related to disease expression. *Journal of Neuroophthalmology* **18**, 81-83.

Taylor, J., and Holmes, G. M. (1913a) Two families, with several members in each suffering from optic atrophy. *Transcripts of the Ophthalmological Society of the United Kingdom.* **33**, 95-115.

Taylor, J., and Holmes, G. M. (1913b) Nervous symptoms associated with optic atrophy of the familial type. *Transcripts of the Ophthalmological Society of the United Kingdom.* **33**, 116-138.

Taylor, W. R., and Wassle, H. (1995) Receptive field properties of starburst cholinergic amacrine cells in the rabbit retina. *European Journal of Neuroscience* **7**, 2308-2321.

Thompson, H. S., Montague, P., Cox, T. A., and Corbett, J. J. (1982) The relationship between visual acuity, pupillary defect, and visual field loss. *American Journal of Ophthalmology* **93**, 681-688.

Tootell, R. B. H., Hamilton, S. L., and Switkes, E. (1988) Functional anatomy of macaque striate cortex, IV: Contrast and magno-parvo streams. *Journal of Neuroscience* **8**, 1594-1609.

Torii, H., Yoshida, K., Kobayashi, T., Tsukamoto, T., and Tanayama, S. (1985) Disposition of idebenone (CV-2619), a new cerebral metabolism improving agent, in rats and dogs. *Journal of Pharmacobiological Dynamics* **8**, 457-467.

Trobe, J. D., Glaser, J.S., and Cassady, J. C. (1980) Optic atrophy: Differential diagnosis by fundus observation alone. *Archives of Ophthalmology* **98**, 1040.

Trotti, D., Danbolt, N. C., and Volterra, A. (1998) Glutamate transporters are oxidant-vulnerable: a molecular link between oxidative and excitotoxic neurodegeneration? *Trends in Pharmacological Science* **19**, 328-334.

Tsao, K., Aitken, P. A., and Johns, D. R. (1999) Smoking as an aetiological factor in a pedigree with Leber's hereditary optic neuropathy. *British Journal of Ophthalmology* **83**, 577-581.

Tso, D. Y. and Gilbert, C. D. (1988) The organization of chromatic and spatial interactions in the primate striate cortex. *Journal of Neuroscience* **8**, 1712-1727.

Turrens, J. M., and Boveris, B. (1980) Generation of superoxide anion by the NADH dehydrogenase of bovine heart mitochondria. *Journal of Biochemistry* **191**, 421-427.

Turski, L., Bressler, K., Rettig, K. J., Loschmann, P. A., and Wachtel, H. (1991) Protection of substantia nigra from MPP+ neurotoxicity by N-methyl-D-aspartate antagonists. *Nature* **349**, 414-418.

Tyler, C. W., Apkarian, P. A., Levi, D. M., and Nakayama, K. (1979) Rapid assessment of visual function: an electronic sweep technique for the pattern VEP. *Investigative Ophthalmology and Visual Science* **18**, 703-713.

Tyler, C. W., Apkarian, P. A., and Nakayama, K. (1978) Multiple spatial-frequency tuning of electrical responses from human visual cortex. *Experimental Brain Research* **33**, 535-550.

Uemura, A., Osame, M., Nakagawa, M., Nakahara, K., Sameshima, M., and Ohba, N. (1987) Leber's hereditary optic neuropathy: mitochondrial and biochemical studies on muscle biopsies. *British Journal of Ophthalmology* **71**, 531-536.

Valentino, M. L., Avoni, P., Barboni, P., Pallotti, F., Rengo, C., Torroni, A., Bellan, M., Baruzzi, A., and Carelli, V. (2002) Mitochondrial DNA nucleotide changes C14482G and C14482A in the ND6 gene are pathogenic for Leber's hereditary optic neuropathy. *Annals of Neurology* **51**, 774-778.

van Gemert, G. W., and Versteeg, J. (1989) Virological investigations in patients with Leber's optic neuropathy. *Documenta Ophthalmologica* **71**, 88-92.

Van Senus, A. H. C. (1963) Leber's disease in the Netherlands. *Documenta Ophthalmologica* **17**, 1-165.

Vanopdenbosch, L., Dubois, B., D'Hooghe, M. B., Meire, F., and Carton, H. (2000) Mitochondrial mutations of Leber's hereditary optic neuropathy: a risk factor for multiple sclerosis. *Journal of Neurology* **247**, 535-543.

Vaphiades, M. S, and Newman, N. J. (1999) Optic nerve enhancement on orbital magnetic resonance imaging in Leber's hereditary optic neuropathy. *Journal of Neuroophthalmology* **19**, 238-239.

Vergani, L., Martinuzzi, A., Carelli, V., Cortelli, P., Montagna, P., Schievano, G., Carrozzo, R., Angelini, C., and Lugaresi, E. (1995) MtDNA mutations associated with Leber's hereditary optic neuropathy: studies on cytoplasmic hybrid (cybrid) cells. *Biochemical and Biophysical Research Communication* **210**, 880-888.

Victor, M. (1993) Persistent altered mentation due to ethanol. *Neurology Clinics* **11**, 639-661.

Victor, J. D., and Mast, J. (1991) A new statistic for steady-state evoked potentials. *Electroencephalography and Clinical Neurophysiology* **78**, 378-388.

Vilkki, J., Ott, J., Savontaus, M. L., Aula, P., and Nikoskelainen E. K. (1991) Optic atrophy in Leber hereditary optic neuroretinopathy is probably determined by an X-chromosomal gene closely linked to DXS7. *American Journal of Human Genetics* **48**, 486-491.

Vilkki, J., Savontaus, M. L., and Nikoskelainen, E. K. (1989) Genetic heterogeneity in Leber hereditary optic neuroretinopathy revealed by mitochondrial DNA polymorphism. *American Journal of Human Genetics* **45**, 206-211.

Vilkki, J., Savontaus, M. L., and Nikoskelainen, E. K. (1990) Segregation of mitochondrial genomes in a heteroplasmic lineage with Leber hereditary optic neuroretinopathy. *American Journal of Human Genetics* **47**, 95-100.

Villegas-Perez, M., Aviles-Trigueros, M., Lafuente, M.P., Rodriguez, M. E., Garcia-Aviles, A., Coll, L., Mayor-Torroglosa, S., Miralles de Imperial, J., and Vidal-Sanz, M. (2002, May) Axonal transport preservation in adult rat retinal ganglion cells protected from ischemia induced cell death by Brimonidine. Poster session presented at the annual meeting of the Association for Research in Vision and Ophthalmology, Sarasota, Florida.

Volterra, A., Bezzi, P., Rizzini, B. L., Trotti, D., Ullensvang, K., Danbolt, N. C., and Racagni, G. (1996) The competitive transport inhibitor L-trans-pyrrolidine-2, 4-dicarboxylate triggers excitotoxicity in rat cortical neuron-astrocyte co-cultures via glutamate release rather than uptake inhibition. *European Journal of Neuroscience* **8**, 2019-2028 **.**

Wakakura M., and Yamamoto N. (1994) Cytosolic calcium transient increase through the AMPA/Kainate receptor in cultured Muller cells. *Vision Research* **34**, 1105-1109.

Wakakura M., and Yokoe J. (1995) Evidence for preserved direct pupillary light response in Leber's hereditary optic neuropathy. *British Journal of Ophthalmology* **79**, 442-446.

Wallace D. C. (1970a) A new manifestation of Leber's disease and a new explanation for the agency responsible for its unusual pattern of inheritance. *Brain* **93**, 121-132.

Wallace DC. (1970b) Leber's optic atrophy: a possible example of vertical transmission of a slow virus in man. *Australas Annals of Medicine* **19,** 259-262.

Wallace D. C. (1986) Mitochondrial genes and disease. *Hospital Practice* **21**, 77-87.

Wallace D. C. (1989) Mitochondrial DNA mutations and neuromuscular disease. *Trends in Genetics* **5**, 9-13.

Wallace, D. W. (1992a) Mitochondrial genetics: a paradigm for aging and degenerative diseases. *Science* **256**, 628-632.

Wallace, D. W. (1992b) Diseases of the mitochondrial DNA. *Annual Review of Biochemistry* **61**, 1175-1212.

Wallace D. C. (1994) Mitochondrial DNA mutations in diseases of energy metabolism. *Journal of Bioenergetics and Biomembranes* **26**, 241-250.

Wallace, D. C., Singh, G., Hopkins, L. C., Lott, M. T., Hodge, J. A., Schurr, T. G., Lezza, A. M., Elsas, J., and Nikoskelainen, E. K. (1985) Maternally inherited diseases of man. In E. Quagliariello, E. C. Slater, F. Palmier, et al. (Eds.), *Achievements and Perspectives of Mitochondrial Research: Biogenesis.* (Vol. II, pp. 427). Amsterdam: Elsevier Science Publishers BV.

Wallace, D. C., Singh, G., Lott, M. T., Hodge, J. A., Schurr, T. G., Lezza, A. M., Elsas, J., and Nikoskelainen, E. K. (1988) Mitochondrial DNA mutation associated with Leber's hereditary optic neuropathy. *Science* **242**, 1427-1430.

Walsh T., J. (1985) *Neuro-Ophthalmology: Clinical Signs and Symptoms* (2nd ed., pp.346) Philadelphia: Lea & Febiger.

Wassle, H., and Boycott, B. B. (1991) Functional architecture of the mammalian retina. *Physiological Reviews* **71**, 447-480.

Wassle, H., Boycott, B. B., and Rohrenbeck, J. (1989) Horizontal cells in the monkey retina: Cone connections and dendritic network. *European Journal of Neuroscience* **1**, 421-435.

Wassle, H., Grunert, U., Martin, P. R., and Boycott, B. B. (1994) Immunocytochemical characterization and spatial distribution of midget bipolar cells in the macaque monkey retina. *Vision Research* **34**, 561-579.

Watanabe, M., and Rodieck, R. W. (1989) Parasol and midget ganglion cells of the primate retina. *Journal of Comparative Neurology* **289**, 434-454.

Watanabe, M., Sawai, H. & Fukuda, Y. (1997) Survival of axotomized retinal ganglion cells in adult mammals. *Clinical Neuroscience* **4**, 233-239.

Watanabe S, Shen J. (1997) Two opposite effects of ATP on the apparent sensitivity of the cGMP-gated channel of the carp retinal cone. *Visual Neuroscience* **14,** 609-615.

Watkins, J. C., and Evans, R. H. (1981) Excitatory amino acid neurotransmitters. *Annual Review of Pharmacology and Toxicology* **21**, 165-204.

Weiner NC, Newman NJ, Lessell S, Johns DR, Lott MT, Wallace DC. (1993) Atypical Leber's hereditary optic neuropathy with molecular confirmation. *Archives of Neurology* **50**, 470-473.

Went, L. N. (1964a) A sex-linked heredo-degenerative neurological disorder associated with Leber's optic atrophy. Part 2. Laboratory investigations. *Journal of Neurological Science* **1**, 81-87.

Went, L. N. (1964b) A sex-linked heredo-degenerative neurological disorder associated with Leber's optic atrophy. Part 3. Genetical aspects. *Acta Genetica* **14**, 220-239.

Whitehouse, D. B., Poole, C. J., Kind, P. R., and Hopkinson, D. A. (1989) Rhodanese isozymes in three subjects with Leber's optic neuropathy. *Journal of Medical Genetics* **26**, 113-115.

Wilichowski, E., Ohlenbusch, A., and Hanefeld, F. (1998) Characterization of the mitochondrial genome in childhood multiple sclerosis. II. Multiple sclerosis without optic neuritis and LHON-associated genes. *Neuropediatrics* **29**, 307-312.

Wilkinson, L. (1999) Statistical methods in psychology journals: guidelines and explanations. *American Psychology* **54**, 594-604.

Wijburg, F. A., Barth, P. G., Ruitenbeek, W., Wanders, R. J. A., Vos, G. D., Ploos Van Amstel, S. L. B., and Schutgens, R. B. H. (1989) Familial NADH: Q_1 Oxidoreductase (Complex I) deficiency: Variable expression and possible treatment. *Journal of Inherited Metabolic Disease* **12** (Supp), 349-351.

Wijburg, F. A., de Groot, C. J., Feller, N., Wanders, R. J. A. (1991) Restoration of NADH-Oxidation in Complex I and Complex III deficient fibroblasts by Menadione. *Journal of Inherited Metabolic Disease* **14**, 293-296.

Wijburg, F. A., Feller, N., de Groot, C. J., Wanders, R. J. A. (1990) - Menadione partially restores NADH-oxidation and ATP-synthesis in complex I deficient fibroblasts. *Biochemistry International* **22**, 303-309.

Wilson, D. R. (1963) Leber's hereditary optic atrophy, some clinical and etiological considerations. *Brain* **86**, 347-362.

Wilson, D. R. (1965a) Leber's hereditary optic atrophy: A possible disorder of cyanide metabolism. *Clinical Science* **29**, 505-515.

Wilson, D. R. (1965b) Skeletal manifestations in Leber's optic atrophy: A possible disorder of cyanide metabolism. *Annals of Physical Medicine*, **44**, 91-95.

Wilson, D. R., and Kline, L.B. (1992) Leber's hereditary optic neuropathy with bilateral distended optic nerve sheaths. *Journal of Clinical Neuro-Ophthalmology* **12**, 73-74.

Wissinger, B., Besch, D., Baumann, B., Fauser, S., Christ-Adler, M., Jurklies, B., Zrenner, E., and Leo-Kottler, B. (1997) Mutation analysis of the ND6 gene in patients with Lebers

hereditary optic neuropathy. *Biochemical and Biophysical Research Communications* **234**, 511-515.

WoldeMussie, E., Craft, D.K., & Wheeler, L. A. (2002) Neuroprotective effect of different formulations of topically applied Brimonidine after calibrated optic nerve injury. Poster session presented at the annual meeting of the Association for Research in Vision and Ophthalmology, Sarasota, Florida.

Woo, S. J., Kim, D. M., Kim, J. Y., Park, S. S., Ko, H. S., and Yoo, T. (2004) Investigation of the association between OPA1 polymorphisms and normal-tension glaucoma in Korea. *Journal of Glaucoma* **13**, 492-5.

Xu, X., Ichida, M. J., Allison, J. D., Boyd, J. D., Bonds, A. B., and Casagrande, V. A. (2001) A comparison of koniocellular, magnocellular and parvocellular receptive field properties in the lateral geniculate nucleus of the owl monkey *(Aotus trivirgatus) Journal of Physiology* **531**, 203-218.

Yamada, K., Mashima, Y., Kigasawa, K., Miyashita, K., Wakakura, M., and Oguchi, Y. (1997) High incidence of visual recovery among four Japanese patients with Leber's hereditary optic neuropathy with the 14484 mutation. *Journal of Neuroophthalmology* **17**, 103-107.

Yamanaka, H. (1971) The mode of inheritance of Leber's disease. *Nippon Ganka Gakkai Zasshi* **75**, 1930-1936.

Yamauchi, T., Kashii, S., Honda, Y., and Akaike, A. (2002, May) Role of mitochondrial K(atp) channel and Pke on the neuro-protection against glutamate neurotoxicity. Poster session presented at the annual meeting of the Association for Research in Vision and Ophthalmology, Sarasota, Florida.

Yang, X. L, and Wu, S.M. (1991) Coexistence and function of glutamate receptor subtypes in the horizontal cells of the tiger salamander retina. *Visual Neuroscience* **7**, 377-382.

Yazejian, B., and Fain, G. L. (1992) Excitatory amino acid receptors on isolated retinal ganglion cells from the goldfish. *Journal of Neurophysiology* **67**, 94-107.

Yen, M. Y., Lee, H. C., Liu, J. H., and Wei, Y. H. (1996) Compensatory elevation of Complex II activity in Leber's hereditary optic neuropathy. *British Journal of Ophthalmology* **80**, 78-81.

Yen, M. Y., Lee, H. C., Wang, A. G., Chang, W. L., Liu, J. H., and Wei, Y. H. (1999) Exclusive homoplasmic 11778 mutation in mitochondrial DNA of Chinese patients with Lebers hereditary optic neuropathy. *Japanese Journal of Ophthalmology* **43**, 196-200.

Yen, T. C., Yeh, S. H. (1995) ^{99m}Tc-HMPAO brain single photon emission computerized tomography in mitochondrial encephalomyopathies. *Chinese Medical Journal (Taipei)* **56**, 287-291.

Yip, H. K., Hu, B., Kau, W. F., and So, K. F. (2002, May) Combined treatment of neurotrophic factors and cytokines enhances survival of neonatal retinal ganglion cells in vitro. Poster session presented at the annual meeting of the Association for Research in Vision and Ophthalmology, Sarasota, Florida.

Yoneda, M., Tsuji, S., Yamauchi, T., Inuzuka, T., Miyatake, T., Horai, S., and Ozawa, T. (1989) Mitochondrial DNA mutation in family with Leber's hereditary optic neuropathy *Lancet* **1,** 1076-1077.

Yu, D., and Eldred, W. D. (2003, May) Interactions of GABA and the NO/cGMP signaling pathway in the retina. Poster session presented at the annual meeting of the Association for Research in Vision and Ophthalmology, Sarasota, Florida.

Zeevalk, G. D., and Nicklas, W. J. (1990) Chemically induced hypoglycemia and anoxia: relationship to glutamate receptor-mediated toxicity in retina. *Journal of Pharmacology and Experimental Therapy* **253**, 1285-1292.

Zeevalk, G. D., and Nicklas, W. J. (1991) Mechanisms underlying initiation of excitotoxicity associated with metabolic inhibition. *Journal of Pharmacology and Experimental Therapy* **257**, 870-878.

Zeevalk, G. D., and Nicklas, W. J. (1992) Evidence that the loss of the voltage-dependent Mg^{2+} block at the N-methyl-D-aspartate receptor underlies receptor activation during inhibition of neuronal metabolism. *Journal of Neurochemistry* **59**, 1211-1220.

Zemon, V. (1984) The VEP: Analysis of functional subsystems in the brain. *Proceedings of the Sixth Annual Conference of the IEEE Engineering in Medicine and Biology Society* **6**, 426-431.

Zemon, V., Buckley, S., Fitzgerald, K. M., Gordon, J., Hartmann, E. E., and Meyer, A. (1999) Objective determination of signal from noise in swept-parameter transient visual evoked potentials (VEPs). *Investigative Ophthalmology and Visual Science* **40**, S824.

Zemon, V., Eisner, W., and Gordon, J. (1994) Transient VEP measures of visual development in children. *Investigative Ophthalmology and Visual Science, Supplement* **35/4**, 1775.

Zemon, V., Eisner, W., Gordon, J., Grose-Fifer, J., Tenedios, F., and Shoup, H. (1995) Contrast-dependent responses in the human visual system: childhood through adulthood. *International Journal of Neuroscience* **80**, 181-201.

Zemon, V., and Gordon, J. (1988) Spatial tuning characteristics of functional subsystems in the visual pathways of humans. *Investigative Ophthalmology and Visual Science, Supplement* **29**, 297.

Zemon, V., Hartmann, E. E., Gordon, J., and Prunte-Glowazki, A. (1997) An electrophysiological technique for assessment of the development of spatial vision. *Optometry and Vision Science* **74**, 708-716.

Zemon, V., Kaplan, and Ratliff, R. (1980) Bicuculine enhances a negative component and diminishes a positive component of the visual evoked cortical potential in the cat. *Proceedings of the National Academy of Sciences of the United States of America* **77**, 7476-7478.

Zemon, V., Kaplan, and Ratliff, R. (1986a) The role of GABA-mediated intracortical inhibition in the generation of visual evoked potentials. In R. Q. Cracco & I. Bodis-Wollner (Eds.), *Frontiers of Clinical Neuroscience: Evoked Potentials*, (Vol III, pp. 287-295). New York, Alan R. Liss.

Zemon, V., and Ratliff, F. (1982) Visual Evoked Potentials: Evidence for lateral interactions. *Proceedings of the National Academy of Sciences of the United States of America* **79,** 5723-5726.

Zemon, V., Victor, J., and Ratliff, F. (1986b) Functional subsystems in the visual pathways of humans using evoked potentials. In R. Q. Cracco & I. Bodis-Wollner (Eds.), *Frontiers of Clinical Neuroscience: Evoked Potentials*, (Vol III, pp. 203-210). New York: Alan R. Liss.

Zeviani, M., Servidei, S., Gellera, C., Bertini, E., DiMauro, S., and DiDonato, S. (1989) An autosomal dominant disorder with multiple deletions of mitochondrial DNA starting at the D-loop region. *Nature* **339**, 309-311.

Zhou, Z. J., Fain, G. L., & Dowling, J. E. (1993) The excitatory and inhibitory amino acid receptors on horizontal cells isolated from the white perch retina. *Journal of Neurophysiology* **70**, 8-19.

Zhou, Z. J., Marshak, D. W., and Fain, G. L. (1994) Amino acid receptors of midget and parasol ganglion cells in primate retina. *Proceedings of the National Academy of Sciences of the United States of America* **91**, 4907-4911.

Zhu DP, Economou EP, Antonarakis SE, Maumenee IH. (1992) Mitochondrial DNA mutation and heteroplasmy in type I Leber hereditary optic neuropathy. *American Journal of Medical Genetics* **42,** 173-179.